Structure/function analyses of neural circuitry controlling courtship behaviours in *Drosophila melanogaster*

A thesis submitted for the degree of
Doctor of Philosophy at the University of Glasgow

by

Anthony James Dornan

Institute of Molecular, Cell and Systems Biology
College of Medical, Veterinary and Life Sciences
University of Glasgow
Glasgow
G12 8QQ
UK

August 2011

Abstract

There has been a continuous production of high quality reports focussing on *fruitless* as the genetic switch for male sexual behaviour in *Drosophila* melanogaster, and on *fruitless*'s contributions to creating a male-specific neural circuit within the CNS. However it has become increasingly clear that *fruitless* is not sufficient in itself to specify the full complement of male-specific behavioural repertoires. One obvious genetic candidate that contributes to the male neural circuit is *doublesex*. *doublesex* has long been known to be pivotal to the specification of the sexually dimorphic adult soma but it's function in specifying sex-specific neural substrates has, up till now, been largely unexplored. While *fruitless* has so far shown to be found only in insects, *doublesex* is a more ancient gene and, as member of the Dmrt family of genes, is both structurally and functionally conserved throughout the animal kingdom. Thus the study of *doublesex* offers great potential for understanding the neuronal, developmental and physiological logic underlying innate and species-specific behaviours, in not one but both sexes, in organisms throughout the animal kingdom.

Using the novel *dsx*^{GAL4} transgenic tool, generated by ends-in homologous recombination at the *doublesex* locus, I have been able to perform a systematic temporal and spatial survey of *doublesex* expression both within, and outwith, the nervous system. Excitingly, as *doublesex* is endogenously expressed in both males and females, this has uncovered profound dimorphic differences in male and female neural substrates. In the male this circuit is shared with *fruitless* (whose expression is restricted to adult males) and has allowed myself, and my colleagues in the Goodwin lab, through functional behavioural analyses, to gain greater understanding into how male-specific behavioural outputs may be generated. Further though, functional analyses impinging on the novel *doublesex* female circuitry has allowed us to gain new insight into the (largely unstudied) role that females play in the courtship ritual. The *dsx* ^{GAL4} transgenic tool, and the insights gained in this study, are also of import in relation to dissecting out mechanisms involved in the post-mating physiological and behavioural changes the female undergoes after successful copulation with a male. As well as this, as *doublesex* is known to play a pivotal role in establishing the dimorphic morphology of the fly, this tool has begun to allow us an understanding of how the assembly of these dimorphic neural circuits is coordinated with the development, and

maintenance, of a sex-specific anatomy and physiology to produce the complete male or female ‘state’; Integrating both mind (fly brain) and body (fly soma).

Preface

“There is no time which flows equally for all observers. Now, sooner, later, and simultaneous are relative to the frame of reference of the observer.”

–Albert Einstein

“There are two kinds of light--the glow that illuminates, and the glare that obscures.”

-James Thurber

Table of Contents

List of Tables

List of Figures

List of accompanying materials

Rideout E.J.*, Dornan A.J.*, Neville M.C.*, Eadie S., and S.F. Goodwin. (2010). Control of sexual differentiation and behavior by the *doublesex* gene in *Drosophila melanogaster*. Nat Neurosci 13(4), 458-66. *Joint primary authors.

Dornan A.J., and S.F. Goodwin. (2008). Fly courtship song: triggering the light fantastic. Cell 133(2), 210-2.

Billeter J.-C., Rideout E., Dornan A.J., and S.F. Goodwin. (2006). Control of male sexual behavior in *Drosophila* by the sex determination pathway. Curr Biol 16(17), R766-R776.

Acknowledgements

I have many people to thank for the various opportunities given to me during the creation of this thesis, but only one person, Stephen Goodwin, to thank for providing the actual facility that allowed this Ph.D. to be completed. Stephen has been remarkable, in that he has successfully steered the difficult waters of maintaining a close friendship while providing the necessary guidance, support and discipline required to see me through to the end. I must also thank Jean-Christophe Billeter, who helped engender in me the belief that I could do this, never failed to provide me with support when requested, honest criticism when needed and friendship always. My thanks also to Megan Neville, for exactly the same reasons, and for providing a calm and clear perspective when the rest of us were working ourselves into an uproar.

I have to thank Elizabeth Rideout, for providing the *dsx*^{GAL4} reagent that underpins the research in this thesis. As Newton wrote to Hooke, "*If I have seen a little further it is by standing on the shoulders of giants*". To the many other members of the Goodwin Lab, both past and present, who tolerated my moods and idiosyncrasies with real humour and as much grace as they could muster; to Suzanne, Hania, Lizzy, Carolina, Michael and John, who each in their way made life in and out of work interesting and fun, you have my gratitude and best wishes.

My eternal gratitude must also go to Julian Dow and Shireen Davies and the Dow/Davies lab, for providing me with safe haven and consistently giving me help, understanding, and a far greater degree of latitude in completing this thesis than could, or should, have been rightly expected.

To my family, I will always be grateful for the patience you have shown me, and the love that is testament in the second, third and fourth chances provided. To my Mum, whom I'm sorry never got to see this completed effort, and to my Dad, I hope this will in some way redress the pain I have caused in past times and confirm the belief you have always held in me. Finally to the three lovely girls who are the most precious things in my life; to Kirstan, Darcy and Marley, who helped complete this thesis through selfless sacrifice and constant love and belief, my thanks and love always.

Author's declaration

I hereby declare that all the work reported in this thesis is my own unless stated otherwise in the text. None of the work has been previously submitted for any other degree at any other institution. All sources of information used in the preparation of this thesis are indicated by reference.

Anthony James Dornan

Glossary

Anatomical Terms

Abdominal Ganglion	Abg
Abdominal nerve trunk	AbNvTk
Accessory Gland	Acg
Antennal lobe	AL
Antennal mechano-sensory and motor centres	AMMC
Apodeme	Apo
Calyx	Ca
Cell body rind	CBR
Central complex	CC or CX
Central nervous system	CNS
Cervical connexion	CvCn
Common oviduct	OvdC
Direct flight muscles	DFM
Ejaculatory bulb	EjB
Ejaculatory duct	EjD
External genital plates	GenPlate
Fan shaped body	Fb
Fat body	FB
Inferior neuropils	INP
Lateral crescent	LC
Lateral horn	LH
Lateral junction	LJ
Lateral oviduct	OvdL
Malpighian tubule	MT
Mesothoracic ganglion	Msg
Mesothoracic triangle	Mst
Metathoracic ganglion	Mtg
Muscle of Lawrence	MOL
Mushroom body	MB
Neuromuscular junction	NMJ
Noduli	NO
Olfactory receptor neuron	ORN
Optic lobe	OL
Ovary	Ov
Ovary flap	OvF
Paravoria	Par
Pars intercerberalis	PI
Peduncle	Ped
Perieosophageal neuropils	PENP
Peripheral nervous system	PNS
Prothoracic ganglion	Prg
Protocerebral bridge	Pb
Proventriculus (cardia)	Provent
Salivary gland	SG
Seminal vesicle	SmV

Seminiferous receptacle	SmRcp
Sex comb	SC
Somatic gonadal precursor cells	SGP
Spermatheca	Spt
Spur	Sp
Stomodeal valve	StomV
Subeosophageal ganglion	SOG or SEG
Superior neuropils	SNP
Transverse bristles	TVB
Vas deferens	VD
Ventral nerve cord	VNC
Ventromedial neuropils	VMNP
Ventrolateral neuropils	VNLP

Genetic Terms

Abdominal-A or B	*Abd-A or Abd-B*
Accessory gland protein	Acp
apterous	*ap*
Broad-complex/Tramtrack/Bric-à-brac	BTB
Canton-Special	CS
Curly of Oster	CyO
don juan	*dj*
doublesex	*dsx*
Doublesex isoforms (female or male)	Dsx^F or Dsx^M
ebony	*e*
embryonic lethal, abnormal vision	*elav*
enhanced Green Fluorescent Protein	eGFP
Flippase site-specific recombinase	FLP
Flippase recognition site	FRT
fruitless (gene)	*fru*
Fruitless (proteins)	Fru
Green Fluorescent Protein	GFP
Gustatory receptor gene	Gr
Gustatory receptor neuron	Grn
head involution defective	*hid*
hermaphrodite	*her*
Humeral	*Hu*
intersex	*ix*
Male-specific Fruitless proteins	Fru^M
Mosaic analysis with a repressible cell marker	MARCM
Membrane-bound mouse lymphocyte marker CD8	mCD8
mini-white	*mw*
nuclear Green Fluorescent Protein	nGFP
nuclear Red Fluorescent Protein	nRFP
octopamine receptor in the mushroom bodies	OAMB
Olfactory receptor neuron	Orn
Phalloidin	Phall
reaper	*rpr*
reversed polarity	*repo*
Serrate	*Ser*
Sex-lethal (gene)	*Sxl*

Sex-lethal (protein)	Sxl
Sex peptide	SP
Sex peptide receptor	SPR
Stable insulated nuclear enhanced GFP	Stinger
Stubble	*Sb*
teashirt	*tsh*
Third multiple of singsong	*TMS*
transformer (gene)	*tra*
Transformer (protein)	Tra
transformer-2 (gene)	*tra-2*
Transformer-2 (protein)	Tra-2
Tubby	*Tb*
Upstream Activating Sequence	UAS
white	*w*
Wild-type	WT
Yeast Transcriptional Activator GAL4	GAL4
yolk protein	*yp*
Zinc finger	Znf

Measurements

Base pair	bp
Centimetre	cm
Centripetal force = to gravitational acceleration	g
Decibel	dB
Degrees Centigrade	ºC
Hour	hr
Hertz	hz
Kilobases	kb
Melting temperature	Tm
Microgram	µg
Microlitre	µL
Micrometre	µm
Micromolar	µM
Milligram	mg
Millilitre	mL
Millimetre	mm
Millimolar	mM
Millisecond	ms
Minute	min
Molar	M
Nanogram	ng
Nanometre	nm
Optical density	O.D.
Second	sec or s

Behavioural Parameters

Courtship index	CI
Cycles per pulse	CPP
Interpulse interval	IPI
Mean pulses per train	MPPT
Proboscis extension response	PER
Pulse trains per minute	PTPM
Song index	SI
Song bouts per Minute	SBPM
Wing extension index	WEI

Chemicals

2' Deoxyribonucleic acid	DNA
Bovine serum albumin	BSA
Carbon dioxide	CO_2
Horseradish peroxidase	HRP
Messenger RNA	mRNA
Phosphate buffered saline	PBS
PBS with Triton-X	PBT
PBS with Triton-X and 5% SNS	PTN
PBS with Triton-X and 0.1% BSA	PAT
Ribonucleic acid	RNA
Ribonuclease A	RNaseA
Normal serum (Sheep or Goat)	SNS or GNS
Tetramethylrhodamine B isothiocyanate	TRITC

Miscellaneous

Analysis of variance	ANOVA
Bacterial artificial chromosome	BAC
Cuticular hydrocarbon	CH
Enteroblast	EB
First, second or third larval molt stage	L1, L2 or L3
Heat shock	hs
Intestinal stem cell	ISC
Look up table	LUT
Neuroblast	NB
Overnight	O/N
Polymerase chain reaction	PCR
P transposable element	P-element
Room temperature	R/T
RNA interference	RNAi
Standard deviation	s.d.
Standard error of the mean	s.e.m.
Tagged image file format	.tif or .tiff

1 Introduction

1.1 Why behaviour?

How we process information about, and respond to, the physical world exists as one of the most profound questions for a multitude of investigative disciplines. Yet, in higher order organisms at least, "…learning and many other higher processes are secondary modifications of innate mechanisms, and … therefore a study of learning processes has to be preceded by a study of the innate foundations of behaviour" (Tinbergen, 1951). This approach to the investigation of behaviours may be summed up in Tinbergen's four questions of ethology:

- Function (adaptive significance)?
- Causation (mechanism)?
- Development (genetics/ontogeny)?
- Evolution (phylogenetic history)?

Behaviour may be seen as the effect of any sensory input, which then results in some form of organismal response. However this broad description may encompass virtually any action by an organism within its environment. For the purpose of this study I would define innate behaviours as those stereotypical patterns of action(s) that may then be defined and in some way quantified, governed solely by the organism's nervous system, which without prior experiential influences occur in direct response to either internal or external stimuli. That these behavioural outputs are fundamentally derived from underlying genetic determinants is implicit in the idea of the heritability of stereotypical/innate behavioural responses. Humans, as higher order animals, may be able to override innate behavioural drives but these drives will still be present, hard wired into us by our genetic make-up. It should be noted that behaviours in general are rarely under the direction of a single gene, but rather are more usually exemplified by polygenic determinants. Molecular genetics and systems biology can, through the application of a mechanistic approach to Tinbergen's questions, attempt to establish the 'innate foundations of behaviour', that is the complete process by which a behavioural output is generated once the stimuli is received. Initially this

requires the identification of species-specific candidate genes (those which appear to influence behaviour in one species, and are therefore likely to influence similar behaviours in other species) (Fitzpatrick et al., 2004). Once a gene (or genes), has (have) been identified as involved in the modulation of a specific behaviour then this provides a gateway into understanding cellular function, allowing us to attempt to understand how, when and in what context the gene might function in the whole organism to contribute to towards the determination of a specific behavioural output (or outputs). Starting from initial sensory processing of the stimuli, to gene response(s) and on through to the regulation of the animal's physiology or direction of motor response(s) by the animal's nervous system. The potential for both short- and long-term changes that may occur in any external environment, coupled with the requirement of an organism to maintain its own 'internal environment' (that is a homeostatic metabolism), necessitates that an organism, and therefore its behaviours, must be responsive to change. The implication being that the genetic substrates that ultimately form the basis for governing an organism's behaviours must also maintain a balance between specifying a stereotypical response while also ensuring that an underlying plasticity exists to allow response to change. Therefore understanding the processes which occur to form the stereotypical behavioural response in an organism may then allow us insight into how changing external environmental pressures on, and/or modification of, the original ancestral genetic processes may then result in the creation of potential speciation factors (Figure 1.1).

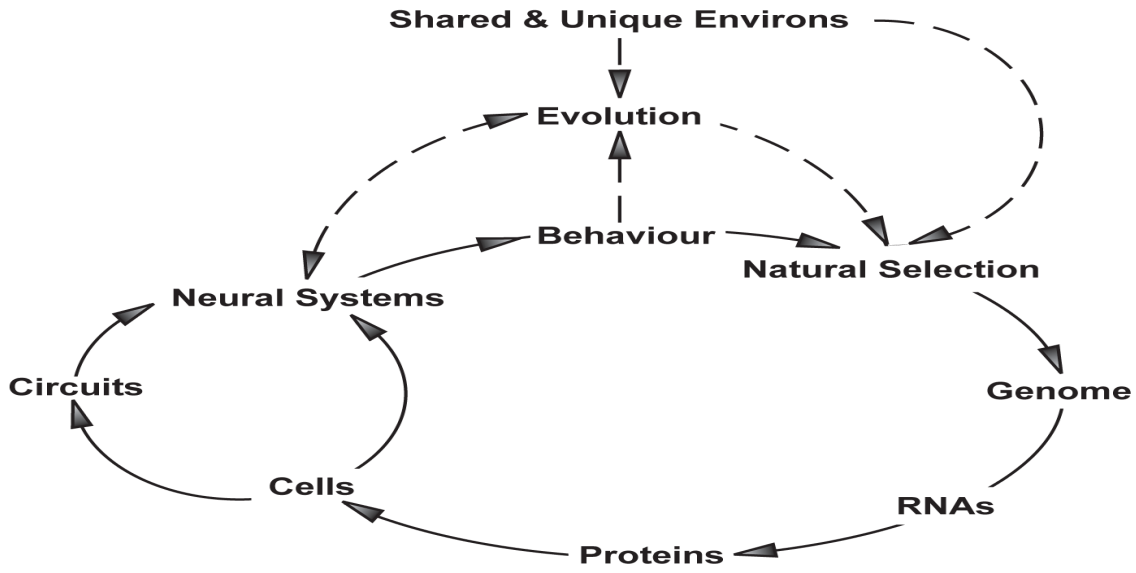

Figure 1-1 Genes to brains to behaviour in higher order animals.
Schematic of the relationship between an organism's genome, physiology and how this is then manifested as a behavioural output (black arrows), and the concomitant direct and indirect factors that might modify this output (dashed arrows).

Finally If how behavioural outputs are governed at a molecular level provides insight into the underlying genetic principles that determine nervous system development, then it follows that sex-specific behaviours provide us with understanding as to how a sexually dimorphic nervous system may be formed, and how this is coordinated with the development and maintenance of a dimorphic organism as a whole. The basis for the investigations that comprise this thesis were dependent upon the creation of a transgenic tool by Elizabeth Rideout as part of her doctoral thesis "Investigating the neurobiological basis underlying the sex-specific production of courtship song in *Drosophila*: the roles of sex determination genes *fruitless* and *doublesex*" (2008) undertaken in the lab of Dr. Stephen Goodwin at the University of Glasgow. Many of the findings derived from the investigations described within the thesis presented here already form the basis for a publication (Rideout et al., 2010). However in this introduction I would wish to merely provide the background information, from historical studies to recent investigative findings, needed to understand the development and genetic context of this transgenic tool. Retaining the actual description and findings of the research associated with this novel transgene to the experimental chapters that follow.

1.2 Courtship behaviours in the model organism Drosophila

Drosophila melanogaster's place as a model organism for genetic study has been established through its use in investigations over the past ~100 years with its use as a model for the study of neurogenetics, once seen as a heretic idea, now firmly entrenched (Bellen et al., 2010; Vosshall, 2007). Our ability to functionally dissect the genetic processes that determine the development of the fly, from egg to adult, has been made possible by the continuing creation, and modification, of a vast range of genetic tools. This has included the identification of visible genetic markers, creation of balancer chromosomes, the ability to carry out mutagenic screens and the use of *P*-element transformation techniques to generate a range of transgenic animals. More recently the sequencing of the *melanogaster* genome, coupled with the development of higher throughput molecular approaches such as microarrays and the various "-omics" in conjunction with more powerful bioinformatic data analyses tools, has ensured that these techniques have been advanced again, allowing for more systemic/holistic analyses of the complete

genome and its products throughout development. This intensity of research and sophistication of investigative processes has also been applied to the study of behaviours (both ‘simple’ and ‘complex’) throughout the life cycle of the fly. One such complex behaviour in *Drosophila* that lends itself well to investigations utilising the range of genetic tools alluded to, due to the stereotypical and easily assayed dimorphic behavioural outputs displayed, is courtship.

1.2.1 Drosophila male courtship behaviours.

Drosophila courtship is largely the remit of the male (the female apparently restricting her actions to receptive, or unreceptive, responses to the male’s forays), and consists of a series of independent, but inter-related, behaviours designed to achieve copulation between the male and female resulting in successful fertilisation of the female’s eggs (Figure 1.2) (Billeter et al., 2006a; Dauwalder, 2008; Dickson, 2008; O'Dell and Goodwin, 2010). The male, in response to visual and olfactory stimulation, will orient on, and follow, a target female (Cook, 1979; Markow, 1987; Tompkins et al., 1983). He will ‘tap’ the female with his forelimbs, presumably gaining non-volatile pheromonal cues from the female (Amrein and Thorne, 2005; Greenspan and Ferveur, 2000; Manning, 1959; Thorne et al., 2005; Venard et al., 1989). Next the male extends and vibrates the wing most adjacent to the female, generating a species-specific courtship song. Courtship song in *melanogaster* is a male-specific behavioural output and consists of “sine-” and “pulse-” song components (Figure 1.2) (Ewing and Bennet-Clark, 1968). Sine-song is a low frequency humming sound with a carrier frequency of approximately 160 Hz in *melanogaster* produced by beating the wing in a manner similar to that seen in flight, which is thought to increase female receptivity (Figure 1.2) (von Schilcher, 1976a, b). Pulse-song is a series of monocyclic pulses, with an intra-pulse carrier frequency of approximately 240 Hz in *melanogaster* (Figure 1.2) (Ewing and Bennet-Clark, 1968; Wheeler et al., 1988; Wheeler et al., 1989). The time between consecutive pulses (the inter pulse interval; IPI) in *melanogaster* is approximately 33ms (Bennet-Clark and Ewing, 1967; Ewing and Bennet-Clark, 1968; Kawanishi and Watanabe, 1980; Shorey, 1962) and provides a species-specific parameter to the song (Bennet-Clark and Ewing, 1967; Ewing and Bennet-Clark, 1968; Kyriacou and Hall, 1980; Kyriacou and Hall, 1982; Kyriacou and Hall, 1986; Ritchie et al., 1999). While the sinusoidal cycling of the IPI, with a period of approximately 55-60 s, has also been shown to contribute a species-specific component to the song

output (Bennet-Clark and Ewing, 1967; Ewing and Bennet-Clark, 1968; Kyriacou and Hall, 1980; Kyriacou and Hall, 1982; Kyriacou and Hall, 1986; Ritchie et al., 1999). That the species-specific components of courtship song are important in the identification of conspecific courting males by target females may be demonstrated by the enhanced levels of courtship success when target females are exposed to song with the IPI cycling of their own species, as opposed to either no song, or song with the incorrect species parameters (Kyriacou and Hall, 1982; Ritchie et al., 1999). If these initial behaviours are successful this will cause the receptive female to slow, allowing the male to lick her genitals, presumably gaining further stimulatory non-volatile pheromonal cues (Tompkins et al., 1983). The male will then attempt copulation. The act of copulation in *melanogaster* is one of "intromission-before-mounting", where the male's genitalia must be properly aligned with the female's for successful coupling (Cook, 1977; Coyne, 1985). During attempted copulation, and copulation, the male curls his abdomen under and forward, rearing upwards, thrusting his head under the female's wings, and grasping her body with his fore- and mid-legs. If successful, copulation itself will ensue whereupon the male transfers a complex package of sperm, to fertilise the female, and seminal fluids, which will alter her behavioural state, increasing ovulation rates, locomotor activity and feeding while reducing her receptivity to further competitive courtship attempts (Aigaki et al., 1991; Carvalho et al., 2006; Häsemeyer et al., 2009; Kubli, 2003; Kubli, 2008, 2010; Yang et al., 2009). These behaviours performed by the male are innate, that is a naïve male reared in isolation is still capable of performing the full repertoire of behaviours when introduced to a female. However that does not say that they are not modifiable, as shown by the alteration in courtship levels induced during courtship conditioning experiments (McRobert et al., 2003; Siegel and Hall, 1979; Siwicki et al., 2005).

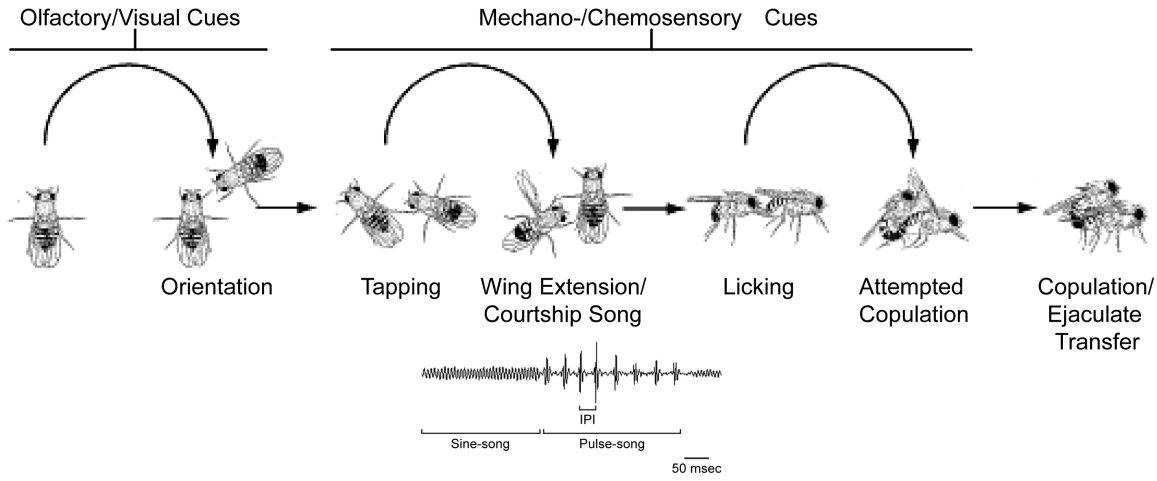

Figure 1-2 Courtship steps performed by a wild-type male *Drosophila* towards a receptive target female.
The male orientates on the target female. The male then taps her abdomen with his foreleg, extends the most proximal wing and generates a species-specific courtship song, licks her genitals with his proboscis, attempts copulation and, if successful, then copulation occurs resulting in the transfer of the ejaculate comprising sperm and seminal fluids. Stimulatory cues that may facilitate courtship behaviours listed above. Male-specific wild-type courtship song trace illustrated below. Sine- and pulse-components, and inter pulse interval (IPI) indicated. Scale bar = 50 msec. Figure adapted from Billeter et al. (2006a).

1.2.2 Drosophila female courtship behaviours

Courtship studies in *Drosophila melanogaster* have almost exclusively focused on the male, as the sequential program of behaviours performed by males are robust and easily quantifiable (Billeter et al., 2006a). The female, by comparison, appears to be largely passive with those female-specific inputs identified to date consisting mostly of subtle rejection behaviours (Connolly and Cook, 1973; Ejima et al., 2001; Spieth and Ringo, 1983). In quantitative terms little is known about what might stimulate these rejection responses or what effects these might then have on the courtship process as a whole. However logically, if the female is to be anything other than an unresponsive participant, she must be in someway actively assessing potential male suitors, not only of species type (*cf.* increased courtship success with the species appropriate courtship song output) but also perhaps of individual fitness, prior to allowing copulation to occur. Presumably forming some assured judgement about her prospective mates via a variety of stimulatory cues, such as audition and pheromonal signaling (Figure 1.2). In some Drosophilids species females exhibit defined acceptance postures, ranging from the female spreading her wings up and out, holding them extended until the male mounts and/or spreading their vaginal plates, which allows, or may even initiate, male attempted copulation (Spieth, 1974; Spieth and Ringo, 1983). Despite these known acceptance postures, there have been few courtship studies assaying

female-specific behaviours compared with those that utilise the act of copulation itself as a measure of female receptivity (Ikeda et al., 1981; Ritchie et al., 1998; Tomaru et al., 1885). This an important consideration in *melanogaster* where, while it has been demonstrated that in response to a courting male receptive females will slow down and cease rejection behaviours, allowing the male to lick her genitals (Spieth and Ringo, 1983), it has also been shown that a persistent male can overcome determined female rejection to successfully copulate (Rideout et al., 2010). However if successful intromission is allowed to occur, the copulating pair will then remain largely stationary (Spieth and Ringo, 1983) and, as stated, the male will then transfer a complex package of sperm, to fertilise the female, and seminal fluids, which will engender a change in the female's behavioural and physiological state. That is increasing the post-mated female's ovulation rates, locomotor activity and feeding, induce upregulation in her innate immune responses, while reducing the female's receptivity to further competitive courtship attempts (Aigaki et al., 1991; Carvalho et al., 2006; Häsemeyer et al., 2009; Kubli, 2003; Kubli, 2008, 2010; Yang et al., 2009).

1.3 The sex determination pathway

Correct manifestation of sexual behaviours is dependent upon the ability to receive, process and respond in a gender appropriate manner to stimuli. This ability to perform sex-specific behaviours therefore also requires the development of a co-ordinated sex-specific anatomy and physiology. The 'complete sexual state' is not merely dependent on the manifestation of physical attributes (both sex- and non-sex-specific). Pivotal to the generation of the appropriate sex-specific behavioural outputs is the development of a sexually dimorphic neuroanatomy. In *Drosophila* this dimorphic nervous system, and the associated sensori-motor effector tissues, is created, and maintained, through the gender appropriate expression of the genes of the sex determination hierarchy (Figure 1.3). Central to the development of the dimorphic nervous system and soma are the transcription factors *fruitless* (*fru*) and *doublesex* (*dsx*), both key genes of the sex determination hierarchy (Figure 1.3) (Billeter et al., 2006a; Christiansen et al., 2002; Cline and Meyer, 1996; MacDougall et al., 1995).

Essentially sex determination in *Drosophila* is determined by the ratio of X to autosomes (X:A) in each cell, activating (in XX females) or repressing (in XY

males) the *Sex lethal* (*Sxl*) gene (Camara et al., 2008; Christiansen et al., 2002). In females the presence of the Sxl protein regulates the *transformer* (*tra*) pre-mRNA, so that an active Tra protein is expressed. The presence or absence of Tra, in conjunction with the non-sex-specific Transformer-2 protein, determines the presence, or form, of both Dsx and Fru proteins, which in turn determine most aspects of the male and female state. Previously *dsx* and *fru* have been defined as heading independent branch points of the sex determination path such that the sex-specific forms of Dsx largely determine male or female somatic morphology outside the nervous system, while the male-specific Fru (Fru^M) proteins determine male sexual behaviour. However it has become clear that these two genes do not work in isolation but rather the complete dimorphic nervous system, and therefore complete wild-type behavioural repertoire, is dependent upon the proper expression of both genes functioning in complement with each other (Billeter et al., 2006b; Kimura et al., 2008; Rideout et al., 2007; Rideout et al., 2010; Siwicki and Kravitz, 2009).

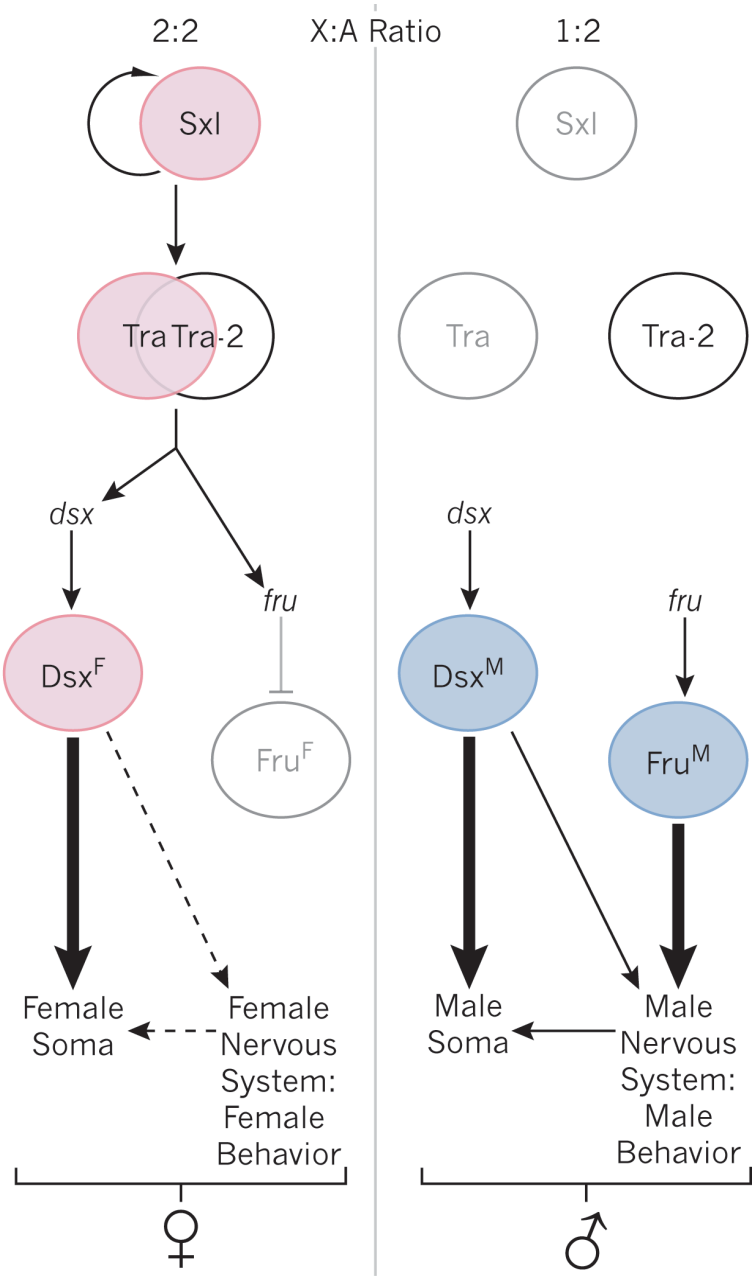

Figure 1-3 Schematic of the sex determination hierarchy highlighting the functional activities of *doublesex* and *fruitless*.
Black lines/bold colours indicate active; grey lines/faded colours indicate inactive or non-functional. Female-specific proteins (pink), male-specific proteins (blue), non-sex-specific proteins (white). *Sex lethal* gene is maintained 'on' in females by positive auto-regulatory splicing of its own pre-mRNA, Sex Lethal (Sxl) protein also controls female-specific splicing of *transformer* pre-mRNA to generate the Transformer (Tra) protein. Tra in conjunction with Tra-2 regulates the splicing of *doublesex* (*dsx*) and *fruitless* (*fru*) so that a functional female-specific form of Doublesex (Dsx^F) protein is formed and the female-specific *fru* pre-mRNAs are not translated into a functional Fruitless (Fru^F) protein. Dsx^F largely determines female somatic structures and external morphology, though has also been shown to impact on female specific behaviours arising from the nervous system (indicated by dashed arrowed line). In the absence of Tra, *dsx* and *fru* are spliced into their functional male Dsx^M and Fru^M proteins. Dsx^M largely determines male somatic structures and external morphology, while Fru^M is required for expression of male behaviours arising from the male nervous system. However Dsx^M has also been shown to be required for the complete organization/complement of some Fru^M expressing neurons and so is also involved in determining the male nervous system. Conversely Fru^M's activity within male-specific structures of the peripheral nervous system may also indicate a function for *fru* within the developing soma of the fly as with the induction of the male-specific muscle of Lawrence. *dsx* appears above *fru* in the linear schematic as it's expression precedes Fru^M's. Figure adapted from Billeter et al. (2006a).

1.4 fruitless

fruitless, or '*fruity*' as it was originally denoted, was first identified in an X-ray mutagenic screen as a behavioural male-sterile mutant by Kulbir Gill (1963). However its importance wasn't fully understood till the Hall lab began investigating the behavioural phenotypes manifested by, and the underlying (neuro-) genetics of, this mutant in the late seventies (Hall, 1978). *fru* is a complex pleiotropic gene with two separate functions; one for male sexual behaviour; the other essential for the viability of both sexes (Fig. 1.4) (Anand et al., 2001; Billeter et al., 2006b; Demir and Dickson, 2005; Dornan et al., 2005; Goodwin et al., 2000; Ito et al., 1996; Lee and Hall, 2001; Lee et al., 2001; Manoli et al., 2005; Ryner et al., 1996; Song et al., 2002; Song and Taylor, 2003; Villella et al., 1997). *fru* has so far only been demonstrated to exist within insect lineages (existing in such diverse organisms as Tribolium, Apis, and Musca) with the mechanism of sex-specific splicing and isoform choice shown to be conserved between *Drosophilidae* and Mosquito, animals separated by ~250M years of evolution (Clynen et al., 2011; Davis et al., 2000; Gailey et al., 2006; Gailey et al., 2000). All Fru proteins contain a common BTB N-terminal domain capable of protein:protein interactions and, through alternative splicing, one of four C-terminal Zinc-finger (Znf) DNA binding domains (A-D) (Billeter et al., 2006a; Goodwin et al., 2000; Ito et al., 1996; Ryner et al., 1996; Usui-Aoki et al., 2000). Transcripts from the most distal of the four *fru* promoters, *fru*-P1, in the absence of the Tra/Tra-2 protein complex, default splices to encode the male specific proteins (the Fru^{M} isoforms; Fru^{MA}, Fru^{MB}, and, Fru^{MC}) (Billeter et al., 2006a; Goodwin et al., 2000; Ito et al., 1996; Ryner et al., 1996; Usui-Aoki et al., 2000). These differ from the proteins produced by the non-sex specific promoters P2, P3 and P4 (the Fru^{Com} isoforms; Fru^{ComA}, Fru^{ComB}, Fru^{ComC}, and Fru^{ComD}) by the inclusion of 101 amino acids upstream of the common BTB domain. Fru^{M} proteins first appear at the beginning of metamorphosis, coinciding with the remodelling of the CNS during which the behavioural repertoire switches from foraging larva to mature adult (Lee et al., 2000).

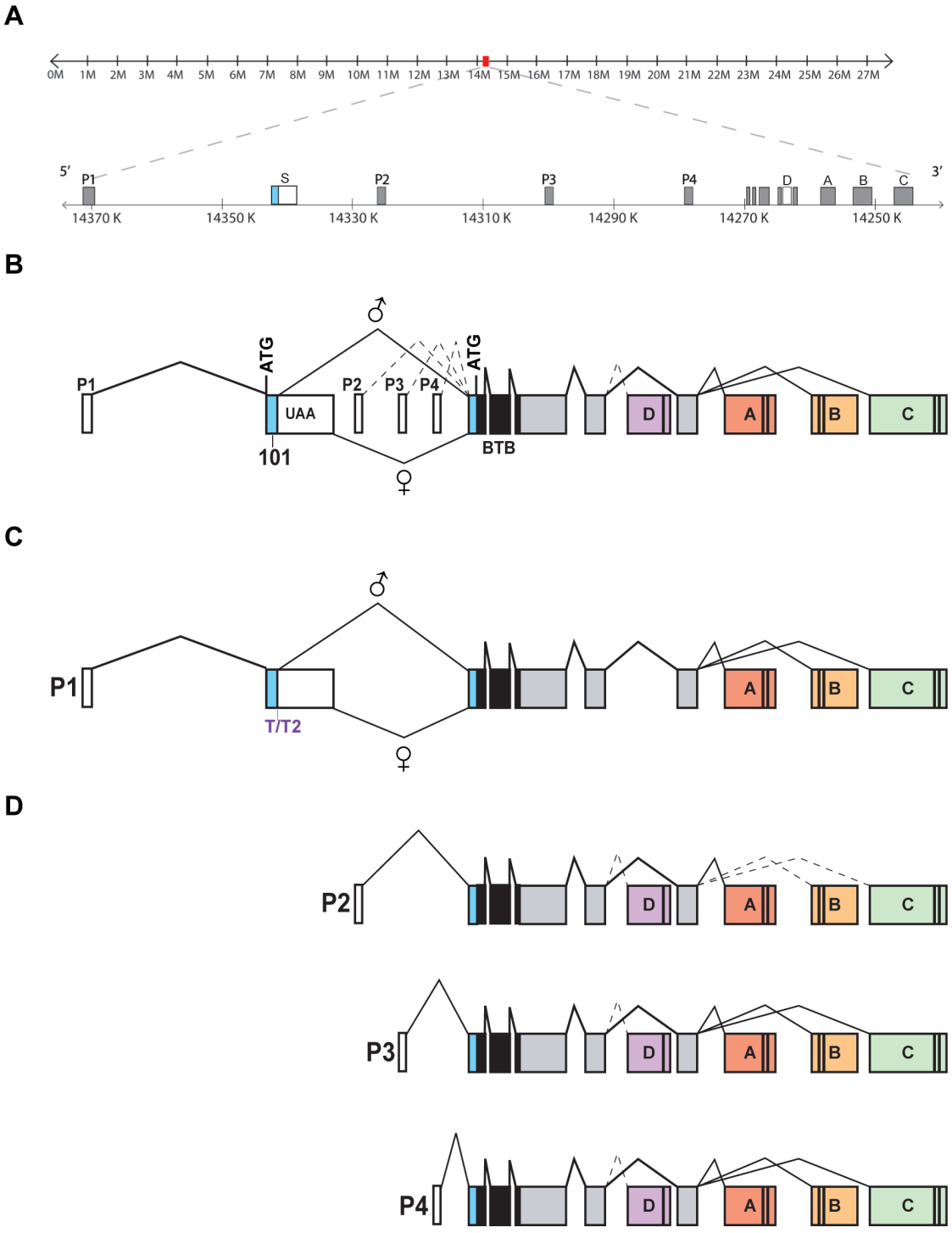

Figure 1-4 Schematic representation of the *fruitless* locus and its predicted transcripts. (A) Right arm of the third chromosome, *fru* locus indicated by the red box (M=megabases). Expanded region of the *fru* locus below, spanning ~150 kb at cytogenetic location 91A7-91B3. Both sex- and non-sex-specific exons represented (grey boxes). Sex specifically spliced exon represented by blue/white box (S). (B) Schematic of *fru* gene, (C) male and female P1 sex-specific predicted transcripts and (D) P2-P4 non-sex-specific predicted transcripts. Arrows indicate transcriptional start sites, non-coding exons (white boxes). Translational start sites (blue boxes). Common BTB domain (black boxes). Grey and coloured boxes sex- and non-sex-specific coding exons. Transcripts from the P1 promoter undergo sex-specifically splicing at the 5' end in the Sex specifically spliced exon by the female specific splice factor Tra in conjunction with the non-sex-specific splice factor Tra-2 (T/T2). P1 male-specific transcripts include an additional 101 amino acids (101). P1-P4 transcripts incorporate through alternative splicing, one of four C-terminal Znf DNA binding domains (A-D). Figures adapted from E. Rideout (unpublished) and Billeter and Goodwin (2004).

Disruption of the male-specific *fru* transcripts results in a concomitant global reduction in the levels of Fru^M expression, absence of expression in subsets of Fru^M-expressing neurons, or absence of specific Fru^M isoforms (Anand et al., 2001; Billeter et al., 2006b; Demir and Dickson, 2005; Dornan et al., 2005; Goodwin et al., 2000; Ito et al., 1996; Lee and Hall, 2001; Lee et al., 2001; Manoli et al., 2005; Ryner et al., 1996; Song et al., 2002; Song and Taylor, 2003; Usui-Aoki et al., 2000; Villella et al., 1997). That *fru* is pivotal to the regulation of male courtship behaviour is demonstrated by the fact that this reduction of expression levels may be directly correlated with a variety of courtship defects; including severe reductions or absence of courtship towards females, failure to produce the pulse-song component of courtship song, increased levels of inter-male courtship, and failure to attempt copulation, as well as the absence of a male-specific abdominal muscle, the muscle of Lawrence (MOL) (Baker et al., 2001; Billeter and Goodwin, 2004; Billeter et al., 2006a; Billeter et al., 2006b; Demir and Dickson, 2005; Dornan et al., 2005; Gailey and Hall, 1989; Gailey et al., 1991; Goodwin et al., 2000; Ito et al., 1996; Manoli and Baker, 2004; Manoli et al., 2005; Ryner et al., 1996; Usui-Aoki et al., 2000; Villella et al., 1997). Although copulation can occur in certain *fru* mutant combinations, these animals often fail to transfer sperm and seminal fluids. Most *fru* mutants are sterile as a result of a combination of these defects. Further support that Fru^M proteins are critical for male courtship has come from the observation that a female constitutively expressing Fru^M (a *'she-male'*) can perform the early steps of the male courtship ritual, though generally at sub-normal levels, that is: initiation, orientation, following, tapping and wing extension towards wild-type females, although no recognisable song is produced and these females never attempt copulation (Demir and Dickson, 2005; Manoli et al., 2005; Rideout et al., 2007). The distribution of Fru^M proteins is highly suggestive, especially with respect to modulation of the underlying behavioural circuitry (Figure 1.5). They are restrictively expressed in subsets of sensory and motor neurons within the adult males' central and peripheral nervous systems (CNS and PNS), in ~2000 neurons of the CNS and in sites in the PNS associated with smell, taste and hearing, all of which have been implicated in the regulation of male courtship behaviours (Billeter and Goodwin, 2004; Billeter et al., 2006a; Billeter et al., 2006b; Demir and Dickson, 2005; Lee et al., 2000).

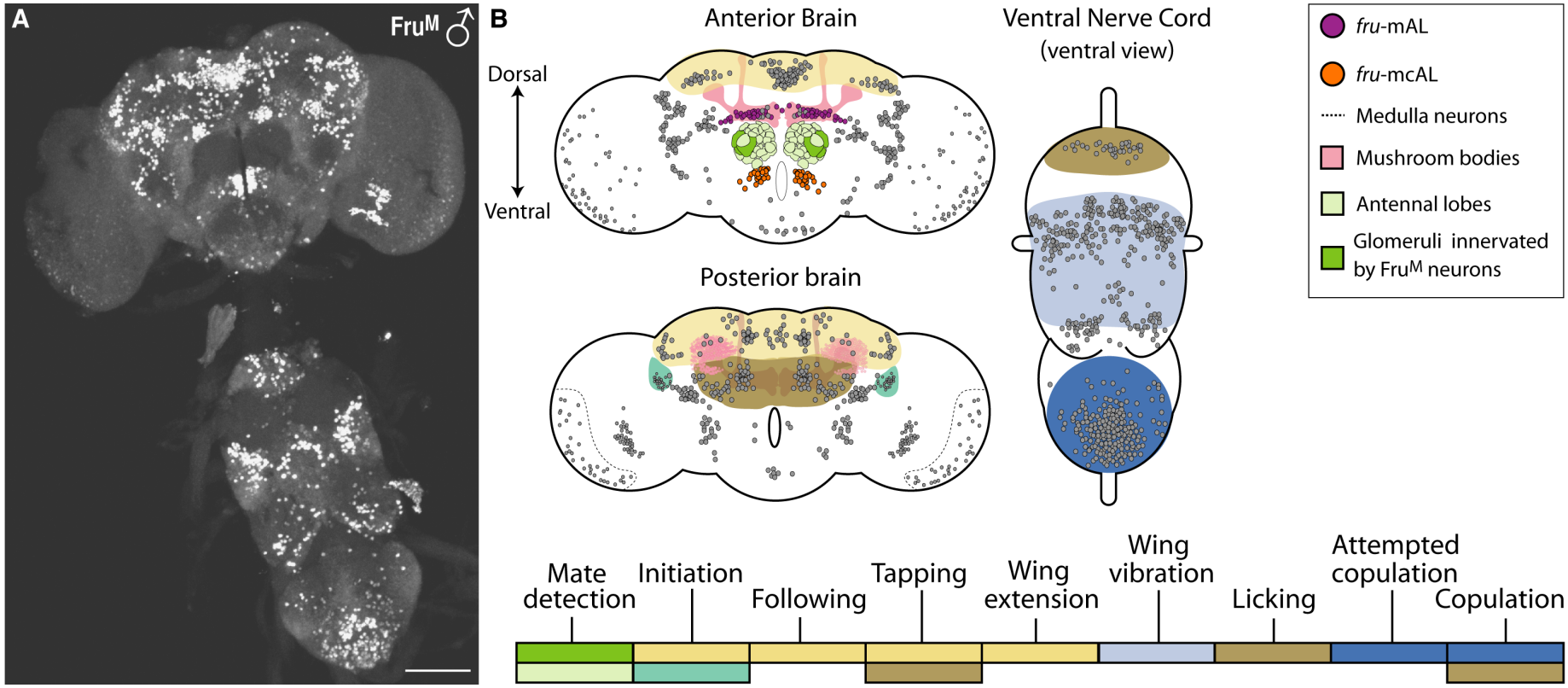

Figure 1-5 Endogenous Fru^M in the adult male CNS.
(A) Endogenous Fru^M expression in a 5 day old adult wild-type male. Ventral view. Scale Bars = 50 µm. Figure taken from Dornan et al. (2005). (B) Cartoon of the overlap of Fru^M-expressing neuronal clusters with neural foci implicated in the modulation of male courtship behavioural outputs. Areas of the adult male CNS associated with the control of specific courtship steps are color-coded and refer to the courtship steps indicated below and to the legend on the right. Fru^M immunoreactivity in neuronal nuclei of the adult male CNS is represented by grey and colored dots. The antennal lobes (light green) are involved in partner discrimination and specific glomeruli (darker green) innervated by Fru^M-expressing odorant receptor neurons are involved in mate recognition. A cluster of cells in the lateral dorsal brain (teal) regulates courtship initiation. The dorsal posterior brain (yellow) is involved in the initiation of courtship, following, tapping, and wing extension. The posterior midbrain (brown) affects licking and copulation. In the ventral nerve cord, the prothoracic ganglion (light purple) is a site associated with the control of tapping; the mesothoracic ganglion (light blue) regulates wing extension and courtship song; and the abdominal ganglion (dark blue) controls attempted copulation and copulation. Figure taken from Billeter et al. (2006a).

This pattern of expression is also important as it highlights anatomical differences that exist between male and female nervous systems (Cachero et al., 2010; Datta et al., 2008; Kimura et al., 2005; Kvitsiani and Dickson, 2006; Rideout et al., 2007; Stockinger et al., 2005; Yu et al., 2010). These differences, both in terms of neuronal numbers and projection patterns, while subtle, still could result in profound dimorphic behavioural outputs. This could be either as a result of intrinsic *fru*-dependent differences, such as in excitability or connectivity within the circuit, where *fru* may function as a transcriptional 'neuromodulator' "blocking out" the dimorphic behavioural program on an extant default circuit. Alternatively *fru* could be acting to control the behavioural circuit extrinsically, that is both males and females possess the circuitry necessary to produce a dimorphic behaviour but only males receive the appropriate input from *fru*-specific 'command neurons'. These two models are not mutually exclusive and indeed there is good evidence for their co-existence (Cachero et al., 2010; Clyne and Miesenböck, 2008; Datta et al., 2008; Dornan and Goodwin, 2008; Kimura et al., 2005; Kvitsiani and Dickson, 2006; Rideout et al., 2007; Stockinger et al., 2005; von Schilcher and Hall, 1979; Yu et al., 2010).

1.4.1 fru is necessary, but not sufficient, for specification of male courtship behaviours

However while *fru* is demonstrably necessary for the specification of male-specific behaviours, it is not sufficient (Demir and Dickson, 2005; Rideout et al., 2007). This may be exemplified by the fact that those male-specific courtship indices performed by females expressing Fru^M are generally performed at subnormal levels with the later steps of courtship never performed at all. That is while these 'she-males' may exhibit appropriate levels of wing extension they do not produce a recognisable courtship song and they never attempt to, or in fact actually, copulate (Rideout et al., 2007). This latter point is not a consequence of the female's anatomy or gravid abdomen precluding the bending necessitated in attempted copulation as earlier sexual mosaic studies had observed animals with complete male CNSs but enlarged/gravid female abdomens still attempting copulation (Hall and Greenspan, 1979). Furthermore, although males null for Fru^M expression show no sexual interest towards females, they are still observed to perform courtship towards other males, evidenced by the occurrence of the anomalous 'chaining' behaviour that occurs when several of these Fru^M-mutant males are

grouped together; indicative of the fact that even without Fru^M expression these males still retain some ability to court. All of this suggesting that further male-specific components are required for formation of the complete adult male behavioural repertoire, requiring the involvement of additional gene expression.

Previous investigations have shown that *tra* mutant females, which express the male-specific isoforms of both *fru* and *dsx*, are able to perform all male-specific behaviours (Bernstein et al., 1992; Kyriacou and Hall, 1980), demonstrating that *tra* must be able to regulate all the downstream events required for courtship behaviour. As previously stated the pivotal genes downstream of *tra* in the SDH are *fru* and *dsx*. It has also been demonstrated that *dsx* expression is not sufficient to specify male-sexual behaviours (Taylor et al., 1994). However it has been shown that males null for Dsx^M perform subnormal levels of courtship behaviours such as wing extension, courtship song, licking and tapping and completely lack the sine-song component of courtship song (McRobert and Tompkins, 1985; Taylor et al., 1994; Villella and Hall, 1996; Waterbury et al., 1999). When you also consider that both isoforms of Dsx have been shown to be expressed in the adult CNS, that Fru^M and Dsx^M co-express within the adult male CNS and that Dsx^M plays a role in the creation of a sexually dimorphic CNS, it would seem obvious to consider *dsx* as a genetic candidate to act alongside Fru^M in the specification of the dimorphic neural substrates underlying the generation of male-specific courtship behaviours (Billeter et al., 2006b; Lee et al., 2002; Rideout et al., 2007; Taylor and Truman, 1992).

1.5 doublesex

Doublesex proteins are part of the Dmrt (*doublesex* and *mab-3*-related transcription factor) family (Raymond et al., 2000; Raymond et al., 1998; Zarkower, 2002). In contrast with *fru*, which has so far only been discovered within insect lineages (Gailey et al., 2006; Salvemini et al., 2010), *dsx* is a more ancient gene being structurally and functionally conserved throughout the animal kingdom (Raymond et al., 2000; Raymond et al., 1998; Zarkower, 2002).

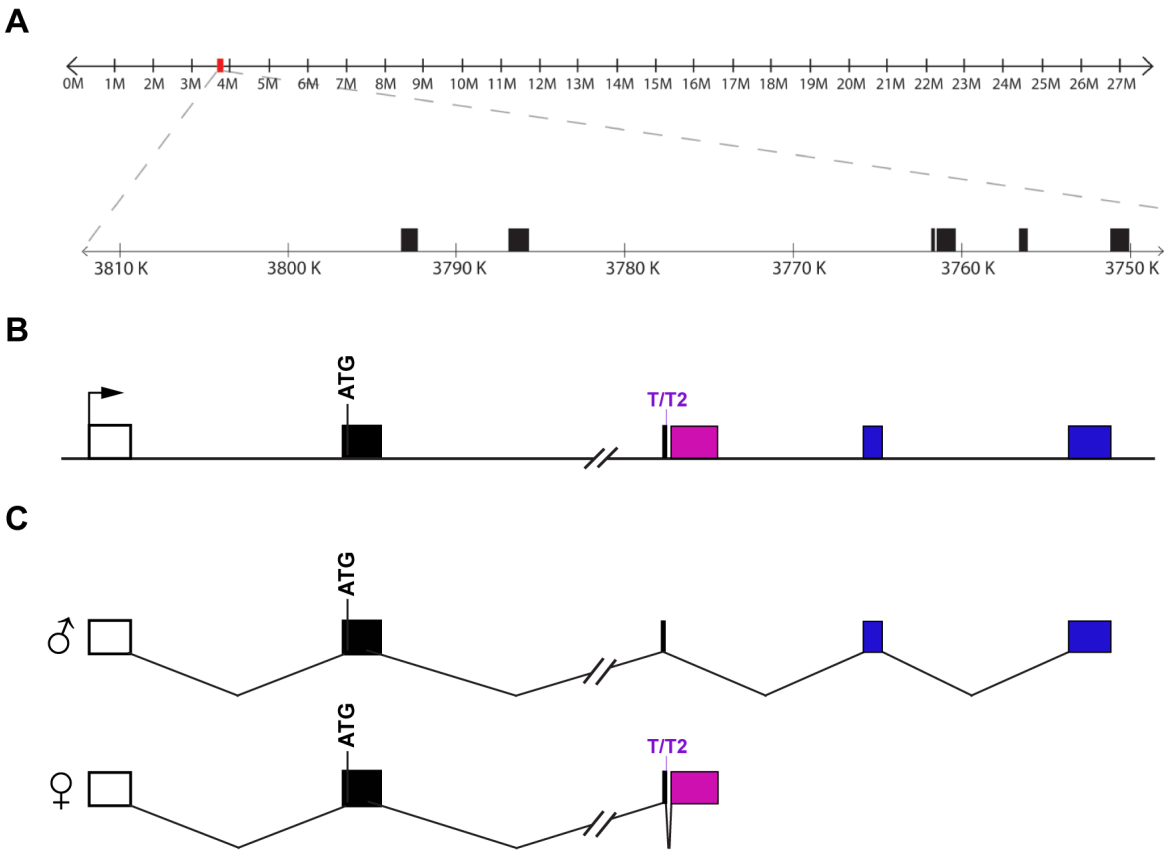

Figure 1-6 Schematic representation of the *doublesex* locus and its predicted transcripts. (A) Right arm of the third chromosome, *dsx* locus indicated by the red box (M=megabases). Expanded region of the *dsx* locus below, spanning ~43 kb at cytogenetic location 84E5-84E6. Both sex- and non-sex-specific exons represented (black boxes). (B) Schematic of *dsx* gene and (C) male and female predicted transcripts. Arrows indicate transcriptional start sites, white box non-coding exon. Black and coloured boxes sex- and non-sex-specific coding exons. Transcripts from the *dsx* locus are sex-specifically spliced at the 3' end by the female specific splice factor Tra in conjunction with the non-sex-specific splice factor Tra-2 (T/T2). Figures adapted from E.Rideout (unpublished) and Rideout et al. (2010).

dsx, as stated, is regulated by *tra* so that in the presence of the Tra/Tra-2 protein complex *dsx* pre-mRNA is spliced into the female form of the protein (Dsx^F), and in the absence of Tra *dsx* pre-mRNA is spliced into the male form (Dsx^M) (Fig. 1.6) (Hoshijima et al., 1991; Ryner and Baker, 1991). Both forms of Dsx are Znf proteins, each transcript is comprised of a common N-terminal domain, containing common domains for DNA binding and mediating protein:protein interactions and, as a result of sex-specific splicing events, divergent C-terminal domains (An et al., 1996; Burtis et al., 1991; Cho and Wensink, 1997; Erdman et al., 1996). The variant C-terminal domains contain sex-specific regulatory elements as well as a homotypic domain that may again mediate protein:protein interactions (An et al., 1996; Cho and Wensink, 1997; Erdman et al., 1996). Generally these isoforms act to both repress genes or paths leading to inappropriate sexual identity in specific tissues, while ensuring genes or paths leading to the appropriate sexual fate are

activated. While wild-type *dsx* functions to determine male and female somatic structure, as stated it has been shown that it is not sufficient to control male sexual behaviour as chromosomally (XX) female flies expressing the male form of *dsx* (Dsx^M), and therefore physiologically male, do not exhibit any male-like behaviours (Taylor et al., 1994). However males lacking *dsx*, which appear intersexual, while able to perform courtship behaviours, do so at greatly diminished levels and fail to generate the sine component of courtship song (Villella and Hall, 1996). This would indicate that *dsx* must figure in the network of genes responsible for determining male sexual behaviour and as such is necessary for the generation of the complete sexually dimorphic nervous system (Billeter et al., 2006a; Billeter et al., 2006b; Kimura et al., 2008; Lee et al., 2002; McRobert and Tompkins, 1985; Rideout et al., 2007; Villella and Hall, 1996). This cooperation of *dsx* in mediation of male courtship behaviour and the sexually dimorphic nervous system has also been indicated by its co-expression with *fru* in a restricted, but highly suggestive, grouping of neuronal clusters and its requirement for the complete organised complement of *fru* expressing neurons in some of these clusters (Billeter et al., 2006b; Rideout et al., 2007; Rideout et al., 2010). Expression of *dsx* begins earlier than *fru*, in the larval stages, however its expression then peaks during the pupal stages at the time when male-specific *fru* expression is at its highest, expression in both genes coinciding with the critical juncture for determination of adult male sexual behaviour (Arthur et al., 1998; Lee et al., 2000; Lee et al., 2002).

1.5.1 doublesex specifies sexual characteristics in male and female soma

As previously described *dsx* in *Drosophila* is central to somatic sex determination and has been shown to be necessary, if not sufficient, for the establishment of both male and female secondary sexual characteristics (Billeter et al., 2006a; Camara et al., 2008; Christiansen et al., 2002; Simpson, 2002). As such, in the absence of the upstream regulators of the *Drosophila* SDH, *Sxl* and *tra*, the male-specific Dsx^M isoform is produced and a default program of male sexual differentiation is followed. This results in a fly with male-specific darkly pigmented dorsal cuticular plates (tergites) on the 5^{th} and 6^{th} abdominal segments, male genitalia and possessing sex-combs, a specialized row of 10-12 densely packed, blunted/thickened and highly pigmented curved mechanosensory bristles orientated longitudinally with respect to the leg, which in *melanogaster* are

restricted to the medial aspect of the distal T1 tarsi of the foreleg (Ahuja and Singh, 2008; Barmina and Kopp, 2007). When *Sxl* and *tra* are active the female-specific Dsx^F isoform is produced, and a female program of sexual differentiation occurs. This results in a fly with a pattern of lighter pigmentation restricted to the dorsal posterior stripe as present on the tergites of both sexes on abdominal segments A2 to A6, female genitalia and, on the area analogous to that of the male sex comb, a row of ~4-5 transverse bristles (TVBs) that are thinner, less pigmented and orientated at ~90º compared to that of the male sex combs (Barmina and Kopp, 2007).

1.5.1.1 Abdominal pigmentation.

In *Drosophila melanogaster* males exhibit darkly pigmented dorsal cuticular plates (tergites) on the 5^{th} and 6^{th} abdominal segments, whereas females display a much reduced pattern of lighter pigmentation restricted to the dorsal posterior stripe as present on the tergites of both sexes on abdominal segments A2 to A6 (Figure 3.5). This dimorphic pattern of pigmentation occurs largely as a consequence of the segmental- and sex-specific expression of *bric-à-brac* (*bab*) under the joint modulation of *dsx* and the homeobox protein, Abdominal-B (Abd-B).

bab has been shown to be capable of repressing pigmentation in segments A2 to A6, however wild type *bab* expression occurs in segments A2 to A6 in females, but only in A2 to A4 in males. This pattern of expression correlates with the repression of pigmentation exhibited in wild type adult male tergites. Abd-B has been shown to be a repressor of *bab* and is expressed in an increasing gradient across segments A5 to A7 (Kopp and Duncan, 2002; Kopp et al., 2000). However as this pattern of expression is monomorphic, Abd-B requires a co-factor to provide sexual specificity. *dsx* mutants are known to exhibit an intersexual phenotype (though as this involves the presence of a greater degree of pigmentation this may be characterised as more ‘male-like’) with respect to the pigmentation of segments A5 and A6 (Jursnich and Burtis 1993; Kopp, Duncan et al. 2000). Latterly it has been demonstrated that *dsx* cooperates with *Abd-B* in determining adult abdominal pigmentation (Jursnich and Burtis, 1993; Kopp et al., 2000; Williams et al., 2008).

This dimorphic pattern of pigmentation therefore results from the combinatorial activities of segmental- and sex-specific factors such that in females Abd-B acting in concert with Dsx^F activates the dimorphic elements of *bab* expression repressing default male pigmentation (Williams et al., 2008). Whereas in males Abd-B activity is overridden by Dsx^M direct repression of these same dimorphic elements in *bab* resulting in male-specific abdominal pigmentation (Williams et al., 2008). In this instance *dsx* is essentially acting as a bimodal molecular switch, oppositely affecting target gene expression in males and females.

1.5.1.2 External genitalia.

The adult terminalia, including the genitalia and analia, originate from the genital disc. This disc, located at the ventral midline, is unique among the imaginal discs as it is unpaired and has a compound origin, being comprised of cells from the embryonic A8, A9 and A10 segments. The cells of these segments form three distinct primordia, each of which possess a defined three-dimensional polarity (anterior/posterior and dorsal/ventral). This polarity again occurs as a consequence of expression of homeotic genes, *abdominal-A*, *Abd-B*, and related genes, such as *caudal* (*cad*), *decapentaplegic* (*dpp*), and *wingless* (*wg*) (Keisman et al., 2001; Sanchez and Guerrero, 2001). The primordia have defined fates, undergoing overt dimorphic development to generate variant morphological tissues in adults of both sexes. Again the homeotic gene *Abd-B*, while monomorphic, appears to act in concert with *dsx*, resulting in a dimorphic pattern of expression. So that in males Dsx^M, in conjunction with Abd-B, positively and negatively regulates *daschund (dac*) expression in the Dpp and Wg domains respectively, whereas in females the opposite occurs with Dsx^F and Abd-B negatively and positively regulating *dac* expression in the Dpp and Wg domains respectively (Keisman et al., 2001; Sanchez et al., 2001; Sancehz and Guerrero, 2001). In the developing male, under the instructive regulation of *dsx*, the male primordium (originating from segment A9) forms the majority of the male genitalia, while the female primordium forms the 8^{th} tergite. In females the female primordium (originating from segment A8), again regulated by *dsx*, develops into most of the female genitalia with the male primordium forming the paravoria. The third primordium derived from segment A10 forms the analia, and is pluripotent, being able to develop into the male or female form of this structure.

In the adult male, the genital plate and, as they are physically attached, the ejaculatory duct and hindgut, undergo a 360º dextral rotation approximately 25-36 into pupal development (Coutelis et al., 2008; Spéder et al., 2006). Abnormally rotated genitalia may occur as a result of aborted rotation, extended rotation, or aberrant plane of rotation (sinistral as opposed to dextral). These phenotypes may be generated via mutations in such diverse genes as the *myosin 31DF* gene that encodes a type ID unconventional myosin, or in *spin*, a novel rotation-specific allele of the *Fasciclin2* (*Fas2*) gene (Adam et al., 2003; Spéder et al., 2006). Neither of these genes appears to be expressed sex-specifically, though their effects clearly imply some male-specific modulation of expression. Nor is there any real indication of interaction with genes of the sex determination hierarchy, though $Fas2^{spin}$ rotation defects are linked to an abnormal endocrine function and an elevated level of juvenile hormone, which is involved in Dsx^F mediated regulation of yolk proteins (Bownes, 1994). However it may be telling that abnormally rotated genitalia are a phenotype common to *tra*, *dsx* and *fru* mutants (Billeter et al., 2006b; Butler et al., 1986; Waterbury et al., 1999), perhaps indicative that factors regulating this process may also be modulated by genes of the sex determination hierarchy (Arbeitman et al., 2010).

Adding a further level of complication to this cascade of development is the expression of non-sex-specific genes with pleiotropic functions that may play instructional roles in sex determination/differentiation via sexually differential levels of expression, or through interaction with, or modulation by, genes of the sex determination hierarchy. Two genes, *branchless* (*bnl*) encoding the fibroblast growth factor (FGF) and *breathless* (*btl*) encoding a fibroblast growth receptor (FGR) are both expressed male-specifically in two bilaterally symmetrical groups of cells adjacent in the male genital disc (Ahmad and Baker, 2002). Dsx^M induced FGF expression has the effect of actively recruiting FGR cells to migrate to the genital disc where they form a novel clonally distinct compartment, which gives rise to the paragonia and vas deferens. In females, expression of Dsx^F represses FGF expression such that there is no recruitment of FGR cells into the genital disc and therefore no development of male-specific structures. Dsx mutants, in which *bnl* is expressed in both males and females, can cause the development of an extra pair of paragonia in males due to ectopic expression of *btl* in the female primordium (Ahmad and Baker, 2002; Hildreth, 1965). This would seem to imply that Dsx^M not only has an instructive role in specifying development of these male-

specific structures, but also a role in regulating where expression of the morphogenetic signal occurs.

In females *intersex* (*ix*) and *hermaphrodite* (*her*) are non-sex-specific genes whose effects are generally manifested in a female-specific manner. *ix*, a putative transcriptional activator, appears to be an obligate partner of Dsx^F binding directly to the N-terminal tail (Chase and Baker, 1995; Christiansen et al., 2002; Garrett-Engele et al., 2002; Waterbury et al., 1999). The effects of disruption of *ix* have been described as entirely female-specific; females appearing intersexual (*cf. dsx* mutant females, though in *ix* mutant females the masculinization effects are less overt), while *ix* mutant males appear normal (Baker and Ridge, 1980; Chase and Baker, 1995). However there is some indication that *ix* expression also impinges on male development, *ix* mutants demonstrating a reduced level of male courtship which may occur in conjunction with, or as a consequence of, alteration in sex-comb morphology and genital bristle morphology (Acharyya and Chatterjee, 2002; McRobert and Tompkins, 1985).

Disruption of *her*, a putative transcription factor encoding a Znf, results in mainly female-specific effects (Pultz et al., 1994). This gene typifies the complexity involved in regulation of adult dimorphic features. *her* has both maternal and zygotic components involved in sexual determination and differentiation (Pultz and Baker, 1995; Pultz et al., 1994). The zygotic non-sex-specific expression of *her* has been shown to function in conjunction with *dsx* in the female, its activity repressed in males by expression of Dsx^M (Li and Baker, 1998a; Li and Baker, 1998b; Pultz and Baker, 1995; Pultz et al., 1994). Her has also been shown to operate in conjunction with Dsx^F to modulate sexual differentiation in abdominal pigmentation and in the bristles of the foreleg and terminal tergites, but male differentiation of these tissues does not require Dsx^M directed suppression of Her function (Li and Baker, 1998a; Li and Baker, 1998b; Pultz and Baker, 1995; Pultz et al., 1994). Some very subtle alteration of dimorphic tissues, *e.g.* extra bristles on the 6^{th} sternite and, again tellingly, rotated genitalia, have also been observed in *her* mutant males, though the occurrence of this as a consequence of alteration of segmental identifiers, rather than representing a true intersexual phenotype, may not be ruled out (Pultz and Baker, 1995; Pultz et al., 1994).

1.5.1.3 Sex Combs

The sex combs are a male-specific structure consisting of a specialized row of 10-12 densely packed, curved, blunted/thickened and highly pigmented mechanosensory bristles orientated longitudinally with respect to the leg, which in *Drosophila melanogaster* are restricted to the medial aspect of the distal T1 tarsi of the foreleg (Ahuja and Singh, 2008; Barmina and Kopp, 2007). In females the analogous area of the distal T1 tarsi of the foreleg contains a row of ~4-5 transverse bristles (TVBs) that are thinner, less pigmented and orientated at ~90º compared with the males sex combs (Barmina and Kopp, 2007). These structures arise from a set of precursor bristles present in both sexes (Barmina and Kopp, 2007; Tokunaga, 1962). The sex combs have been shown to facilitate copulation and increase copulatory success in *D. melanogaster* (Ng and Kopp, 2008). It has been speculated that they may achieve this by performing a mechanical role in allowing males 'precision' grasping of the female's abdomen and perhaps in spreading the female's wings (Cook, 1977; Coyne, 1985; Spieth, 1952). This maybe of importance as the process of copulation in *D. melanogaster* is one of "intromission-before-mounting", where the male's genitalia must be properly aligned with the female's for successful coupling (Cook, 1977; Coyne, 1985). As *D. melanogaster* receptive females, while generally quiescent, are not completely still this requires the male to have some mechanical assurance that proper alignment of the genitalia has occurred (Cook, 1977; Coyne, 1985). Alternatively the morphology of the sex combs may affect the female's decision as to the fitness of the courting male (Markow et al., 1996; Ng and Kopp, 2008).

Sex comb development is under the control of the sex determination hierarchy, demonstrated by the fact that in experiments where the male foreleg has been feminised by ectopic expression of *tra* no sex combs are formed (Ng and Kopp, 2008) and that *dsx*-null mutants appear to possess a sex comb structure that is intermediate between males and females in bristle number, morphology and orientation (Baker and Ridge, 1980; Steinmann-Zwicky et al., 1990) while global expression of Dsx^M using a heat-shock promoter fusion construct results in transformation of much of the bristles on all legs in both sexes, with the most complete effects visible in the basitarsal areas (Jursnich and Burtis, 1993). This determination and differentiation by the sex determination hierarchy of tissues to form, or not, the sex comb is cell autonomous (Baker and Ridge, 1980). However

the subsequent orientation of these bristles is dependent upon the number/ratio of male versus female bristles present in the row; implying that there exists also a non-cell autonomous interaction between the bristles present, providing sex-specific identifiers to determine sex comb positional morphology (Baker and Ridge, 1980).

Restriction of the sex combs normally to the distal T1 tarsi of the male foreleg demonstrates that, apart from the requirement for male-specific determinants, segmental and patterning identifiers (along the proximal-distal axis and restricted to the prothoracic, rather than meso- or metathoric, legs) are essential for proper sex comb formation. Again interaction between the dimorphically expressed genes of the sex determination hierarchy and monomorphically expressed patterning genes *engrailed* (*en*), *Polycomb* (*Pc*), *extra sex combs* (*esc*), and *bab* are key to the regulation of the differentiation and determination of tissues in males and females, and the restriction of the sex combs to males (Couderc et al., 2002; Godt et al., 1993; Steinmann-Zwicky et al., 1990; Struhl, 1982).

en, whose expression in the legs is restricted to the foreleg discs in males and females, acts to negatively regulate sex comb formation such that loss of function results in ectopic sex comb formation on the foreleg (Couderc et al., 2002; Godt et al., 1993). *Pc*, *esc*, and *bab*, which again are expressed monomorphically but this time in all leg discs, act to negatively regulate sex comb formation such that loss of function mutations can result in ectopic sex comb formation on all legs (Couderc et al., 2002; Godt et al., 1993). Importantly while these ectopic sex combs are rarely (if ever) complete, they appear only on the distal portion of the tarsi and are restricted to males (Couderc et al., 2002; Godt et al., 1993; Steinmann-Zwicky et al., 1990).

The homeotic gene *Sex combs reduced* (*Scr*) is unusual in that it is dimorphically expressed. Expression is restricted to the area corresponding to sex comb development in males in the prothoracic leg alone but not in the coincident area in females (Barmina and Kopp, 2007). Sex combs are entirely absent in *Scr*-null clones, while *Scr* hypomorphs demonstrate a significant loss in sex comb formation (Barmina and Kopp, 2007; Struhl, 1982). Ectopic expression of *Scr* results in formation of additional sex combs, but again only in the distal portion of

the tarsi and only in males. It should also be noted that these ectopic sex combs are not complete and fail to completely rotate (Barmina and Kopp, 2007).

That sex combs never develop in females, either through the over-expression of *Scr* or through loss-of-function mutations in *en*, *Pc*, *esc* and *bab* indicates that additional sexual identifiers (i.e. *dsx*) are necessary to induce sex comb formation (Barmina and Kopp, 2007; Couderc et al., 2002; Godt et al., 1993; Steinmann-Zwicky et al., 1990). It is clear that Dsx^M acts in a positive regulatory manner to induce sex comb formation (Barmina et al., 2005; Jursnich and Burtis, 1993; Ng and Kopp, 2008; Waterbury et al., 1999) but there is also some indication that Dsx^F can act in a negative manner to repress sex comb formation, though this is effectively masked by direct competition of endogenous Dsx^M expression (Waterbury et al., 1999).

1.5.1.4 Summation

As transcription factors, the sex-specific isoforms of Dsx have been shown to act as a bimodal molecular switch, exerting opposite effects on target gene expression in males and females. Examples of this have been shown for both the *Yolk protein* (*Yp*) genes, and the *bab* gene. Dsx^F activates *Yp* genes exclusively in the female fat body, whereas Dsx^M represses their transcription (reviewed in Bownes, 1994). Similarly, in females the Hox protein Abd-B and Dsx^F activate *bab* expression, repressing default male pigmentation; whereas in males Dsx^M directly represses *bab*, resulting in male pigmentation (Williams et al., 2008). In comparison, Shirangi et al. (2009) identified the *desaturaseF* (*desatF*) gene, which encodes an enzyme involved in the production of sexually dimorphic pheromones, as a novel Dsx^F target. Although in this case Dsx^M has no apparent regulatory role, demonstrating the possibility for alternative mechanisms of gene regulation such as the requirement for *dsx* in only one sex for differential, and therefore sex-specific, gene expression (Goldman and Arbeitman, 2007; Shirangi et al., 2009). In effect the generation of the complete morphological sexual state is dependent on a complex development program of independent and inter-dependent genetic factors, both sex- and non-sex-specific, acting both in a cell autonomous and non-autonomous manner. Our understanding of how this dimorphic program is effected in the adult fly has to date largely been dependent upon global over-expression and mutant analyses of genes identified to be involved in these paths. This limits

the ability to interpret any effects observed, as anomalies in development may occur in the dimorphic program of development through a variety of mechanisms; through ectopic expression of genes of the sex determination hierarchy spatially, in cells or tissues not usually expressing sexual identifiers; through inappropriate temporal expression in cells or tissues which may, or may not, express sexual identifiers; through inappropriate expression of positional identifiers; or through impingement or activation of unrelated functions of the pleiotropic genes involved in these paths. Indeed non-specific over-expression of Dsx^{M} has been shown to result in lethality (Jursnich and Burtis, 1993). Targeting the *dsx* locus would allow the restrictive manipulation of *dsx*-expressing cells, with the subsequent assessment of any affects on the development of secondary sexual characteristics in both males and females confirming the efficacy of the transgenic tool to reiterate known functions of *dsx* while gaining further insight into how these morphogenic programs might then operate.

1.6 Neurobiological dissection of behavioural substrates

1.6.1 General neuro-anatomy

The *Drosophila* CNS is formed from several nerve centres, or ganglia, comprised of a cortex or ‘cell body rind’ (CBR) and neuropil. The CBR is a layer formed from the cell bodies of neurons and surface- or rind-associated glia. The neurons of the CBR are comprised of differing sub-classes or -types of neurons, though these may essentially be divided into two major classes; the interneurons, which contribute solely to the synaptic complexity of the CNS itself; and the efferent neurons whose dendrites and cell bodies lie within the CNS but whose axons extend outwith the CNS to peripheral targets. The neuropil forms the inner part of the brain and contains neural fibres and synaptic arborisations, as well as neuropil-associated glial cells. The neuropil can be categorized into two types; the synaptic neuropil formed from neural projecting fibres and synaptic arborisations; and the connecting fibre neuropil, which refers to those neural fibres that are devoid of synapses. This latter neuropil includes fascicles (i.e. fibre bundles that connect two areas of the ipsi-lateral hemisphere; also referred to as tracts or bundles), commissures (i.e. fiber bundles that connect two areas of the contra-lateral hemispheres), and chiasmata.

The synaptic neuropil has been divided/compartmentalized into anatomical regions that are comprehensively and mutually exclusive purely via physical descriptors of the overall make-up of these nervous tissues (Miller, 1950; Strausfeld, 1976). These designated neuropil regions were originally defined via the overt changing densities associated with the projecting fibres of the associated cell bodies. These boundaries have been further refined using using synaptic markers such as anti-*nc82* or -*Synapsin* antibodies, as well as pan-neuronal ectopic expression of pre-synaptic-targeted reporter genes such as *n-syb*::GFP or *syt*::HA, and finally glial processes and bundles of connecting fibres that can used as readily identified physical landmarks.

The insect CNS neuronal processes differ from their mammalian counterparts as they are unipolar, with a single process extending from the cell body (Strausfeld and Meinertzhagen, 1998). The cell body itself comprises the nucleus surrounded by a shell of cytoplasm called the perikaryon. The perikaryon contributes a neurite that extends toward its final synaptic target, with this synaptic connection arising from an axon connected to a dendritic arborisation, responsible for signal integration and inter-cellular communication.

Further complexity to this system arises from the connections that arise from the peripheral nervous system (PNS), which consists of peripheral nerves, neuromuscular junctions and sensory receptors that allow the fly to receive, transmit and respond to sensory stimuli. The cell bodies of the PNS are typically bipolar and their axonal projections extend to supply the first-order input into the CNS (Caldwell and Eberl, 2002; Stocker, 1994; Strausfeld and Meinertzhagen, 1998).

The CNS is divided into two inter-dependent and inter-connected sets of ganglia: the brain located in the head capsule, which is then connected by the cervical connexion to the ventral nerve cord (VNC) that extends longitudinally in to the ventral part of the thorax. The most distal portion of the VNC, the abdominal ganglia (Abg), extends an abdominal nerve track (AbNvTk) to supply tissues within the abdomen.

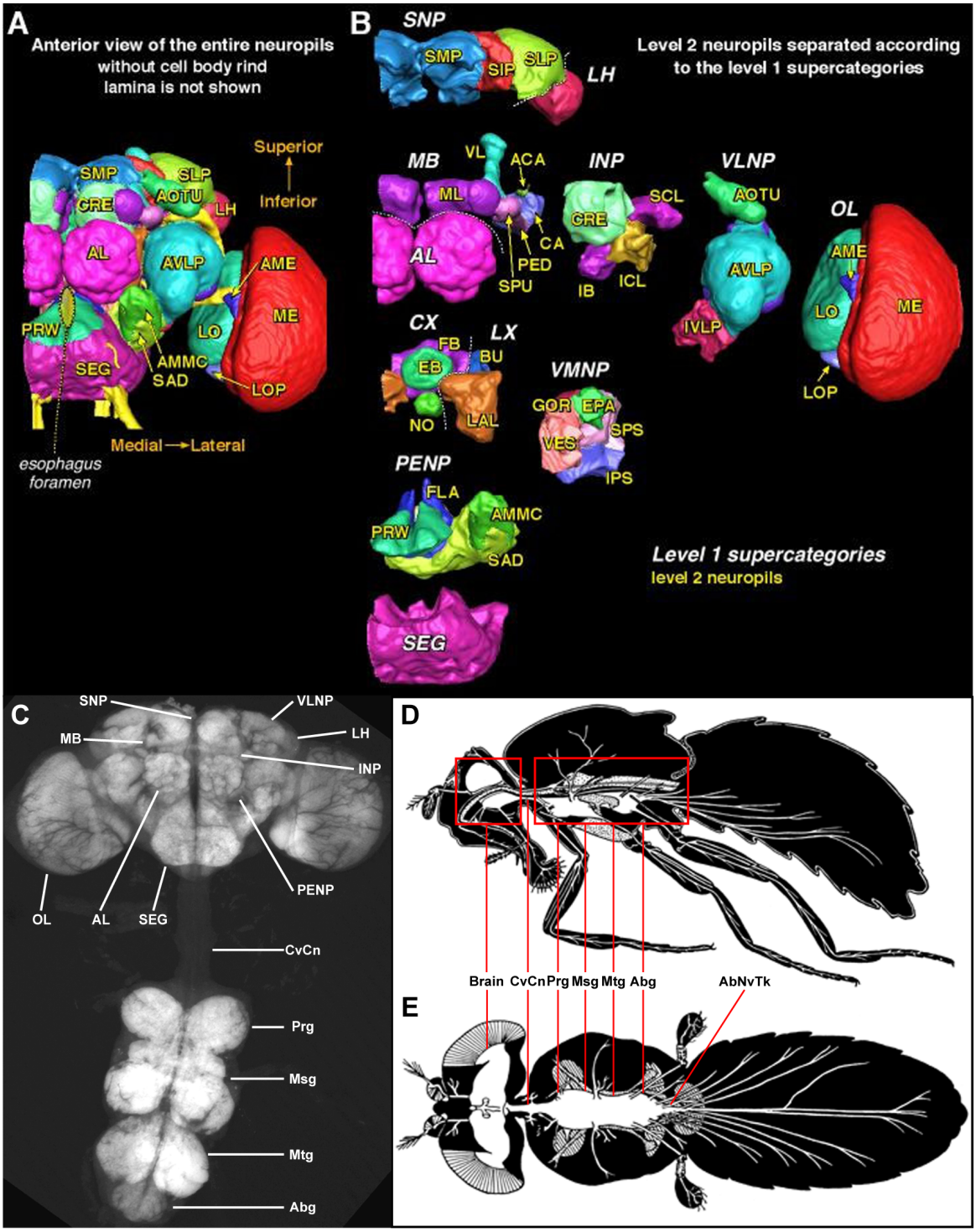

Figure 1-7 Modern and historical representations of the *Drosophila* nervous system. (A) Overall and (B) expanded 3D reconstructions of the regions of the *Drosophila* brain neuropil. The 'level 1' neuropil supercategories indicated are optic lobe (OL), mushroom body (MB), central complex (CX), lateral complex (LX), ventrolateral neuropils (VNLP), lateral Horn (LH), superior neuropils (SNP), inferior neuropils (INP), antennal lobe (AL), ventromedial neuropils (VMNP), periesophageal neuropils (PENP) and subeosophageal ganglion (SEG). (C) 5 D adult CNS stained with anti-nC82 to realize all neuropil. SNP, MB, OL, AL, SEG, PENP, INP, LH and VNLP indicated in brain. Cervical connexion (CvCn) and prothoracic (Prg), mesothoracic (Msg), metathoracic (Mtg) and abdominal (Abg) ganglia indicated in VNC. (Ventral view; superior, top) (D) Lateral and (E) sagittal cartoon representations of the *Drosophila* CNS, *in situ* within the body, with major axonal projections into surrounding somatic regions. Brain and VNC (red boxes). Brain, CvCn, Prg, Msg, Mtg, Abg and abdominal nerve trunk (AbNvTk) indicated. (A-B) Figures taken from BrainName Working Group (In submission, 2011). (D-E) Figures adapted from Miller (1950).

1.6.1.1 The brain

The complexity of the brain is such that only a rudimentary definition of the ganglia is possible, however historically, using developmental and evolutionary criteria, the insect brain has been divided into three main neuromeres; the protocerebrum; the deutocerebrum; and the tritocerebrum). Lying lateral to these structures are the bilaterally paired optic lobes (OLs). For an overall interactive review of the structures listed within this section see http://www.virtualflybrain.org/site/stacks/index.htm. or http://flybrain.neurobio.arizona.edu/. A reformation of these neuroanatomical structures, based on our greater understanding of the both the developmental logic underlying the generation of the final physical adult structures coupled with a greater insight into the functional relationship these structures have with one another, has resulted in the “BrainName Working Group’s” proposed ‘coordinated nomenclature system for the insect brain’ (in submission, 2011).

The protocerebrum is the most dorsal of these three brain regions and is created from a variety of complex neuropils that include, but are not limited to, the mushroom bodies (MBs), the central complex (CC), the lateral complex (LC), the lateral horns (LH) and such more loosely designated areas as the ventero-lateral and ventero-medial neuropils (VLNP and VMNP). Again these regions may be subdivided into more discrete regions of interdependent neuropil. So that the MBs, bilaterally paired lobed neuropil structures that in many species also possess cap-like extensions proximally in the superior-posterior brain, are formed from the calyxes, pedunculi, spurs and lobes. The CC, a group of midline neuropil structures, comprises the central body (CB), in turn formed from the fan shaped and ellipsoid bodies (FB, or upper division of the CB; and EB or lower division of the CB respectively), noduli (NO) and the protocerebral bridge (PB). Other regions are seen as discrete single anatomical areas such as the LH, bilaterally paired regions of neuropil flanking the posterior-superior protocerebrum receiving projection neuronal terminalia from various regions of the brain such as the antennal and olfactory lobes (AL; OL). Also associated with protocerebrum are structures such as the superior protocerebral bridge (SPB) and the pars intercerebrialis (PI). The PI runs fully ventero-dorsally through the superior protocerebrum and contributes several neuro-secretory cells, both locally and distally to the CNS (Pathak and Ghosh, 1990). Beyond these mere anatomical

descriptions, continued research into the neuropil substructures has elucidated some of the functional contributions these structures perform within the CNS and the organism as a whole; in behaviours such as locomotion, olfactory learning and courtship visual learning (the MBs) and walking, flying and visual learning (the CC) (Fahrbach, 2006; Heisenberg, 2003; Ilius et al., 1994; Martin et al., 1998; Martin et al., 1999; Pan et al., 2009; Zars, 2000).

The deutocerebrum lies ventral to the protocerebrum and again encompasses major substructures such as the AL and the antennal mechano-sensory and motor centres (AMMCs). The Als are large bilateral paired glomeruli that receive a number of sensory inputs, most obviously from the antennae via the antennal nerves. The olfactory sensory fibres arising from the third antennal segments project to the ALs while the first and second antennal segments fibres, which arise mainly from mechanoreceptors terminate in the lateral deutocerebrum in the AMMCs.

The tritocerebrum lies displaced ventrally in the brain, separated by a central foramen created by the passage of the oesophageal tract, and is the least defined neuromere in *Drosophila*. However it contains parts (though not all) of the peri-, sub- and oesophageal ganglia, which generally themselves are positioned inferiorally in the brain and, as individual neuropil regions, extend ventero-dorsally (Rajashekhar and Singh, 1994). The tritocerebrum gives rise to descending and ascending neurons as well as receiving sensory fibres from the proboscis via the labial nerves as well as inputs from other gustatory receptors and other neuropils. Neurosecretory fibres projecting from the PI also appear input to this region (Rajashekhar and Singh, 1994).

The optic lobes (OL) are large masses of neuropil associated with the deutocerebrum lying laterally to the central brain. These structures are responsible for the processing of visual information received from the fly’s compounds eyes. The OLs are comprised of three main regions of neuropils arranged proximal to distally, with respect to the central brain, into the lamina, medulla and lobular complexes (LA; ME; and LO respectively). Each region of neuropil is associated with cell bodies which lie distally in the case of the LA and ME, and posteriorally in the case of the LO (Meinertzhagen and Hanson, 1993).

1.6.1.2 The ventral nerve cord

As stated the VNC is connected to the brain via the cervical connexion and extends longitudinally into the ventral part of the thorax (Miller, 1950). The VNC is itself subdivided into four main regions, which, running cephalic to caudal, are defined as the pro-, meso- and meta-thoracic (Prg; Msg; and Mtg respectively) and abdominal ganglia (Abg) (Miller, 1950) The Prg, Msg and Mtg give rise to, among other structures, three bilaterally paired nerves that project ventrally to the legs as well as paired nerves dorsally in the Msg that project to the direct flight muscles, wings and halteres. Paired nerves arising from the Abg form the abdominal nerve trunk (AbNvTk) to ramify on structures within the abdomen (Miller, 1950).

1.6.2 Sexually dimorphic neuroanatomical features in Drosophila

It would seem a basic tenet that to direct sex-specific behavioural outputs an organism requires the formation of a dimorphic nervous system. Generally in neurogenetics there exists the unspoken assumption that dimorphisms in neural structures will equate to alteration in behavioural outputs between the sexes. However without the demonstration of real function we cannot assume a change in neural substrates results in a change in behaviour, nor that in the absence of a dimorphic behavioural output the underlying neural substrate is the same (de Vries and Södersten, 2009). Indeed until recently in *Drosophila* there have been few readily identified sexually dimorphic anatomical features between the CNSs of males and females. Historically however gynandromorph studies in both male and female *Drosophila* have demonstrated that alteration of the gender of specific loci within the CNS will then reflect on the mosaic animal's ability to direct gender appropriate sex-specific behaviours (Ferveur and Greenspan, 1998; Hall, 1977, 1979; von Schilcher and Hall, 1979). Studies over the past few years have begun to elucidate clear, though often subtle, differences in neural substrates, both in terms of gene expression within neurons and in physical differences such as in alterations in neural connectivity, that exist between males and females, which clearly demonstrate the requirement in *Drosophila* for the sculpting, and maintenance, of a sexually dimorphic nervous system.

Within the brain it has been demonstrated that the MBs in females contain a greater number of neuronal fibres than males (Technau, 1984). While Heisenberg et al. (1995) demonstrated that the lobulas and medullas in the optic lobes, and

the calyxes of the MBs are larger in males. Indeed this increase in the lobular and medullar size actually overcompensates for the larger number of optic lobe columns females possess due to the larger number of ommatidia in their eyes (Heisenberg et al., 1995; Rein et al., 2002). It is speculated that the significant increase in the size of the male optic lobes may be due to the presence of visual neural circuitry required for male courtship tracking, similar to that present in calliphorid and muscid flies (Hausen and Strausfeld, 1980; Strausfeld, 1980; Strausfeld, 1991).

That females constitutively expressing Fru^{M} can perform the early steps of the male courtship ritual is compelling evidence that there exists in both sexes a default neural circuitry, which appears to be normally only active in specifying sex-specific behavioural outputs in males (Demir and Dickson, 2005). This is supported by the fact that females may be artificially induced via optogenetics to perform recognisable 'male-like' courtship song (Clyne and Miesenböck, 2008). However while the ectopic expression of fru^{GAL4} can realize a recognizable *fruitless* neural circuit in females, some clear dimorphic differences have been identified at the neuroanatomical level. Kimura et al. (2005) demonstrated that females possess a significantly smaller number of neurons in the *fru*-mAL cluster as compared with males due to a process of programmed cell death (PCD) occurring in the absence of Fru^{M} and that, as a consequence, there exists differences in the axonal projections and therefore the connectivity of the associated neurons. This alteration in connectivity has been implicated in the shaping of the male courtship posture with respect to unilateral wing extension towards a target female (Koganezawa et al., 2010). Kimura et al. (2008) then demonstrated that the *fru*-P1 cluster implicated in courtship initiation is absent in females due to a process of PCD, this time as a consequence of the expression of Dsx^{F}. Fru^{M} expression in the brain has also been demonstrated as necessary for the male-specific enlargement of three olfactory glomeruli, and importantly these glomeruli are specifically innervated by fru^{GAL4}-expressing ORNs (Kondoh et al., 2003; Stockinger et al., 2005). It is speculated that these ORNs might therefore be responding to sex-specific pheromonal cues (Kondoh et al., 2003; Stockinger et al., 2005). Datta et al. (2008) demonstrated that a neural circuit beginning with a fru^{+} ORN that responds to the male-specific pheromone cis-vaccenyl acetate, innervates one of these male-specifically enlarged olfactory glomeruli (DA1), which then sends a glomerular projection into the LH with a demonstrated male-specific

pattern of axonal arborisation. The dimorphic pattern of arborisation within this particular neural circuit is Fru^{M} dependent (Datta et al., 2008). Mapping of this circuit as a whole has since been extended to comprise four neurons, connected by three synapses (Ruta et al., 2010). Three of the neurons in the described circuit are overtly dimorphic and identify a male-specific neuropil that integrates inputs from multiple sensory systems and sends outputs into the VNC to terminate in the thorax and Abg (Ruta et al., 2010). Rideout et al. (2007) also showed that the number of *fru*^{GAL4}-expressing neurons in the Msg of females was significantly reduced and that Fru^{M} and Dsx^{M} cooperation is necessary to obtain the full complement of *fru*-expressing neurons in the male. This dimorphism exists in the area demonstrated to contain a localised song-pattern generator, and again Fru^{M} and Dsx^{M} cooperation has been demonstrated as necessary for the specification of the song circuitry and production of wild-type male-specific courtship song (Rideout et al., 2007; Rideout et al., 2010; von Philipsborn et al., 2011). Further recent clonal analyses have identified candidate neural circuits that may be responsible for initiation and modulation of courtship song (von Philipsborn et al., 2011). Importantly the neurons implicated in these circuits are either male-specific or exhibit male specific neural connectivity, the assumption being that once again Fru^{M} and Dsx^{M} expression masculinises a default circuit to generate a male-specific behavioural output (von Philipsborn et al., 2011). In the Abg Dsx^{M} has been shown to act on a group of neuronal stem cells to prolong neurogenesis into early metamorphosis resulting in a greater number neurons with respect to females, in which these stem cells stop dividing at the late larval stage (Taylor and Truman, 1992). Again in the Abg, Fru^{M} and Dsx^{M} expression have been shown to be necessary for the complete population and appropriate organisation of a set of male-specific serotonergic cells, which then project to parts of the male internal genitalia (Billeter et al., 2006b). Also projecting from the A5 segment of the VNC exists a male-specific (MIND) motorneuron in which expression of Fru^{M} induces formation of the male-specific somatic structure, the Muscle of Lawrence, and associated dimorphic neuromuscular junction (Billeter and Goodwin, 2004; Nojima et al., 2010). Projections arising from male-specific gustatory receptor neurons of the PNS into the CNS also demonstrate a dimorphic pattern of midline chiasmatic crossing in the Prg, again through positive inductive signalling by Fru^{M} and Dsx^{M}, with perhaps negative signalling by Dsx^{F} in females (Mellert et al., 2010; Possidente and Murphey, 1989).

These differences in neural substrates between the sexes have also been demonstrated in recent studies utilising clonal analyses to map neural connectivity in males and females (Cachero et al., 2010; Datta et al., 2008; Kimura et al., 2008; Kimura et al., 2005; Rideout et al., 2010; Ruta et al., 2010; von Philipsborn et al., 2011; Yu et al., 2010). These investigations not only demonstrated the existence of sex-specific neuronal clusters but also dimorphisms in the projections associated with shared neuronal clusters and consequent alterations in connectivity associated with these varying differences between the CNSs of the sexes (Cachero et al., 2010; Datta et al., 2008; Kimura et al., 2008; Kimura et al., 2005; Rideout et al., 2010; Ruta et al., 2010; von Philipsborn et al., 2011; Yu et al., 2010). Associated with these investigations was the demonstration that volumetric differences existed between male and female standardised brains, with male and female expanded regions (MERs and FERs) present in areas of significant dimorphisms in neural projections and connectivity (Cachero et al., 2010).

1.7 GAL4/UAS binary system

Classical forward genetics employed techniques for delineating gene function via the impairment of gene expression. This approach, while valid, was limited in the scope of investigative approaches available and was reliant on the random nature of the mutagenesis screens performed. Latterly reverse genetic approaches, especially in the ‘post-genomic age’, has expanded the ability of investigators to elucidate gene function by the direct manipulation of gene function(s): via analyses ranging from quantification of transcriptional gene expression to the characterisation of the consequent resultant phenotypic effects. One of the most important tools today in the arsenal of *Drosophila* geneticists with respect to these forms of investigations is that of the GAL4/UAS binary system of targeted gene expression (Brand and Perrimon, 1993; Duffy, 2002).

The GAL4 gene encodes a yeast transcription activator protein that directly binds to four related 17 bp sites, that together define an enhancer-like element described collectively as the upstream activating sequence (UAS), which are essential for the transcriptional activation of these GAL4-regulated genes (Giniger *et al*., 1985; Ptashne, 1988). Fischer et al. (1988) were able to demonstrate that ectopic GAL4 expression could activate the transcription of a gene engineered to be under the control of the UAS element (reporter genes). Importantly, as GAL4

has no endogenous targets in Drosophila, it appeared to produce no deleterious effect on endogenous gene expression in the transgenic fly. Brand and Perrimon (1993) then extended these findings in the development of the *in vivo* GAL4/UAS binary system for targeted gene expression in *Drosophila*. The ability of this system to describe the temporal-spatial expression pattern of a gene and latterly, via a variety of GAL4 responsive UAS transgenics, to then impinge on gene function, have provided investigators with a plethora of investigative tools and approaches for the elucidation of the genetic underpinnings of *Drosophila* development and the specification of behaviours (Duffy, 2002; Jones, 2009; McGuire et al., 2004). Since the first inception of the GAL4/UAS system investigators have consistently increased and improved on the transgenic tools available, developing more and more sophisticated ways in which to alter and assess gene expression, both in terms of the GAL4 drivers available and in the number and form of GAL4 responsive transgenic tools (Duffy, 2002; Jones, 2009; McGuire et al., 2004; Simpson, 2009)

1.7.1 Intersectional techniques

While the GAL4/UAS binary system has proved a powerful, flexible and highly valuable tool for the characterisation and functional dissection of gene expression within the fly, like any system it can manifest faults (expression patterns that do not reiterate the endogenous gene, 'leaky' transgenes, off target and dose-dependent effects and alteration of gene transcription profiles) and limitations (lack of isoform- or gene-specific restricted patterns of expression spatially and/or temporally) etc. As such, coincident with development of the GAL4/UAS binary system, alternate methods for targeting and functional impinging upon gene expression within *Drosophila* have been developed (McGuire et al., 2004; Simpson, 2009). Many of these alternate methodologies can in fact be used in conjunction with the GAL4/UAS system. Thereby broadening the reach of the individual approaches by complementary use of the systems and allowing a finer restriction of targeted expression within subsets of a more general population of cells by the coincident employment of the strategies than would otherwise be achieved with each of the systems when used individually.

One example of this strategy of refining the expression patterns driven in GAL4 lines is via employment of the yeast protein Gal80, which binds and inhibits

the transcriptional activation domain (AD) of Gal4 effectively preventing GAL4 responsive UAS gene expression (Ma and Ptashne, 1987; Pfeiffer et al., 2010a; Pilauri et al., 2005; Suster et al., 2004; Yun et al., 1991). GAL80 may be expressed in a gene-specific or temperature sensitive manner allowing spatial or temporal targeted suppression of GAL4 activity in a subset of cells of the overall population that would normally express the driver (Jones, 2009). This ability to repress GAL4 activity has been used to great effect in conjunction with the previously developed FLP/FRT site-specific recombinase system (Golic and Lindquist, 1989; Liu and Hou, 2008; Struhl and Basler, 1993; Xu and Rubin, 1993) in the development of the mosaic analysis with a repressible cell marker (MARCM) system (Lee and Luo, 1999; Liu and Hou, 2008). In this system the dominant repressor (GAL80) of a transgenic cell marker is placed in trans to a mutant gene of interest. Mitotic recombination events between homologous chromosomes via heat shock activation of the FLP/FRT site-specific recombinase system then generate homozygous mutant cell or cells, which are exclusively labelled by activated expression of the transgenic marker due to loss of the repressor, effectively creating unique mosaic animals (Lee and Luo, 1999). Indeed these positively marked cells can even be made homozygous mutant for a particular gene of interest and/or modified with additional effector transgenes in an otherwise wild-type environment (Lee and Luo, 1999). This system has proved itself invaluable for lineage analysis, the tracing of neural circuitry, and high-resolution mosaic analysis of gene function (Liu and Hou, 2008; Luo, 2007).

Complementary binary gene targeting systems in *Drosophila*, independent of GAL4, have also been developed. One such system is the LexA/LexAop binary system, which encodes the bacterial (*E. coli*) transcriptional activator LexA fused to a C-terminal activation domain derived from GAL4 or VP16 (Sadowski et al., 1988), this allows it to drive *in vivo* transcription of reporter transgenes in *Drosophila* whose promoters contain multimerized LexAop motifs (Lai and Lee, 2006a; Szüts and Bienz, 2000). Another alternate binary system is the “Q” system, which utilises gene-specific ‘QA’ trans activators binding to multimerized ‘QUAS’ responsive transgenes with direct repressors and activators of the transcriptional drivers this time derived from *neurospora* (Potter and Luo, 2011; Potter et al., 2010). The advantages of developing these complementary systems are manifold, allowing intersectional strategies employing the LexA or Q systems in conjunction with the vast array GAL4 drivers and UAS responsive transgenic lines for refining

gene expression patterns and manipulating the sub-populations of cells, as well as creating the opportunity to perform both GAL4-independent and 'coupled' MARCM analyses (Lai and Lee, 2006a), thereby further increasing the level of refinement that may be applied to the functional analyses of exclusively labeled cells or clonal groups (Pfeiffer et al., 2010a; Shang et al., 2008).

1.8 Homologous Recombination

Historically mutations in a gene of interest have been isolated using *P*-element- or mutagenic (ethane methyl sulphonate or isotope induced) mediated screens; however these techniques are generally non-specific, reliant on the screening of a number of mutagenic 'events' for alterations within a gene of interest. Gene targeting by homologous recombination utilises *P*-element transformation techniques (see http://engels.genetics.wisc.edu/Pelements/index.html) (Engels, 1996; Rubin and Spradling, 1983) to direct targeted insertions, deletions or alterations to a specific genetic locus in *Drosophila* (Rong and Golic, 2000). Homologous recombination also has the advantage of allowing the direct manipulation of very large genes with multiple promoters and/or protein isoforms, and genes with complex *cis*-acting regulation, thereby making it ideal for disrupting or altering specific aspects of a gene's function (Bi and Rong, 2003). The technique of homologous recombination has, since it was first described, been successfully employed to engineer a number mutations and/or modifications at a variety of loci within the *Drosophila* genome (Demir and Dickson, 2005; Manoli et al., 2005; Rideout et al., 2010; Robinett et al., 2010; Rong and Golic, 2000, 2001; Rong et al., 2002; Stockinger et al., 2005).

1.8.1 Strategies for homologous recombination

Homologous recombination in *Drosophila* requires the generation of a 'donor' *P*-element construct, containing regions of homology to that of the chosen targeted gene. The required amount of donor to target homology may range from 2.9 kb to 8.9 kb, though typically around 4 kb has proven to be sufficient (Bi and Rong, 2003; Hasty et al., 1991a; Rong and Golic, 2000, 2001; Rong et al., 2002). The engineered donor element must also contain *P*-element transposition sequences and FRT sites at each of the extreme 5' and 3' ends flanking the regions of homology, as well as a marker gene element (such as *mini-white*$^{+}$; *mw*$^{+}$), and a

recognition site for the site-specific endonuclease I-*Sce*I. This donor element is initially randomly inserted into the genome via *P*-element transformation (Rubin and Spradling, 1983) before the actual process of homologous recombination may begin.

Depending on the desired end product the donor construct design is tailored to employ one of two strategies for gene targeting by homologous recombination. These variant stratagems are described as ‘ends-out’ or ‘ends-in’; with the ends-out strategy more often used to generate a null mutation within the gene of interest, while the more complex process of ends-in strategy may be used to generate more subtle mutations such as the creation of small deletions or insertions, or the disruption of a single isoform of the targeted gene (Bi and Rong, 2003; Rong and Golic, 2000).

1.8.2 Ends-out versus ends-in strategies

The ends-out strategy involves a donor construct with the donor/target regions of homology separated by a marker gene and an I-*Sce*I endonuclease recognition site, which should itself not be in close proximity to either the marker gene or the regions of homology. This strategy is described as a ‘one-step’ process, compared with the ends-in strategy (Rong and Golic, 2000, 2001; Rong et al., 2002). Essentially following the donor element’s random insertion into the genome, the transgenic fly is crossed to a strain carrying both a site-specific recombinase (FLP) and endonuclease (I-*Sce*I). The progeny of this cross undergo a defined heat shock protocol at an experimentally established developmental time point (usually early in development), which causes the donor element to be excised from the genome and induces a double strand break. This results in a mobilised and linearised donor element that may then be integrated into the targeted locus via homologous recombination. The successful recombinant event may be scored for via the presence of expression of the marker gene (i.e the appearance of eye colouration in a w^- genetic background due to the incorporation of a transgenic donor element carrying the mw^+ genetic marker) followed by use of molecular techniques (PCR, Southern and/or Northern blotting) to confirm successful integration at the chosen locus. As stated the ends-out stratagem is used to generate a null form of the targeted gene of interest. This may be achieved in one of two ways, dependent on the region chosen for the donor/target homology in the

generation of the donor construct (Rong and Golic, 2000; Rong *et al*., 2002). If the region of donor/target homology consists of sequences set within the targeted locus, then the gene will be disrupted by the insertion of the donor construct into the targeted gene locus. However if the region used to create the donor/target homology consists of sequences flanking the desired locus, then the entire gene should be replaced by the donor construct (Bi and Rong, 2003).

The ends-in strategy is generally described as a more complex 'two-step' process in which the donor element contains a marker gene and three regions of donor to target homology separated by the I-*Sce*I and I-*Cre*I site-specific endonuclease recognition sites, which again should not be in close proximity to either the marker gene or regions of homology (Rong et al., 2002). Essentially once the donor element has been randomly inserted into the genome then the pattern of crosses and heat shock regimen follows that described above with the ends-out strategy. However due to the construction of the donor element associated with this strategy, rather than disrupting endogenous gene expression by generating a null mutation, this recombinant event results in a duplication of the targeted gene locus. The successful recombinant event may again be scored for by the appearance of phenotypic expression of the inserted transgenic genetic marker again followed by use of molecular techniques (PCR, Southern and/or Northern blotting) to confirm successful integration at the chosen locus. Following this the second step of the overall ends-out process may performed in which the duplication at the locus, and with it the inserted genetic marker, may be resolved by crossing the recombinant transgenic fly to a strain carrying the heat shock inducible I-*Cre*I site-specific endonuclease. The progeny of this cross undergo a defined heat shock protocol at an experimentally established developmental time point, which again induces a double-strand break in the locus that may be subsequently repaired via homologous recombination (Rong et al., 2002). This event may result in the resolution of the duplication at the locus and the elimination of the marker gene which may then be scored for by the loss of the previously observed phenotypic expression (i.e the disappearance of eye colouration and return to a w^- genetic background due to the elimination of the transgenic mw^+ genetic marker) (Rong et al., 2002).

1.8.2.1 Targeting GAL4 to the *dsx* locus

An ends-in strategy for targeting of the *dsx* locus by HR was successfully undertaken by Dr. Elizabeth Rideout as part of her Ph.D. research in the lab of Dr. Stephen Goodwin (2008; Div. of Molecular Genetics -FBLS, Univ. of Glasgow) (Figure 1.7). An ends-in strategy was adopted as it had been previously reported that, in yeast and mammalian systems at least, the ends-out scheme for HR was less efficient (Hastings et al., 1993; Hasty et al., 1991b). Also, at the time this scheme was undertaken, a number of studies had demonstrated the successful application of the ends-in protocol and the targeting vectors for this strategy had been made freely available (Bi and Rong, 2003; Rong and Golic, 2000, 2001; Rong et al., 2002; Stockinger et al., 2005). Finally while the ends-in system also allowed for the elimination of the marker gene from the targeted locus, the duplication at the *dsx* locus was not resolved, likely as a result of a polymorphism subsequently discovered in the I-*Cre*I site in the targeting vector pED22 (J. Walker, unpublished data).

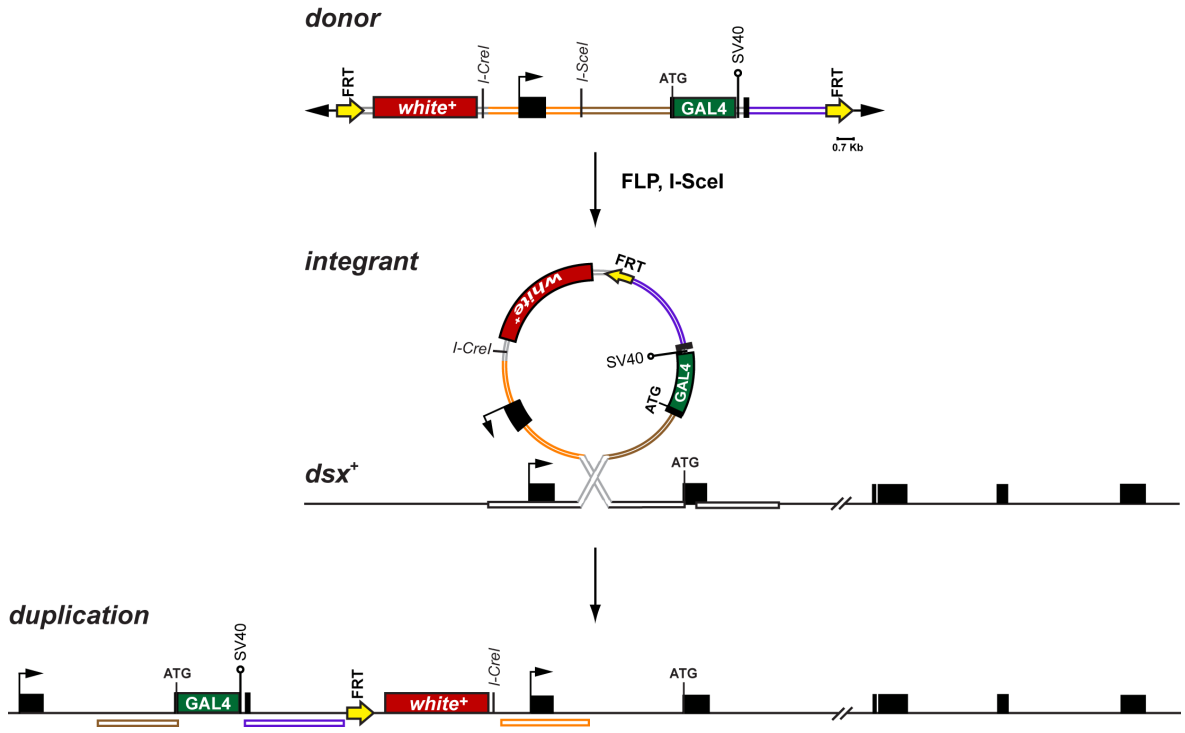

Figure 1-8 Schematic of the ends-in strategy for targeting GAL4 to the *dsx* locus by homologous recombination.
To obtain the successful integration of the GAL4 insert into the *dsx* locus, a transgenic fly line was initially generated containing a *dsx P*-element targeting construct (donor) located on the second chromosome. The donor *P*-element contained the two FLP-recombinase recognition FRT sequences (yellow arrows), the I-*Cre*I recognition site, the I-*Sce*I recognition, the GAL4 open reading frame (green), and three regions of homology to the *dsx* locus: fragment I (orange), fragment II (brown), and fragment III (purple). Solid black boxes indicate the position of exons and black arrows represent transcriptional start sites of endogenous *dsx* genomic sequence. The donor sequence was next excised and linearised using *hs-FLP* and *hs-I-SceI*, respectively resulting. A recombination event at the *dsx* locus resulting in successful integration of the donor element (integrant) at the locus was detected by the observable phenotypic expression of the *white*$^{+}$ marker (duplication). Figure adapted from Rideout et al., 2010.

It should be noted that since its first description in 2000 till 2005, only ~50 examples of successful homologous recombination have been demonstrated. One reason for this may be that while the benefits of development of a successful recombinant targeted to a specific gene of interest may be manifest, the costs with respect to time and effort employing the HR stratagems within a lab, especially if the end-results prove to be negative, may not be viewed as worth the risk. As a consequence of this alternate strategies for gene targeting are continuing to be developed. However the need to overcome a limitation in, or the ability to improve on, an extant system can only manifest as that system is being applied in investigations, nor can it be easily predicted what new technology may arise, nor how development in novel technologies might be applied to problems that exist outwith the predicted systems they are developed in. All of which continues to

ensure that the future avenues of research remain both exciting and completely unpredictable.

1.9 Aims and objectives

Together, gene specific targeting to insert a GAL4 element by homologous recombination into a gene's locus, in conjunction with GAL4 responsive reporter genes, allows the opportunity to develop a comprehensive spatial-temporal survey of an endogenous gene's expression throughout development. Further, this topographical understanding of the gene's expression may then be expanded by functional analyses, using the vast array of GAL4 responsive transgenic tools developed to manipulate gene expression in conjunction with appropriate instersectional tools. The gene targeting of *dsx* provides a prime exemplar for how these techniques can allow the investigation into a gene's (and its isoforms') expression pattern(s). With a process of somatotopic mapping and functional analyses providing insight into the genetic underpinnings that might operate to generate specific behavioural outputs.

In the case of the dimorphically expressed *dsx* gene this allows us the opportunity to investigate the developmental process from which the dimorphic soma and the nervous systems might arise. Initially this requires that the transgenic tool, previously generated by Elizabeth Rideout by ends-in HR at the *dsx* locus, is validated; demonstrating that it reiterates endogenous *dsx* gene expression and known functions in both males and females. Following this the transgenic reagent may be then used to create a comprehensive spatio-temporal survey of *dsx* expression within the developing nervous systems of males and females, and compare this expression in *wild-type* and mutant backgrounds, as well as establishing those tissues in which gender-specific identifiers are required in determination of the final adult state. These spatio-temporal surveys may then be combined with functional analyses, wherein *dsx*-expressing neurons may be directly manipulated, providing a somatotopic map of how these *dsx*-specific neurons and tissues function in the adult male and female in the generation of sex-specific behavioural outputs. Thereby providing insight into the developmental logic for how these, and other, potential sexually dimorphic circuits are formed and how these systems might then be coordinated with gender-appropriate physiology

and sensori-motor tissues to generate sex-specific behavioural outputs in the dimorphic adult.

The questions posed by these investigations represent, in small part at least, what should be viewed as one of the ultimate goals of neurogenetics; investigating the underlying genetic principles that determine the sexually dimorphic nervous system, relating this to how the nervous system then governs specific behavioural output(s) and how this is coordinated with the gender appropriate physiology; and perhaps gaining new insight into how these innate mechanisms may be modified to then determine species-specific behaviours.

2 Material and Methods

2.1 Drosophila

2.1.1 Drosophila melanogaster stocks

A description of all the *Drosophila* stocks used in this work can be found in Table 2.1. A full description of all mutations and balancer chromosomes used can be found in FlyBase (http://www.flybase.co.uk).

Strain/Genotype	Description	Reference
Isogenised Strains		
Canton-Special (Canton-S; CS)	Isogenic wild-type strain.	Flybase.
white^{honey} (*w*^{h})	*w* mutant allele isogenised to CS.	Flybase.
Balancer chromosome strains		
w^{h};*ap*^{Xa}/*CyO*;+	Strain isogenised to CS. Second chromosome balancer Curly of Oster(*CyO*) and dominant marker (*ap*^{Xa}).	Flybase.
TM3,Sb,Ser, e/TM6B,Tb,Hu,e	Strain isogenised to CS. Third chromosome balancers *Third Multiple of Singsong* (*TM*) 3 and 6B.	Flybase.
GAL4 Lines		
+; +; *dsx*^{GAL4}/*TM3*, *Sb*, *Ser*, *e*	GAL4 element inserted into *doublesex* (*dsx*) locus via ends-in HR.	Rideout et al., 2010.
+; +; *dsx*^{GAL4}/*TM6b*, *Tb*, *Hu*, *e*	GAL4 element inserted into *dsx* locus via ends-in HR.	Rideout et al., 2010.
+; +; *dsx*^{GAL4}, *P{w*$^{+mc}$*= UAS-mCD8::GFP.L}*LL6/*TM3*, *Sb*, *Ser*, *e*	GAL4 element inserted into *dsx* locus, recombined with a fusion protein between mouse lymphocyte marker CD8 and Green Fluorescent Protein (GFP).	Rideout et al., 2010.

Strain/Genotype	Description	Reference
Dp(1:Y)B^{S}; *dsx*^{GAL4}*/TM3, Sb, Ser*, *e*	GAL4 element inserted into *dsx* locus via ends-in HR, carrying a marker used for transformation experiments. haplo-X vs. diplo-X progeny identified by Bar-marked Y chromosome.	Rideout et al., 2010.
+; +; *dsx*^{GAL4}, *Df(3R)fru*$^{4-40}$*/TM6B,Tb,Hu,e*	GAL4 element inserted into *dsx* locus via ends-in HR recombined with chromosomal deletion of at least 70 kb covering *fru* locus, removing transcripts from P1 and P2 transcripts.	Rideout et al., 2010.
fru^{GAL4}*/TM3,Sb,Ser*	GAL4 knock-in at the *fru* locus by homologous recombination. Drives expression in all *fru* neurons. Homozygous courtship behaviour defective, partially fertile.	Stockinger et al., 2005
UAS Reporter Transgenes		
y^{1}*,w**; *P{ w*$^{+mc}$*=UAS-mCD8::GFP.L}*LL5; +	Fusion protein between mouse lymphocyte marker CD8 and the Green Fluorescent Protein (GFP). Labels cell membranes, highly concentrated in neuronal processes.	Lee and Luo, 1999.
Y^{1}*,w**; *Pin*^{Yt}*/CyO*; *P {w*$^{+mc}$*=UAS-mCD8::GFP.L}*LL6	Fusion protein between mouse lymphocyte marker CD8 and the Green Fluorescent Protein (GFP). Labels cell membranes, highly concentrated in neuronal processes.	Lee and Luo, 1999.
W^{1118}; +; *P{w*$^{+mc}$*=UAS-StingerII}*	Stable insulated nuclear enhanced Green Fluorescent Protein (GFP).	Barolo et al., 2000.
w^{1118}; *P{w*$^{+mc}$*=UAS-RedStinger}4*/*CyO*	Nuclear dsRed Flourescent Protein (RFP).	Flybase.
UAS-*synaptotagmin*–HA	Pre-synaptic marker recombined with Human influenza hemagglutinin (HA) tag.	Kimura et al., 2005.

Strain/Genotype	Description	Reference
Sex Determination Transgenes		
w*; *UAS-tra*$^{IR\ No.2560}$; +	VDRC RNA interference *transformer* (*tra*) specific line.	Dietzl et al., 2007.
W*; +; *UAS-tra*$^{IR\ No.2561}$	VDRC RNA interference *tra* specific line.	Dietzl et al., 2007.
W*; +; *UAS-tra-2*$^{IR\ No.8868}$	VDRC RNA interference *transformer-2* (*tra-2*) specific line.	Dietzl et al., 2007.
W*; +; *UAS-tra-2*$^{IR\ No.\ 24499}$	VDRC RNA interference *tra-2* specific line.	Dietzl et al., 2007.
W*; *UAS-fru*$^{IR\ No.\ 105005}$; +	VDRC RNA interference *fruitless* (*fru*) specific line.	Dietzl et al., 2007.
W*; *P{ w*$^{+mc}$*=UAS-tra*^{F}*}*^{2057}; +	GAL4 reponsive UAS Female-specific splice variant of the *tra* gene.	Ferveur et al., 1995.
y, w*; +; *P{ w*$^{+mc}$=UAS-*dsx*^{M}*}*	GAL4 reponsive UAS male-specific splice variant of the *dsx* gene.	Lee et al., 2002.
Y, w*; +; *P{ w*$^{+mc}$*=UAS-dsx*^{F}*}*	GAL4 reponsive UAS female-specific splice variant of the *dsx* gene.	Lee et al., 2002.
Sex Determination Mutants		
w*;+;*dsx*^{1}*/TM3,Ser*	Homozygous individuals are intersexual in appearance. Spontaneous loss of function mutation in *dsx*.	Hidreth, 1965.
Dp(1;Y)B^{S}*Y*; +; *Df(3R)dsx*^{15}*/TM6B,Tb,Hu,e*	Deletion covering the *doublesex* (*dsx)* locus, from cytogenetic location 84D11-84E8.	Baker et al., 1991; Taylor et al., 1994; Ring and Martinez Arias 1993.
In(3R)dsx^{23}*,dsx*^{23}*,Ubx*$^{bx-1}$*,sr*^{1}*,e*^{s}*/TM3,Sb*^{1}	Homozygous intersexual in appearance.	Duncan and Kaufman, 1975; Baker et al., 1991.
w^{1}*; +; dsx*^{43}*/TM3,Ser*	*dsx* deficiency, causes females to develop as pseudomales when heterozygous with *dsx*^{Swe}.	Baker et al., 1991; Waterbury et al., 2000.

Strain/Genotype	Description	Reference
w^1;+; dsx^{Sw}/TM3,Ser, e (dsx^{Dom})	Small deletion in female-specific splice acceptor site in *dsx*. Dominant mutation where females heterozygous with deficiency dsx^{43} develop as pseudomales.	Baker and Wolfner, 1988; Nagoshi and Baker, 1990; Waterbury et al., 1999.
w^a;+;tra^1/TM2	Homozygous chromosomal females differentiate as males. Spontaneous deletion removing most of the *transformer* (*tra*) locus.	Sturtevant, 1944; Butler et al., 1986.
Dp(1;Y)B^SY;+;Df(3L)st-J7	Chromosomal deletion covering the *tra* locus, from cytogenetic location 73A2-73B2.	Belote et al., 1990; Cunniff et al., 1997.
***fruitless* Alleles**		
fru^F/TM3,Sb,Ser,e	*fruitless* (*fru*) P1 transcripts are constitutively spliced in the male form due to the deletion of the entire female-specific S exon which contains the Tra/Tra-2 binding site.	Demir and Dickson, 2005
fru^M/TM3,Sb,Ser, e	*fru* transcripts are constitutively spliced in the female form due to a mutation in the male splice donor site.	Demir and Dickson, 2005
Df(3R)fru^{4-40}/TM6B, Tb, Hu, e	Chromosomal deletion of at least 70 kb covering *fru* locus, removing transcripts from P1 and P2 transcripts.	Anand et al., 2001.
Miscellaneous		
elav-GAL80	GAL80 repressor of GAL4 driven by embryonic lethal abnormal vision (elav) promoter in post-mitotic neurons.	Rideout et al., 2010.
w^-; *ppk-GAL80; ppk-GAL80*	GAL80 repressor of GAL4 driven by the *pickpocket* (*ppk*) promoter.	Yang et al., 2009.

Strain/Genotype	Description	Reference
w^{-}; *tsh-Gal80*/*Cyo*	GAL80 repressor of GAL4 driven by the *teashirt* (*tsh*) promoter.	Julie Simpson, Janelia Farm, VA, USA.
y,w FRT19a; UAS-nlacZ,UAS-mCD8::GFP, UAS-p35; MKRS/+	GAL4 responsive UAS transgenic reporter expressing anti-apototic anti-caspase *p35* gene.	Rideout et al., 2010.
UAS-TNT$_G$	GAL4 responsive UAS transgene expressing tetanus neurotoxin light chain.	Sweeney et al., 1995.
w; P{dj::GFP}*	*don juan-* (*dj-*) *GFP*. eGFP linked to a spermatozoa flagellar mitochondrial protein driven by the β*2 tubulin* promoter.	Santel et al., 1997.
w; P{sp-SP::GFP}*	*sex-peptide-* (*SP-*) *GFP*. GFP linked to the sex-peptide specific protein driven by the *SP* promoter.	Villella et al., 2006
ppk::eGFP	*pickpocket* (*ppk*) promoter fusion expressing enhanced GFP.	Grueber et al. 2003; Yang et al., 2009.
y w; UAS-pStingerII, lexAop-FRT-tdTomato::Nls; fru$^{PI.LexA}$	GAL4 responsive UAS nGFP transgene in conjunction with *fru*^{PI} driven nulear Tomato via LexA/LexAop binary system.	Mellert et al., 2010

Table 2-1 *Drosophila* stocks used in this study.
"*w" or "*y**" indicates that the precise allele for *w* or *y* is unknown.**

Fly strains were raised as per Billeter and Goodwin (2004), unless stated otherwise. *dsx*^{GAL4} lines and all transgenes are in a *w*$^{+}$ background for behavioural studies.

2.1.2 Wild-type strain

Unless otherwise stated the wild-type strain used in this study was *Canton-Special* (Canton-S; CS).

2.1.3 Sex determination mutant genotypes

Null mutations in the *transformer* (*tra*) gene were obtained using heterozygous combinations of $tra^{1}/Df(3L)st\text{-}J7$ (as per Billeter *et al*., 2006). Null mutations in the *doublesex* (*dsx*) gene were obtained using heterozygous combinations of either $dsx^{1}/Df(3R)dsx^{15}$ or $In(3R)dsx^{23}/Df(3R)dsx^{15}$ (as per Villella and Hall, 1996). The dsx^{Sw} allele was always examined in trans to *dsx* deficiency stock dsx^{43} (as per Waterbury *et al*., 2000). Transformation experiments employed a $Dp(1:Y)B^{S}$; dsx^{GAL4} */TM3, Sb* stock; haplo-X vs. diplo-X progeny identified by *Bar*-marked *Y* chromosome. The fru^{M} and fru^{F} alleles were always examined *in trans* to $Df(3R)fru^{4\text{-}40}$ (as per Demir and Dickson, 2005).

2.1.4 Fly husbandry

Drosophila stocks were raised on 'Glasgow' *drosophila* medium. Stocks were maintained at room temperature in the laboratory (~22ºC). Unless otherwise stated for genetic crosses and experiments, the flies were mated and their progeny raised either in an incubator or a designated fly room at 25°C at 45% humidity in 12:12 hr light-dark cycles. RNAi crosses were performed at 29°C.

Glasgow Medium: 10 g agar, 15 g sucrose, 30 g glucose, 35 g dried yeast, 15 g maize meal, 10 g wheat germ, 30 g treacle, and 10 g soy flour per litre of distilled water.

2.1.5 Outcrossing of transgenic strains into an isogenised wild-type background

All generated transgenic strains were outcrossed to isogenise their genetic background with that of a *Canton-S* wild type strain. White-eyed virgin females of the *Canton-S* (w^{h}) strain were collected and crossed to red-eyed males of the line of interest. The *mini-white* marker was used to follow the transgene throughout the outcrossing procedure. At the F1 stage, one orange-eyed virgin female was crossed to three *Canton-S* (w^{h}) males. At the F2 stage, one orange-eyed virgin female was crossed again to Canton-S (w^{h}) males. This process was repeated for at least five generations. After outcrossing, a single virgin female was collected and crossed to three sibling males, and the homozygous progeny from this cross were used to generate the final outcrossed stock.

2.1.6 Embryo collection plates

Drosophila adult females were allowed to lay eggs on grape juice agar plates for approximately 16 - 24 hrs, after which the embryos were collected from the plates.

Grape Juice Agar: 20 g agar, 26 g sucrose, 52 g glucose, 7 g dried yeast, and 9% (v/v) preservative free grape juice per litre of distilled water.

For this media, distilled water was heated to boiling to dissolve the agar. The remaining reagents were then added and allowed to dissolve. The media was allowed to cool to 60°C before being supplemented with Nipagin M (4-hydroxybenzoic acid methylester, 10% (w/v) in absolute ethanol) to inhibit fungal growth.

2.1.7 Dissection Techniques

2.1.7.1 Whole Mount Dissection of Adult CNS and/or somatic tissues

Unless otherwise stated for adult dissections flies were aged for 5 days prior to dissecting, except in the case of pharate adults. After light CO_2-anaesthesia, flies were immersed in ethanol for 5 sec. They were then transferred into 300 µl phosphate-buffered saline (PBS; 137 mM NaCl, 2.7 mM KCl, 10 mM Na_2HPO_4, 2 mM KH_2PO_4) on a blacked-out concave dissecting slide. Their wings and legs were removed using No. 5 Biology Grade dissection forceps (Dumont). The brain was exposed by first removing the proboscis, and then by tearing the head capsule in half by pulling at the lower corner of each eye. The brain was left attached to the rest of the body by the cervical connexion. The abdomen was then severed using dissection scissors. The forceps were used to cut the thoracic cuticle transversely at the midline from posterior/caudal to anterior/cephalic severing the cuticle surrounding the cervical connexion. The dorsal cuticle with attached muscles and then oesophagus would be lifted away to reveal the dorsal surface of the ventral nerve cord (VNC). The VNC, with Brain attached, would then be gently lifted from the thorax. Finally the whole isolated CNS would be transferred using a siliconised Pasteur pipette to a dish for fixation and incubations.

In the case of dissections requiring the abdominal nerve trunk (AbNvTk) to remain attached to the internal genitalia the dissection is as above, except the abdomen would be left attached and the abdominal and thoracic cuticle would be severed at the midline from the anal plates up to the cervical connexion. The dorsal cuticular structure then would be lifted away and the internal genitalia lifted out ensuring the AbNvTk remained attached to both the genitalia and VNC. The final stages of the dissection would then proceed as normal.

Axonal degeneration experiments involved performing axotomies at specific points on the legs of newly eclosed flies. The flies were then isolated and aged for seven days prior to any behavioural assays and/or CNS dissections being performed (as described above).

Somatic tissues such as the internal genitalia, guts, proboscis, appendages etc. are removed as required and treated as per the protocol described above. For cuticular preps the cuticles were excised using dissecting forceps and, if required, muscle and fat body scraped away to present the cuticle alone.

2.1.7.2 Whole Mount Pupal CNS

Wandering 3rd instar (L3) larvae make their way out of the food and up the side of the vial. These would be collected and sexed by the size of their gonads (Ashburner, 1989). Sexed L3 larvae would be transferred onto 3M Whatman paper in a 50 mm Petri dish humidified with an underlying tissue moistened with water. These larvae would then evert their spiracles and stop moving, developing into white pre-pupae (Bainbridge and Bownes, 1981). The pupae would then be aged at 25°C for a fixed time period. Pupae at the desired stage would be transferred to 300 µl PBS on a blacked-out concave dissecting slide for dissection. The operculum would first be removed using forceps. The rest of the pupal case would then get gently peeled off to reveal the pupa. A slit would be made with forceps along the dorsal part of the abdomen, extending to just below the top of the brain. A Gilson P20 micropipette fitted with a yellow tip would then be used to jet 20 µl of PBS in and out of this opening, which clears the inside of the thorax and allows visualization of the pupal CNS. The CNS would be dislodged from surrounding connective tissues with continued gentle jetting of PBS until the whole CNS could be lifted from the capsule using the forceps. The whole isolated CNS would then

be transferred using a siliconised Pasteur pipette to a dish for fixation and incubations.

2.1.7.3 Whole Mount Larval CNS and/or somatic tissues

L3 larvae were gently selected with forceps and transferred to PBS. Larvae were sexed according to the size of their gonads (Ashburner, 1989). No. 5 dissecting forceps were then used to tear a small opening in the caudal end of the larvae. The mouthparts were then firmly taken hold of by one set of forceps and, using the other forceps, the cuticle was slid along effectively inverting the larvae while leaving the internal tissues intact and *in situ*. The desired tissues (CNS, imaginal disc, gonads, fat body etc.) could then be removed for processing.

2.1.7.4 Embryo Collection

Approximately 100 females and 50 males were pooled in an inverted plastic beaker and allowed to lay eggs on a plastic Petri dish containing grape juice agar medium with a dab of yeast paste (dried yeast dissolved in distilled water, which is subsequently heat inactivated) covering the open bottom of the beaker. Flies were allowed to lay overnight at 25°C on the plate, and the plate was removed the following morning for collection. Embryos were detached from the egg laying plate using a paintbrush and a stream of distilled water, and collected in a fine-mesh sieve.

2.2 Visualisation Techniques

2.2.1 Immunofluorescence

2.2.1.1 Incubations for larval, pupal and adult tissues.

All samples dissected and treated as per Lee et al. (2000) and Billeter and Goodwin (2004). Samples were dissected in PBS and fixed in 4% paraformaldehyde (in PBS) for 20 min on ice, except for preparations involving incubation with *fruitless* antibody, which were fixed in 2% paraformaldehyde (in PBS) for 20 min on ice. Samples were then washed three times in PBS for 15 min each, three times in PBT (1xPBS, 0.4 % Triton X-100), and incubated for 1 hr in PTN (PBT, 5% normal goat serum; Scottish Diagnostics and Molecular Probes). The specimens were incubated at 4ºC overnight in PTN containing the primary

antibody at the appropriate concentration (see table 2.2). They were washed four times in PBT for 1 hr each and incubated in PTN containing the appropriate species-specific fluor-conjugated secondary antibody (see table 2.3) either for 4 hr at room temperature or overnight at 4ºC. They were washed four times in PBT for 1 hr and three times in PBS for 30 min. Stained specimens were mounted in VectaShield (Vector Lab) on Polylysine treated microscope slides (BDH).

2.2.1.2 Embryonic incubations

Embryos were collected as described previously, and dechorionated by placing the sieve into a 50% solution of bleach in distilled water for exactly 3 min, after which the embryos were washed thoroughly with distilled water to remove all traces of bleach. The embryos were then transferred to 5 ml heptane in a glass container using a paintbrush, and 5 ml of 4% paraformaldehyde (in PBS) was added, and the solution was shaken vigorously. The embryos were fixed for 10 -30 mins at room temperature. After fixation, the aqueous bottom layer was completely removed, and a 5 ml solution of 95% methanol/5% EGTA (ethylene glycol tetra-acetic acid, pH 8.0) was added to the glass container, and swirled gently. De-vitellinized embryos sank to the bottom of the container. Embryos were then transferred to a clean 1.5 ml Eppendorf tube containing 1.0 ml of PBS using a Pipette with a cut tip. After the embryos had fallen to the bottom of the tube, most of the PBS was removed and several drops of PAT (PBS, 1% Triton-X, 0.1% bovine serum albumin) were added. The embryos were then washed an additional three times with PAT, followed by two washes in PBS. To mount, the PBS was removed and VectaShield (Vector Lab) was added, and the embryos were transferred to a polylysine slide for viewing.

2.2.1.3 Phalloidin muscle preparations

Muscle preparations were fixed for 30 min in 4% (w/v) paraformaldehyde (in PBS). Preparations were then washed three times for 10 min per wash in PBS, followed by a single wash in PBT (PBS, 0.5% (v/v) Triton-X). The preparations were then incubated with 100 nM TRITC- (tetramethylrhodamine B isothiocyanate) conjugated phalloidin (F-Actin specific fungal toxin; Sigma) for 20 min. The preparations were given three 10 min washes with PBT, followed by three 10 min washes in PBS before being mounted in VectaShield (Vector Lab) on a slide.

2.2.1.4 Primary and secondary antibodies employed in immunofluorescent investigations

Antibody	Description	Dilution	Source/Reference
Anti-Fru^M	Rat, polyclonal against male-specific 101 aa domain of Fru^M.	1:300	Lee et al., 2001
Anti-Fru^M	Rabbit, polyclonal against male-specific 101 aa domain of Fru^M.	1:400	Billeter et al., 2006b
Anti-Dsx	Rat, polyclonal against common DM DNA-binding domain of Dsx.	1:50	Sanders and Arbeitman, 2008
Anti-Horseradish Peroxidase (Anti-HRP)	Cy3 conjugated affinity purified goat polyclonal against HRP.	1:300	Jackson ImmunoResearch Laboratories
Anti-HRP::Cy3	Cy3-AffiniPure conjugated Goat Anti-HRP.	1:400	Jackson ImmunoResearch Laboratories
Anti-Serotonin (Anti-5HT)	Rabbit, polyclonal against 5-Hydroxytryptamine.	1:500	Sigma
Anti-mCD8	Rat, monoclonal against mouse lymphocyte marker CD8a-subunit.	1:20	Caltag Laboratories
Anti-Green Fluorescent Protein (Anti-GFP)	Rabbit, polyclonal against GFP.	1:1000	Invitrogen Molecular Probes
Anti-Elav	Rat, mononclonal against Elav.	1:5	DSHB (Univ of Iowa)
Anti-nc82	Mouse, monoclonal against Bruchpilot (neuropil marker)	1:6	DSHB (Univ of Iowa)

Antibody	Description	Dilution	Source/Reference
Anti-HA	Rat ,monoclonal against human influenza Hemagglutinin	1:1000	Invitrogen Molecular Probes
Phalloidin-TRITC	TRITC- (tetramethylrhodamine B isothiocyanate) conjugated Phalloidin (F-Actin specific fungal toxin).	100 nm	Sigma

Table 2-2 Primary antibodies used in this study.

Antibody	Description	Dilution	Source/Reference
Anti-rat IgG-Alexa Fluor 488	Goat, polyclonal against rat IgG, conjugated to Alexa Fluor 488.	1:600	Invitrogen Molecular Probes
Anti-rabbit IgG-Alexa Fluor 488	Goat, polyclonal against rabbit IgG, conjugated to Alexa Fluor 488.	1:600	Invitrogen Molecular Probes
Anti-rat IgG-Alexa Fluor 546	Goat, polyclonal against rat IgG, conjugated to Alexa Fluor 546.	1:600	Invitrogen Molecular Probes
Anti-rabbit IgG-Alexa Fluor 546	Goat, polyclonal against rabbit IgG, conjugated to Alexa Fluor 546.	1:600	Invitrogen Molecular Probes
Anti-mouse IgG-Alexa Fluor 546	Goat, polyclonal against mouse IgG, conjugated to Alexa Fluor 546.	1:600	Invitrogen Molecular Probes
Anti-mouse IgG-Alexa Fluor 405	Goat, polyclonal against mouse IgG, conjugated to Alexa Fluor 405.	1:600	Invitrogen Molecular Probes

Table 2-3 Secondary antibodies used in this study.
IgG stands for Immunoglobulin Gamma.

2.2.2 Confocal Microscopy

Stained whole mount preparations were examined using a Zeiss LSM 510 Meta confocal micro-system equipped with x10, x20, x40 (oil immersion), and x63 (oil/water immersion) objectives. The Diode laser excites in the visibe spectrum at 405 nm. The Ar laser can excite fluorophores with the following wavelengths in the visible spectrum: 458, 477, 488 and 514 nms. The He/Ne lasers of the can excite fluorophores with the following wavelengths in the visible spectrum: 543 and 633 nms. Alexa fluor-405-conjugated secondary antibodies excited with the 405 nm line and emit at ~420 nms. Alexa fluor-488-conjugated secondary antibodies excited with the 488 nm line emit at ~520 nms. TRITC-conjugated phalloidin and the Alexa Fluor 546-conjugated secondary antibodies excited with 543 nm line emit at ~575 nms.

For multi-track (multiple fluorophore labels) imaging, each wavelength was sequentially scanned for each optical section through the sample to excite each fluorophore individually and avoid bleed-through.

2.2.3 Image Processing

After acquisition of confocal images, the images files were opened with Ziess LSM software and transformed into “maximum-Z-stack projections” which superimpose serial optical sections into a single image. Unless stated otherwise images presented in this study represent maximal Z stack projections.

Pseudocolours were added to images generated by confocal microscopy using the software ‘Image J’ (National Institutes of Health, Washington) with the ‘Look Up Table’ function (‘LUT’). For single track/single flourochrome preparations no pseudocolour was applied as greyscale provides a higher degree resolution for the image. A green LUT was applied to images obtained from samples stained with Alexa fluor 488-conjugated secondary antibodies; and a magenta LUT was applied to samples stained with either Alexa fluor 546-or TRITC-conjugated secondary antibodies. LUTs replaced the greyscale value produced by the confocal microscope with colours. If a third flourochrome label was present this was kept in greyscale. Three-dimensional (3D) reconstruction of confocal stacks were performed using the Image J software using the ‘Maximum Projection’ function, which is a flattened composite of the brightest pixels found through the vertical (or

Z) axis of a given number of optical sections. Pseudocoloured 3D reconstructions or individual optical sections for co-localisation experiments were merged either using the Image J 'RGB Stack Merge' plug-in and saved as .tiff files or the individual flourochrome images were saved as .tiff (Tagged Image File Format) files, opened in Adobe Photoshop 7.0. converted into RGB mode and then merged as layers. These .tiff images files were processed, with brightness and contrast adjusted if necessary, using Adobe Photoshop 7.0. (Adobe Systems Inc., San Jose, CA). Figures were then assembled using Adobe Illustrator 10 (Adobe Systems Inc., San Jose, CA).

2.2.4 Cell Counts

For cell counts, stacks of optical sections obtained by confocal microscopy were opened using the LSM reader plugin (Input-output) in 'Image J' software (National Institutes of Health, Washington). The optical slices were converted into RGB colour mode (Image type) and then the slices were examined sequentially, and all labelled nuclei were marked manually using the point tool with automatic advancement of the slice (Auto-Next slice). After all optical slices had been examined and nuclei marked, the number of marked nuclei were counted and recorded.

2.2.5 Whole mount imaging

Epifluorescence microscopy was performed using a Zeiss SteREO Lumar.V12 Stereomicroscope, captured via a Zeiss Mrm Axiocam. Bright field microscopy for imaging of tarsi was performed using a Zeiss Axioskop 2 microscope using 5x, 10, and 20x objectives and captured via a Zeiss Mrm Axiocam. White balance was adjusted using the 'Level' Function in the 'Image' menu. Abdominal cuticular and external genital preps were obtained using a Zeiss Stemi 2000-C mount dissecting microscope with attached Sony cyber-shot digital camera. Images generated by the digital cameras were saved and stored as .tiff files. Images obtained by conventional microscopy were processed using Adobe Photoshop 7.0 (Adobe Systems Inc., San Jose, CA). Brightness and Contrast adjusted if necessary. Processed images were saved as .tiff files. Figures were assembled using Adobe Illustrator 10 (Adobe Systems Inc., San Jose, CA).

2.3 General Molecular Biology Protocols

2.3.1 Quantification of Nucleic Acids

The amount of DNA or RNA in a sample was estimated by taking Optical Density (O.D.) measurement at a wavelength of 260 nm using a NanoDrop 1000 spectrophotometer (Thermo Scientific). An $O.D._{260}$ =1 corresponded to ~50 µg/ml of double stranded DNA. An $O.D._{260}$ =1 corresponded to ~40 µg/ml of double stranded RNA.

2.3.2 Polymerase Chain Reaction (PCR)

Taq polymerase (New England Biolabs) was used for diagnostic PCR, and Phusion high fidelity DNA polymerase (New England Biolabs) was used for applications requiring high fidelity amplification. The PCR mix was set according to manufacturer's instruction. For PCR using *Taq* polymerase (New England Biolabs) the conditions were the following: initial denaturation- 5 min at 95ºC; denaturation- 50 sec at 94ºC, annealing- 40 sec at a temperature °C appropriate to the primer pair employed as determined by TmºC – 5ºC, extension- 1 min at 72ºC, where denaturation through extension was repeated for 30-35 cycles, followed by a final extension at 72ºC for 5 min.

Primer Name	Sequence (5'-3')	Tm (ºC)
dsx-dsxJFSeq	AGTTGAAGCGAAGGCGTTTC	61.8
dsx-dsxJRSeq	TGCTGAGGAGTCAAACGG	58.4
G0-for	CAAGTGCTCCAAAGAAAAACCG	66.5
G0-back	CTTCCGATGATGATGTCGCAC	55.0
rp49-for	TCCTACCAGCTTCAAGATGAC	66.0
rp49-rev	GTGTATTCCGACCACGTTACA	66.0

Table 2-4 Primers used in this study for the generation of PCR random primed probes for Northern analysis.

2.3.3 Primer Design

Primers used in this study were designed with the help of MacVector 7.2.2 (Oxford Molecular) software purchased from Invitrogen. The T_m of primers was calculated using MacVector software. The primers were ordered from Sigma-Aldrich (Dorset, UK). A description of the primers used for PCR can be found in Table 2.4.

2.3.4 Northern blotting of PolyA+ mRNA

2.3.4.1 Isolation of total RNA

Whole sexed flies of the appropriate genotypes were collected and snap frozen in liquid nitrogen and stored at -80ºC. RNA isolation preparation was performed under ribonuclease-free (RNAse-free; RF) conditions using RF materials. Whole RNA isolation was performed on 1 gm of collected flies per sample contained in a 50 ml centrifuge tube. 10 ml of the phenolic TRIzol Reagent (Invitrogen) was added and the materials emulsified using a Polytron PT10/35 GT benchtop homogenizer on a ST-P10/600 Stand with a 5mm Polytron generator attached for 1 minute at maximal speed from the moment the tissues were sufficiently thawed to liquid state. The homogenised mixture was incubated for 5 min at R/T prior to addition of 2 ml Chloroform. The sample tubes were inverted/shaken and then incubated for 3 min at R/T. The samples were then centrifuged at 12000 rcf for 15 min at 4ºC to pellet insoluble materials such as cuticle and achieve phase separation. The upper aqueous phase containing the RNA were then transferred to a new 50 ml centrifuge tube without disturbing the lipid meniscus separating the upper from lower layer and insoluble pelleted materials. 5 mls of isopropyl alcohol was then added to each sample, the samples inverted and then incubated for exactly 10 mins at R/T to precipitate the RNA. The samples were then centrifuged at 12000 rcf for 10 min at 4ºC to pellet the precipitated RNA. The supernatant was then removed and the pellet washed with 10 ml of ice cold 75% ethanol. The samples were than centrifuged at 12000 rcf for 5 min at 4ºC. Remove The supernatant was carefully removed and the pellet allowed to air-dry for ~5 min. The pellet was resuspended in 1 ml of RNAse-free water. Samples were then stored at -20ºC. RNA samples were then quantified (Nanodrop 1000 Spectrophotometer, Thermo Scientific) and 10 µg of each sample were then run on a 1% agarose MOPS/Formaldehyde denaturing gel at 5 volts/cm (using Ambion's NorthernMax Kit) with 5 µg 0.24-9.5 kb RNA ladder (Life Technologies) to assay integrity of the RNA samples visually via realisation on a ultra violet (UV) trans-illuminator.

2.3.4.2 Isolation of PolyA+ mRNA

Isolation of PolyA+ mRNA from 500 µg starting material of total RNA samples performed using the PolyATtract® mRNA Isolation Systems (Promega) via a

biotinylated oligo(dT) primer that hybridizes at high efficiency in solution to the 3´ poly(A) region present in *Drosophila* mRNA. The hybrids are captured and washed at high stringency using streptavidin coupled to paramagnetic particles and a magnetic separation stand. The mRNA is eluted from the solid phase by the addition of RNAse-free deionized water. A 0.1 volume of 3M sodium acetate (pH 5.2) and 1.0 volume of isopropanol was added to the eluate mRNA samples, then incubated at –20ºC overnight. The samples were then centrifuged at 12000 g at 4ºC for 10 min to pellet the mRNA. The supernatant was removed and the RNA pellets resupended in 1ml of 75% ethanol before centrifuging again at 12000 g at 4ºC for 10 min. The supernatant was removed and the pellets allowed to air dry ~5 min. The pellets were then resuspended in 5 µl volumes of RNAse-free deionized water.

2.3.4.3 Northern blotting

The total amount of each mRNA samples in a 5 µl volume was run at 5 volts/cm on a 1% agarose MOPS/Formaldehyde denaturing gel (NorthernMax Kit; Ambion) with 5 µg 0.24-9.5 kb RNA ladder (Life Technologies) using the Owl B3 Mini Gel System with built-in recirculation (‘Buffer Puffer’; Thermo Scientific). The denaturing gel underwent capillary blotting onto BrightStar-Plus positively charged nylon membrane using the NorthernMax (Ambion) kit reagents. After overnight transfer the RNA was fixed to the membrane via UV crosslinking at $12x10^4$ µJ/cm^2 using a Stratalinker (Stratagene).

2.3.4.4 Preparation and labelling of PCR DNA probes with ^{32}P

Probes were created by a 3´ exonuclease-deficient Klenow fragment of DNA polymerase I [(exo-) Klenow] random labelling a random hexanucleotide primer/template DNA complex with a nucleotide reaction mix containing 5ul of (3000 Ci/mmol) [α–^{32}P]dCTP using the Prime-It II Random Primer Labeling Kit (Stratagene). The subsequent reaction mix was purified of non-incorporated [α–^{32}P]dCTP radio-nucleotide using Micro Bio-Spin Columns with Tris buffer (BioRad).

Probes were denatured by boiling for ~2 min before snapping back on ice and were used at a concentration of between $0.5x10^7$ - $1x10^6$cpm/ml in the hybridisation buffer.

2.3.4.5 Incubations and washing

Membranes were prehybridised at 42ºC for >3 hr in ULTRAhyb (Ambion) Ultrasensitive Hybridization Buffer (preheated to 65ºC). Membranes were then hybridised overnight at 42ºC. The probe/hybridisation buffer was removed and the membrane washed in NorthernMax Low Stringency Wash Buffer #1 (2X SSC or SSPE, 0.1% SDS; Ambion) for 5 min at R/T. The membrane was then washed twice for 5 min in NorthernMax Low Stringency Wash Buffer #1 at 42°C. The membrane was then washed twice for 15 min in NorthernMax High Stringency Wash Buffer #2 (0.1X SSC or SSPE, 0.1% SDS; Ambion) at 42°C.

2.3.4.6 Autoradiography

Autoradiography of probed filters was carried out at –70ºC in a cassette with intensifying screens and exposed to Konica Medical film, for as long as required. Films were developed using a Kodak X-Omat X-ray film processor.

2.3.4.7 Re-screening filters

Membranes required to be re-screened with different probes were allowed to have the previous probe decay off naturally before undergoing pre-hybridisation and hybridisation as described above.

2.4 Behavioural Analyses

2.4.1 Equipment

2.4.1.1 Chambers

Prior to behavioural recordings, flies were introduced into the appropriate chamber by aspiration through a small opening in the side of the chamber. For locomotion, courtship behaviour and song recordings, round chambers 1 cm in diameter and 0.4 cm in height with a nylon mesh base were used, courtship latency was measured in larger round chambers (2 cm diameter x 4 mm height). The chambers have a Perspex top to allow the camera to record the movements and activities of the flies.

2.4.1.2 Cameras

A Sony DCR VX2100E camera was used for all behavioural song recordings. The camera was mounted on an adjustable mount, and prepared for the recording by turning the power dial to ‘Camera’. The camera was then positioned over the recording chamber, and the image on the LCD screen was sharpened using the focus and zoom rings. The audio input cable was connected to the MIC jack, and the input was switched to LINE. Sony Mini-DV (60 min SP) tapes were used in the camera. During the recording, each tape was given a name, and the date, genotype, time recording started, time recording ended, comments on recording, and eventual file name were noted on a logging sheet.

2.4.1.3 Insectavox

The Insectavox (Gorczyca and Hall, 1987) is an integrated enclosure in which the courtship song of *Drosophila* males was recorded. The enclosure consists of three separate compartments: one containing a modified electret condenser microphone, a second containing the electronics (attenuator, pre-amplifier circuit, and a capacitor), and a third containing a low noise power supply and a transformer. The microphone is contained in an acoustically insulated compartment to minimize the environmental noise on the recording. For recordings, the courtship chamber was placed directly onto the microphone, and the flies were viewed through a glass lens in the top of the Insectavox.

2.4.2 Computing

2.4.2.1 Computer

All computations for behavioural analyses were performed on a Power Mac G5 (Apple).

2.4.2.2 Digitising and Compressing

Behavioural recordings were digitized and compressed using FootTrack (v2.3.2) software (T-Squared Software). To digitise the tapes, the camera was connected to the G5 by a firewire cable. The tapes were then rewound, and to start digitizing, FootTrack was opened, and the ‘New Tape’ command under the ‘File’ menu was selected. The tape was given a name, and the type of tape selected was Hi8, with

a 60 min recording time. Next, the ‘Import’ command was selected, and the ‘OK’ button was clicked. Digitised files were stored by FootTrack as .dv extensions.

Digitised files were compressed using FootTrack software. Files to be compressed were highlighted and the ‘Compress’ option was selected. The type of compression selected was H.164. Compressed files were stored by FootTrack as .mov extensions.

Files stored in FootTrack as .mov extensions were given names corresponding to the file names given on the initial behaviour logging sheet. Each tape was named by highlighting the file by clicking on the snapshot and pressing the ‘i’ button.

2.4.2.3 LifeSong X

The LifeSong X program was obtained from J. Hall, A. Villella and J. Rieffel at Brandeis University (Villella *et al*., 2005).

2.4.3 Behavioural analyses

For behavioural assays flies were raised at 21°C in a 12:12 hr light:dark cycle. Individual virgin adults were collected and aged for 5 - 7 days post-eclosion at 25°C and assays carried out at 25°C.

2.4.3.1 General sensiro-motor behavioural analyses

Locomotion: Activity was measured in round courtship chambers (1 cm diameter × 4 mm high). 10 min recordings of single males were made, and the number of times the fly crossed a line across the middle of the chamber during the recording were counted (Kulkarni and Hall, 1987;Villella *et al*., 1997). Activity was measured as the number of line crossings per minute.

Flight: 200 (for winged) or 20 for (‘de-winged’) flies of the appropriate genotypes were dropped in at the top of a 500 ml graduated cylinder the inside wall (5 cm in diameter) of which was coated in paraffin oil. When released into the cylinder, flies with wild-type flight capabilities immediately initiate flight, striking the wall and becoming embedded in the oil near the top. Flies lacking flight capability drop farther before becoming stuck. Thus the distribution of flies over the vertical length of the cylinder is a function of flying capability (Benzer 1973; Elkins et al., 1986).

Olfaction: Flies of the appropriate genotypes were collected and aged for 4 - 7 days post-eclosion. These flies were then stored in single-sex groups of five individuals in clear plastic 2.5 x 9.5 cm culture vials without medium for 3-6 hr before testing. The vials were marked with two lines, 3 and 6 cm from the bottom. A cotton swab dipped in benzaldehyde (Sigma) was inserted so the tip lined up against the 6 cm mark, protruding centrally ~1 cm below the cellulose wool plug. The vial was placed on its side and the flies were given 15 sec to recover from the disturbance during the insertion of the plug with swab. Then 10 counts of the number of flies in the bottom compartment of the vial, demarcated by the 3 cm line, were taken at 5 sec intervals, starting from the 15 sec recovery time point. The behaviour of the flies in the vial was quantified as the "avoidance score", calculated as the number of flies in the bottom sector of the vial, averaged over the 10 measurements (Mackay et al., 1996). Ten replicate assays were done of males and of females for four concentrations of benzaldehyde ranging from 0 – 0.6%.

Taste: Flies used for measuring proboscis extension reflex (PER; Goredesky-Gold et al., 2008) were aged for 1 – 2 days following eclosion as older flies are more easily damaged during the handling process and produce lower responses. Prior to testing, flies were starved in vials for approximately 21 hrs on filter paper saturated in distilled water to prevent dehydration. For each experiment, flies (>70 males and females of varying genotypes) were anesthetized using CO_2 and affixed by the middle of their dorsal thorax to the tip of a wooden swab stick using 2 µl of Tissue Tack Adhesive (Electron Microscopy Sciences). Immobilized flies were placed horizontally and allowed to recover for 3 hrs at 25ºC. Before initial testing, flies were permitted to drink water to satiation from a pipette tip. Similarly, flies were also offered water to satiation between stimulations. Tarsal PER assays were conducted using a micropipette (Eppendorf) containing the experimental appetitive and aversive solutions (100 mM Sucrose and 75 mM Caffeine respectively) to stimulate anterior tarsi bilaterally (Goredesky-Gold et al., 2008). Flies were retested with water applied to the tarsi at the end of each sweetener test. Trials in which flies responded to water were not included in the analyses as the responses to the sweeteners were considered non-specific. Flies were typically tested with 1 – 6 stimuli during a single assay. Testing of one stimulus was completed before beginning the next stimulus with an interstimulus interval of 3 – 5 min.

2.4.3.2 Male courtship behavioural analyses

Males tested for fertility were collected at eclosion (kept in groups ≤10) and aged for 5 days. Then they were placed individually in food vials containing three wild-type virgin females of the same age. All vials were scored for presence of larval progeny over a 7 day period (Gailey and Hall, 1989). Vials containing a dead male and no progeny were discounted. Females in vials in which no progeny were apparent after 7 day were then re-mated with wild-type males to then assure the receptivity/fertility of these target females.

Courtship behaviour was as described in Villella et al. (1997) and was measured in the chambers as described above. Essentially an individual male aged 3 - 5 days old (of varying genotype) and a single wild-type CS virgin ‘target’ female of the same age were introduced into the chamber and observed for a 10 min period. The courtship index (CI) was measured as the proportion of time in 10 min that the ‘courter’ spent exhibiting courtship behaviours towards the ‘target’ female (as per Villella *et al*., 1997). Courtship behaviours are defined here as: following, orientation, tapping, wing extension, and abdominal curling/attempted copulation.

Courtship initiation is the time elapsed between introduction of flies and first exhibition of courtship behaviour by the male towards the target female (as per Villella et al., 1997).

% Mating in a 4 hr period was the number of male flies, as a percentage, that were observed successfully copulating within this time frame as (Rideout et al., 2010).

2.4.3.3 Male courtship song analyses

Several courtship song parameters were calculated, including the number of pulse trains per minute (PTPM) (Villella *et al*., 1997), the number of sine song bouts per minute (SBPM) (von Schilcher, 1976), the mean number of pulses per train (MPPT) (Villella *et al*. 1997), the number of cycles per pulse (CPP) (Villella *et al*. 1997), and the interpulse interval (IPI) (Kawanishi and Watanabe, 1980). PTPM was calculated as (total number of pulses in 5 min recording/time in sec of recording) x 60. SBPM was calculated as (total number of bouts of sine song in 5 min/time in sec of recording) x 60. MPPT was calculated as the average number of pulses per train from all pulse trains where number of pulses was >2. CPP was

calculated as the number of peaks per pulse from the first 10 pulse trains where pulses/train >10. IPI was calculated as the mean time between consecutive pulses in a pulse train, and was calculated from all pulse trains where the number of pulses per train >2.

2.4.3.4 Female courtship behavioural analyses

Females tested for fertility were collected at eclosion (kept in individual vials) and aged for 5 days. Then they were placed individually in food vials containing three wild-type virgin males of the same age. All vials were scored for presence of larval progeny over a 7 day period (Rideout et al., 2010). Vials containing a dead female and no progeny were discounted. Males in vials in which no progeny were apparent after 7 days were then re-mated with wild-type females to then assure their fertility.

Egg laying was measured by counting the number of eggs present per day in vials in which individual females (of varying genotypes) were introduced to three wild-type males (Rideout et al., 2010). After one day the females and males were transferred to a fresh vial and the old vial was then examined for the presence of eggs. This assay was performed over five days. Any set of vials in which the target female died during the assay was discounted. To aid in the detection of the (white) eggs, inactivated charcoal was added to the food (prior to being added into the vial) rendering the food colour black.

% Copulating over time is a measure of the number of females (of varying genotypes) observed to successfully copulate with a wild-type male, measured in ten min intervals over a 1 hr period (Rideout et al., 2010).

Locomotion during mating was a measure of the number of times a copulating pair crossed a demarcated line in the courtship chamber per min during the time spent copulating (as per Waterbury et al., 1999).

Copulation duration was the observed time (in sec) elapsed between the beginning of mating and its termination (as per Billeter et al., 2006a).

% re-mating is a measure of the number of females (of varying genotypes) that were successfully re-mated by the same wild-type male over a 4 hr period (Rideout et al., 2010).

For sperm and SP transfer experiments (as per Villella et al, 2006), target females of appropriate genotypes and control and test (GFP expressing) males were collected and aged for 5 days. Male and female pairs were introduced into a courtship chamber and observed over a 2 hr time period for successful copulation. When copulation was observed the female then had her internal genitalia dissected and examined 15 min after mating to assay the presence of the sperm/seminal package as indicated by a GFP signal.

2.5 Statistics

Behavioural means compared using Tukey-Kramer HSD statistical test where indicated. For Fisher's exact test used for fertility assays, 2-tail p-values were compared to wild-type. Egg laying data subjected to Dunnett's test with wild-type as the set control. Cell counts were subjected to Student's t-test. For song analyses the IPI for each genotype was calculated as the mean of *n* intramale means. CI, WEI, and SI values were transformed using the square root arcsine transformation to approximate normality. These transformed values were subjected to one-way ANOVA analysis. Untransformed values for PTPM, SBPM, MPPT, CPP, and IPI were subjected to one-way ANOVA. Statistical tests performed with JMP v6.0 software (SAS Institute).

3 Characterisation of the novel *dsx*^{GAL4} allele

3.1 Molecular characterisation of the novel *dsx*^{GAL4} allele

Extensive and varied molecular and genetic analyses have been performed at the *dsx* locus yet there still remains much to be discerned as to when and where *dsx* is active within the developing fly and how this activity then results in establishing a complete dimorphic adult. This is in part due to the limitations of the genetic tools available for marrying our understanding of the underlying genetic processes involved in *dsx* expression with the end point physiological and behavioural processes (both sex- and non-sex-specific) that delineate male and female adult flies. Therefore, as previously described (see section 1.8.2.1), to allow detailed anatomical, neuro-anatomical and functional analyses of *dsx*-expressing cells to be performed, the technique of ends-in homologous recombination was employed by Dr. Elizabeth Rideout in 2007 to insert the coding sequence of the yeast transcription activator protein GAL4 into the first, non-sex-specific, coding exon of *dsx*, creating a tandem duplication (Figure 3.1) (Rideout et al., 2010).

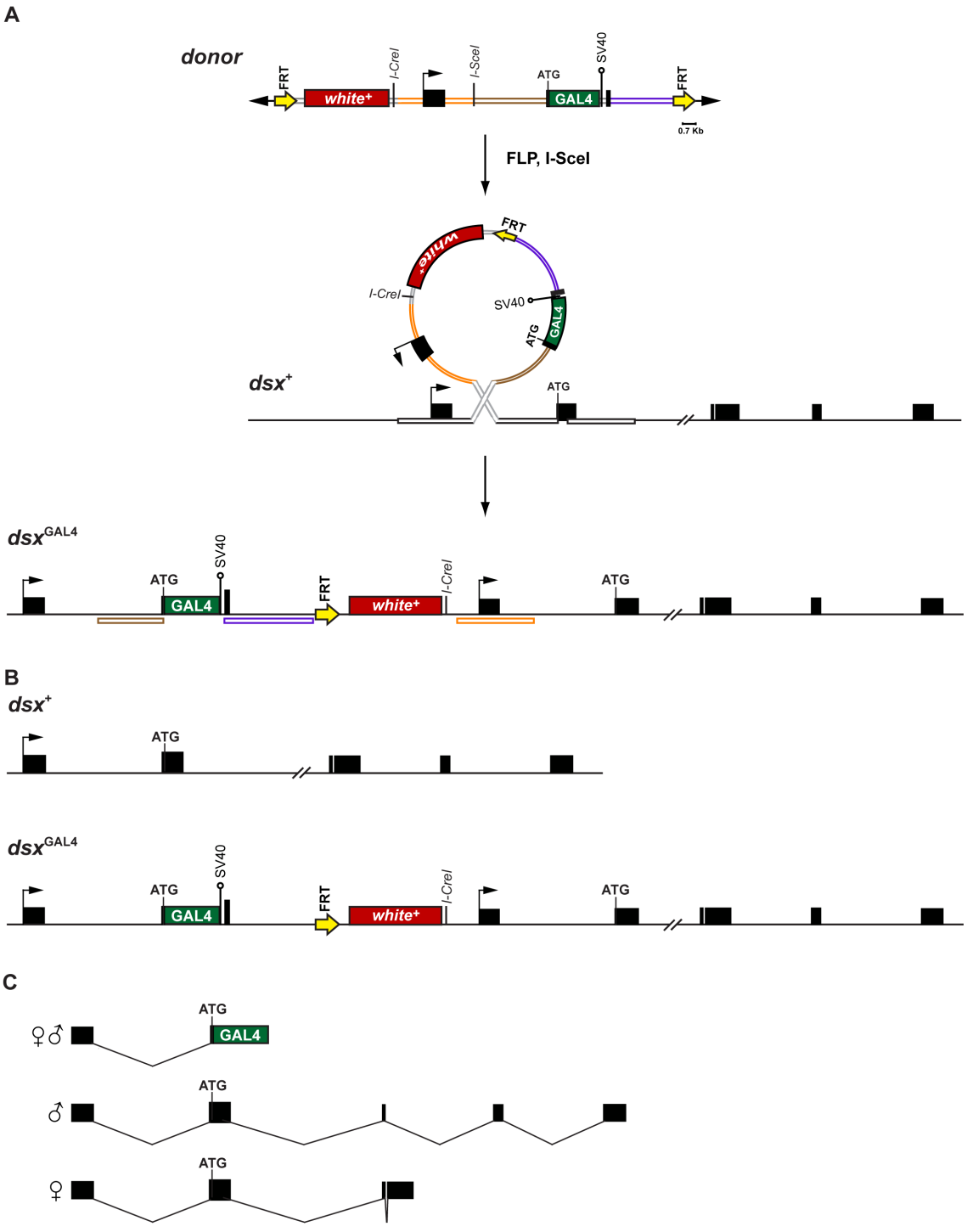

Figure 3-1 Schematic of the integration of GAL4 into the *dsx* locus and the predicted resultant transcripts for the *dsx*^{GAL4} allele.
(A) To arrive at the *dsx*^{GAL4} transgenic line a transgenic fly containing the *dsx* P-element targeting (donor) construct located to the second chromosme was generated. The donor P-element contained two FLP-recombinase recognition FRT sequences (yellow arrows), an I-*Cre*I recognition site, a I-*Sce*I recognition site, the GAL4 open reading frame (green box), and three regions of homology to the endogenous *dsx* locus: fragment I (orange): fragment II (brown): and fragment III (purple). Solid black boxes represent position of exons, and raised black arrows represent transcriptional start sites. Following integration of the donor P-element the donor sequence was excised and linearised using *hs-FLP* and *hs-I-SceI* respectively. Recombination to the *dsx* locus was detected by the third chromosome expression of the *white*$^{+}$ marker in an *ey-FLP* background (*dsx*^{GAL4}). (B) Comparative schematic representation of *dsx* (*dsx*$^{+}$) and *GAL4* knock-in allele (*dsx*^{GAL4}). (C) Schematic representations of the predicted male and female *dsx*^{GAL4} locus transcripts. Figures adapted from Rideout et al. 2010.

As the resulting integrant is essentially a duplication of the locus, it is predicted that the allele should express a GAL4 product that reiterates the endogenous gene expression in conjunction with that of the endogenous gene transcripts. I therefore performed Northern blot analyses of sexed adult polyA+ mRNA from wild type *Canton-S* (CS) and dsx^{GAL4} flies to confirm that this resulting allele, designated dsx^{GAL4}, produced both the expected endogenous wild type *dsx* and GAL4-containing transcripts in both sexes (Figure 3.2) (Rideout et al., 2010). The DSX probe hybridizes to the first non-sex-specific coding exon common to all *dsx* transcripts (Figure 3.2), comprising nucleotides 980-1762 (GenBank Acc. AY060257), and should therefore result in the identification of two male-specific and one female-specific set of transcripts (Burtis and Baker, 1989). In wild type CS males the DSX probe detected two bands: one 2.8 kb and one 2.6 kb band. In CS females a single 2.7 kb band was detected with the DSX probe. In homozygous dsx^{GAL4} males and females, the transcripts detected were the same size as those observed in wild type males and females, indicative that no disruption of endogenous *dsx* transcription had occurred. The GAL4 probe hybridizes to the GAL4 coding region, nucleotides 499-844 (GenBank Acc. K01486). No GAL4-positive transcripts were detected in either wild-type CS males or females, whereas a single transcript of approximately 2.9 kb was observed in both dsx^{GAL4} homozygous males and females, again indicative that GAL4 is being actively transcribed only in the dsx^{GAL4} flies.

When homozygous, or examined *in trans* with the *dsx* deficiency ($Df(3R)dsx^{15}$), neither male nor female dsx^{GAL4} flies exhibited any overt morphological abnormalities either in internal genitalia (including neuronal innervations ramifying on the genitalia) or external sexual characteristics (data not shown). As well, fertility for both male and female dsx^{GAL4} flies was unaffected ($p>0.05$, $n>45$**)** (Rideout et al., 2010). As such I concluded that the insertion of an operative GAL4 sequence into the *dsx* locus resulted in no overt disruption of endogenous *dsx* gene function

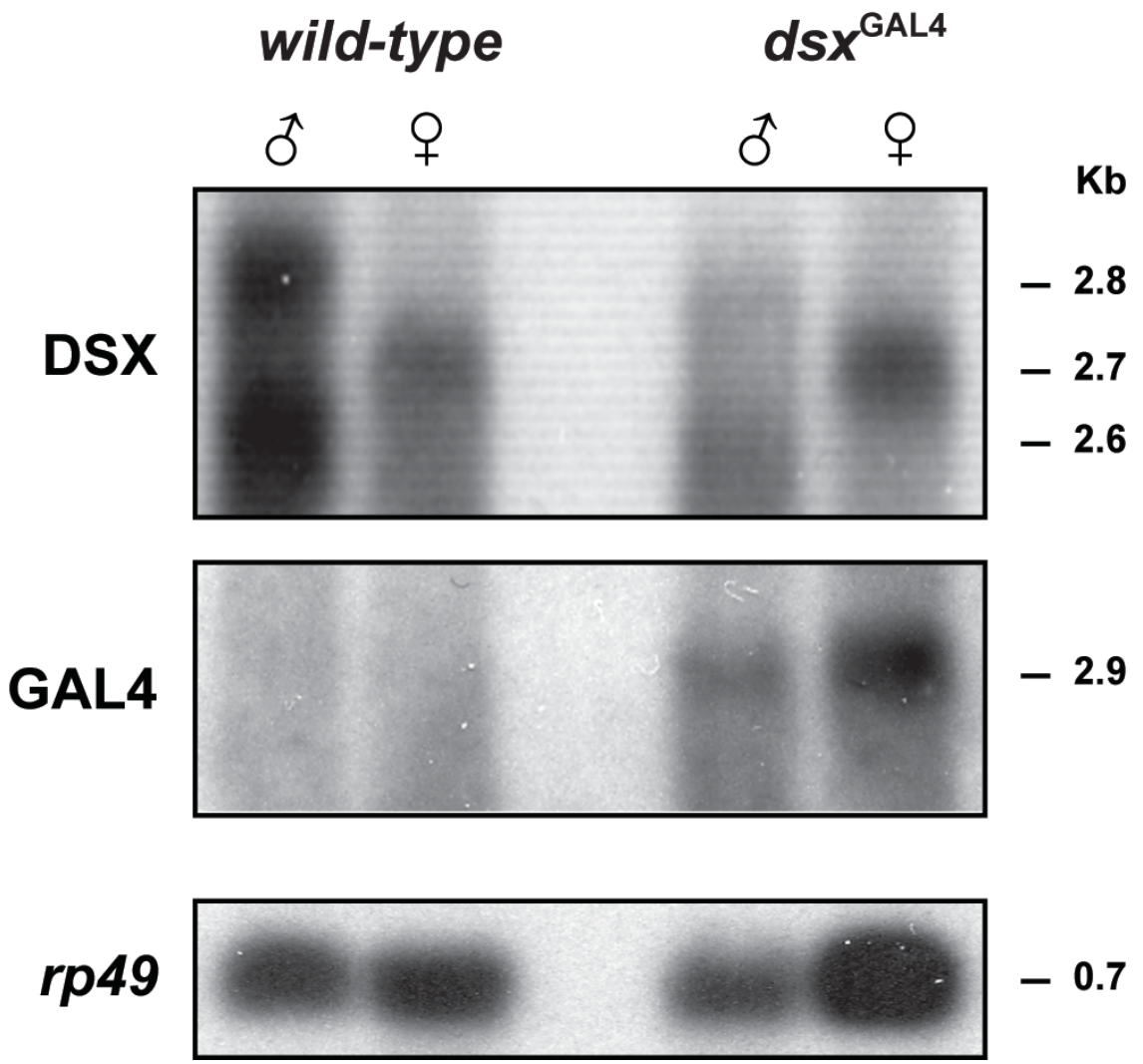

Figure 3-2 Northern blot analysis of sexed adult polyA+ mRNA from wild-type *Canton-S* (*CS*) and *dsx*^{GAL4} flies.
The DSX probe hybridised to the first non-sex-specific coding exon common to all *dsx* transcripts (nucleotides 980-1762; GenBank Acc. AY060257), resulting in the detection of two (one 2.8 kb and one 2.6 kb) bands in males and a single (2.7 kb) band in females. In males and females homozygous for the *dsx*^{GAL4} allele the transcripts detected were the same size as observed for wild-type males and females. The GAL4 probe hybridised to the GAL4 coding region (nucleotides 499-844; GenBank Acc. K10486). No GAL4-positive transcripts were detected in either wild-type males or females, whereas a single (2.9 kb) band was observed in both males and females homozygous for the *dsx*^{GAL4} allele. The blot was subsequently probed with *rp49* to determine RNA loading for each lane. Figure adapted from Rideout et al. 2010.

3.2 *dsx*^{GAL4} reiterates endogenous *dsx* expression

It has been previously demonstrated that Dsx is expressed in both the male and female pupal and adult CNSs in a small population of neurons (Billeter et al., 2006b; Lee et al., 2002; Rideout et al., 2007; Sanders and Arbeitman, 2008). To confirm the *dsx*^{GAL4} allele's ability to reiterate endogenous dsx expression in both sexes I performed colocalisation experiments using a *dsx*-specific antibody (kind gift of Michele Arbeitman), which localizes to the nuclei (Sanders and Arbeitman, 2008) and a GAL4 responsive transgenic reporter expressing nuclear GFP driven

by *dsx*^{GAL4}. These experiments demonstrated that the novel *dsx*^{GAL4} allele directs GAL4 expression in all described *dsx*-expressing neuronal clusters in pupal and adult CNSs of both sexes (Figures 3.3 and 3.4) though it does not completely reiterate expression in all endogenous *dsx*-expressing cells (Lee et al., 2002). However this iteration of *dsx's* endogenous expression pattern within the CNS compellingly demonstrates the *dsx*^{GAL4} allele's sensitivity and specificity as a reporter of *dsx*.

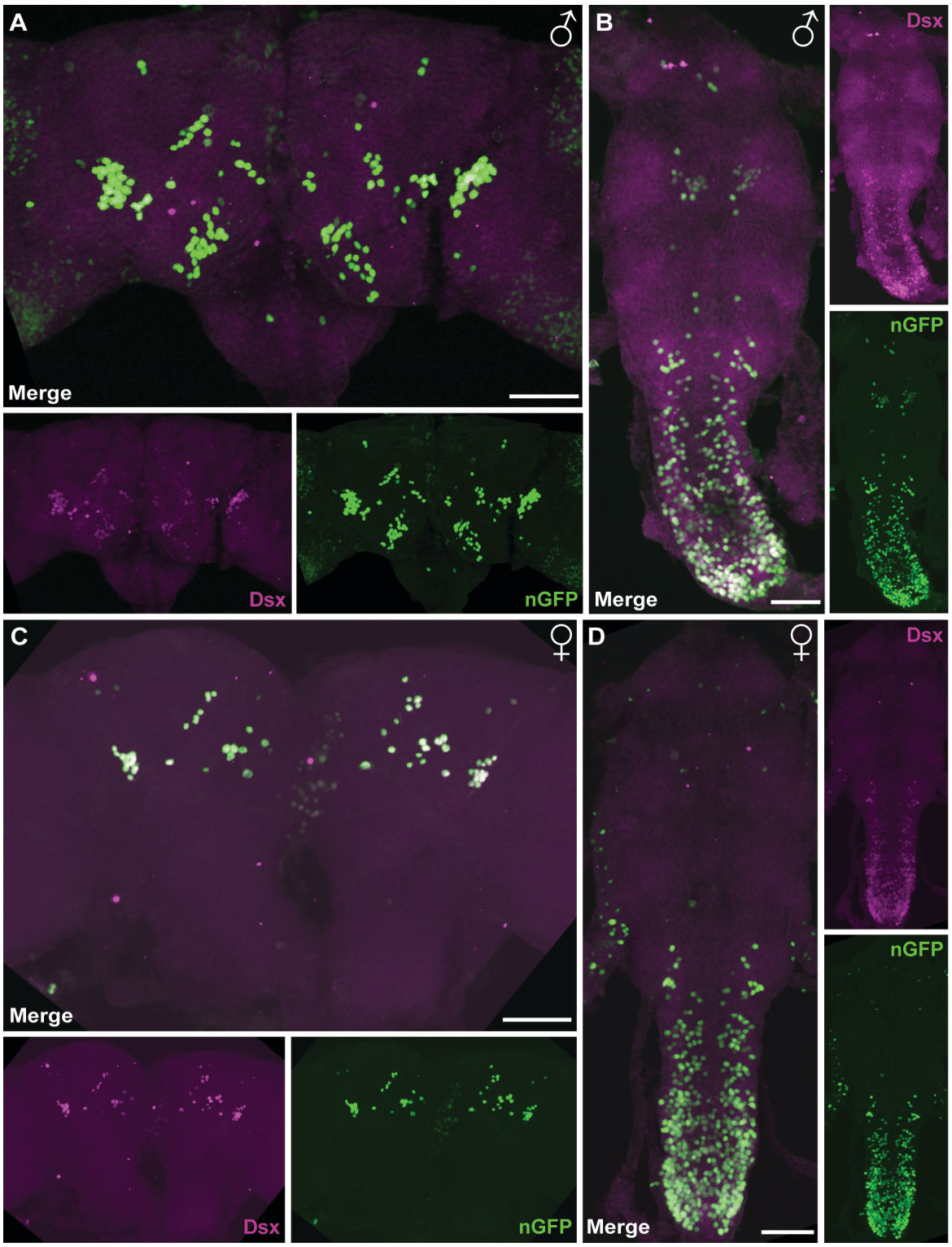

Figure 3-3 Co-expression of *dsx*^{GAL4} responsive nGFP and Dsx in male and female 2 day old pupal CNSs.
Male *dsx*^{GAL4} expressing UAS-StingerII co-stained with anti-Dsx (A) brain and (B) VNC. Female *dsx*^{GAL4} expressing UAS-StingerII co-stained with anti-Dsx (C) brain and (D) VNC. nGFP, green. Dsx, magenta. Ventral view, anterior up. Scale bar = 50 µm.

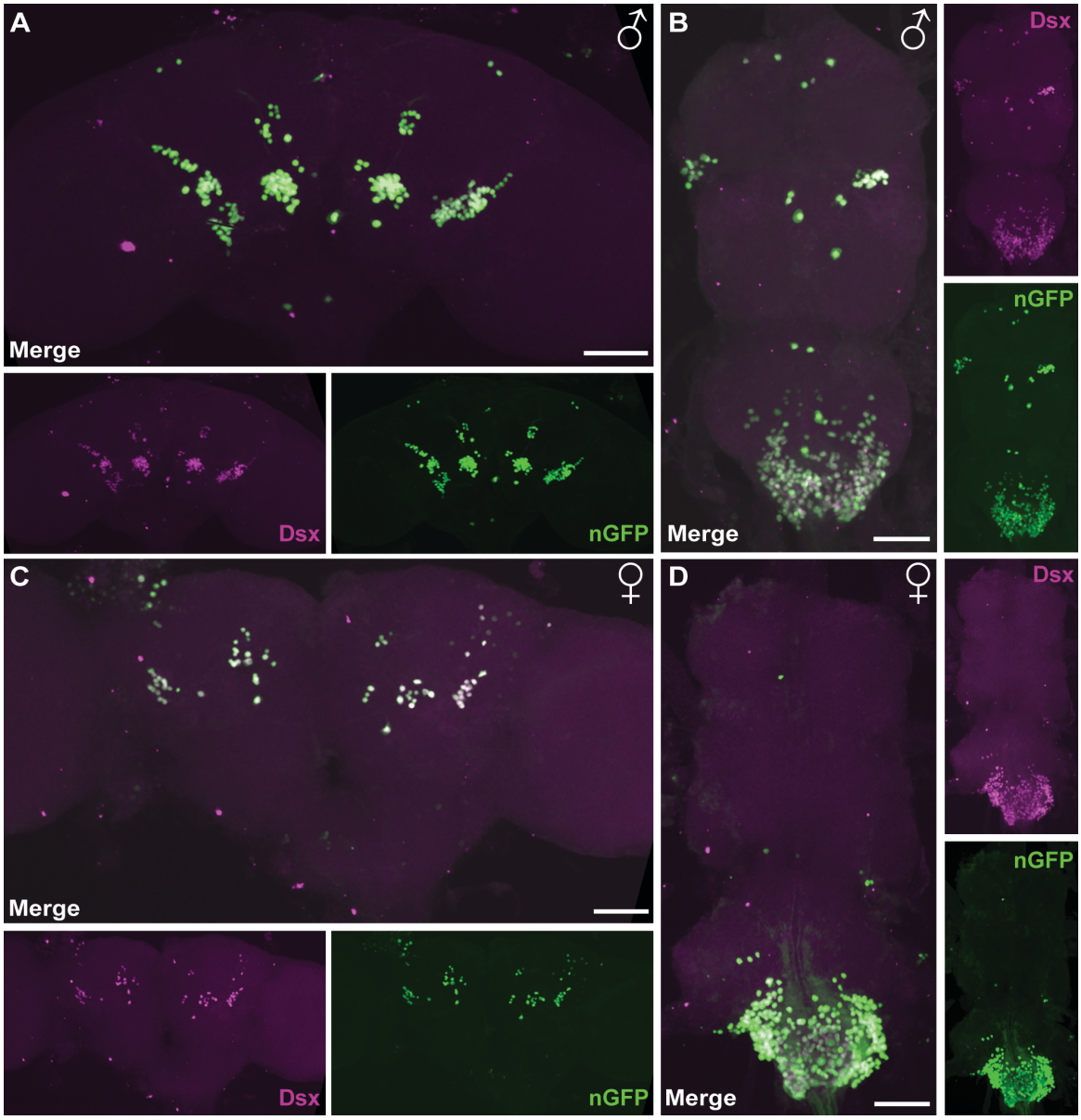

Figure 3-4 Co-expression of *dsx*^{GAL4} responsive nGFP and Dsx in male and female 5 day old adult CNSs.
Male *dsx*^{GAL4} expressing UAS-StingerII co-stained with anti-Dsx (A) brain and (B) VNC. Female *dsx*^{GAL4} expressing UAS-StingerII co-stained with anti-Dsx (C) brain and (D) VNC. nGFP, green. Dsx, magenta. Ventral view, anterior up. Scale bar = 50 µm.

3.3 *dsx*^{GAL4} can direct a sex-specific program of morphogenesis

3.3.1 dsx directed somatic sexual determination and differentiation of secondary sexual characteristics

As previously described *dsx* is central to somatic sex determination in *Drosophila* and has been shown to be necessary, though not sufficient for the establishment of both male and female somatic sexual characteristics (Billeter et al., 2006a; Camara et al., 2008; Christiansen et al., 2002; Simpson, 2002). *dsx* encodes

transcription factors which may act independently, in concert, or in parallel with other regulatory agents (Camara et al., 2008; Christiansen et al., 2002; Simpson, 2002). In the fly two sex-specific *dsx* isoforms maybe transcribed; the male-specific Dsx isoform (Dsx^M) or the female-specific Dsx isoform (Dsx^F), transcription of these sex-specific *dsx* isoforms dependent upon upstream elements of the sex determination hierarchy (SDH) (Camara et al., 2008; Christiansen et al., 2002; Simpson, 2002). In the absence of the upstream regulators of the *Drosophila* SDH, *Sxl* and *tra*, the male-specific Dsx^M isoform is produced and a program of male sexual differentiation is occurs by default. This results in a fly with male-specific darkly pigmented dorsal cuticular plates (tergites) on the 5^{th} and 6^{th} abdominal segments, male genitalia and possessing sex-combs, a specialized row of 10-12 densely packed, blunted/thickened and highly pigmented curved mechanosensory bristles orientated longitudinally with respect to the leg, which are restricted to the medial aspect of the distal T1 tarsi of the foreleg (Ahuja and Singh, 2008; Barmina and Kopp, 2007) (Figure 3.5A). When *Sxl* and *tra* are active the female-specific Dsx^F isoform is produced, and a female program of sexual differentiation occurs. This results in a fly with a pattern of lighter pigmentation restricted to the dorsal posterior stripe as present on the tergites of both sexes on abdominal segments A2 to A6 (Figure 3.5B), female genitalia and, on the area analogous to that of the male sex comb, a row of ~4-5 transverse bristles (TVBs) that are thinner, less pigmented and orientated at ~90º compared to that of the male sex combs (Barmina and Kopp, 2007) (Figure 3.5B).

3.3.2 Effects of restricted overexpression of the male- and female-specific Dsx isoforms via GAL4 responsive transgenes

As stated above the ability of *dsx* to determine secondary sexual characteristics had been established through analyses of mutants, or ubiquitous over-expression of the Dsx isoforms (Baker and Ridge, 1980; Jursnich and Burtis, 1993; Steinmann-Zwicky et al., 1990). I restrictively manipulated the sex of dsx^{GAL4}-expressing cells, assaying the consequences of over-expressing either Dsx^M or Dsx^F on secondary sexual characteristics, in order to establish dsx^{GAL4}'s ability to direct a sex-specific program of morphological development. Over-expression of Dsx^M resulted in masculinized XX females with male-like abdominal pigmentation and overt, with respect to thickness, orientation and pigmentation, though incomplete, with respect to bristle number, sex combs (Figure 3.5E; Table 3.1)

(Rideout et al., 2010). However the genitalia, while masculinized, were abnormally rotated and often malformed (Figure 3.5E) (Rideout et al., 2010). Expression of ectopic Dsx^M had no apparent effect on development in XY males (data not shown). Therefore, whilst Dsx^M is sufficient to manifest much of the male-specific programs of development, it is unable to overcome all effects of endogenous Dsx^F. Over-expression of Dsx^F resulted in XY males with female-like abdominal pigmentation, genitalia, and bristles morphologically more similar to TVBs in pigmentation and orientation (Figure 3.5F; Table 3.2), though with a slight but still significant increase in bristle number (4.7 ± 0.53 SD, n=28 vs 4.01 ± 0.53 SD, n=34**;** p<0.0001, Student's t-test) (Rideout et al., 2010). Again expression of ectopic Dsx^F had no apparent effect on development in XX females (data not shown). Thus Dsx^F appears sufficient to direct a female-specific program of development even when competing with endogenous Dsx^M production.

3.3.3 Effects of restricted overexpression of the female-specific Tra^F isoform via a GAL4 responsive transgene

Ectopic over-expression of the female-specific isoform of *tra* has been shown to result in female somatic differentiation (McKeown et al., 1987; McKeown et al., 1988; O'Dell et al., 1995; Rideout et al., 2010). As such I again restrictively manipulated the sex of dsx^{GAL4}-expressing cells, assaying the consequences of over-expressing Tra^F on the development of secondary sexual characteristics. Over-expression of Tra^F in XY males resulted in female-like abdominal pigmentation and intersexual genitalia (Figure 3.5H). The sex combs, although clearly showing the effects of feminisation, notably in the significantly reduced number of bristles, still appeared to be more masculine in bristle morphology in terms of thickness, pigmentation and orientation (Figure 3.5H; Table 3.1). Surprisingly however XX females expressing ectopic Tra^F appeared to have undergone some masculinising effects, rendering the genitalia more intersexual in appearance. The TVBs also appeared to have been masculinised with respect to pigmentation, orientation and number of bristles, presenting as more 'sex comb-like' (Figure 3.5G; Table 3.2).

3.3.4 Effects of restricted expression of RNA-mediated gene interference (RNAi) specific to genes of the sex-determination hierarchy via GAL4 responsive transgenes

XX female flies homozygous for loss-of-function *tra* or *tra-2* mutations are sexually transformed, developing as pseudo-males, indistinguishable from normal XY males in morphology and behaviour, though they are sterile (Baker and Ridge, 1980; Belote and Baker, 1987; Rideout et al., 2010). Using RNA interference I restrictively knocked-down endogenous Tra and Tra-2 specifically in dsx^{GAL4}-expressing cells. Strikingly, XX females developed as phenocopies, closely matching *tra* and *tra-2* loss-of-function mutants; exhibiting male-like abdominal pigmentation and genitalia and overt sex combs with respect to thickness, orientation and pigmentation, though incomplete with respect to bristle number (Figure 3.5G, H; Table 3.1) (Rideout et al., 2010). RNA interference of either Tra or Tra-2 had no apparent effect on development in XY males (data not shown).

While RNA interference of Fru would not be predicted to impinge on external sexual morphology, this was assayed in case interference of Fru^{M} would directly, or indirectly through repression of related male-specific identifiers, affect the *dsx*-mediated morphogenic program, particularly with respect to sex comb development in males. No overt effect was observed in XY males with respect to pigmentation, genitalia and sex combs (data not shown; Table 3.1) or with XX female morphological development (data not shown; Table 3.2) and both males and females were fertile (n=30; $p>0.05$).

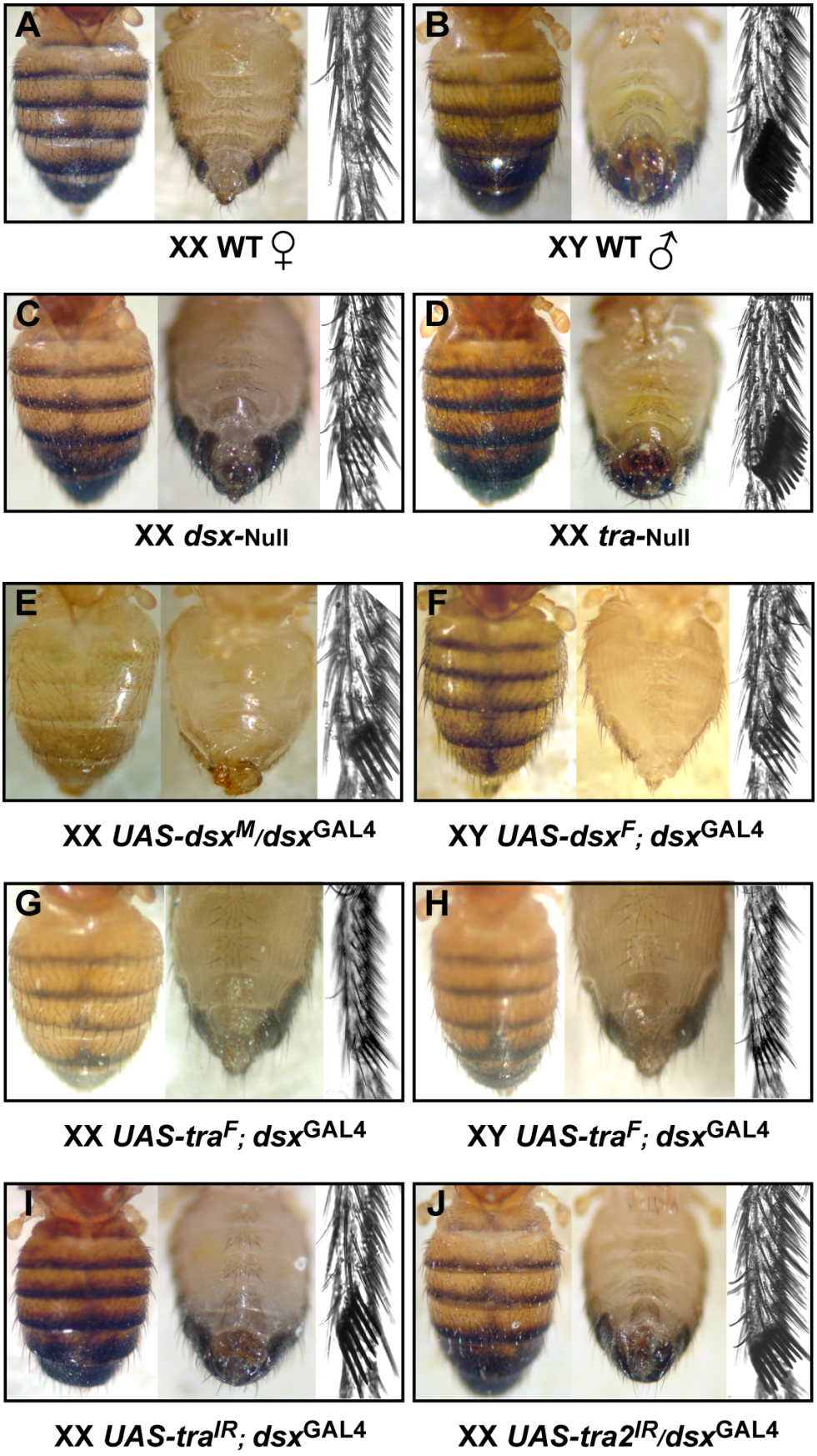

Figure 3-5 *dsx*^{GAL4} transformation of somatic sexual characteristics.
Shown are as follows; dorsal abdominal cuticular pigmentation; external genitalia; and foreleg basitarsal detail. (A) XY and (B) XX wild-type animals. (C) XX *dsx*-null intersexual animal. (D) XX *tra*-null pseudo-male. (E) XX *dsx*^{GAL4}/UAS-*dsx*^{M} pseudo-male. (F) XY UAS-*dsx*^{F}; *dsx*^{GAL4} pseudo-female. (G) XX UAS-*tra*^{F}; *dsx*^{GAL4} masculinised female.(H) XX UAS-*tra*^{F}; *dsx*^{GAL4} feminised male. (I) XX UAS-*tra*^{IR}; *dsx*^{GAL4} and (J) and XX *dsx*^{GAL4}/UAS- *tra-2*^{IR} pseudo-males.

Genotype (haplo-X) males	Mean no. of sex comb bristles
+/Y; +/+; *dsx*^{GAL4}/+ [a]	10.15 ± 1.02 (34)
yw^{-}/Y; +/+; *dsx*^{GAL4}/ UAS-*dsx*^{F} [b]	4.80 ± 0.41 (30) *, **
w^{-}/Y; UAS-*tra*^{F}/+; *dsx*^{GAL4}/+ [b]	6.20 ± 1.10 (30)*
w^{-}/Y; UAS- *tra*$^{IR(2560)}$/+; *dsx*^{GAL4}/+ [a]	5.62 ± 0.71 (32) *, ***
w^{-}/Y; +/+; *dsx*^{GAL4}/UAS- *tra*$^{IR(2561)}$ [a]	5.33 ± 0.61 (30) *, ***
w^{-}/Y; +/+; *dsx*^{GAL4}/UAS- *tra-2*$^{IR(24499)}$ [a]	5.5 ± 0.57 (30) *, ***
w^{-}/Y; +/+; *dsx*^{GAL4}/UAS- *tra-2*$^{IR(8868)}$ [a]	5.87 ± 0.91 (32) *
w^{-}/Y; UAS-*fru*^{IR}/+; *dsx*^{GAL4}/+ [a]	10.08 ± 1.08 (36)

Table 3-1 Comparison of repression of sex comb in 3 day old adult *dsx*^{GAL4} males expressing various GAL4 responsive transgenes.
Mean number bristles± standard deviation, n's in brackets. * p<0.0001 compared to +/Y; +/+; *dsx*^{GAL4}/+. ** *P*<0.05 compared to *w*$^{-}$/Y; +/+; *dsx*^{GAL4}/UAS- *tra*$^{IR(2560)}$ and (2561) and *w*$^{-}$/Y; +/+; *dsx*^{GAL4}/UAS- *tra-2*$^{IR(8868)}$ and (24499). *, * *P*<0.001 compared to *w*$^{-}$/Y; UAS-*tra*^{F}/+; *dsx*^{GAL4}/+ (Student's t-test). [a] Flies raised at 29ºC. [b] Flies raised at 25ºC.**

Genotype (diplo-X) females	Mean no. of sex comb or transverse bristles
+/+; +/+; *dsx*^{GAL4}/+ [a]	4.09 ± 0.51 (34)
yw^{-}/+; +/+; *dsx*^{GAL4}/ UAS-*dsx*^{M} [b]	5.87 ± 0.73 (30) *, **
w^{-}/+; UAS-*tra*^{F}/+; *dsx*^{GAL4}/+ [b]	4.71 ± 0.53 (30) *
w^{-}/+; UAS-*fru*^{IR}/+; *dsx*^{GAL4}/+ [a]	4.04 ± 0.53 (26)

Table 3-2 Comparison of induction of sex comb-like bristles in 3 day old adult *dsx*^{GAL4} females expressing various GAL4 responsive transgenes.
Mean number bristles ± standard deviation, n's in brackets. * *P*<0.0001 compared with +/+; +/+; *dsx*^{GAL4}/+. ** *P*<0.0001 compared with *w*$^{-}$/+; UAS-*tra*^{F}/+; *dsx*^{GAL4}/+ (Student's t-test). [a] Flies raised at 29ºC. [b] Flies raised at 25ºC.

3.4 Discussion

I have, through these investigations, demonstrated that an operative GAL4 element has been successfully integrated into the endogenous *dsx* locus via homologous recombination. Importantly the integration of this novel construct has not impinged on normal gene expression and the transgenic line remains viable and fertile, i.e. both male and female flies homozygous for the dsx^{GAL4} allele appears to be wild-type in gross morphology and fertility (a more detailed analyses of behaviours for both sexes will be examined in this study later). Also I have demonstrated that the dsx^{GAL4} allele reiterates endogenous *dsx* expression within the CNS and, finally, manipulating *dsx* function specifically in dsx^{GAL4}-expressing cells can reprise the functional roles of endogenous *dsx* in establishing external sexual morphology, demonstrating the validity of this tool for future studies.

Previous studies have shown that Dsx functions as a homodimer but that the ectopic presence of one isoform could potentially interfere with activity of the other by forming a heterodimer (Erdman et al., 1996). As both Dsx isoforms can bind the same enhancer elements, the presence of ectopic isoform homodimers could also potentially compete with endogenous homodimers for these sites, thereby altering normal/gender appropriate gene regulation (Erdman et al., 1996). With this in mind, over-expression of the female Dsx isoform in XY males achieved a more complete transformation to female sexual morphology, despite the presence of endogenous Dsx^{M}. Implying that in direct competition Dsx^{F} instructive and repressive signals may effectively override Dsx^{M} activity. The masculinisation of XX females by over-expression of Dsx^{M} was less complete especially with respect to the formation of the genitals, which appeared malformed and abnormally rotated. This last point maybe telling as, while it is unclear whether the abnormal orientation of the genital plate is caused by repression, extension or alteration of the nomal (i.e sinistral) direction of rotation, it would seem to imply that the presence of Dsx^{F} negatively affects the action of the male-specific rotation of the genital plate and thus that this process is *dsx*-dependent (Arbeitman et al., 2010). So while with cuticular pigmentation it appears that Dsx^{M} is equal to Dsx^{F}, with respect to the determination and differentiation of tissues in the genitalia and sex combs it appears that Dsx^{M} is less capable of directly competing with Dsx^{F} and thereby overriding female-specific morphogenic cues.

Feminisation via expression of Tra^F in XY males was again incomplete. This may be less surprising as it has been shown that in dsx^{Swe} XX females, which therefore also express Dsx^M, the presence of the male Dsx isoform appears to counteract the feminising effects of expressing Tra^F (Waterbury et al., 2000). That the genitalia presented as intersexual and abnormally orientated *cf. tra* hypomorphs (Butler et al., 1986) reinforces the findings that this process is *tra*/*dsx* dependent (see Arbeitman et al., 2010). What was surprising was to observe that XX females expressing ectopic Tra^F appeared masculinised. One reason for this could be that the exogenous Tra protein is competing with endogenous Tra to form an attenuated Tra/Tra-2 splicing complex, or may be directly binding to the splice recognition sequence blocking the splicing machinery. Either way this competition could reduce the binding efficiency of the Tra/Tra-2 protein complex and thereby impede the efficiency of the female-specific splicing event with some level of transcription therefore defaulting to the Dsx^M isoform. With respect to this Savarit et al. (1999) reported using *UAS-*tra^F in females to effectively ablate normal pheromonal production in these females.

Finally RNA interference of Tra or Tra-2 in XX females was compelling, effectively phenocopying the morphology of *tra*-nulls, which appear as pseudo-males. The effectiveness of these transformations compared with the Dsx^M masculinisation experiment is probably reflective of the fact that there is less chance of direct competition occurring between exogenous and endogenous isoforms in these animals. This again emphasising the potential problems of competition when overexpressing one isoform in the presence of the other. RNA interference directed at endogenous Tra in all *dsx*-expressing cells ensured a marked reduction in the production of Dsx^F and significantly negated the repressive effects this isoform might have on the male-specific program of development. Again as splicing of the Dsx^M isoform is the default state this would also explain why this masculinisation appears more successful than the feminisation experiment using Tra^F. However the fact that overexpression of Dsx^F achieved complete feminisation is indicative of the repressive strength of Dsx^F even in competition with endogenous Dsx^M. That these Tra^{IR} and Tra-2^{IR} transformations were not wholly complete, again with respect to the number of sex-comb bristles, may be ascribed to the fact that gene expression is generally not completely knocked-down by single-copy expression of RNAi constructs, and

so some female-specific identifiers could still be transcribed to compete with the male-specific program of development.

While the overall success of these transformation experiments is sufficient to argue the efficacy of the *dsx*^{GAL4} allele as a tool to reiterate known functional roles for *dsx* in determining the somatic sexual characteristics in both males and females, it would still be of real interest to see if the levels of transformations may be improved. One approach would be to sensitise the genetic background the transformations are performed in using deficiencies for *dsx* (and perhaps other genes of the SDH). Thereby reducing the amount of endogenous *dsx* present to compete with the ectopically expressed protein (*c*.f. Waterbury et al., 1999). As well quantitative RT-PCR experiments would allow more insight into the varying levels of transcripts being produced in flies expressing both their endogenous *dsx* isoform and the differing transgenic construct transcripts. More in depth molecular characterization of the splicing events and potential competitions which may occur between both the variant isoforms of *dsx* itself and with the other constituent members of the SDH may also provide valuable data as to how the stereotypical dimorphic fly is finally achieved.

Generally *dsx*, through the production of sex-specific isoforms in relevant tissues, appears to function as a bimodal switch, providing both instructive and repressive signals to regulate downstream signaling-molecules and transcription factors, either independently or in combination with various cofactors, to ensure the proper determination and differentiation of dimorphic tissues. Further complexity may occur via alternate mechanisms of gene regulation such as the requirement for *dsx* in only one sex for differential, and therefore sex-specific, gene expression (Goldman and Arbeitman, 2007). However delineating *dsx*'s particular role in these processes may be complicated by the effect of 'canalization' (Waddington, 1942); the requirement to generate a uniform morphology ensuring some degree of 'redundancy' is retained in the system due to homeostatic pressures. Thus genes and paths independent of the sex determination hierarchy may act to ameliorate some of the effects resulting from disruption of *dsx* gene expression in the developing adult (resistance to perturbation competing with phenotypic plasticity). This is supported by the fact that while *dsx* is necessary to the morphogenic program of development in males and females (and clearly is pivotal in determining most morphological sexual

characteristics), it is not sufficient for all aspects of these programs. Other genes have also been shown to be required for aspects of *dsx*-independent morphological sexual differentiation, i.e. *dissatisfaction* has been shown to be *tra* dependent/*dsx* independent in determining the correct sex-specific motor neuronal innervation of the ventral A5 abdominal muscles implicated in correct abdominal curling in courtship males and in the circumfrential uterine wall muscles implicated in egg laying in females (Finley et al., 1998; Finley et al., 1997). While Fru^M has been shown necessary in the soma for the formation of the male-specific Muscle of Lawrence via induction by a Fru^M-expressing male-specific neuron (Billeter and Goodwin, 2004; Nojima et al., 2010) and in the CNS it is required for the specification of male-specific neuro-anatomical features (Billeter et al., 2006b; Datta et al., 2008; Kimura et al., 2005; Kondoh et al., 2003; Rideout et al., 2007; Ruta et al., 2010; Stockinger et al., 2005). Again the roles these genes play in the process of sex determination serves to emphasise the potential for other genes to be involved in somatic terminal differentiation processes, with morphogenic processes that may directly or indirectly impinge upon the sex determination pathway (for example those that determine stereotypical dimorphism in body size), and with potential roles in sex determination that have yet to be characterised.

Finally as morphological sexual traits are some of the most rapidly divergent characteristics in *drosophila* (Haerty et al., 2007), the potential alteration in sex-specific traits, occurring as a consequence of differential or altered gene expression in response to (both sex- and non-sex-specific) selective pressures, provides insight into how these changes could result in the development of novel sex- and species-specific identifiers (Ahuja and Singh, 2008; Haerty et al., 2007).

4 Spatiotemporal expression of *dsx*^{GAL4} in the nervous system of males and females

Behavioural genetic studies originally indicated a neural aetiology for *dsx* related behavioural phentoypes (Ferveur and Greenspan, 1998; Hall, 1979; Hall and Greenspan, 1979; Kido and Ito, 2002; Tompkins and Hall, 1983; Tompkins et al., 1983). This premise gained further validation with the demonstration that *dsx* is expressed in a dimorphic manner in the pupal and adult CNS (Lee et al., 2002; Sanders and Arbeitman, 2008). Further, Dsx^{M} has been shown to be co-expressed with Fru^{M} in a restricted subset of neurons and *dsx* and *fru* have been shown to collaborate in the determination and organisation of specific neuronal clusters implicated in the specification of reproductive behaviours such as those involved in male copulation and in generating the potential for male-specific courtship song (Billeter et al., 2006b; Kimura et al., 2008; Rideout et al., 2007; Rideout et al., 2010; Sanders and Arbeitman, 2008; von Philipsborn et al., 2011). *dsx* has been shown to be regulate this dimorphic pattern of expression in an isoform-specific and dose-dependent manner utilising a variety of processes to achieve its final expression within the CNS (Kimura, 2011; Sanders and Arbeitman, 2008). However the studies involved have been limited by the sensitivity of the reagents available and in the inability to perform anything but the most gross manipulations of the cells demonstrated to be *dsx*-expressing in the developing fly.

Having demonstrated the dsx^{GAL4} allele's validity as a reporter of endogenous *dsx* expression and, following the tenet that to understand function you must first understand structure, I utilised the dsx^{GAL4} allele to direct expression of a variety GAL4 responsive reporters in order perform a systematic and comprehensive survey of the expression of *dsx* throughout development in the nervous system of both males and females. The results of this survey are telling, not only in describing *dsx* expression with respect to the topology of behaviourally relevant neural regions but also in the dynamic manner of temporal expression, which culminates in the final adult dimorphic pattern of expression.

dsx has also been shown to regulate the development of specific sense organs of the peripheral nervous system in the foreleg and genitalia (Hildreth, 1965). Again characterisation of mutants, or the effects of ubiquitous over-expression of *dsx* isoforms, has demonstrated the necessity for *dsx* expression in somatic tissues involved in secondary sexual characteristics. These findings indicate that *dsx* is expressed in tissues beyond the CNS, an assumption

supported by microarray analyses (Chintapalli et al., 2007). However again, due to a lack of amenable reagents, this expression has never has never been systematically characterised. As such I performed a comprehensive survey of *dsx*^{GAL4} outwith the CNS and found a pattern of expression that was both restricted and revealing in the tissues and manner of expression.

4.1 Establishment of dimorphic *dsx*^{GAL4} neural circuitry in the central nervous system of male and female

As stated above, to understand the contribution of *dsx* in sculpting the mature neural architecture of males and females, which ultimately directs sex-specific behavioural outputs, it is necessary to know not only where *dsx* is expressed in the CNS but also to try to gain insight into how this final level of expression is achieved (as per question three of Tinbergen's four questions of ethology; ontogeny). This requires the characterisation of not only *dsx* neuronal expression in both sexes throughout development but also the resulting associated pattern of projections and synaptic interactions. Describing not only the differences, but also the similarities, in expression between the sexes providing insight into how both non-sex- and sex-specific behavioural outputs may be modulated by gene expression directing the final assembly of neural circuitry within the developing male and female animal.

4.1.1 dsx^{GAL4} neuronal expression in males and females throughout development

Using *dsx*^{GAL4} to express nuclear GFP I was able to systematically describe the full pattern of *dsx*^{GAL4} expression in both males and females within the developing CNS. Realisation of this pattern of expression clearly demonstrates a profound difference in neuronal cell numbers and in the *dsx*-determined neuronal architecture between males and females. This data provides a time line progression of the dynamic manner in which these neuronal clusters develop, are maintained or lost, and therefore provides insight into the processes underlying how the final adult dimorphic circuitry is eventually derived.

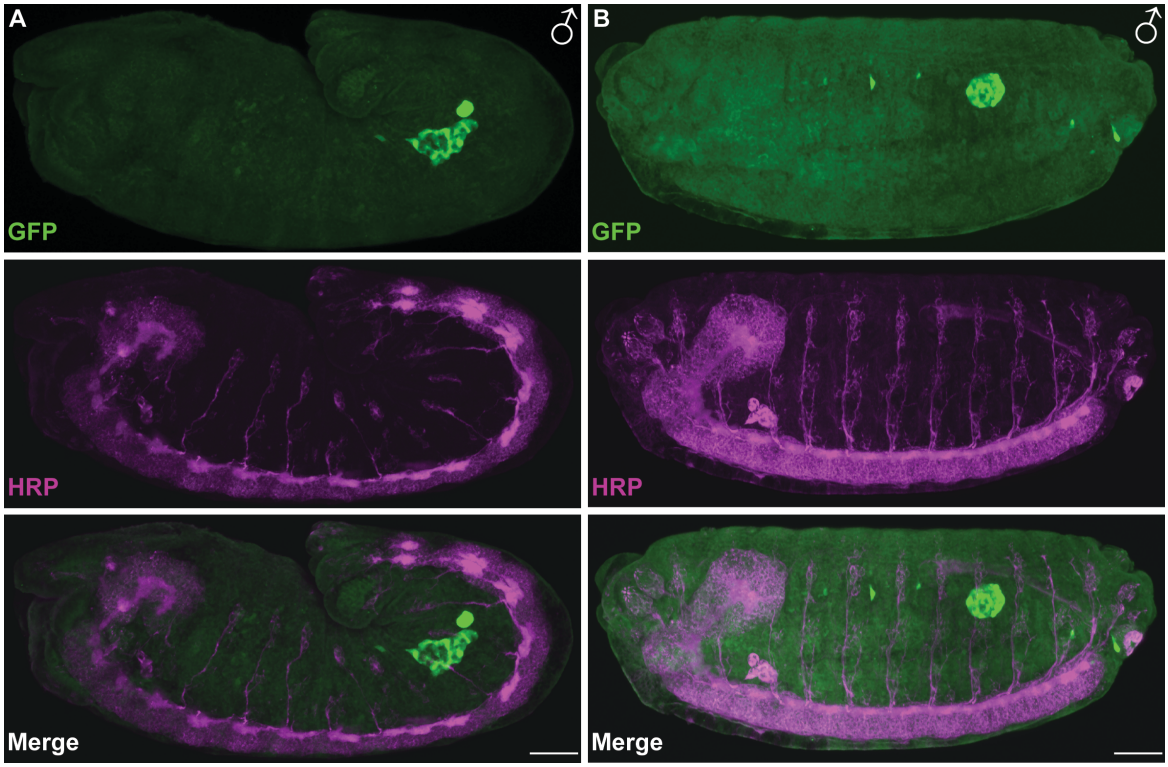

Figure 4-1 *dsx*^{GAL4} driven nuclear GFP in the embryo demonstrating a lack of expression in the nervous system.
(A) Stage 11 – 12 and (B) Stage 14 – 15 male embryos counterstained with the neural tissue specific marker anti-HRP (magenta) (Jan and Jan, 1982; Snow et al., 1987) demonstrating no co-expression with *dsx*^{GAL4} driven nGFP (green). Cephalic, left; ventral, bottom. Stages as per Hartenstein, 1993. (B) as per Rideout et al., 2010. Scale Bars = 50 µm.

While *dsx*^{GAL4} specified expression is apparent by stage 11 -12 in the embryo and persists into the developing larvae (see http://flymove.uni-muenster.de/; (Hartenstein, 1993) co-expression with the nervous tissue specific reagent anti-HRP demonstrated that this expression is neither in the CNS nor the PNS (Figure 4.1) (Jan and Jan, 1982; Snow et al., 1987). This expression, exhibited outwith the embryonic nervous system, will be discussed in the following chapter.

TABLE 4.1. Single-labelling with GFP applied to CNSs from *dsx*^{Gal4} flies crossed to UAS-*StingerII* (nGFP)

Neuronal clusters	L3 Larvae		0-24hr Pupae		48hr Pupae		5-7 day old Adults	
	Male	Female	Male	Female	Male	Female	Male	Female
Brain								
1 -pC1[a]	20 ± 4.8 (12)	5 ± 1.9 (12)	36 ± 1.4 (10)	7 ± 2.5 (10)	43 ± 6.0 (12)	9 ± 3.8 (12)	57 ± 5.0(10)	9 ± 2.0 (10)
2 -pC2[a]	47 ± 8.4 (12)	23 ± 5.9 (13)	54 ± 8.4 (10)	23 ± 6.6 (10)	54 ± 8.2 (12)	17 ± 5.2 (12)	77 ± 3.1 (10)	11 ± 1.9 (10
3 -pC3[a]	6 ± 2.7 (12)	4 ± 1.3 (5)	4 ± 1.5 (20)	2 ± 2.3 (12)	5 ± 0.8 (10)	3 ± 1.5 (12)	14 ± 1.0 (10)	6 ± 1.4 (10)
4 -aDN[a]	n.a.	n.a.	3 ± 0.4 (20)	3 ± 0.5 (12)	2 ± 0.5 (10)	2 ± 0.3 (12)	2 ± 0 (10)	2 ± 0 (10)
5 -SN[a]	n.a.	n.a.	n.a.	n.a.	1 ± 0 (12)	1 ± 0 (12)	1 ± 0 (10)	0 ± 0 (12)
Ventral Nerve Cord								
6 -TN1[a]	0 ± 0 (10)	0 ± 0 (10)	0 ± 0 (20)	0 ± 0 (12)	16 ± 2.6 (14)	0 ± 0 (20)	22 ± 1.7 (10)	0 ± 0 (10)
7 -TN2[a]	0 ± 0 (10)	0 ± 0 (10)	n.a.	n.a.	10 ± 1.3 (16)	12 ± 2.9 (16)	7 ± 3.0 (10)	0 ± 0 (10)
9 -Abg[b]	66 ± 4.8 (5)	32 ± 8.0 (5)	214 ± 16.2 (10)	44 ± 7.7 (6)	342 ± 34.2 (8)	388 ± 52.4 (10)	277± 22.1 (10)	312 ± 15.9 (10)

Table 4-1 Single-labelling with GFP applied to CNSs from *dsx*^{Gal4} flies crossed to UAS-*StingerII* (nGFP).
[a]Neuronal cluster away from CNS midline. Count represents one cluster per hemisegment of the CNS. [b]Neuronal cluster spans the CNS midline. Count given is for the complete VNC. Counts represent mean ± standard deviation. n's listed in parentheses. Table modified from Rideout et al., 2010.

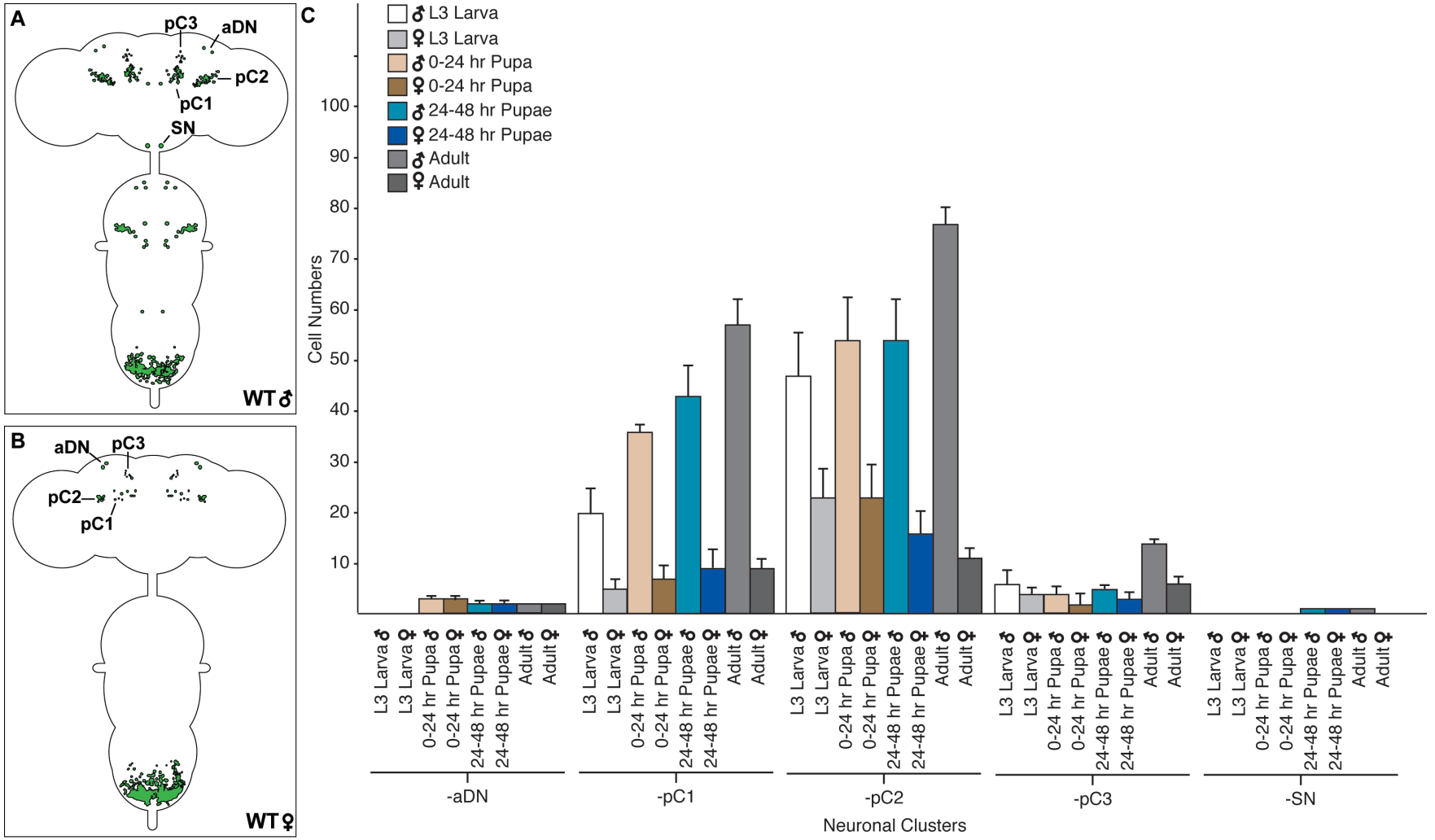

Figure 4-2 Graphical representation of the distribution of *dsx*^{GAL4} driven nGFP expression in the brain throughout development.
(A-B) Schematic representation of *dsx*^{GAL4} neuronal expression in the adult male (A) and female (B) CNS. Neuronal clusters in the brain indicated as per Lee et al. 2002 and Rideout et al. 2010. (C) Graphical representation of cell counts for each neuronal clusters from L3 larvae to adult in males and females. Counts represent mean ± standard deviation.

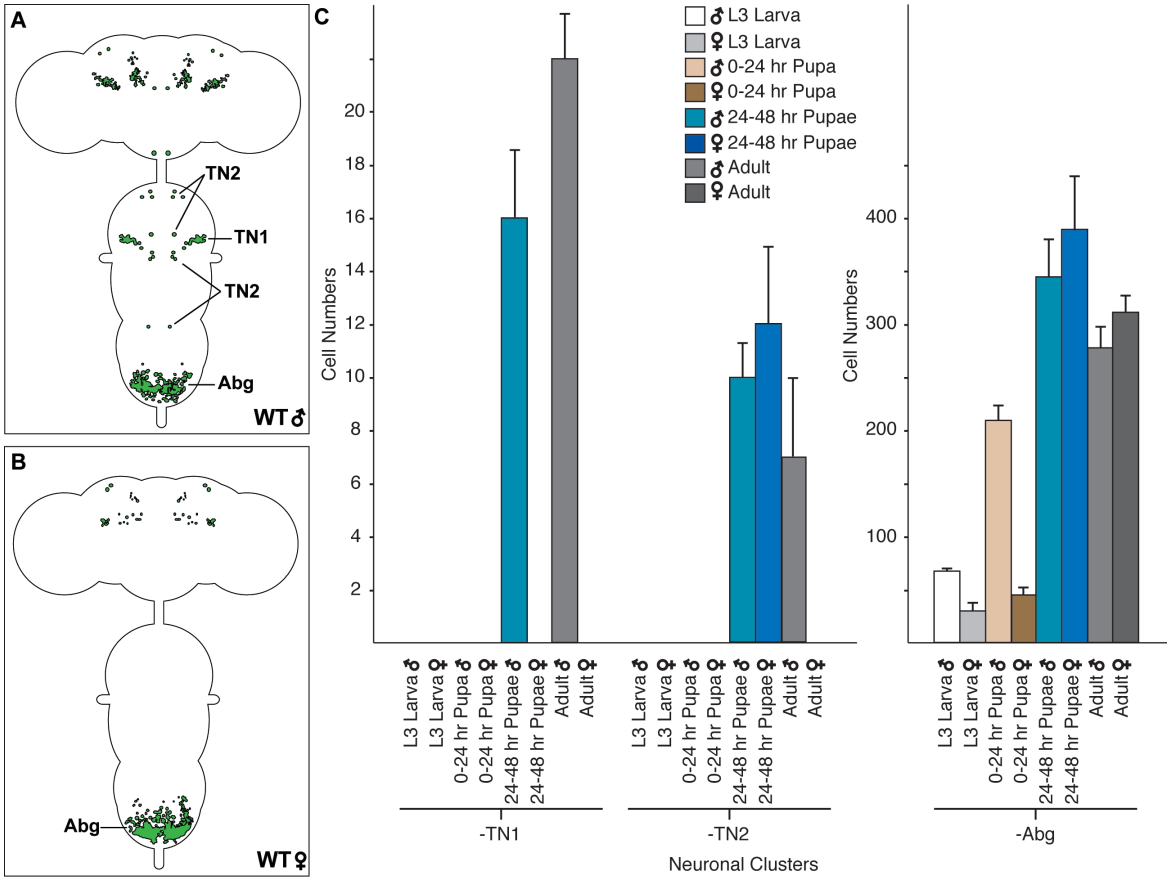

Figure 4-3 Graphical representation of the distribution of *dsx*^{GAL4} driven nGFP expression in the ventral nerve cord throughout development.
(A-B) Schematic representation of *dsx*^{GAL4} neuronal expression in the adult male (A) and female (B) CNS. Neuronal clusters in the VNC indicated as per Lee et al. 2002. (C) Graphical representation of cell counts for each neuronal clusters in male and female VNCs from L3 larvae to adult. Counts represent mean ± standard deviation.


A
nC82
GFP
B
nC82
GFP
C
♂
nC82
GFP
D
♀
nC82
GFP
E
♂
nC82
GFP
F
♀
nC82
GFP
G
♂
nC82
GFP
H
♀
nC82
GFP
I
♂
nC82
GFP
J
♀
nC82
GFP

Figure 4-4 *dsx*^{GAL4} driven nuclear GFP expression in the developing CNSs of males and females.
(A) L1 larva, no expression apparent (anterior right; ventral bottom). (B) L2 larva, expression in a bilateral cluster of cells (white box) at distal tip of the Abg (anterior right; dorsal view). (C) L3 male larva, expression apparent in the *dsx*-pC1, -pC2, -pC3 and -Abg clusters. No *dsx*-TN1 and -TN2 neurons expression is observed. (D) L3 female larva, expression in the *dsx*-pC1, -pC2, -pC3 and -Abg clusters, though reduced in numbers with respect to the male. (E) 0-24 hr male pupa, expression apparent in the *dsx*-aDN, -pC1, -pC2, -pC3 and -Abg clusters. No *dsx*-TN1 and -TN2 neurons expression is observed. (F) 0-24 hr female pupa, expression in the *dsx*-aDN, -pC1, -pC2, -pC3 and -Abg clusters, though reduced in numbers with respect to the male. (G) 48 hr male pupa, expression in the *dsx*-aDN, -pC1, -pC2, -pC3, -SN, -TN1, -TN2 and -Abg clusters. (H) 48 hr female pupa, expression in the *dsx*-aDN, -pC1, -pC2, -pC3, -SN, -TN2 and -Abg clusters. All clusters remain reduced in numbers with respect to the male except in the *dsx*-Abg. (I) 5-day-old adult male, expression in the *dsx*-aDN, -pC1, -pC2, -pC3, -SN, -TN1, -TN2, and -Abg clusters. (J) 5-day-old adult female, expression in the *dsx*-aDN, -pC1, -pC2, -pC3, and -Abg clusters. Expression is no longer apparent in the *dsx*-SN and -TN2 cells. All clusters remain reduced in numbers with respect to the male except the *dsx*-Abg. Counts for designated clusters given in Table 4.1. Cluster designation as per lee et al., 2002 and Rideou et al., 2010. nGFP realised with anti-GFP antibody (green) and neuropil counterstained with anti-nC82 (magenta). Unless noted, all views ventral, anterior up. Scale bar = 50 µm. Figure as per Rideout et al. 2010.

Again no expression is observed in the CNS of L1 larva of either sex (Figure 4.4A). Expression becomes apparent in L2 larvae, restricted to a bilateral cluster of cells in the distal tip of the Abg in both male and females (Figure 4.4B). In L3 larvae this pattern of expression has expanded, with increased numbers of cells in the Abg, though no other cells are observed in the developing VNC (Figures 4.2, 4.3 and 4.4C,D; Table 4.1). Expression was also observed in cells in the brain in distinct clusters topographically consistent with the *dsx*-pC1 and –pC2 clusters, previously described in pupae and adults (Figures 4.2 and 4.4C,D; Table 4.1; (Lee et al., 2002). A novel non-sex-specific cluster, superior to the described *dsx*–pC1 and –pC2 clusters but still lying in the dorsal protocerebral compartment of the brain was also identified (Figures 4.2 and 4.4C,D; Table 4.1). In keeping with the established nomenclature this cluster was given the designation *dsx*-pC3 (Rideout et al., 2010). At this juncture the L3 larval pattern of expression is now noticeably dimorphic. A scattering of *dsx*^{GAL4}-expressing cells may also be observed in the optic lobes, however as the numbers of cells exhibiting expression was highly variant, and expression was often occluded or artifactually enhanced by expression in adjoining tissues, no definitive counts of these cells was possible. No expression in cells consistent with that of the *dsx*-aDN neurons described in pupa and adults of either sex, or in the male specific *dsx*–SN neurons was observed in larval brain (Figures 4.2 and 4.4C,D and Table 4.1).

This dimorphic pattern of expression exhibited in L3 larvae continues into pupariation with the male *dsx*-PC1, -pC2 and especially -Abg neuronal populations

expanding incrementally while the rest remain essentially static (Figures 4.2, 4.3 and 4.4E,F; Table 4.1). At this point the only anteriorly positioned cells, the non-sex specific *dsx*-aDN neurons become apparent in males and females, though at this stage this is a bilateral cluster of three neurons (Figures 4.2 and 4.4E,F; Table 4.1). Following from this a key moment in the developmental timeline is 48 hrs into pupariation, a point during the rapid metamorphosis of the CNS from one that determines the behaviour of the foraging larva to one that determines the behaviour of the mature adult (Arthur et al., 1998). At this juncture the male-specific *dsx*-SN and –TN2 neurons and –TN1 neuronal clusters appear (Figures 4.3 and 4.4G,H; Table 4.1). Again the male *dsx*-Abg neuronal continues to expand incrementally, however now so to does the female *dsx*-Abg cluster, which overtakes the male with respect to neuronal numbers (Figures 4.3 and 4.4G,H; Table 4.1). These changes in expression patterns in both male and female CNSs are indicative that this period is pivotal in the sculpting of the mature dimorphic neural architecture and by corollary may be of importance in the establishment of the neural substrates that govern sex-specific behavioural outputs Consistent with this is the finding that this time point in early pupal development is critical in the establishment of the neural substrates that govern sex-specific reproductive behaviours (Arthur et al., 1998; Belote and Baker, 1987).

As stated in addition to the previously described *dsx*-pC1, -pC2 and -aDN neuronal clusters in the adult posterior brain a further *dsx*-expressing cluster, *dsx*-pC3, was observed positioned superior to *dsx*-pC1 and -pC2 (Figures 4.3 and 4.4I,J and Table 4.1). The *dsx*-pC1, -pC2 and -pC3 clusters have higher numbers of neurons in males (Figures 4.2 and 4.4I vs. J and Table 4.1). The *dsx*-pC1, -pC2 and -pC3 clusters lie in the dorsal inferomedial, infero- lateral and superomedial protocerebrum, respectively, surrounding the mushroom body calyces; regions which have, through mosaic analyses, been implicated in sex-specific behaviours in both sexes (Ferveur and Greenspan, 1998; Hall, 1977, 1979). In the suboesophageal ganglion (SOG), two male-specific neurons, *dsx*-SN, were present (Figures 4.2 and 4.4I).

Describing the development of the dsx^{GAL4} neurons highlights the 48 hr pupal stage as a critical point of divergence between the sexes. At this point *dsx*-SN and -TN2 cells arise in both sexes, but these cells then disappear specifically in adult females (Figures 4.3, 4.4 and Table 4.1). The *dsx*-TN1 neuronal clusters

also appear at this point in males, but never females (Figures 4.3, 4.4 and Table 4.1). Until the 48 hr pupal stage, the number of *dsx*^{GAL4}-Abg neurons is consistently higher in males vs. females (Figure 4.3, 4.4 and Table 4.1). Programmed cell death (PCD) has been shown to be a key method of determining the final adult *dsx* expression (Kimura, 2011) and the *dsx*-TN1 clusters have specifically been shown to be specified in an isoform and dose-dependent manner which results in a process of sex-specific PCD ensuring that these neurons only normally develop within the adult male (Sanders and Arbeitman, 2008). It would seem not unreasonable to assume that the reduction in neuronal numbers between pupa and adult, especially with respect to the disappearance of the *dsx*-SN and –TN2 neurons in the female, occurs as a result of sex-specific PCD. It is this progression in the development of the *dsx*-specific neurons, culminating in the adult CNS in expression in ~640 neurons divided into 9 groups in males, and ~370 neurons divided into 5 groups in females (Figures 4.2 – 4.5 and Table 4.1) which results in, as will be seen in the following section, overt and substantial dimorphisms in the topology of the associated axonal projections and synaptic pattern of expression.

4.1.2 dsx^{GAL4} determined expression of projections and synaptic patterns in male and female adult brains

Following this developmental survey of the neuronal populations within the CNS of both males and females I then examined the neural architecture of adult CNSs, as determined by the projections and synaptic patterning associated with these neurons. Describing the potential dimorphic substrates that maybe shaped by *dsx*^{GAL4} sex- and non-sex-specific expression within these previously identified neuronal cells and clusters.

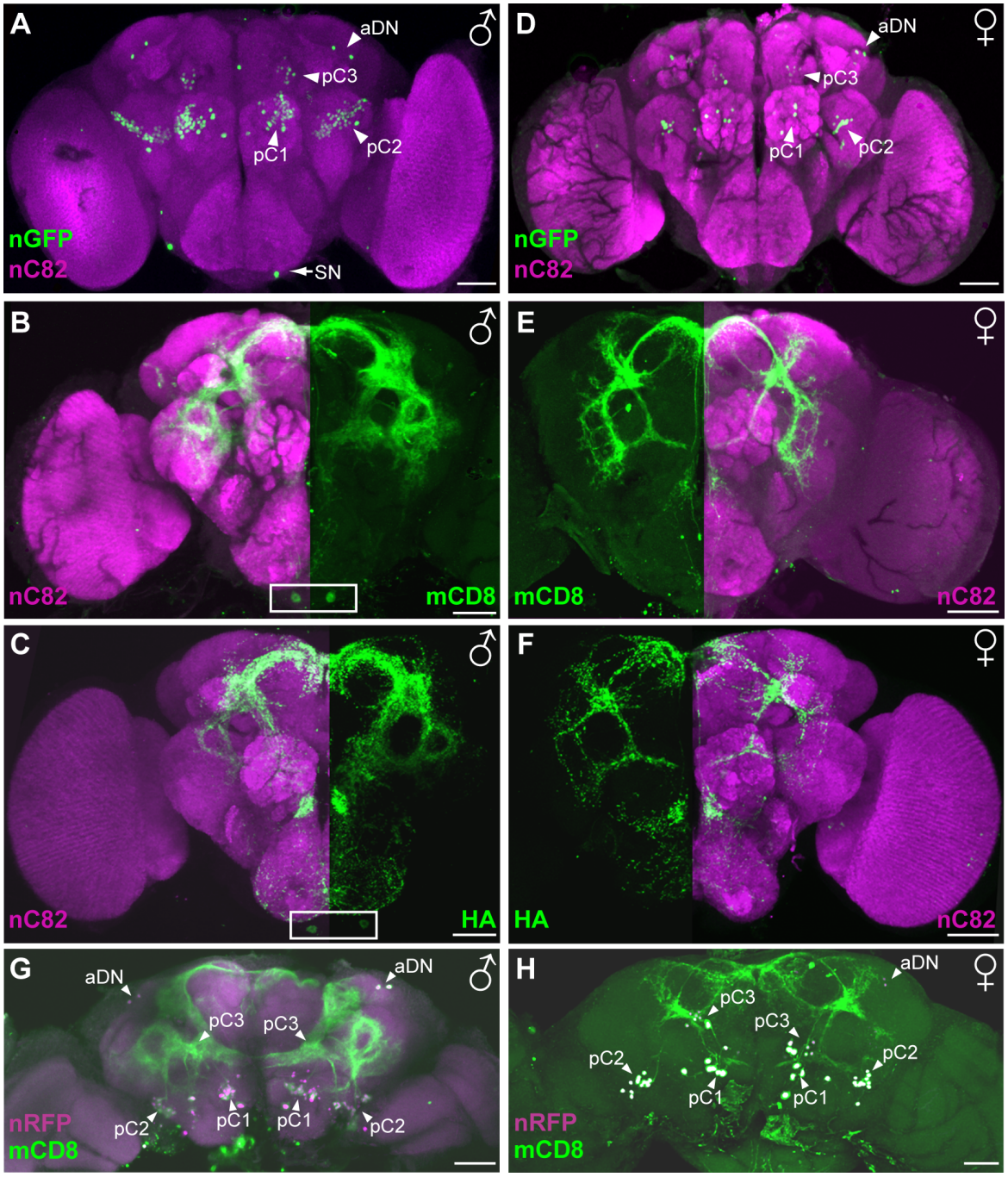

Figure 4-5 Sexually dimorphic expression of *dsx*^{GAL4}-neurons and associated projections and synapses in the brains of 5 day old adult males and females.
(A-C) Male brains (A) dsx neuronal clusters (arrowheads, A), male-specific SN neurons (only one cell in plane of focus, arrow, A). The cell bodies of pC1, pC2 and pC3 are located in the dorsal inferomedial, inferolateral and superomedial protocerebral areas, respectively. SN cells position is shown in the box (B –C). (D–F) Female brain. (D) dsx neuronal clusters (arrowheads, D). Neuronal cell bodies expressing UAS- *pStingerII* (nGFP) are shown in A and D. GFP staining is shown in green. Neuronal projections expressing UAS-*mCD8::GFP* (membrane-bound GFP) are shown in B, E, I and K. mCD8 staining is shown in green. Expression of UAS-*synaptotagmin* (pre-synaptic marker tagged with HA) is shown in (C) and (F). HA staining is shown in green. Neuropil was counterstained with antibody to nC82 (magenta). Ventral views; anterior top. (G-H) UAS-*RedStinger*; *dsx*^{GAL4}, UAS-*mCD8::GFP* male (M) and female brain (N). Dsx neuronal clusters are indicated by arrowheads. mGFP, green; nRFP, magenta. Horizontal view, ventral top. Scale bars = 50 µm. Figure modified from Rideout et al., 2010.

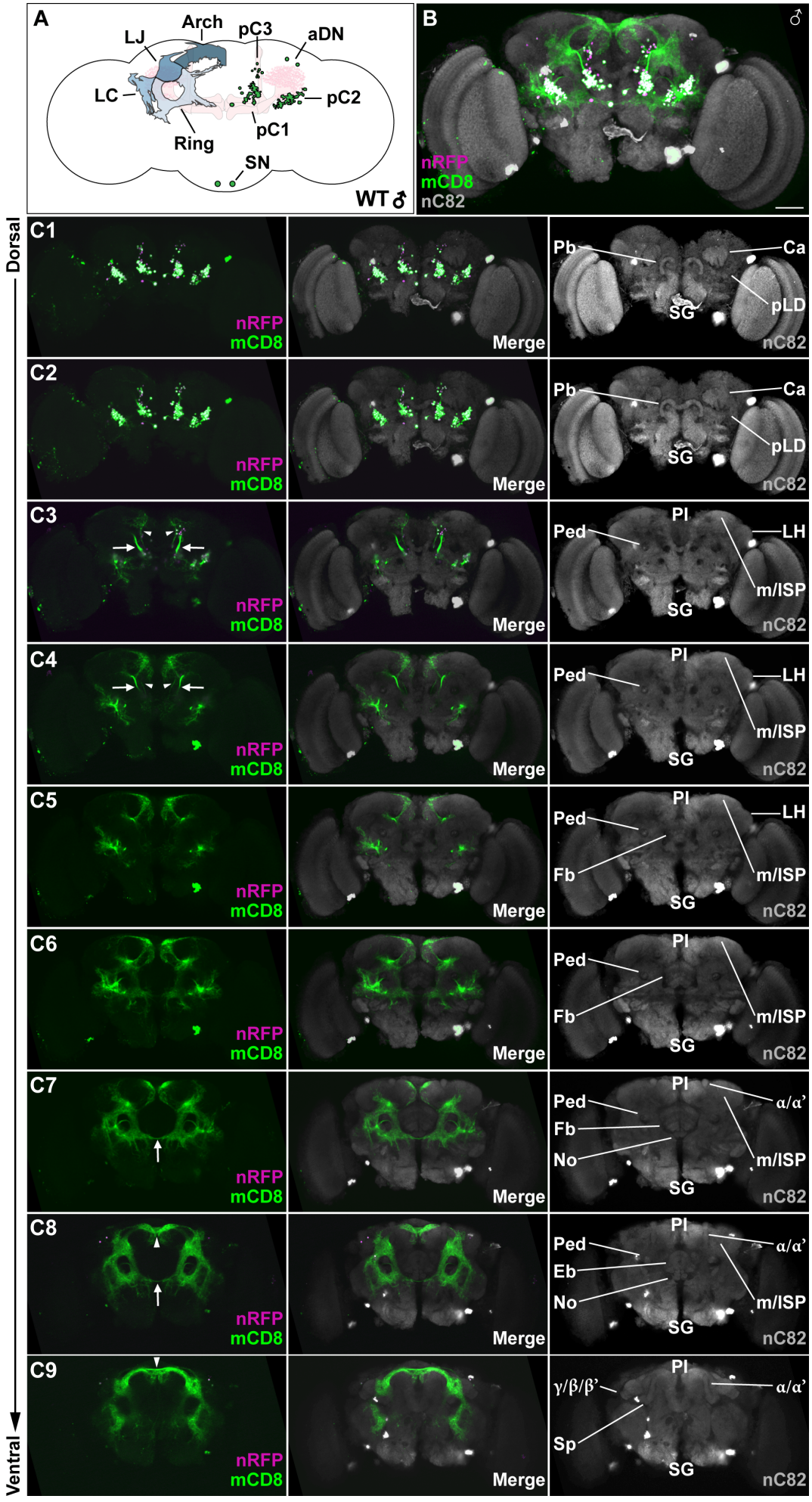
A
Arch
LJ
pC3
aDN
LC
pC2
pC1
Ring
SN
WT ♂
B
♂
nRFP
mCD8
nC82
Dorsal
Ventral
C1
C2
C3
C4
C5
C6
C7
C8
C9
nRFP
mCD8
Merge
Pb
Ca
pLD
SG
nC82
Ped
PI
LH
m/ISP
Fb
No
Eb
α/α'
γ/β/β'
Sp

Figure 4-6 *dsx*^{GAL4} nuclear and membrane-bound fluorescent protein expression in the brain of a 5 day old adult male highlighting the topographical positioning of the *dsx* neurons and their associated projections.
(A) Schematic representation of *dsx*^{GAL4} neuronal expression in the adult male brain. Neuronal clusters in the brain indicated as per Lee et al., 2002 and Rideout et al., 2010. Lateral protocerebral complex (Arch; LJ, lateral junction; LC, lateral crescent; Ring) indicated as per Yu et al., 2011. (B) Maximal Z Projection stack of a 5 D adult *dsx*^{GAL4} male brain expressing nuclear RFP (magenta) and membrane-bound GFP (green). Neuropil counterstained with antibody to nC82 (gray). Dorsal view, anterior top. Scale bar = 50 µm. (C1-9) Subsections of Z projection slices, progressing dorsally to ventrally, of the *dsx*^{GAL4} male brain shown in (B) highlighting expression in the *dsx* neurons (nRFP, magenta) and their associated projections (mCD8, green) with respect to neuro-anatomical landmarks. (C3) and (C4) Arrows indicate primary antero-ventrally hooking fascicular bundle originating from *dsx*-pC1. Arrowheads indicate secondary superiorally projecting fascicular bundle and associated dendritic arborisation terminating in the medial dorsal superior protocerebrum. (C7) and (C8) Arrows indicate inferior antero-dorsal commissural bridge. (C8) and (C9) Arrowheads indicate superior antero-dorsal commissural bridge. Calyxces (Ca); protocerbral bridge (Pb); posterior lateral deutocerebrum (pLD); suboesophageal compartment (SOG); pars intercerebralis (PI); medial and lateral superior protocerebrum (m/lSP); lateral horn (LH); peduncle (Ped); fan-shaped body (Fb); noduli (No); alpha lobes (α/α'); ellipsiid body (Eb); gamma and beta lobes (γ/β/β'); and spur (Sp) indicated.

In the adult male brain, moving ventro-dorsally cell projections appear positionally associated with the previously described *fru*-mcAl cluster (Lee et al. 2000) and the antennal mechanosensory neuropil (see Supplementary Video 1, Rideout et al., 2010). Synaptic expression appears intensified at this locality (see Figure 4.5C vs F). From here projections may be seen both inferior, forming a plexus in the anterior suboesophageal ganglion (SG) compartment wherein the *dsx*-SN neurons lie and superior, running dorsally with respect to the antennal lobes (AL) and laterally to the oesophageal cavity, to the anterior superior protocerebrum (Figures 4.5; see Supplementary Video 1, Rideout et al., 2010). Projections in the superior protocerebrum (SP) appear to be forming a commissural bridge connecting the two hemispheres (Figures 4.5 and 4.6; see Supplementary Video 1, Rideout et al., 2010). Projections are apparent in the anterior lateral protocerebrum (both superior and inferior; aSLP, aILP) running superior to the beta (β) and gamma (γ) lobes of the mushroom bodies (MBs) and along the lateral edge of the alpha (α) and alpha' (α') MB lobes (Figures 4.5 and 4.6; see Supplementary Video 1, Rideout et al., 2010). Projections bifurcating around the distal ends of the α, α' lobes form part of the trans-midline SP bridge, most likely part of the antero-dorsal commissure, (Figures 4.5 and 4.6; see Supplementary Video 1, Rideout et al., 2010). Dorsal projections, running laterally to the ellipsiod body (Eb) and around the peduncle (P), connect this bridge to the superior and inferior posterior lateral protocerebrum (Figures 4.5 and 4.6; see Supplementary Video 1, Rideout et al., 2010). Projections are also apparent forming an inferior antero-dorsal commissural bridge (running below the noduli,

ellipsiid and fan shaped body; Fb; Figures 4.5 and 4.6) extending into a further plexus in the dorsal SG compartment, in which are present the two large male-specific *dsx*-SN neurons (Fig. 4.5A-C and Table 4.1), and then on through the cervical connection (see Supplementary Video 1, Rideout et al., 2010). Projections from the two *dsx*-SN neurons extend both contra-, as well as ipsi-laterally into the brain. Again there is an increased level of synaptic expression associated with this plexus in the male, notably at the position of the *dsx*-SN neurons (Figure 4.5; Rideout et al., 2010). The dorsal most projections are associated with supramedial, inferomedial and inferolateral areas surrounding the calyxes of the MBs juxtaposed to, or associated with, Kenyon cell bodies (Figures 4.5 and 4.6; Rideout et al., 2010), finally terminating in the *dsx*-pC1, -pC2 and –pC3 neuronaL clusters. All these described projections contribute to parts of the arch, ring, lateral junction and lateral crescent forming the lateral protocerebral complex (Yu et al., 2010).The inferomedial projections arise from, or project to, the previously described *dsx*-pC1 neuronal cluster as well as the novel *dsx*-pC3 cluster (Lee et al. 2002; Figures 4.5A-C and 4.6). In males the *dsx*-pC1 clusters' position within the circuit, the fact that it has been previously shown to co-localise with FruM (Rideout et al., 2007) and its characteristic axonal bundle, running anterodorsally up before hooking round anteroventrally (Figure 4.7), identifies it as containing cells of the *fru*-P1 cluster (Kimura et al., 2008). The *dsx*-pC1 cluster contributes to the projections running to the inferolateral areas of the MBs, ramifying on the *dsx*-pC2 neuronal cluster (Figure 4.5 and 4.6) and other regions within the lateral junction (Yu et al., 2010). As well as the primary antero-ventrally 'hooking' fascicle, the *dsx*-pC1 cluster has a secondary fascicular bundle which projects superiorally terminating in an extensive dendritic arborisation in the medial dorsal SP and may synapse with neurons from the novel *dsx*-pC3 neuronal cluster (Figure 4.6). The *dsx*-pC3 cluster, exists superior to the *dsx*-pC1 cluster, contiguous to the point where the -pC1 projections hook anteroventrally, and can be seen not only contributing to the lateral protocerebral complex but also contributing projections to the tritocerebral loop associated with the SG compartment and the *dsx*-SN neurons (Yu et al., 2010). All these clusters are connected via their projections, both ipsi-laterally as well as contra-laterally to the corresponding set of neuronal clusters, to form a complete bilateral circuit (Figures 4.5 and 4.6).

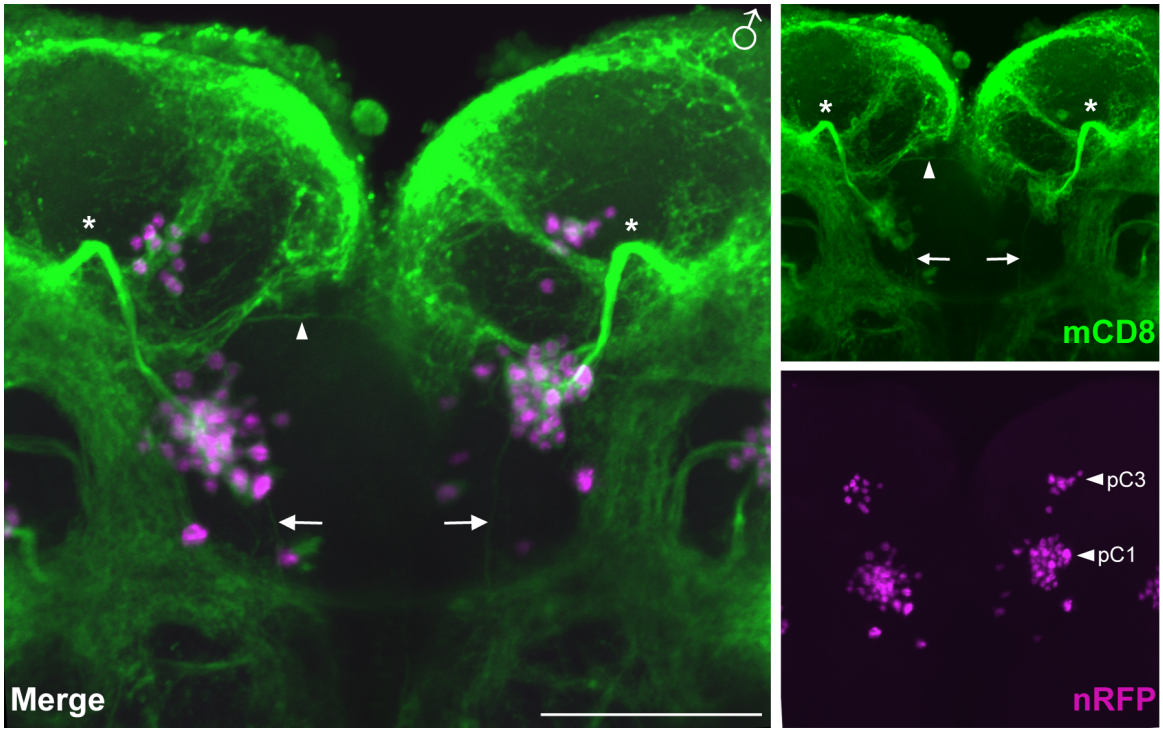

Figure 4-7 Detail of the *dsx*-pC1 neuronal clusters in the adult male brain demonstrating the associated distinct stereotypical axonal projection pattern.
5 D *dsx*^{GAL4} adult brain expressing UAS-RedStinger (nRFP, magenta) and UAS-mCD8::GFP (mCD8, green). Asterisk indicates the stereotypical anteroventral 'hook' associated with the projections of the *dsx*-pC1/*fru*-P1 neuronal complex (Kimura et al., 2008; Rideout et al., 2010). Arrows indicate projections associated with *dsx*-pC3 and the SG compartment. Arrowhead indicates projection between the *dsx*-pC1 clusters. Dorsal view, anterior top. *dsx* neuronal clusters indicated as per Lee et al. 2002 and Rideout et al 2010. Scale Bars = 50 µm.

In the adult female brain this pattern of expression described in the male brain is largely reiterated, though at an overtly attenuated level reflective of the overall decrease in the number of extant cells within the *dsx*-neuronal clusters and associated projections (Rideout et al., 2010). As a case in point Robinett et al. (2010) describe that they are able to discern the presence of the subpopulation of *fru*-P1 neurons within the larger *dsx*-pC1 cluster as these contribute to, or form, a *dsx*-specified anterior SP bridge (*cf.* Kimura et al. 2005) implying that this part of the *dsx* determined neural architecture is purely male-specific. However my examination of the *dsx*^{GAL4} specified projection patterns in females showed that this bridge is still present in females, though at a greatly attenuated level (Rideout et al., 2010). Implying that, while this structure is overtly reduced in comparison with the male, there exist projections that form a bridge in the correspondent region in the female, perhaps associated with neurons of the female *dsx*-pC1 cluster. Again in the absence of the male-specific *dsx*-SN cells, it would appear that there is a much reduced level of synapses within the SG compartment and

that projections directed to this area appear to run predominantly ipsi-laterally with reduced, or absent, contra-lateral projections (Figure 4.5E, F; see Supplementary Video 1, Rideout et al., 2010). These examples serving to underlie the point that while the pattern of expression between males and females may appear topographically similar, that is not to say that there are not significant alterations in connectivity between the male and female *dsx*^{GAL4} neural architecture, both in how the projections interact with corresponding regions of the *dsx*^{GAL4} specified neuronal substrates and how they might interact with other areas within the CNS (Cachero et al., 2010; Yu et al., 2010). Again further somato-topic mapping of these neurons and clusters, their associated projections and neural connectivity as per Cachero et al., 2010 and Yu et al., 2010 using clonal analyses will allow elucidation of the presence or absence of projections associated with *dsx*-specified neural substrates and their direct relation to other neuroanatomical structures providing a clearer understanding of the relationship these cells have within the varying neural circuits involved in higher order processing of sensory inputs. Following this, structure/function analyses can then be performed to dissect out how these individual components of the overall dimorphic neural architecture might then contribute to individual modalities of non-sex- and sex-specific behavioural outputs (Datta et al., 2008; Kimura et al., 2008; Kohatsu et al., 2011; von Philipsborn et al., 2011).

4.1.3 The neuronal cluster dsx-pC2 is comprised of two distinct subsets in males but not females

Historically *dsx*-pC2 has been described as a single cluster in both males and females (Lee et al., 2002). However in pupal and adult brains, while only one distinct *dsx*-pC2 cluster is apparent in the female, the cluster is often ‘split’ into two distinct medial (*dsx*-pC2m) and lateral (*dsx*-pC2l) subsets in the male (Figure 4.8). This is evident in Figure 4 of Lee et al. (2002) though is not described as such in the text and again is referred to in Robinett et al. (2010) though they do not ascribe the medial and lateral clusters as male-specific. These distinct subsets appear to contribute separate axonal fascicles to the overall *dsx*-neural circuitry (Figure 4.8B). It would be tempting to speculate that the increased population of neurons in the male –pC2 cluster (this increase particularly associated with adult development; see Figure 4.2 and Table 4.1), presenting as it does into medial and lateral clusters, actually represents the development in the pupa and adult of a

further novel male-specific cluster, which again contributes to the increased complexity associated with the *dsx*-specified male neural circuitry.

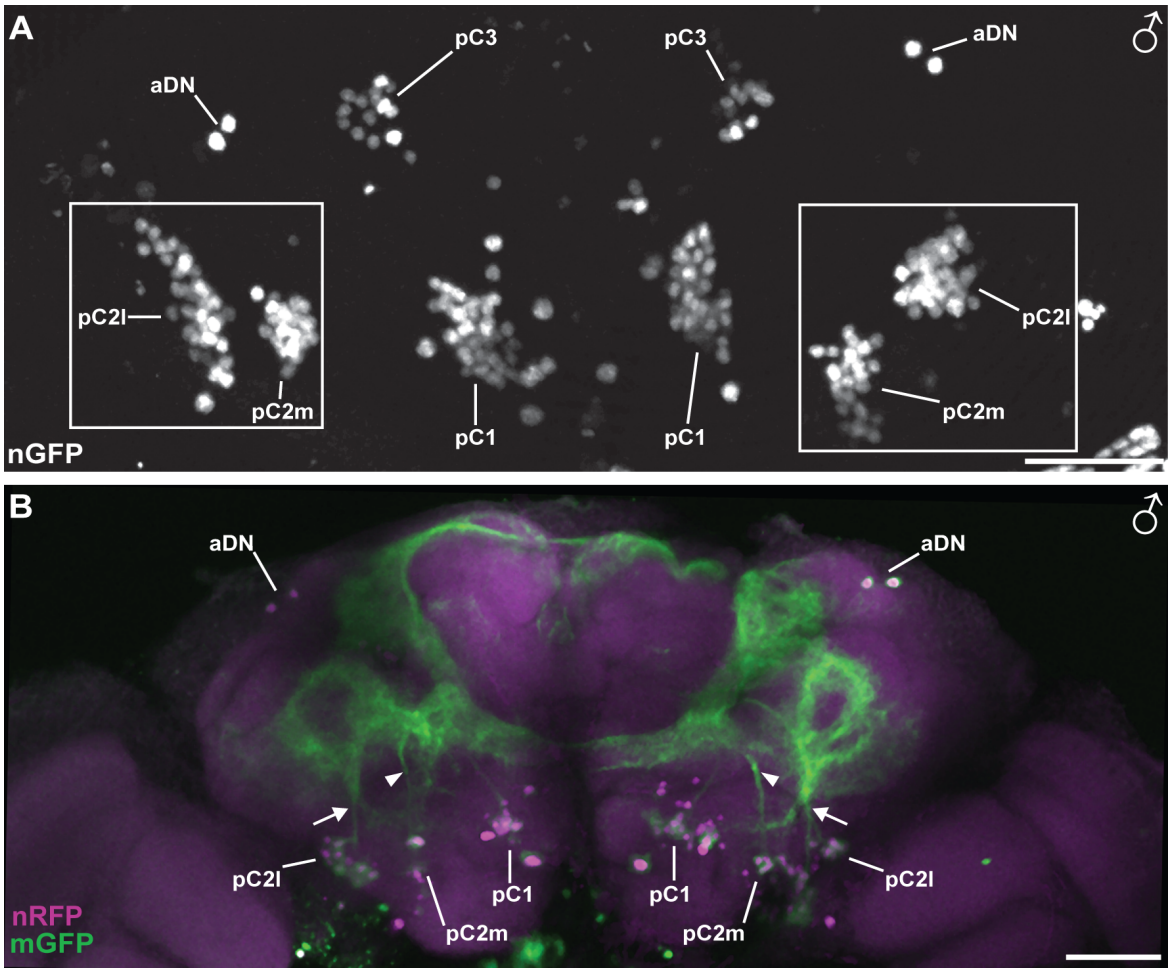

Figure 4-8 Demonstration of distinct medial and lateral subsets of the *dsx*-pC2 neuronal cluster in pupa and adult male brains.
(A) Detail of 2 D *dsx*^{GAL4} pupal brain expressing UAS-StingerII (nGFP). *dsx* neuronal clusters indicated (Dorsal view, anterior top). (B) Detail of a horizontal plane of view 5 D *dsx*^{GAL4} male adult brain expressing UAS-mCD8::GFP (mGFP, green) and UAS-StingerII (nGFP, magenta). Distinct individual fascicles associated with *dsx*^{GAL4}-pC2m (arrowheads) and *dsx*^{GAL4}-pC2l (arrows). *dsx* neuronal clusters indicated. Full maximal confocal stack of this image shown previously in Figure 4.5 (Horizontal view, ventral top). *dsx* neuronal clusters as per Lee et al. 2002, Rideout et al 2010 and Robinett et al. 2010. Scale Bars = 50 µm.

4.1.4 dsx^{GAL4} determined expression of projections in male and female adult VNCs

In the adult male VNC, moving ventro-dorsally there are extensive projections from the foreleg entering the prothoracic ganglia to form a strong plexus including, most notably, a contralateral commissural bridge (Figures 4.9 and 4.10; see Supplementary Video 2, Rideout et al., 2010) within this plexus run superiorally and inferiorally, making what seems to be 'junctional' connections with *dsx*-TN2 cells (Figures 4.9 and 4.10; see Supplementary Video 2, Rideout et al., 2010). The

TN2 cells are described as a set of large male-specific bilaterally paired cells, again which colocalise with Fru^M (Rideout et al., 2010), positioned medially along the longitudinal plane of the VNC from the Prothoracic to Metathoracic ganglia (Figures 4.9 and 4.10; Lee et al., 2002; see Supplementary Video 2, Rideout et al., 2010). These are connected together by contra-lateral commissural projections as well as ipsi-laterally to the circuit as a whole (Figures 4.9 and 4.10; see Supplementary Video 2, Rideout et al., 2010). However the TN2 cells do not all lie in the same ventro-dorsal plane within the VNC, this 3-dimensionality (positioned in not only the x and y but also z axes) adding to the complexity of the architecture of the associated projections (see Figure 4.10). Moving ventro-dorsally a bilateral pair of TN2 neurons (MsTN2'; Figure 4.10) is initially apparent in the Msg. Directly below this a bilateral group of two TN2 neurons (MsTN2"; Figure 4.10) is observed along with a bilateral pair of TN2 neurons (PrMsTN2'; Figure 4.10) positioned between the Prg and Msg. Both these sets of TN2 neurons lie in a plane with, and flank, the *dsx*-TN1 clusters (TN1; Figure 4.10). Also observed in this plane is a bilateral group of two TN2 neurons (MtTN2'; Figure 4.10) in the Mtg. Dorsal to these neurons lies a bilateral group of two TN2 neurons (PrTN2'; Figure 4.10) in the Prg. Finally directly below these in the Prg the dorsal most bilateral pair of TN2 neurons (PrTN2"; Figure 4.10) maybe observed. Projections are present from the mid- and hindlegs to TN2 cells in the VNC, however they are very much reduced in number compared with those in the foreleg and as such are difficult to visualise. Notably, a set of projections are apparent in the medial Msg at the site of the *dsx*-TN1 neuronal clusters which connect to the associated TN2 cells as well as the contra-lateral commissural bridge (Rideout et al., 2010) forming a 3 dimensional (in the x, y and z axes) 'plexus' of connecting projections (Yu et al., 2010). The *dsx*-TN1 clusters again are male-specific and have been shown to colocalise with Fru^M (Rideout et al., 2007). Inferior to this, another more attenuated plexus of projections is apparent in the MsMtg. Again this plexus of projections is seen to form a contra-lateral commissural bridge and appears to have projections originating, or terminating, within the medial Msg at the site of the *dsx*-TN2 cells (Figures 4.9 and 4.10; see Supplementary Video 2, Rideout et al., 2010).

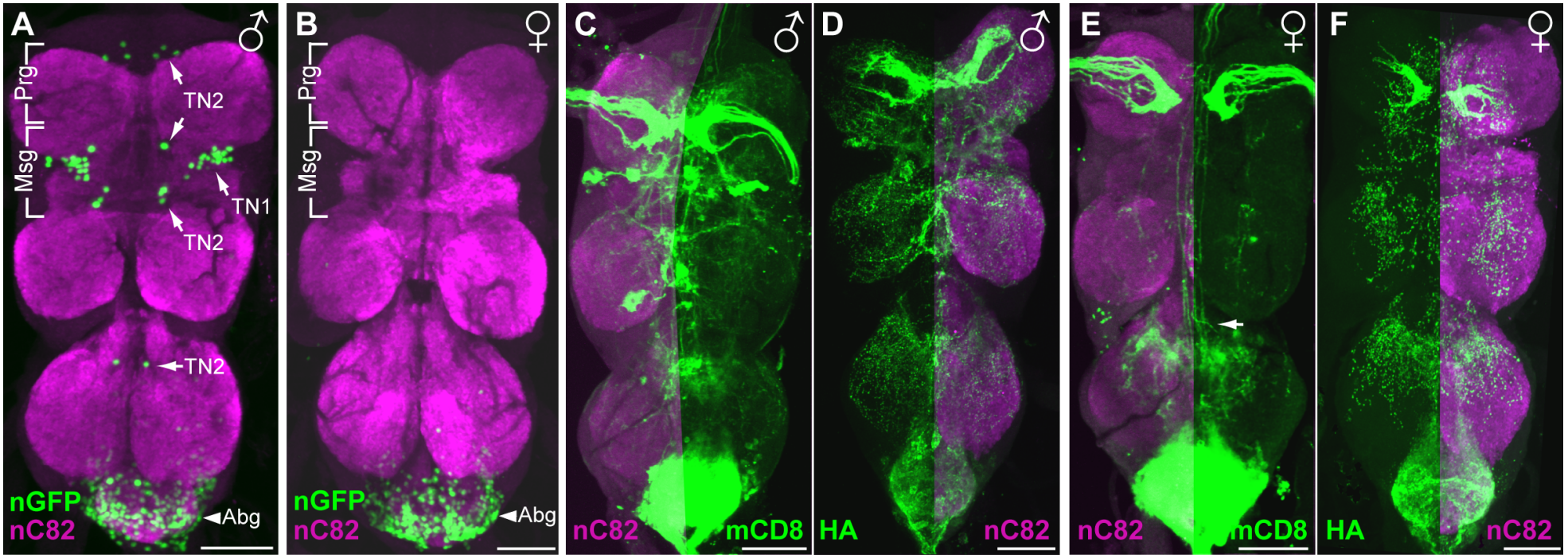

Figure 4-9 Sexually dimorphic expression of *dsx*^{GAL4}-neurons and associated projections and synapses in the VNCs of 5 day old adult males and females. (A) Male VNC, Abg cluster (arrowhead), male-specific TN1 and TN2 neurons (arrows). (B) Female VNC, Abg cluster (arrowhead). (C-D) Male VNCs exhibiting axonal projection (C) and synaptic (D) patterns of expression associated with the male *dsx*^{GAL4} neurons. (E-F) Female VNCs exhibiting axonal projection (E) and synaptic (F) patterns of expression associated with the female *dsx*^{GAL4} neurons. Hindleg contralateral projection (arrow, E). Neuronal cell bodies expressing UAS- pStingerII (nGFP) are shown in A and B. nGFP, green. Neuronal projections expressing UAS-mCD8::GFP (membrane-bound GFP) are shown in C and E. mCD8, green. Expression of UAS-synaptotagmin (pre- synaptic marker tagged with HA) is shown in D and F. HA, green. Neuropil was counterstained with antibody to nC82 (magenta). Ventral views; anterior top. Scale bar = 50 µm. Figure modified from Rideout et al. 2010.

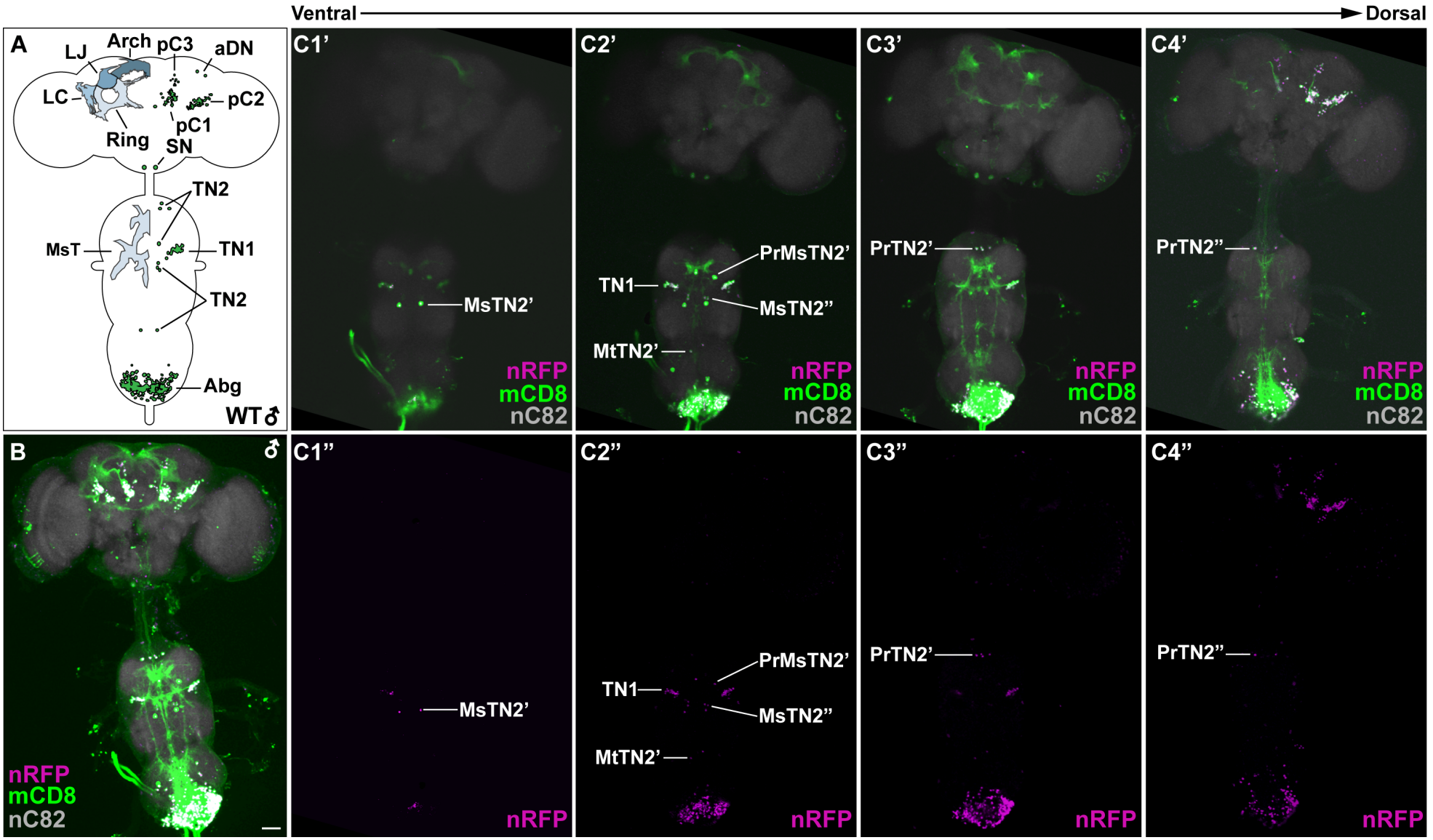
Ventral
Dorsal
A
LJ
Arch
pC3
aDN
LC
pC2
pC1
Ring
SN
TN2
MsT
TN1
TN2
Abg
WT♂
C1'
MsTN2'
nRFP
mCD8
nC82
C2'
PrMsTN2'
TN1
MsTN2"
MtTN2'
C3'
PrTN2'
C4'
PrTN2"
B
♂
C1"
C2"
C3"
C4"

Figure 4-10 *dsx*^{GAL4} nuclear and membrane-bound fluorescent protein expression in the CNS of a 5 day old adult male highlighting the topographical positioning of the male-specific neurons and their associated projections in the VNC.
(A) Schematic representation of *dsx*^{GAL4} neuronal expression in the adult male CNS. Neuronal clusters in the CNS indicated as per Lee et al., 2002 and Rideout et al., 2010. Lateral protocerebral complex (Arch; LJ, lateral junction; LC, lateral crescent; Ring) and mesothoracic triangle (MsT) indicated as per Yu et al., 2011. (B) Maximal Z Projection stack of a 5 day adult *dsx*^{GAL4} male CNS expressing nuclear RFP (magenta) and membrane-bound GFP (green). Neuropil counterstained with antibody to nC82 (gray). Dorsal view, anterior top. Scale bar = 50 µm. (C1-4) Subsections of Z projection slices, progressing ventrally to dorsally, of the *dsx*^{GAL4} male CNS shown in (B), highlighting expression in the male-specific neurons (nRFP, magenta) and their associated projections (mCD8, green) in the VNC. (C1') and (C1") Expression in a bilateral pair of TN2 neurons (MsTN2') in the Msg indicated. (C2') and (C2") Expression in a bilateral pair of TN2 neurons (PrMsTN2') between the Prg and Msg, in a bilateral group of two TN2 neurons (MsTN2"), and the TN1 cluster (TN1) in the Msg, and in a bilateral group of two TN2 neurons (MtTN2') in the Mtg indicated. (C3') and (C3") Expression in a bilateral group of two TN2 neurons (PrTN2') in the Prg indicated. (C4') and (C4") Expression in a bilateral pair of TN2 neurons (PrTN2") in the Prg indicated.

Dorsally to this, projections run ipsi-laterally along the VNC both superiorally, with at least 8 major fascicles (4 bilateral pairs) running through the cervical connection (Figure 4.11; n = 10) and inferiorally, to the abdominal ganglion (Abg) where the most distal projections appear to form a large overt plexus with the Abg (Figures 4.9 and 4.10).

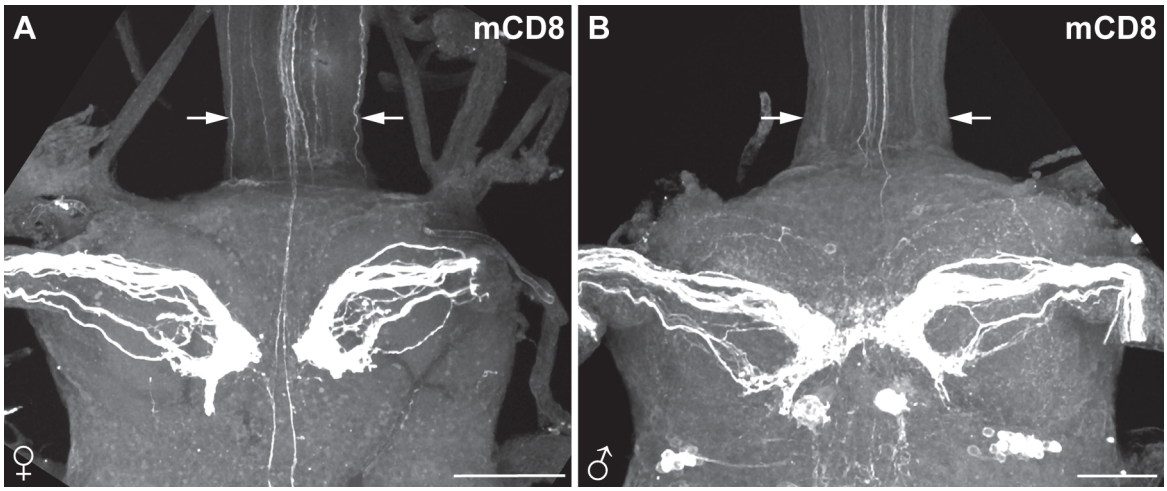

Figure 4-11 Detail of the major fascicles associated with *dsx*^{GAL4} expression projecting through the cervical connections in 7 day old adult males and females.
Detail of the prothoracic and cervical region of the VNC in (A) female and (B) male VNCs of *dsx*^{GAL4} adults expressing UAS-mCD8::GFP (membrane bound GFP). Arrows in (A) highlight a lateral pair of major fascicles not apparent in (B). n = 10. Scale bar = 50 µm.

Again a population of cells within the Abg colocalises with *fru*-specific cells including some, but not all of the male-specific serotonergic (SAbg) neurons (Billeter et al., 2006b). *dsx*^{GAL4} appears to be expressed in 3 of the ventral (Figure 4.12A) and 3 of the dorsal (Figure 4.12B) SAbg neurons. This is in keeping with what would be predicted from the findings of Billeter et al. (2006a) which

demonstrated that expression of *dsx* was necessary for the determination of the full complement of SAbg neurons, with Fru^{MC} then required for the proper organisation of the neurons into their discrete clusters. These neurons send serotonergic positive projections through the abdominal nerve trunk (AbNvTk) to ramify on the ejaculatory duct, accessory glands, vas deferens and seminiferous tubules of the internal genitalia (Billeter et al., 2006b). A lower level of dsx^{GAL4} GFP driven expression is also observed in innervation ramifying on the testes but this does not colocalise with serotonin (Figure 4.12C, D).

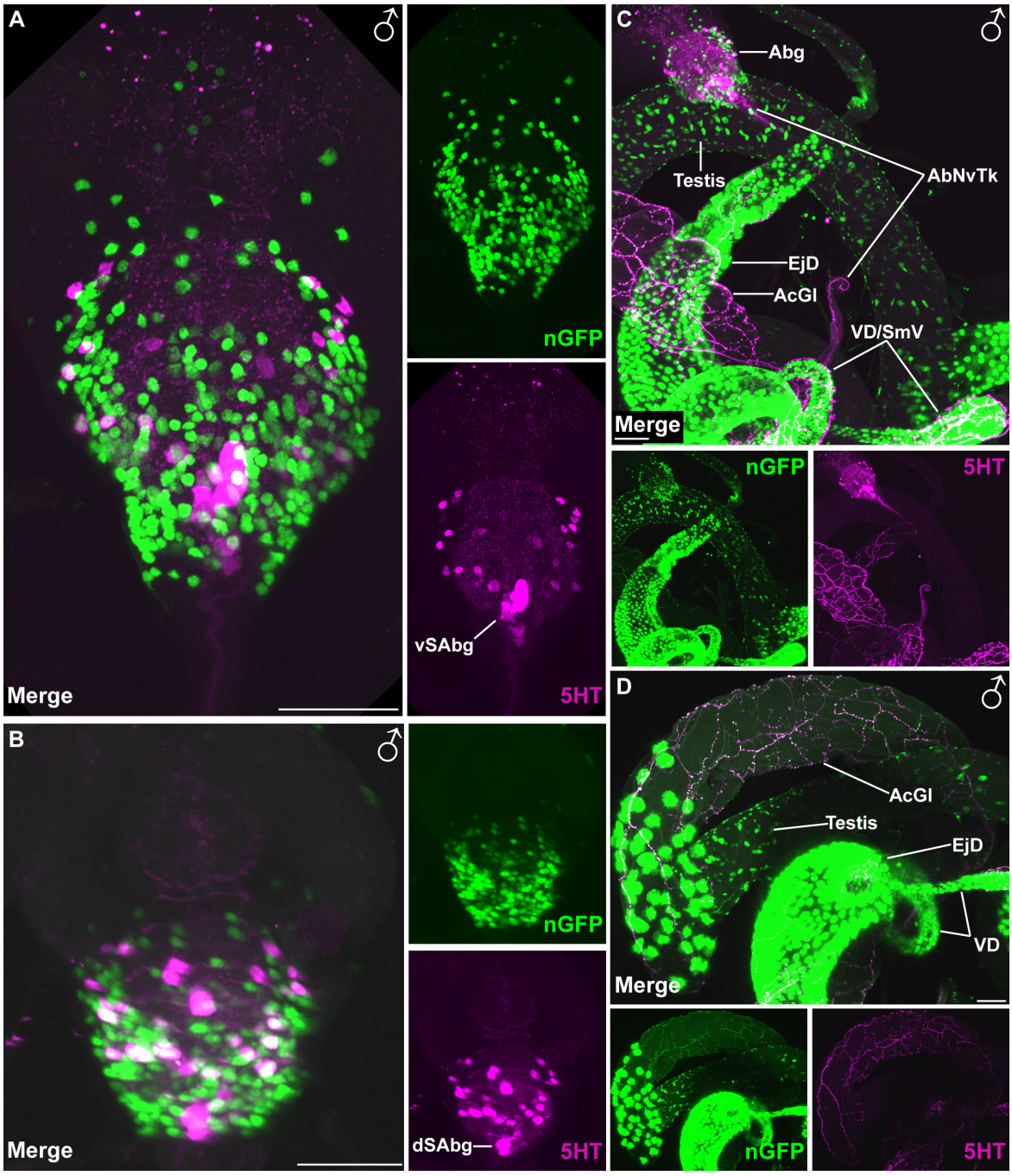

Figure 4-12 Colocalisation of serotonin (5HT) with *dsx*^{GAL4} nGFP expression in the abdominal ganglia and internal genitalia of 5 day old adult males.
(A-B) Detail of the abdominal ganglia expressing *dsx*^{GAL4} nuclear GFP co-stained with anti-serotonin in the VNCs of 5 day old adult males. (A) Ventral and (B) dorsal views, anterior top. Ventral (vSAbg; A) and dorsal (dSAbg; B) male-specific serotonergic clusters indicated (Billeter et al., 2006b). (C) VNC attached by its abdominal nerve track (AbNvTk) to the internal genitalia and (D) detail of the internal genitalia in a 5 day old adult male expressing *dsx*^{GAL4} in a 5 day old adult male expressing *dsx*^{GAL4} nuclear GFP co-stained with anti-serotonin. Testis; ejaculatory duct, EjD; accessory gland, AcGl; and vas deferens/ seminiferous vesicles, VD/SV indicated. Nuclear GFP (nGFP), green; serotonin (5HT), magenta. n = 10. Scale bar = 50 µm.

In the adult female VNC, as in the brain, the pattern of expression of projections is similar to that in the male but at an overtly attenuated level reflective of the overall decrease in the number of neuronal clusters and associated projections (Figures 4.9; see Supplementary Video 2, Rideout et al., 2010). Most conspicuous however is the absence of contralateral projections within the VNC (Figure 4.9E). This is most notable with respect to the projections running from the foreleg into the prothoracic ganglion, which do not form a trans-commissural bridge (Figures 4.9; see Supplementary Video 2, Rideout et al., 2010). As females lack the *dsx*-TN1 and -TN2 cells there is also a complete absence of the plexus of projections including the trans-midline projections originating, or terminating, within the medial Msg and Mtg (Figure 4.9E). There are some female-specific dimorphisms apparent such as an increase in the number of axonal bundles in the cervical connection. Here there appears to be at least 10 major fascicles (5 bilateral pairs) connecting the brain to the VNC, as opposed to four major fascicles in the male, presumably reflective of the increased cell population in the Abg, and therefore an increase in associated ascending and descending neuronal projections, with respect to the male (Figure 4.11). These fascicles also exhibit an altered 3-dimensional topographic distribution within the cervical connection. This presumably reflects the dimorphic distribution of neuronal populations within both the VNC and the brain between males and females and the consequent altered neural architecture resulting from both the shared and altered relationship these neurons have to one another.

Realization of these expression patterns clearly demonstrates significant differences in neuronal cell numbers, projections and synapses in *dsx*-determined neural architecture in areas of the brain associated with sex-specific behavioural foci. Overall differences in the dimorphic neural circuitry are profound and indisputably are associated with male and female expanded regions (MER and FERs) in the brain (Cachero et al., 2010). It is tempting to speculate that the assembly of these neural networks, and the sex-specific differences in neural organization that arise as a consequence, must go to shape the different behavioural outputs observed in males and females.

4.2 Transgenic intersectional tools that impinge on dsx^{GAL4} expression in the central nervous system

embryonic lethal abnormal vision-GAL80 (*elav*-GAL80; a kind gift from S. Sweeney) targets the expression of the GAL4 inhibitor GAL80 specifically to post-mitotic neurons using the *elav* promoter (Lee and Luo, 1999). To validate this intersectional tool I, in conjunction with Dr. Elizabeth Rideout, examined dsx^{GAL4}-nuclear GFP expression in neuronal and non-neuronal tissues in the presence of *elav*-GAL80. We were able to show that marker expression is indeed specifically and comprehensively suppressed throughout the adult CNS (Rideout et al., 2010). This tool may therefore be used to identify *dsx* expression in neuronal cells associated with various tissues in the adult fly. Further, expression of this tool may be used to repress the expression, and therefore negate the effects, of other transgenic tools used to impair neuronal activity thereby establishing the neuronal aetiology of any observed behavioural phenotypes associated with manipulation of dsx^{GAL4} expressing cells (see Chapter 7 of this study).

teashirt-GAL80 (*tsh*-GAL80) drives expression of the GAL4 inhibitor GAL80 using the *tsh* promoter (Clyne and Miesenböck, 2008; Lee and Luo, 1999). *tsh* a homeotic gene with pleitropic effects, is required globally for segmental identity throughout the entire trunk (thorax and abdomen) and has a critical requirement for the proper identity of the anterior prothorax. It is this latter role that is of interest, as this region should see the specific repression of expression within the Msg, the area in which the *dsx*-TN2 neuronal clusters are expressed. To validate this intersectional tool I examined dsx^{GAL4}-nuclear GFP expression in the adult CNS in the presence of *tsh*-GAL80. Examination of the CNSs in adult males demonstrated that marker expression is indeed specifically and comprehensively suppressed in the *dsx*-TN1 clusters as well as the two smaller bilateral pairs of *dsx*-TN2 neurons in the Msg and Mtg (Figure 4.13C, D). Associated with this repression of expression in the Msg is the complete absence, or at least severe reduction, of the axons derived from or projecting to these cells (Figure 4.13D). Expression of this transgenic tool does not appear to impinge on expression of any other cells and neuronal clusters or their associated projections within the VNC and brain (Figure 4.13C, D). Therefore this tool may be of use in studies for delineating a role for the *dsx*-TN1 neuronal clusters in the generation of male-specific courtship song (*cf*. Clyne and Miesenböck, 2008).

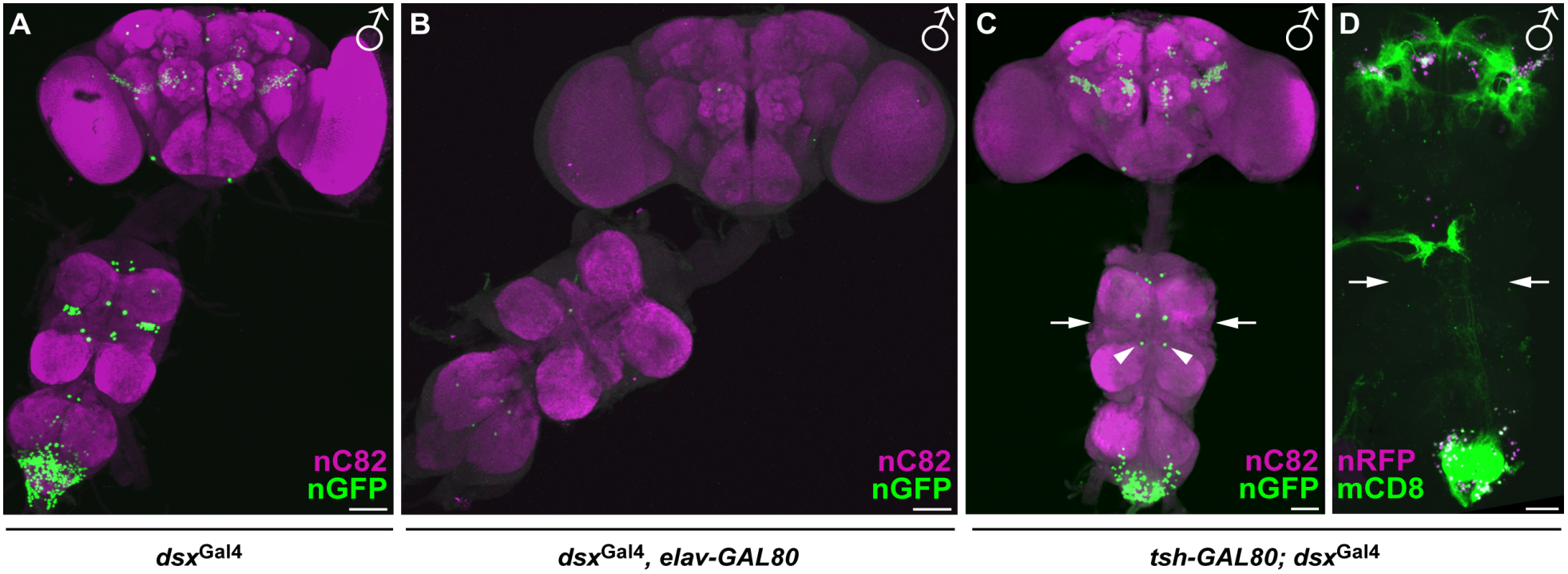

Figure 4-13 Demonstration of specific repression of *dsx*^{GAL4} nuclear GFP or RFP expression by concomitant expression of either *elav*-GAL80 or *tsh*-GAL80 in the CNSs of 5 day old adult males.
(A) UAS-StingerII; *dsx*^{GAL4}, (B) UAS-StingerII; *dsx*^{GAL4}, *elav*-GAL80 and (C) *tsh*-GAL80/UAS-StingerII; *dsx*^{GAL4} CNSs. Nuclear GFP (nGFP), green; neuropil counterstained with antibody to nC82 (nC82), magenta. (D) *tsh*-GAL80/UAS-RedStinger; *dsx*^{GAL4}UAS-mCD8::GFP CNS. Membrane-bound GFP (mGFP), green; nuclear RFP (nRFP), magenta. Arrows indicate missing *dsx*-TN1 clusters (C, D). Arrowheads indicate missing *dsx*-TN2 neurons (C). Ventral views, anterior top. (A-B) as per Rideout et al. 2010. n ≥ 10. Scale Bars = 50 µm.

4.3 dsx^{GAL4} expression in the peripheral nervous system

With the demonstrated expression of *dsx*^{GAL4} within the CNS there must almost certainly be, as a consequence, coincident expression (both motor and sensory) within the peripheral nervous system (PNS) in specific associated tissues. This has been demonstrated in other studies (Kimura et al., 2008; Mellert et al., 2010; Rideout et al., 2007; Robinett et al., 2010) and has already been exemplified in this study by the described expression within the Abg and internal genitalia in the male (Billeter et al., 2006b; Rideout et al., 2010). In the following sections of this chapter, I not only describe the *dsx*^{GAL4} expression pattern in the forelegs of adult males and females, which exhibit sexually dimorphic expression of gustatory sensilla (Nayak and Singh, 1983; Possidente and Murphey, 1989), but also attempt to give some indication as to possible interactions *dsx*^{GAL4} neurons in the forelegs might make with higher order processing centres and the effects loss of these sensory receptors might have on *dsx* neural organisation and, ultimately, on the behavioural outputs associated with these sensilla. Further to this in the following chapter while describing *dsx*^{GAL4} expression patterns in the soma, almost inevitably there may be indicated roles for *dsx*^{GAL4} expression in the associated PNS of the specific tissues observed.

4.3.1 dsx^{GAL4}-expressing cells include gustatory receptors

In the foreleg *dsx*^{GAL4} expression demonstrated a significant difference in cell numbers in males, both in the metatarsus (96 ± 14.4 SD, n=7) and tarsi 5 - 2 (72 ± 10.0 SD, n=7), as compared to females (77 ± 12.4 SD, n=8; and 58 ± 9.7 SD, n=7; for the metatarsus and tarsi 5 - 2 respectively; Figure 4.14A). Some, but not all, of these cells are neuronal, indicated firstly by membrane-bound GFP aggregate formation at the point of the receptor cell body (data not shown) and secondly by consequent reduction in cells numbers apparent with the concomitant expression of the neuronal GAL4 repressor *elav*-Gal80 (Rideout et al., 2010). More *dsx*^{GAL4}-expressing cells are repressed in males than females, suggesting there are a more neurons in the male foreleg, a finding in keeping with the observations of Possidente and Murphey 1989.

Interestingly, females exhibited a significantly higher number of *dsx*^{GAL4}-cells in the hindleg both in the metatarsus (84 ± 12.2 SD, n=10) and tarsi 5 - 2 (42

± 8.7 SD, n=10) compared to males (60 ± 16.7 SD, n=9, and 18 ± 7.1 SD, n=9 for the metatarsus and tarsi 5 - 2 respectively) (Figure 4.14B).

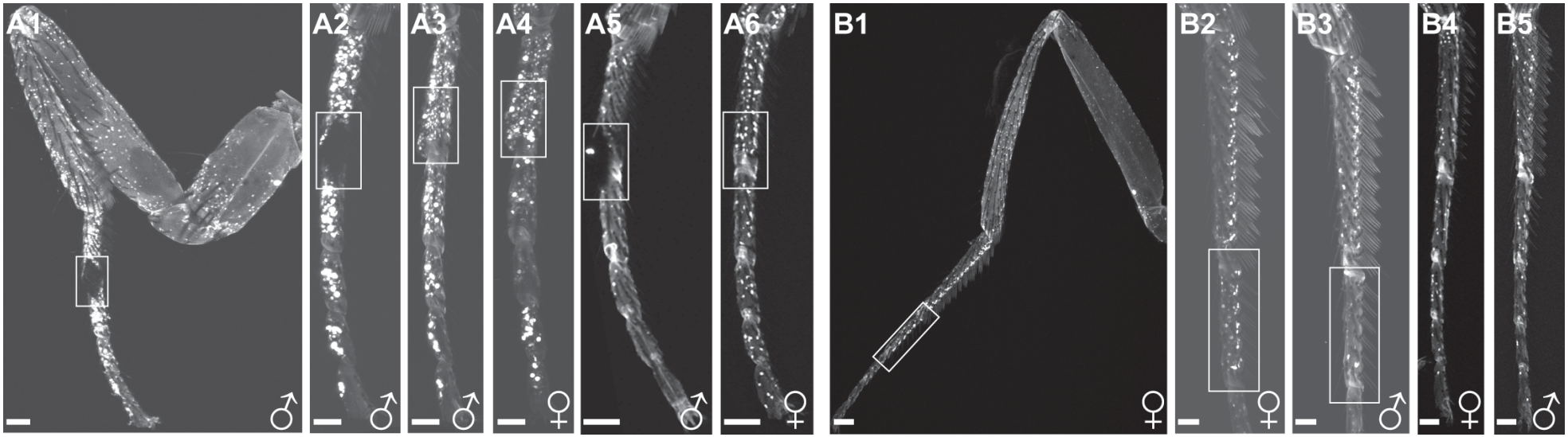

Figure 4-14 Sex-specific *dsx*^{GAL4} expression of nuclear GFP in the fore- and hindlegs of adult males and females.
(A1-6) Sexually dimorphic expression pattern in the foreleg with increased numbers of cells in the male tarsi, especially associated with the male metatarsal sex comb. (A1) Male foreleg (medial aspect), male-specific metatarsal sex comb (boxed). (A2) Detail of the tarsi and metatarsus of the male foreleg (medial aspect). Metatarsal sex comb (boxed). (A3) Detail of the tarsi and metatarsus of the male foreleg (lateral aspect). Metatarsal sex comb (boxed). (A4) Detail of the tarsi and metatarsus of the female foreleg (lateral aspect). Area consistent with that of the male metatarsal sex comb (boxed). (A5) Detail of the tarsi and metatarsus of the male foreleg (medial aspect) also expressing *elav*-Gal80, showing an obvious, but not complete, reduction in the *dsx*^{GAL4}-nGFP expression, indicating not all labelled cells are neuronal. Metatarsal sex comb (boxed). (A6) Detail of the tarsi and metatarsus of the female foreleg (medial aspect) also expressing *elav*-Gal80, persistence of *dsx*^{GAL4}-nGFP expression indicating labelled cells are not neuronal. Area consistent with that of the male metatarsal sex comb (boxed). (B1-5) Sexually dimorphic expression pattern in the hindleg with increased numbers of cells in the female tarsi and metatarsus. (B1) Female hindleg, tarsi 2-3 (boxed). (B2) Detail of the tarsi and metatarsus of the female foreleg, tarsi 2-3 (boxed). (B2) Detail of the tarsi and metatarsus of the male hindleg, tarsi 2-3 (boxed). (B4) Detail of the tarsi and metatarsus of the female hindleg, also expressing *elav*-Gal80, showing an obvious, but not complete, reduction in the *dsx*^{GAL4}-nGFP expression, indicating not all labelled cells are neuronal. (B5) Detail of the tarsi and metatarsus of the male hindleg, also expressing *elav*-Gal80, showing an obvious, but not complete, reduction in the *dsx*^{GAL4}-nGFP expression, indicating not all labelled cells are neuronal. (A1-5) as per Rideout et al., 2010. n ≥ 9. Scale bar = 50 µm.

As it is known that performing axotomy, the severing of axons from their cell bodies, can cause the associated projections distal to the point of transection to degenerate (MacDonald et al., 2006) I, in conjunction with Dr. Elizabeth Rideout, performed a series of leg amputations on *dsx*^{GAL4} flies expressing membrane-bound GFP (Rideout et al., 2010). Amputation of the foreleg below the sex comb in males, or at the equivalent point in females, showed no apparent degeneration in projections in either sex (data not shown) though this is not to say that some axonal projections are not lost from the overall fascicular bundle. However when amputations were performed above the sex comb, or again at the equivalent point in females, no prothoracic projections were observed in either sex (Figure 4.15). These projections must therefore originate in close proximity to the basitarsal area associated with the sex comb and, as only gustatory neurons are known to cross the midline in the VNC, some of the male-specific projections must be gustatory.

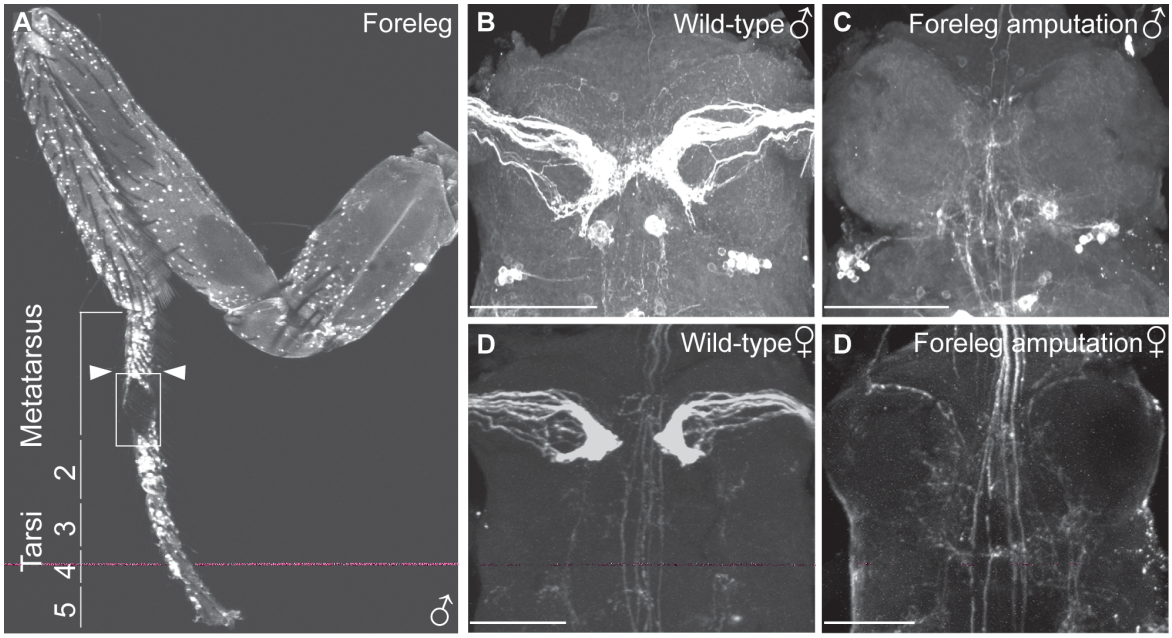

Figure 4-15 Effects of basitarsal axotomy on the prothoracic axonal projections in 7 day old adult males and females.
(A) Male foreleg (medial aspect), sex comb (boxed). Metatarsus and tarsal segments indicated. (B) Wild-type male (D) and wild-type female prothoracic axonal projections. Atrophied male (C) and atrophied female (D) prothoracic axonal projections, post-amputation. The point of amputation is indicated by arrowheads in A. n ≥ 10. Scale bar = 50 µm. Figure as per Rideout et al., 2010

As I had observed a significantly larger number of *dsx*^{GAL4}-expressing cells in the female hind leg as compared to males I also performed axotomies at the join between the hindlegs and the thorax to test if this would have any overt effect on the observed projection patterns. Complete amputations of the hindleg had no

obvious effect on projection patterns within the VNC in either sex, apart from that the apparent loss of a single contra-lateral fascicle from the hind-leg projecting into the female MtAbg (data not shown).

4.3.2 Axotomy performed on male forelegs significantly effects dsx^{GAL4} expression in specific clusters of the brain

It is known that non-sex-specific gustatory neurons in the foreleg send ispsi-lateral projections to the prothoracic ganglion and on through the cervical connection to higher order processing centres in the brain, while (male) sex-specific gustatory neurons in the foreleg contribute both ispso- and contra-lateral projections (Koganezawa et al., 2010; Mellert et al., 2010; Possidente and Murphey, 1989; Wang et al., 2004). Indeed it has been shown that amputation of one of the forelegs above the sex comb can severely affect the courtship behavioural outputs of an adult male (Koganezawa et al., 2010). Axotomy at this point significantly changing the male courtship 'posture' by increasing bilateral, as opposed to unilateral, wing extension; thereby altering the tonal characteristics of the courtship song generated and, presumably as a consequence of this, reducing courtship success (Koganezawa et al., 2010). I decided to examine the effect that performing various amputations on the adult foreleg might have on the associated *dsx* neural architecture in the CNS, initially with a view to determining if the neuronal pattern of expression within the Msg, which has been described as the localised 'song pattern generator' (Clyne and Miesenböck, 2008), was in any way altered. In the VNC the male-specific *dsx*-neurons appear largely unaffected; there was no observed reduction *dsx*^{GAL4} expression in either of the *dsx*-TN1 clusters even in the animals with double amputations (data not shown; n=9); there were observed reductions in the *dsx*-TN2 cells specific to the Prg and Msg but the number and position of neurons affected were so variant that quantification was not possible. However, as may be seen below, it became clear that it was specific *dsx*-neuronal clusters in higher-order processing centres that appeared most affected as a consequence of performing axotomies on the forelegs.

In males, while it appears that transecting neurons in the foreleg below the sex comb still affects specific *dsx* neuronal clusters, the major effects are seen to occur when the point of amputation is above the sex comb. These effects are exacerbated if a double axotomy (one leg below the sex comb, the other above) is

performed. The reduction *dsx*^{GAL4} expression in neuronal clusters is predominantly associated with the clusters in the hemisphere ipsi-lateral to the side of the amputation, but some effects are also apparent on the corresponding contra-lateral clusters. The two clusters affected are *dsx*-pC1 and –pC2 (Figures 4.16, 4.18 and Table 4.2) while the –pC3 clusters (Figures 4.16, 4.18 and Table 4.2) and -aDN and –SN neurons remain unaffected on either side (Figures 4.16, 4.18 and Table 4.2). The more extreme reductions in neuronal cell counts are observed in the *dsx*-pC2 neurons, more specifically the –pC2l clusters (Figures 4.16, 4.18 and Table 4.2). This apparent bias in the reduction of *dsx*-pC2l as opposed to –pC2m neurons again emphasising that *dsx*-pC2 is in fact comprised of two distinct clusters and that at least a sub-population of neurons within the –pC2l cluster maybe male-specific. This reduction in neuronal numbers is surprising, however it has previously been shown that amputation of the olfactory receptor neurons in crayfish leads to not only a degeneration of the receptor cell endings in the ipsi-lateral olfactory lobe (the contra-lateral lobe remains unaffected) but also causes a 'trans-synaptic response' in which the number of higher order neurons is also observed to decrease (Sandeman et al., 1998). Amputation of the crayfish antennae leading to a loss of projection neurons and (more specifically) interneurons from the brain after loss of the afferent input, through a process of PCD (Sandeman et al., 1998) and it maybe that a similar process is occurring to cause a decrement in neurons in specific clusters in the brains of the amputated flies examined here.

In females no decrement in any cluster is observed even with animals undergoing a double amputation. Surprisingly in fact there appears to be a slight, though still significant, increase in the *dsx*-pC1 and –pC2 clusters (Figure 4.17 and Table 4.2). Again no changes were observed in the *dsx*-pC3 clusters (Figure 4.17 and Table 4.2) or the *dsx*-aDN neurons (Table 4.2). Whether the observed increases are a real consequence of the amputations, perhaps the loss of some anterograde signals from the projecting neurons inhibiting female-specific PCD or prolonging neuroblast formation, or are an artefact of the cell counts needs further investigation.

Table 4.2 Comparison of *dsx*^{GAL4} nuclear GFP expression in brains 7 days after axotomy in males and females above and/or below the sex comb, or a position corresponding to the region of the sex comb

		7 day old Adult Males							
	Dsx Neuronal clusters[1]	WT No Amputation [2]	Single amputation below the sex comb		Single amputation above the sex comb		Double amputation above and below the sex comb	
			Ipsi-lateral side to that of the non-amputated leg	Ipsi-lateral side to that of the amputated leg	Ipsi-lateral side to that of the non-amputated leg	Ipsi-lateral side to that of the amputated leg	Ipsi-lateral side to the amputated leg below the sex comb	Ipsi-lateral side amputated leg above the sex comb
Brain neuronal counts								
1	*dsx*-pC1[3]	57 ± 5.0 (10)	50 ± 7.4 (6)*	48 ± 3.2 (6)*	49 ± 8.2 (6)*	43 ± 10.0 (6)*	36 ± 8.1 (9)*	38 ± 5.1 (9)*
2	*dsx*-pC2[3]	77 ± 3.1 (10)	75 ± 5.2 (6)	67 ± 0.9 (6)*	68 ± 3.8 (6)	53 ± 11.5 (6)*	55 ± 7.3 (9)*	37 ± 10.0 (9)*
2a	*dsx*-pC2M[3]	n/a	28 ± 3.1 (6)	28 ± 4.5 (6)	29 ± 2.5 (6)	31 ± 6.0 (6)	25 ± 3.7 (9)*	18 ± 4.5 (9)*
2b	*dsx*-pC2L[3]	n/a	48 ± 5.4 (6)	40 ± 5.4 (6)	39 ± 2.9 (6)	23 ± 10.0 (5)*	31 ± 5.6 (9)*	20 ± 6.3 (9)*
3	*dsx*-pC3[3]	14 ± 1.0 (10)	13 ± 1.9 (6)	13 ± 0.8 (6)	14 ± 1.1 (6)	14 ± 1.0 (6)	13 ± 1.4 (9)	13 ± 1.4 (9)
4	*dsx*-aDN[3]	2 ± 0.5 (10)	0 ± 0.0 (6)	0 ± 0.0 (6)	0 ± 0.0 (6)	0 ± 0.0 (6)	0 ± 0.0 (9)	0 ± 0.0 (9)
5	*dsx*-SN[3]	1 ± 0 (10)	1 ± 0 (6)	1 ± 0 (6)	1 ± 0 (6)	1 ± 0 (6)	1 ± 0 (9)	1 ± 0 (9)
		7 day old Adult Females						
	Dsx Neuronal clusters[1]	WT No Amputation [2]	Single amputation below the position corresponding to the sex comb		Single amputation above the position corresponding to the sex comb		Double amputation above and below the position corresponding to the sex comb	
			Ipsi-lateral side to that of the non-amputated leg	Ipsi-lateral side to that of the amputated leg	Ipsi-lateral side to that of the non-amputated leg	Ipsi-lateral side to that of the amputated leg	Ipsi-lateral side to the amputated leg below the sex comb	Ipsi-lateral side amputated leg above the sex comb
Brain neuronal counts								
1	*dsx*-pC1[3]	9 ± 2.0 (10)	12 ± 0.9 (6)*	11 ± 1.4 (6)	12 ± 0.8 (5)*	12 ± 0.8 (5)*	12 ± 0.9 (6)*	13 ± 2.5 (5)*
2	*dsx*-pC2[3]	11 ± 1.9 (10)	14 ± 0.9 (6)*	16 ± 0.9 (6)*	14 ± 2.6 (5)*	14 ± 2.6 (5)*	14 ± 0.9 (6)*	17 ± 2.4 (5)*
3	*dsx*-pC3[3]	6 ± 1.4 (10)	6 ± 0.5 (6)	7 ± 1.0 (6)	6 ± 1.1 (5)	6 ± 1.3 (4)	6 ± 0.5 (6)	7 ± 1.2 (5)
4	*dsx*-aDN[3]	0 ± 0.0 (10)	0 ± 0.0 (6)	0 ± 0.0 (6)	0 ± 0.0 (5)	0 ± 0.0 (5)	0 ± 0.0 (6)	0 ± 0.0 (5)
5	*dsx*-SN[3]	1 ± 0.0 (10)	1 ± 0.0 (6)	1 ± 0.0 (6)	1 ± 0.0 (5)	1 ± 0.0 (5)	1 ± 0.0 (6)	1 ± 0.0 (5)

Table 4-2 Comparison of *dsx*^{GAL4} nuclear GFP expression in brains 7 days after axotomy in males and females above and/or below the sex comb, or a position corresponding to the region of the sex comb.
[1]Nomenclature for *dsx* neuronal clusters as per Lee et al., 2002, Rideout et al., 2010 and this study. [2] Number of nuclei expressing *dsx*^{GAL4} responsive UAS-nGFP ± standard deviation as per Rideout et al. 2010. [3]Neuronal cluster away from CNS midline. Count represents one cluster per hemisegment of the CNS. Counts represent mean ± standard deviation. n's listed in parentheses. **P*<0.005 for male counts 1, 2, 3, 4 and 5 in comparison to WT (no amputation), and for counts 2a and 2b in comparison to counts for ipsi-lateral side with no amputation. **P*<0.005 for female counts 1, 2, 3, 4 and 5 in comparison to WT (no amputation).

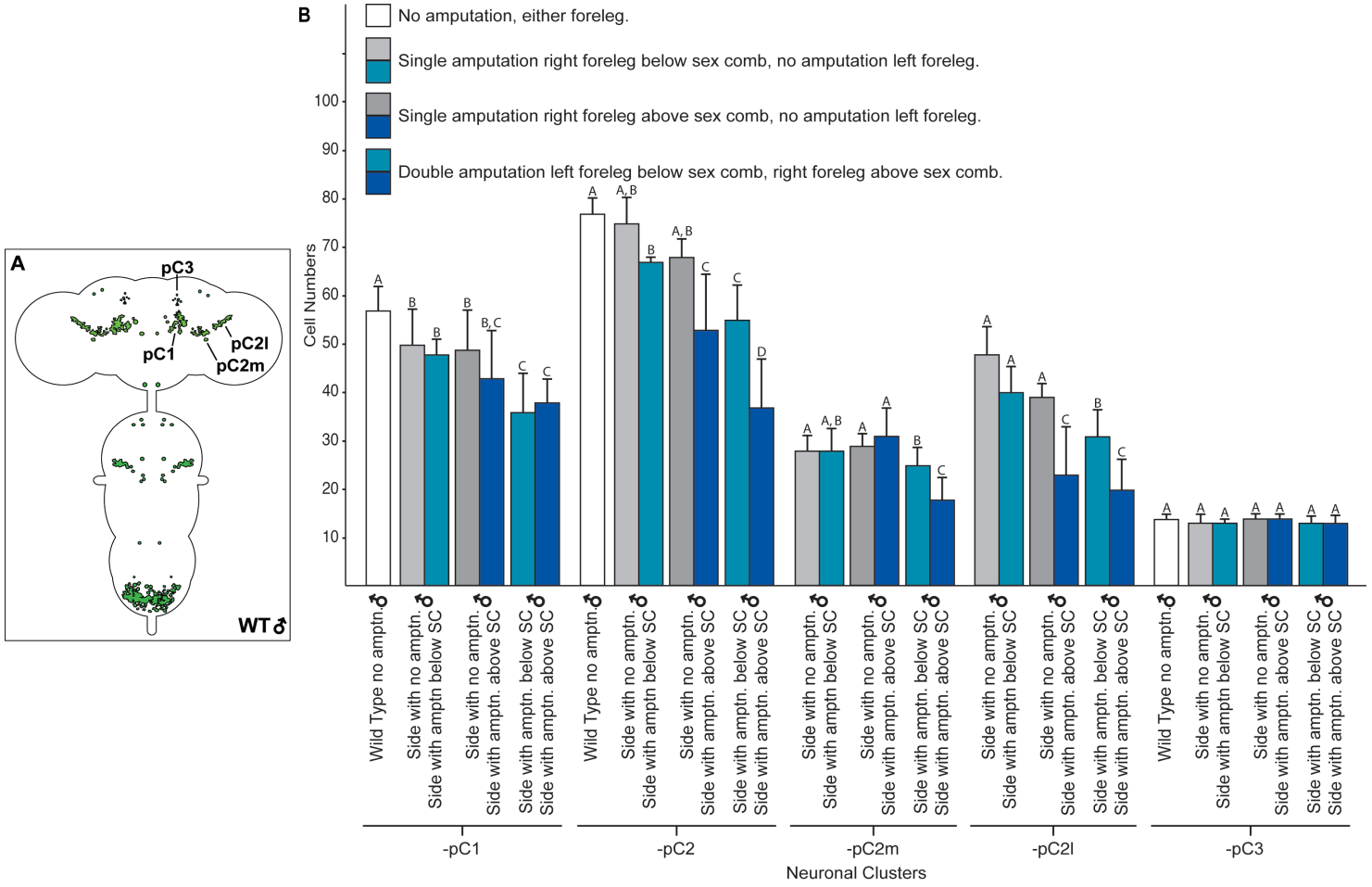

Figure 4-16 Graphical representation of the effect on *dsx*^{GAL4} nuclear GFP expression in 7 day old adult male brains after performing various axotomies to the forelegs above and/or below the sex comb.
(A) Schematic representation of *dsx*^{GAL4} neuronal expression in the adult male brain. Neuronal clusters as per Lee et al., 2002 and this study indicated. (B) Graphical representation of neuronal cell counts for each cluster after performance of described axotomy. Counts not connected by same letter above error bar represent groups within individual clusters that are significantly different (*P*<0.005) according to Student's T-test.

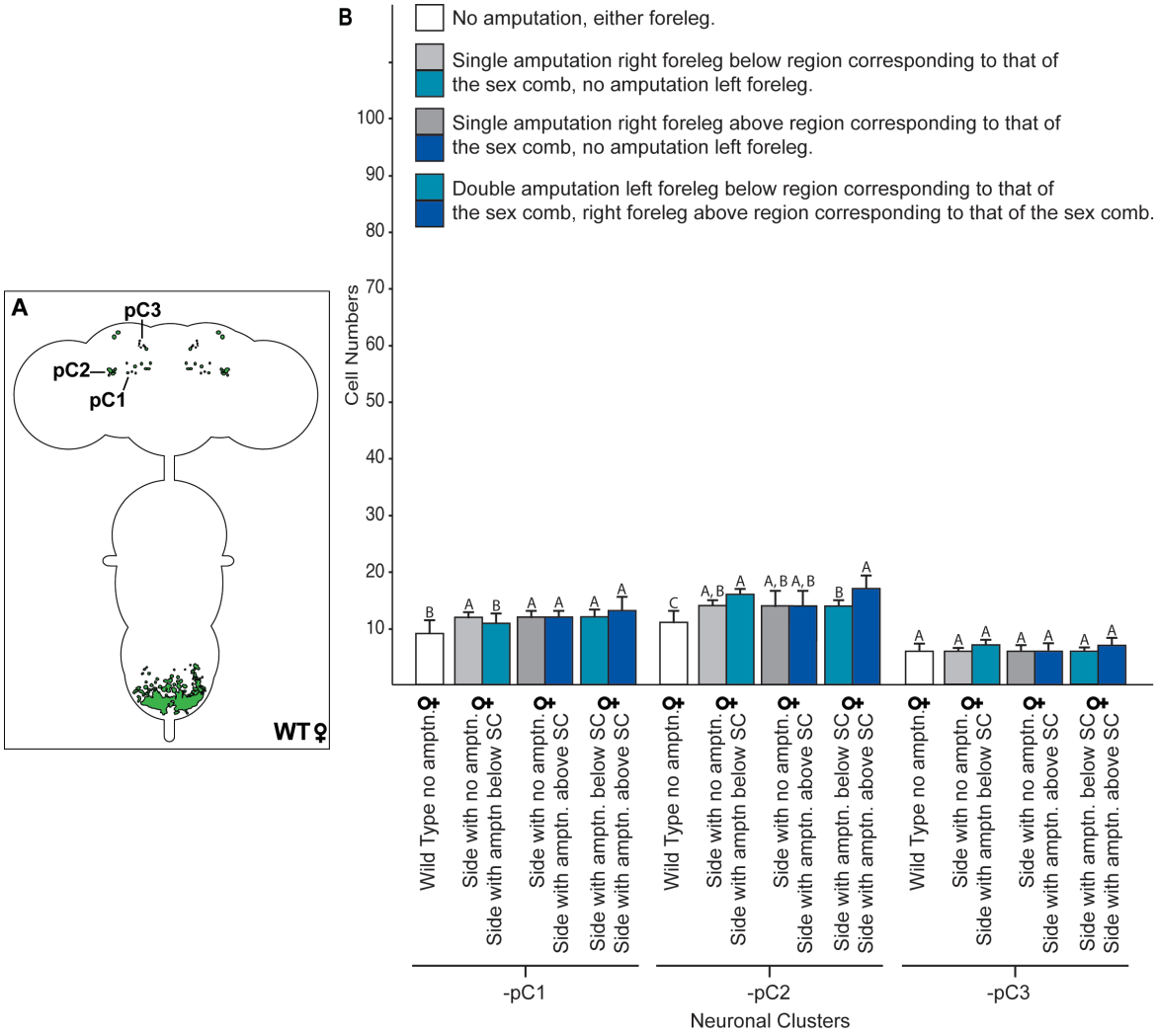

Figure 4-17 Graphical representation of the effect on *dsx*^{GAL4} nuclear GFP expression in 7 day old adult female brains after performing various axotomies to the forelegs above and/or below a region corresponding to the position of the sex comb.
(A) Schematic representation of *dsx*^{GAL4} neuronal expression in the adult female brain. Neuronal clusters as per Lee et al., 2002 indicated. (B) Graphical representation of neuronal cell counts for each cluster after performance of the described axotomy. Counts not connected by same letter above error bar represent groups within individual clusters that are significantly different (*P*<0.005) according to Student's T-test.

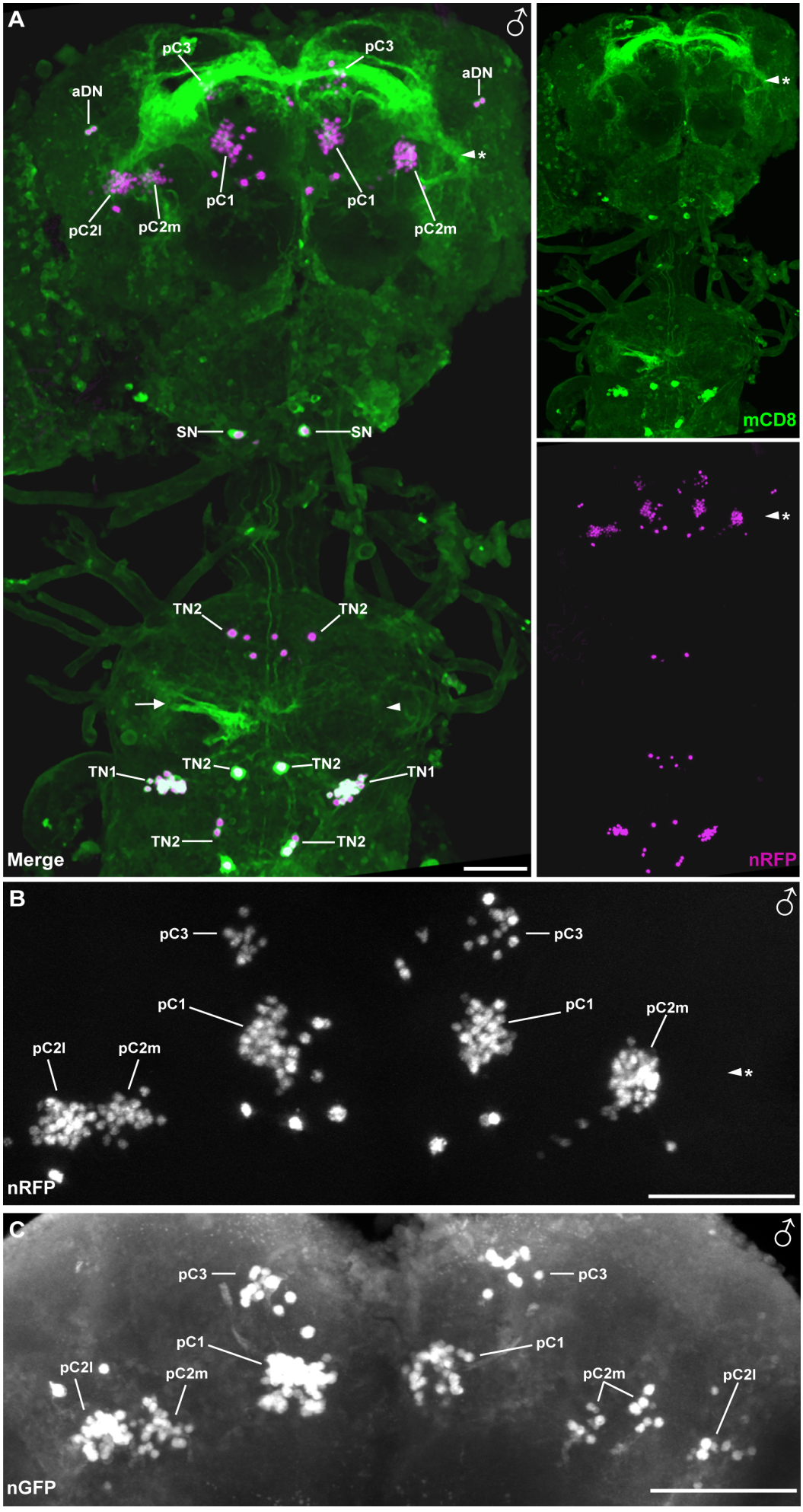
A
♂
aDN
pC3
pC3
aDN
pC2l
pC2m
pC1
pC1
pC2m
SN
SN
TN2
TN2
TN1
TN2
TN2
TN1
TN2
TN2
Merge
mCD8
nRFP
B
♂
pC3
pC3
pC1
pC1
pC2m
pC2l
pC2m
nRFP
C
♂
pC3
pC3
pC1
pC1
pC2l
pC2m
pC2m
pC2l
nGFP

Figure 4-18 Demonstration of the reduction of *dsx*^{GAL4} expression in *dsx*-pC1 and -pC2 neuronal clusters after axotomy of forelegs in 7 day old adult males.
(A) Detail of the brain and VNC of a *dsx*^{GAL4} adult male expressing both nuclear RFP (nRFP, magenta) and membrane-bound GFP (mGFP, green), in which axotomy has been performed below the sex comb on the foreleg associated with the left side and above the sex comb on the foreleg associated with the right side. Unimpaired ascending projections associated with gustatory neurons on left side (arrow). Absent ascending projections associated with gustatory neurons on right side (arrowhead). Left-hand *dsx*-pC2l cluster on side ipsi-lateral to the amputation above the sex comb appears completely absent (arrowhead asterisk). (B) Higher magnification detail of the brain from image (A) highlighting the absence of the pC2m cluster (arrowhead asterisk). (C) Higher magnification detail of a *dsx*^{GAL4} adult male brain expressing nuclear GFP demonstrating the severe reduction that may be associated with the left-hand *dsx*-pC1, -pC2m and -pC2l neuronal clusters after axotomy on the ipsi-lateral foreleg above the sex comb. Ventral views, anterior up. Scale bar = 50 µm.

4.4 Discussion

I have, through this spatial-temporal survey, been able to observe significant neuro-anatomical dimorphisms between males and females arising both from differences in neuronal numbers in homologous clusters and the presence of sex-specific neurons and neuronal clusters. While the resultant *dsx*^{GAL4} neural architecture may, superficially at least, appear similar between males and females, the increased neuronal numbers associated with both sex- and non-sex specific neuronal clusters and neurons in males have the potential to greatly expand neural complexity via increasing axonal density, connectivity and synaptic weight. These observed differences may be highly instructive as even small alterations in expression in individual neurons and neuronal clusters can result in profound differences in the architecture of the associated projections and synapses (Cachero et al., 2010; Datta et al., 2008; Kimura et al., 2008; Yu et al., 2010). One consequence of dimorphic differences in the paths these projections follow and connections they form may be altered processing of sensory inputs. Inputs which again (adding a further dimension of complexity) may themselves be sex- or non-sex specific. This altered processing potentially resulting in the generation of dimorphic behavioural motor outputs (*cf.* Yu et al., 2010). That is not to say that altered neural substrates need necessarily generate dimorphic behavioural responses, nor that shared neural circuitry may not be utilized to generate sexually dimorphic behavioural outputs. However it would appear telling that those areas in which sexually dimorphic *dsx*^{GAL4} expression is exhibited in the CNS have previously been demonstrated to be important with respect to sex-specific behaviours in both males and females (Billeter et al., 2006a; Ferveur and Greenspan, 1998; Hall, 1977, 1979; Villella and Hall, 2008; von Schilcher and Hall, 1978). As noted in Yu et al., (2010) neurons that exist in both sexes but possess

altered connectivity appear to belong to circuits either involved in sensory input reception or in the generation of motor outputs, while those sex-specific neurons and/or neuronal clusters appear to be involved in higher-order processing of the stimuli with respect to dimorphic behavioural outputs. These dimorphic neurons contributing to a greater degree towards the generation of male- and female-specific neuro anatomical structures associated with the described lateral protocerebral complex (Yu et al., 2010). It is not unreasonable to assume that the described *dsx*^{GAL4} pattern of expression in these regions also operates in a similar manner. The close approximation of the *dsx*^{GAL4} specific neuronal clusters and their associated projections to the MBs and structures of the central complex also speaks to the close relation these neural substrates may have in the integration of external stimuli and gender-appropriate behavioural responses. Further this may also involve prior social experience, as the MBs and central complex structures are key to such higher-order processing functions as olfactory and visual memory formation (Fahrbach, 2006; Heisenberg, 2003; Pan et al., 2009). It should be emphasised that courtship behaviour, in males certainly, is not just an innate but also modifiable behaviour, males needing to learn to discriminate appropriate female specific acceptance and rejection cues (Billeter et al., 2006a). As these structures also exist in the female and the relationship between the neural substrates appears largely reiterated, it would be tempting to extend this to females, who perhaps need to learn from social experience to judge potential mates for fitness. Again clonal analysis coupled with functional dissection of the described neural circuitry will provide greater insight into the individual function of the described *dsx*^{GAL4} neurons and associated neural architecture.

This survey also provides a time line progression of the dynamic manner in which these neuronal clusters develop, are maintained or lost, and therefore provides insight into the processes underlying how the final adult dimorphic circuitry is eventually derived. One process, PCD, has previously been demonstrated to be necessary to the sculpting of *dsx*-specified neural substrates (Kimura, 2011; Kimura et al., 2008; Rideout et al., 2010; Sanders and Arbeitman, 2008) and it would appear that PCD may also occur in some of the *dsx*^{GAL4} neurons/neuronal clusters observed during the development from foraging larva to mature adult (*cf*. section 6.4). While expression in the CNS is first apparent in the L2 larval stage, perhaps indicative of an early non-sex-specific role in the determination of the larval neural substrate, dimorphic expression only becomes

apparent from the L3 larval stage onwards. This is in keeping with the idea that metamorphosis is occurring not just to achieve the adult sexually dimorphic physical state but also the sexually dimorphic 'mental' state; that is to ensure that a sexually dimorphic neural circuitry is specified as well. During this development it would seem significant that the 48 hr stage of pupariation appears to be a pivotal moment in determining the final adult dimorphic male and female CNSs, as this time point has previously been identified as critical in the establishment of the neural substrates that govern sex-specific reproductive behaviours (Arthur et al., 1998; Belote and Baker, 1987). Again it is not unreasonable to assume that the creation of these differences during the developmental assembly of the circuits would consequently be functionally relevant to the generation of distinct adult sexual behaviours in both males and females.

This restricted expression of *dsx*^{GAL4} in the CNS implies that any associated expression within the PNS will be restricted as well. However where there is, or indeed isn't, expression within structures associate with the PNS is in itself instructive. It has previously been demonstrated that the direct flight muscles, used to generate male-specific courtship song, need not themselves possess a dimorphic morphology but rather they may be controlled in a sex-specific manner to produce a male-specific behavioural output (Rideout et al., 2007). Yet as has also been demonstrated, other tissues, such as the genitalia or the gustatory receptors on the foreleg, do require a dimorphic morphology to ensure proper sensorimotor processing of sex-specific behaviours (Billeter et al., 2006b; Mellert et al., 2010; Rideout et al., 2010) and unsurprisingly have been shown in this study to exhibit *dsx*^{GAL4} expression. Further complexity may be seen to occur due to *dsx* dimorphic expression in endocrinal tissues involved in neuromodulation as discussed in the following chapter (Chapter 5).

As per the observations of Koganazawa et al., (2010) male flies which have had foreleg axotomies just after eclosion (either a single amputation above the sex comb or with a double amputation, one above and one below the sex comb), when exposed to a receptive target female after 7 days isolation, displayed aberrant bilateral wing extension and took longer to successfully copulate. Koganezawa et al. (2010) postulated that the courtship deficits they observed occurred as a direct consequence of the atrophy of ascending projections from male-specific gustatory sensilla resulting in aberrant, or loss of, synaptic signalling to higher-order

processing centres, specifically the *fru*-mAL clusters. They further speculated that misdirection of male-specific courtship motor outputs specifically related to wing extension and courtship song generation was a consequence of loss of both positive unilateral non-volatile pheromonal cues (that would normally arise from the amputated tarsi's contact with the target female) and the loss of contra-lateral inhibitory cues between the two correspondent *fru*-mAL clusters (Koganezawa et al., 2010). A similar method of reciprocal excitatory/inhibitory signalling has been shown to modulate the courtship behaviour, via transient pheromonal exposure to the left and right antennae, in the silk moth Bombyx mori (Kanzaki et al., 1994). However Koganezawa et al. (2010) reasoning for suggesting that these behavioural phenotypes are derived from aberrant synaptic signalling to the *fru*-mAL clusters is due solely to the proximity of the *Gr32a*- expressing sensory neurons arbors with these clusters. While their model has real value, the loss of neurons in the *dsx*-pC1 and –pC2 neuronal clusters after axotomy may equally be, with the associated loss of proper processing of sensory stimuli, responsible for the aberrant behavioural outputs observed in these animals. As *dsx*-pC1 intersects with a sub-population of male-specific *fru*-P1 neurons (Rideout et al., 2010), known to be involved courtship initiation (Kimura et al., 2008) a significant reduction in the neuronal population of this cluster could clearly affect the initial parts of the courtship sequence (discussed in further detail in section *6.3.2*). Further the *fru*-P1 cluster itself has since been identified as comprising neurons of the *fru*-posterior Medial Protocerebral (pMP) -e clone, a cluster of 'third-order' neurons associated with the olfactory circuit (Cachero et al., 2010), a circuit known to be of importance for sensory stimulation leading to courtship initiation (Billeter et al., 2009; Ferveur, 2005b; Jallon, 1984). The *dsx*-pC2 cluster(s) colocalises with the *fru*-P cluster (Lee et al., 2000; Rideout et al., 2010), which has laterally been identified as comprising clusters *fru*-P2 to –P4 (Kimura et al., 2008). *dsx*-pC2m is positionally related to the *fru*-P2 cluster, while *dsx*-pC2l is more obviously related to *fru*-P4 (discussed in further detail in section *6.3.3*). *fru*-P2 has latterly been identified as comprising neurons from the *fru*-posterior Inferior Protocerebrum (pIP) –a, a cluster of 'second order' neurons of the auditory neural circuit, *fru*-IP-h and *fru*-pMP-f clones, clusters of 'higher interneurons' again associated with the auditory neural circuitry (Cachero et al., 2010). While *fru*-P4 has since been identified as comprising neurons from the *fru*-pIP-e clone, a cluster of 'higher interneurons' associated with the visual neural circuitry (Cachero et al., 2010). *fru*-pIP-e neurons exhibit an extensive pattern of expression, contributing to all of

lateral protocerebral complex and the corresponding areas via the protocerebral bridge (Yu et al., 2010), as well as both ipsi- and contra-lateral projections to the SOG (Cachero et al., 2010). More recently the *fru*-P1 (*fru*-pMP4) and *fru*-pIP10 neurons, whose expression is, at the very least, contiguous with neurons in the *dsx*-pC1 and –pC2 clusters, have been identified as mediating the 'decision' to initiate song production in the male (von Philipsborn et al., 2011). It is reasonable to argue that all these circuits maybe of real importance to male-specific copulatory behavioural outputs and that the significant reduction in neuronal numbers within any of these clusters may impair synaptic signaling pathways in the amputated animals leading to the aberrant behavioural motor outputs observed in this study and in Koganezawa et al. (2010). However as amputated male-flies were only observed visually, to confirm that bilateral wing extension was occurring and that courtship latency was extended prior to dissection, with no objective measurements of these specific courtship indices, further studies need to be performed to validate these assertions. Again these observations, and the subsequent dissections of CNSs, were made on 7 day old males that had been isolated from the time of amputation just after eclosion. It would be interesting, with respect to the concept of synaptic plasticity, to examine the brains of males that have undergone axotomies at different points in development. Also, perhaps more importantly, to examine the effect that earlier, and/or repeated, exposure to target females may have on the apparent atrophy of these specific neuronal clusters within the brain (with perhaps a reduction or amelioration of the observed courtship deficits). Finally it would important to attempt to reproduce these effects by perturbation of synaptic activity within specific neuronal clusters and even sub-populations of these clusters.

It has been previously demonstrated that defects in sensory and proprioceptive feedbacks can adversely effect courtship song production (Ewing, 1979b; Tauber and Eberl, 2001b), song providing not only species information but also an indicator of fitness for mate-selection. It is of interest to note therefore that tonal quality of song production may be altered by changes in not only in sensory input but also higher order processing (Clyne and Miesenböck, 2008) and finally by alteration of motor output control and that these changes in song production effecting female receptivity have the potential to act as a speciation determinant. The profound effects that alterations in the presence, or absence, of just a few neurons can have on the overall neural architecture, specifically in the connectivity

of higher order processing centres with the sensori-motor inputs and outputs speaks to how dimorphisms may occur and laterally to how dimorphic behavioural outputs may then arise. Implicit in this however there is not only the requirement for a dimorphic nervous system to interpret and process sensory inputs and stimuli in a sex-specific manner, but also the requirement for gender-appropriate somatic tissues to generate the appropriate motor responses. As such the following chapter will describe a spatial survey of the presence, and absence, of dsx^{GAL4} expression outwith the nervous system and what insight the described patterns of expression can provide in the specification of the complete male or female animal.

5 Spatiotemporal expression of *dsx*^{GAL4} outwith the nervous system of males and females

dsx is central to sex determination and for the establishment of somatic sexual characteristics in both males and females (Billeter et al., 2006a; Camara et al., 2008; Christiansen et al., 2002; Simpson, 2002). However, as with the CNS, the specific pattern of where, and when, *dsx* expression occurs has been really been determined by the circumstantial evidentiary effects associated with impairing, or over-expressing, *dsx* function in the fly (as reviewed in Camara et al. 2008 and Christiansen et al., 2002). Studies have demonstrated that *dsx* can act to regulate non-sex-specific transcription factors and cell signalling molecules in specific tissues and cells during development into adults, in a sex-specific manner indicative that *dsx* is itself expressed in a developmentally precise manner (as reviewed in Camara et al. 2008 and Christiansen et al., 2002). Studies employing temperature sensitive mutants have demonstrated that *dsx* potentially acts at different developmental time-points to effect differing sex-specific outcomes dependent on the cell lineage, indicative that *dsx* is expressed in a dynamic manner within the developing fly (as reviewed in Camara et al. 2008 and Christiansen et al., 2002). This concept of a dynamic, but restricted, pattern of expression for dsx^{GAL4} has already been demonstrated in the CNS in this study (Rideout et al., 2010). Finally, as the determination of most aspects of sexual differentiation is cell autonomous (with some the exceptions; see Camara et al., 2008), it is as important to register those tissues in which dsx^{GAL4} may not be expressed, indicative that only specific (sexually physiologically relevant) tissues require a sexual identity. Again it should be emphasised that this process of sexual determination in somatic tissues does not occur in isolation, but rather must occur in a co-ordination with the development of the sexually dimorphic nervous system, with all of these processes for the regulation of sexual determinants culminating in the generation of a mature, sexually dimorphic, adult fly. As such I undertook to perform a spatio-temporal survey outwith the CNS to gain a comprehensive idea of which tissues exhibit dsx^{GAL4} expression and when this expression occurs.

5.1 Expression within the developing embryo appears male-specific

As stated in section 4.1 dsx^{GAL4} specified expression is apparent by stage 11 -12 in the embryo (http://flymove.uni-muenster.de/) and persists into the developing larvae (Figures 4.1 and 5.1) (Hartenstein, 1993). However co-expression with the

nervous tissue specific reagent anti-HRP demonstrated that this expression was neither in the CNS nor the PNS (see Figure 4.1) (Jan and Jan, 1982; Snow et al., 1987). In stage 11-12 embryos expression is apparent in cells that appear morphologically and positionally to be somatic (and potentially male-specific) gonadal precursor cells (GPCs) (Hempel and Oliver, 2007), in keeping with previously delineated *in situ* expression analysis of *dsx* transcripts (http://insitu.fruitfly.org/cgi-bin/ex/report.pl?ftype=1&ftext=CG11094) (Tomancak et al., 2002) (Figure 5.1A). These cells go on to coalesce in the later stages to form the gonad and this pattern of expression is continued into the larva and then pupa (Rideout et al., 2010; Robinett et al., 2010) (Figures 5.1 – 5.3) suggesting that there is an early requirement for sexual determinants and, following this, a continuous need for maintenance of sexual identity throughout development (Hempel and Oliver, 2007). In keeping with previous findings (Hempel and Oliver, 2007) this expression pattern is male-specific; as preparations of dsx^{GAL4} embryos containing the GAL4 responsive transgene *UAS-pStingerII* (expressing nGFP) ~50% of the population of embryos exhibited no fluorescent signal (Barolo et al., 2000); no co-expression ocurred between embryos expressing the female-specific *sex-lethal* promoter construct conjugated to GFP (kind gift of B. Oliver) and dsx^{GAL4} driving expression in the GAL4 responsive transgene *UAS- Red Stinger* (expressing nRFP; data not shown); and only males resulted from embryos selected for their gonadal fluorescent signal which were allowed to develop into adults, while only females developed from embryos in which this signal is absent (n>35).

By stage 13-14 embryos expression is also apparent in cells that appear morphologically and positionally to be developing oenocytes (Bodenstein, 1950; Gutierrez et al., 2007; Hartenstein et al., 1992) (Figure 5.1B2). This expression again persists throughout embryonic development through to L3 larval stages (Rideout et al., 2010) (Figure 5.3). While expression appears to only occur in the male embryos, lower levels of expression cannot be ruled out in female embryos as very faint levels of expression in oenocytes may be detected in female L3 larvae.

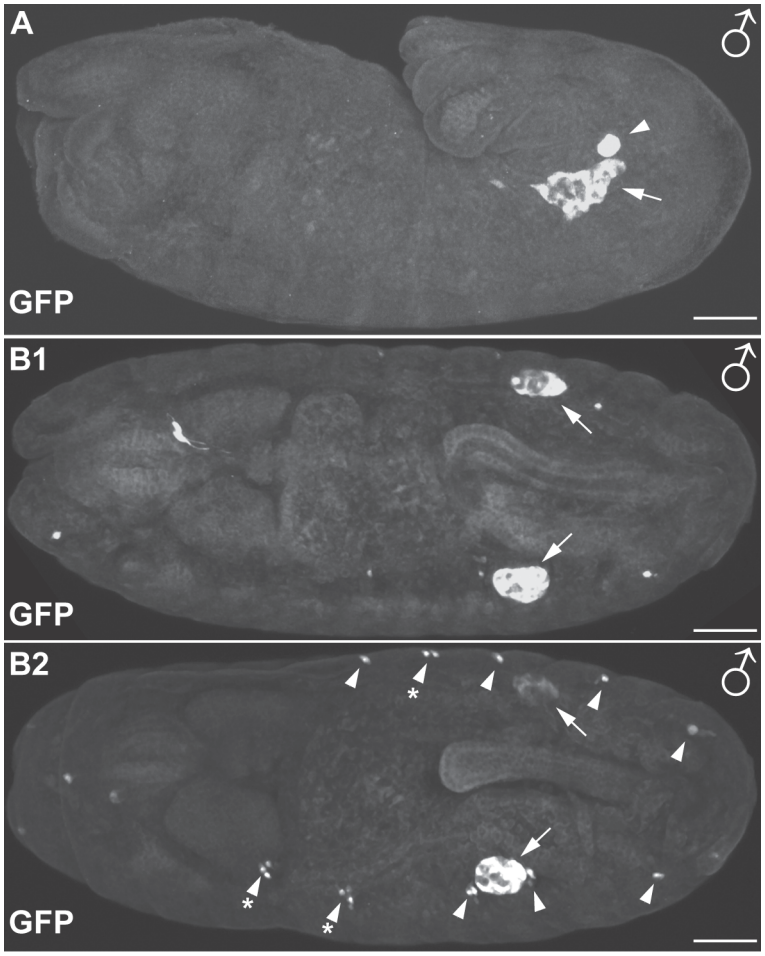

Figure 5-1 *dsx*^{GAL4} driven expression of nuclear GFP in the male embryo.
(A) Stage 11 – 12 and (B1-2) Stage 15 – 16 *dsx*^{GAL4} male embryos expressing nGFP. (A) Highlighting migratory somatic (arrow), and potentially male-specific (arrowhead), gonadal precursor cells. (B1) Detail of confocal sections highlighting expression in gonads (arrows). (B2) Detail of confocal sections highlighting expression in developing oenocytes (arrowheads). Asterisks indicate multiple oenocytes in clusters. Cephalic, left; ventral, bottom. (A) also used in Figure 4.1. Stages as per Hartenstein, 1993. Scale Bars = 50 µm.

5.2 *dsx*^{GAL4} expression persists and expands in the somatic tissues of the developing larvae and pupae

As stated the expression in the male gonads persists throughout larval development into the pupa (Rideout et al., 2010) (Figure 5.2). In the differentiating gonad a high level of expression is exhibited in the basal pole, potentially including male-specific gonadal precursor cells (DeFalco et al., 2003; Robinett et al., 2010) with a lesser level of expression at the apical pole (Figure 5.2) as is described in Robinett et al. (2010). The basal pole also comprises terminal epithelial cells, which go to form, or contribute to, the transitional junction between the developing gonad and the rest of the 'mature' adult internal genitalia, specifically the seminiferous vesicles and vas deferens (Robinett et al., 2010). The apical pole contains within it the hub cells, a cluster of specialized somatic cells required for

germline stem cell maintenance (Hempel and Oliver, 2007; Robinett et al., 2010). As well as this there appears to be expression in cyst cells in the larval and 0 - 48 hr pupal gonads (Hempel and Oliver, 2007; Robinett et al., 2010). Both the hub and cyst cells have previously been demonstrated to express Dsx^{M} from embryonic stage 15 through to the adult (Hempel and Oliver, 2007). Expression in the 72 – 96 hr pupa appears to be strongly reminiscent of the pattern exhibited later in the adult testes, including the development of a surrounding network of cells and apparent fine neurites ramifying on the body of the testis, while the higher level of expression observed in the developing basal pole appears to continue in the adult seminiferous vesicles and vas deferens (Figure 5.2).

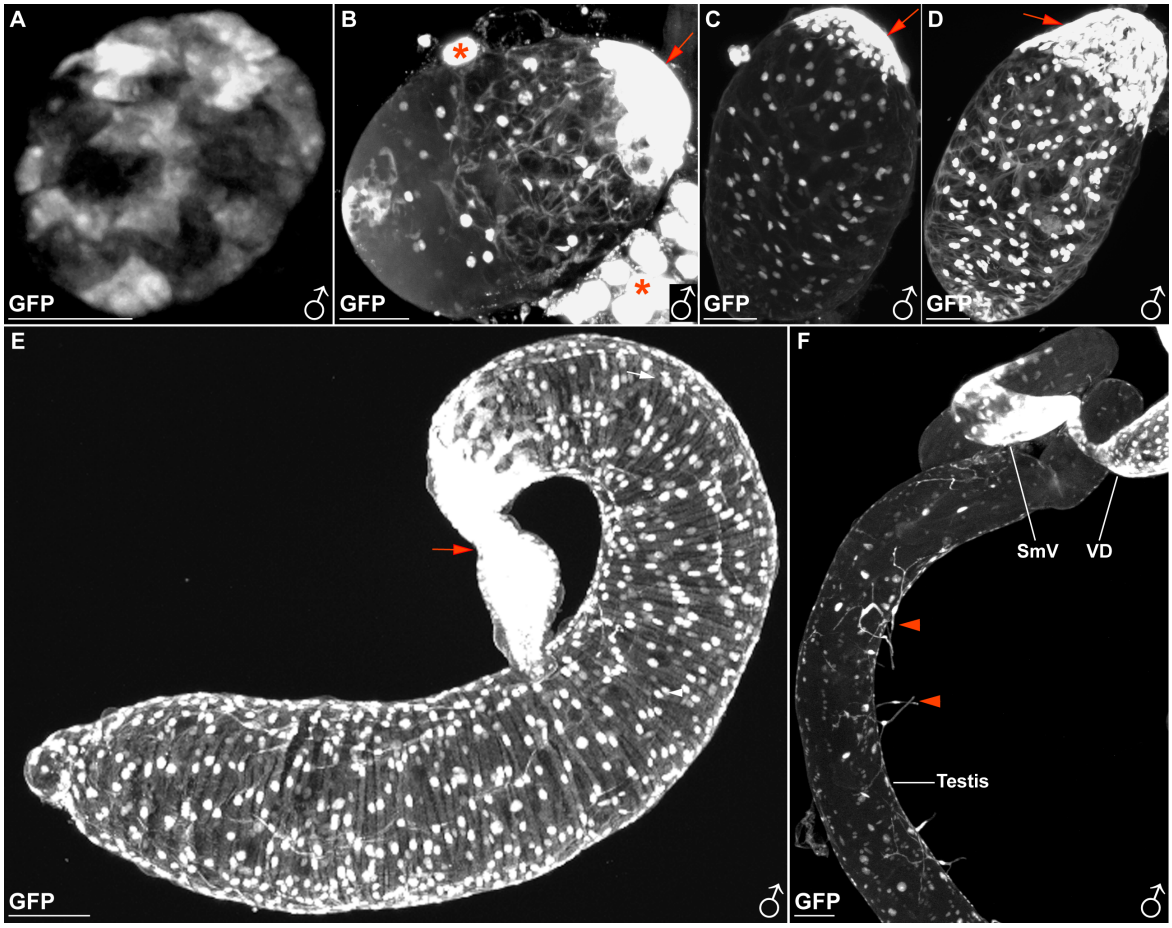

Figure 5-2 Developmental progress of *dsx*^{GAL4} driven expression of nuclear GFP in the male gonad and testis.
(A) Stage 15 embryonic male gonad. Stages as per Hartenstein, 1993. Scale Bars = 10 µm. (B) L3 larval male gonad. Terminal epithelial cells at the basal end, arrow. Fat body cells, asterisks. (C-E) Male pupal gonads. (C) 0 - 24 (D) 24 - 48 and (E) 72 - 96 hr pupal gonad. Terminal epithelial cells at the basal end, arrows. (E) Detail of 5 D adult male testis. Fine network of neurites ramifying on testis indicated by arrowheads. seminiferous vesicle (SmV), vas deferen (VD) and testis indicated. (D-E) as per Rideout et al., 2010. (B-F) Scale Bars = 50 µm.

Expression in the oenocytes in the male larvae also persisted (Figure 5.3) and was also now detectable in the female larvae, though at a much reduced level (data not shown). This overt expression in the male oenocytes, as opposed to the much fainter level of expression observed in the female, provides a novel example of dimorphic expression in larval tissue, providing further evidence that the mechanisms of sex determination, occurring in specific and restricted patterns, are a continuous process throughout development.

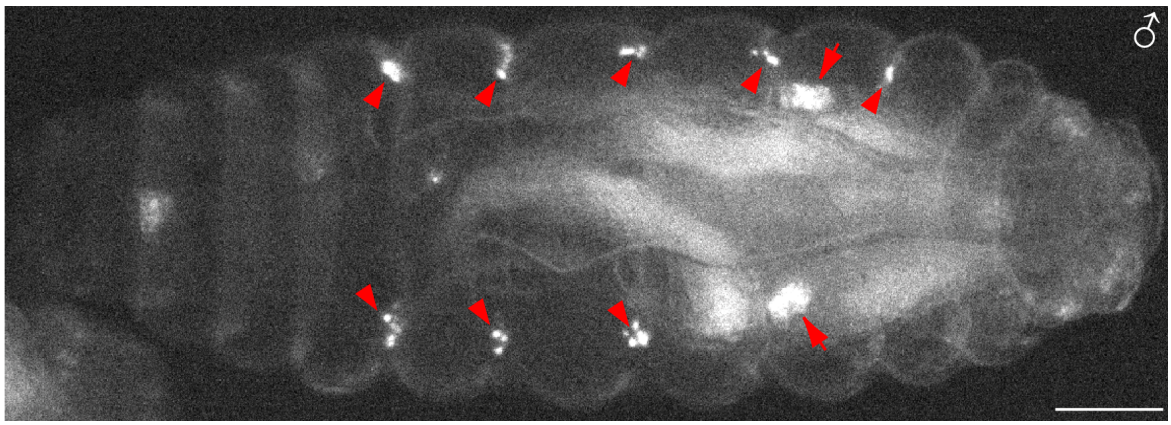

Figure 5-3 *dsx*^{GAL4} driven expression of nuclear GFP in the male L1 larva.
Whole mount image, highlighting expression in the gonads (arrows) and clusters of oenocytes (arrowheads). Cephalic left, dorsal view. Figure as per Rideout et al., 2010. Scale bar = 100 µm.

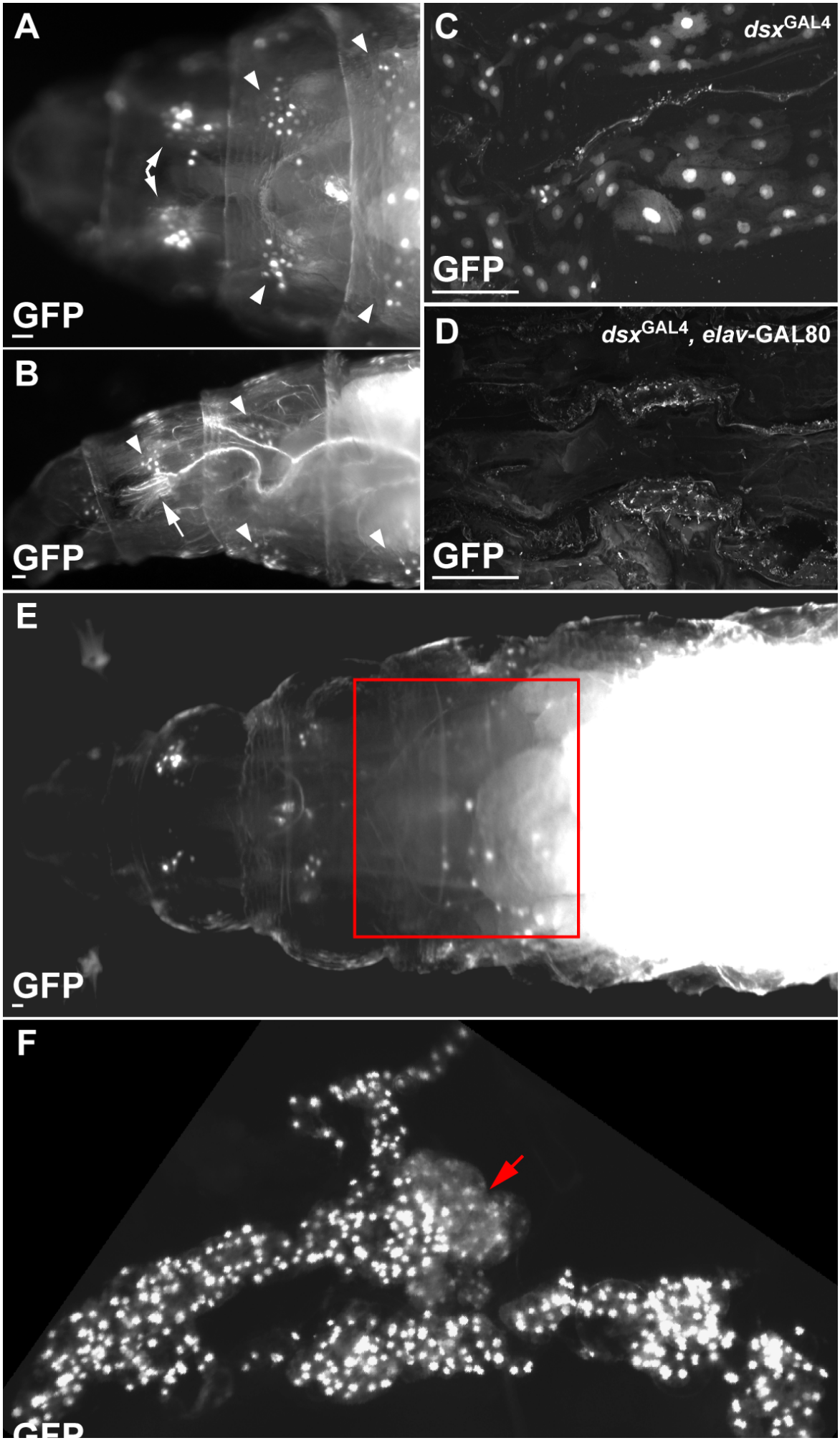
A
GFP
B
GFP
C
dsxGAL4
GFP
D
dsxGAL4, elav-GAL80
GFP
E
GFP
F

Figure 5-4 *dsx*^{GAL4} driven expression of nuclear GFP in the cuticle and fat body of the larvae. (A) Anterior (cephalic) dorsal view and (B) anterior (cephalic) side view detail of whole mount L3 larvae highlighting discrete clusters of sub-cuticular cells present in each hemisegment (arrowheads). Position of the anterior spiracles indicated (arrows). (C) Internal view of the L3 larval cuticular wall exhibiting sub-cuticular cells expressing nGFP driven by *dsx*^{GAL4}. (D) Internal view of the L3 larval cuticular wall demonstrating comprehensive repression of expression of nGFP driven by *dsx*^{GAL4} by concomitant expression of *elav*-GAL80 in these sub-cuticular cells. (E) Anterior (cephalic) dorsal view detail of whole mount L3 larva highlighting the overt level of expression within the fat body. Proportionally lower level of expression in the most anterior portion of the fat body highlighted (red box). (F) *dsx*^{GAL4} driven nGFP expression in the complete larval fat body. Proportionally lower level of expression in the most anterior portion of the fat body highlighted (red arrow). (A-F) This pattern of expression is the same for both sexes. (A, F) as per Rideout et al., 2010. Scale Bars = 50 µm.

While *dsx*^{GAL4} expression persists within the oenocytes and gonads throughout larval development, this expression becomes obscured in the L3 larvae by the high level of expression exhibited by the larval fat body (Figure 5.4) (Rideout et al., 2010; Robinett et al., 2010). This expression occurs in both males and females and is maintained into the adult (Rideout et al., 2010; Robinett et al., 2010). It should be noted that, while generally this expression appears consistent throughout rest of the fat body, the anterior most (cephalic) portion exhibits a proportionally lower level of *dsx*^{GAL4} driven expression than the majority of the fat body (Figure 5.4E–F).

Also apparent by the L3 larval stage is expression in peri-cuticular cells in the larval cuticular wall of each hemisegment (Figure 5.4). This is restricted to discrete clusters in the anterior (cephalic) segments but, moving dorsally, expression of cells extends to ring each segment of the body wall. That these cells may be neuronal in origin is indicated by the fact that *dsx*^{GAL4} driven nGFP expression in these cells was specifically and comprehensively repressed in the presence of *elav*-GAL80 (Figure 5.4D). As yet the function of these cells remains unknown, though it would be tempting to speculate, due to their position and morphology, that they are involved in proprioception or perhaps nociception. Something which could perhaps be tested by assaying of thermal (hot or cold) or mechanical transduction of the nociceptive/locomotor defense responses in *dsx*^{GAL4} flies expressing TNT or by attempting to initiate nociceptive or mechanical locomotor responses via optogenetic techniques (Hwang et al., 2007; Zhong et al., 2010; Zimmermann et al., 2009).

5.3 *dsx*^{GAL4} is expressed in a restricted manner in a subset of the imaginal discs.

Several previous genetic studies have directly, or indirectly, indicated that *dsx* functions during the development of particular imaginal discs (Baker and Ridge, 1980; Chatterjee et al., 2011; Hildreth, 1965; Keisman et al., 2001; Rideout et al., 2010; Robinett et al., 2010). As such it was unsurprising to observe *dsx*^{GAL4} nGFP expression exhibited in a restricted manner in some, but not all, imaginal discs of the developing larvae. Again, where *dsx*^{GAL4} expression is observed, the patterns of expression exhibited appeared to be the same in both sexes. Implying that specific tissues require gender appropriate modulation to arrive at their final dimorphic structures in both males and females. It is of real interest therefore to describe which imaginal discs expressed *dsx*^{GAL4}, though it must be emphasized that these descriptions are restricted to the discs of third instar wandering larvae, and that these patterns of expression may be altered at differing developmental time points between the sexes.

While little to no expression is apparent in the clypeolabrum, dorsal prothorax (humeral), and midleg discs (Figure 5.5A and D), some expression in a scattering of cells, mostly associated with the apical stalk, does seem apparent in the haltere, labial, wing and perhaps hindleg discs (Figure 5.5A, E-G). Again this paucity of expression levels may not seem surprising as these structures exhibit no overt dimorphisms, but it should be emphasized that this not to say that *dsx* may not function in modulating these tissues at a later point in development. This maybe evidenced by the onset of expression of *dsx*^{GAL4} in cells in the mid- and hindlegs 48 hrs after pupariation in both sexes (data not shown).

I was unsurprised to observe high levels of expression in the eye/antennal, foreleg and genital discs as all of these tissues have been shown to possess dimorphic features in their adult structures. In the eye/antennal disc strong levels of expression occur in a grouping of cells in the central area of the antennal region associated with the third or fourth antennal segments, and a second cluster of cells in the eye portion of the disc in an area closely associated with the morphogenetic furrow (Figure 5.5A-B). The predominant pattern of *dsx*^{GAL4} expression in the foreleg disc occurs in a distally located crescent shape with a scattering of cells throughout the main body of the disc. Latterly Robinett et al.

(2010) showed that this region did not co-express with *engrailed*, therefore locating it to the anterior compartment of the disc. They did however show that it to co-localised with *sex combs reduced* and *bric-a-brac*, identifying it as the region where the tarsal segments, and therefore coincidentally in males the sex combs, develop. Finally the highest levels of expression may be observed in both the male and female genital discs (Figure 5.5H- I). That all parts of the primordia of these tissues give rise to dimorphic structures in the adult (as discussed in the Introduction and Chapter 3) via isoform-specific determination and repression of tissues (Chatterjee et al., 2011; Keisman et al., 2001; Sánchez et al., 2001; Sánchez and Guerrero, 2001), would explain the extensive nature of the exhibited expression. In keeping with this idea of a sex-specifically determined topography there are clearly visible regional variations in the patterns of expression, with generally reduced levels at the lateral and ventral (basal) edges and higher levels in bilaterally symmetrical patterns associated with the central portions of the in both the male and female genital discs.

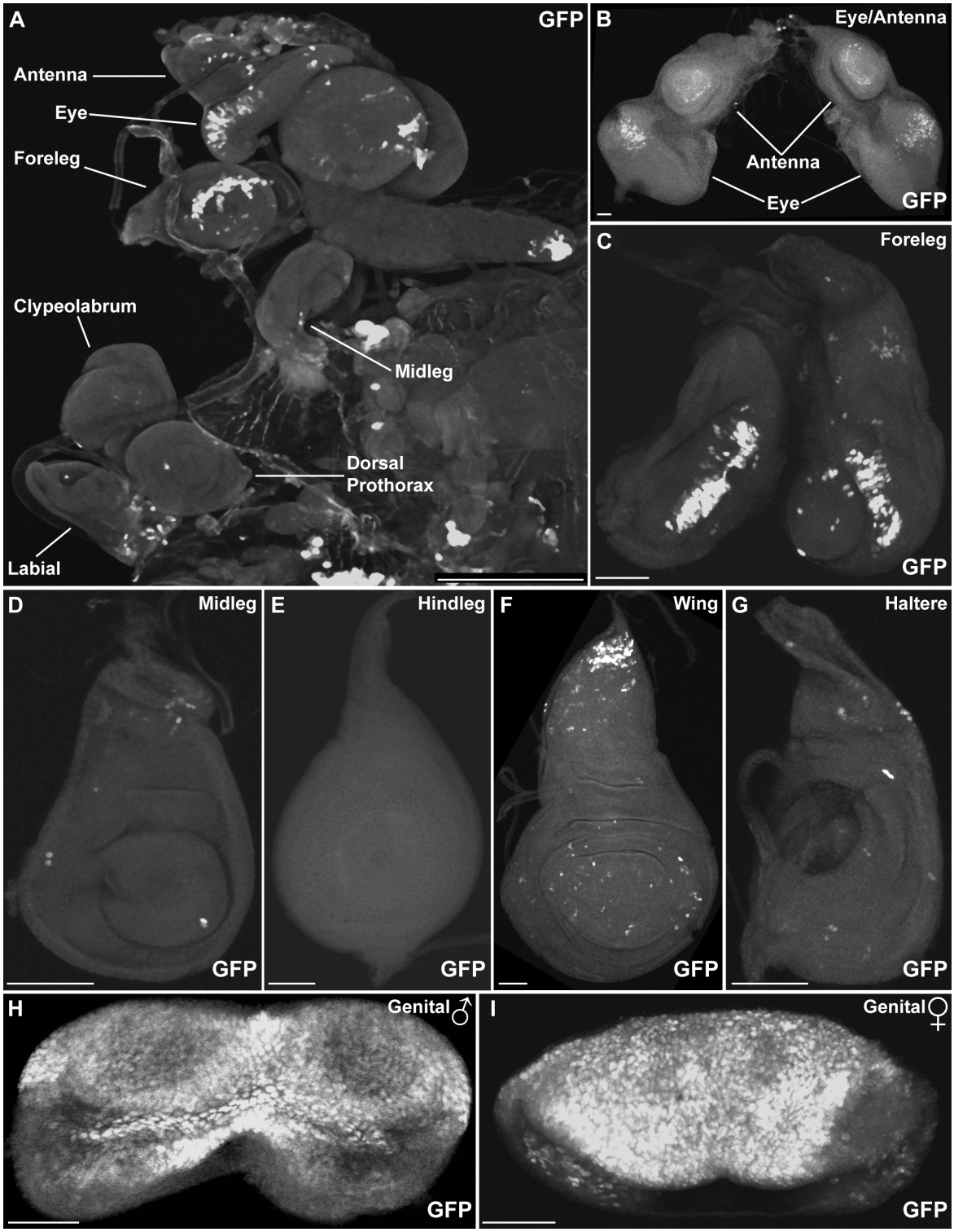

Figure 5-5 *dsx*^{GAL4} driven expression of nuclear GFP in the imaginal discs of L3 larvae. (A) Detail of male 'inverted' larva with *in situ* CNS and associated imaginal discs (listed). Anterior/cephalic left, ventral below. (B) Pair of eye/antennal discs. Individual regions of discs indicated. (C) Pair of foreleg discs. (D) Midleg disc. (E) Hindleg disc. (F) Wing disc. (G) Haltere disc. (A-G) This pattern of expression is the same for both sexes. (H) Male genital disc. (I) Female genital disc. (H-I) Dorsal top, ventral bottom, anterior to ventral view. Scale Bars = 50 µm.

5.4 *dsx*^{GAL4} expression in the mature adult

The extensiveness of *dsx*^{GAL4} expression in the mature adult may be evidenced by the levels of expression of *dsx*^{GAL4} driven fluorescent protein exhibited in whole fly preps realised via epi-fluorescent excitation (Figure 5.6). The resultant fluorescent signals representing the summation of expression within the nervous system, internal organs and peri-cuticular cells.

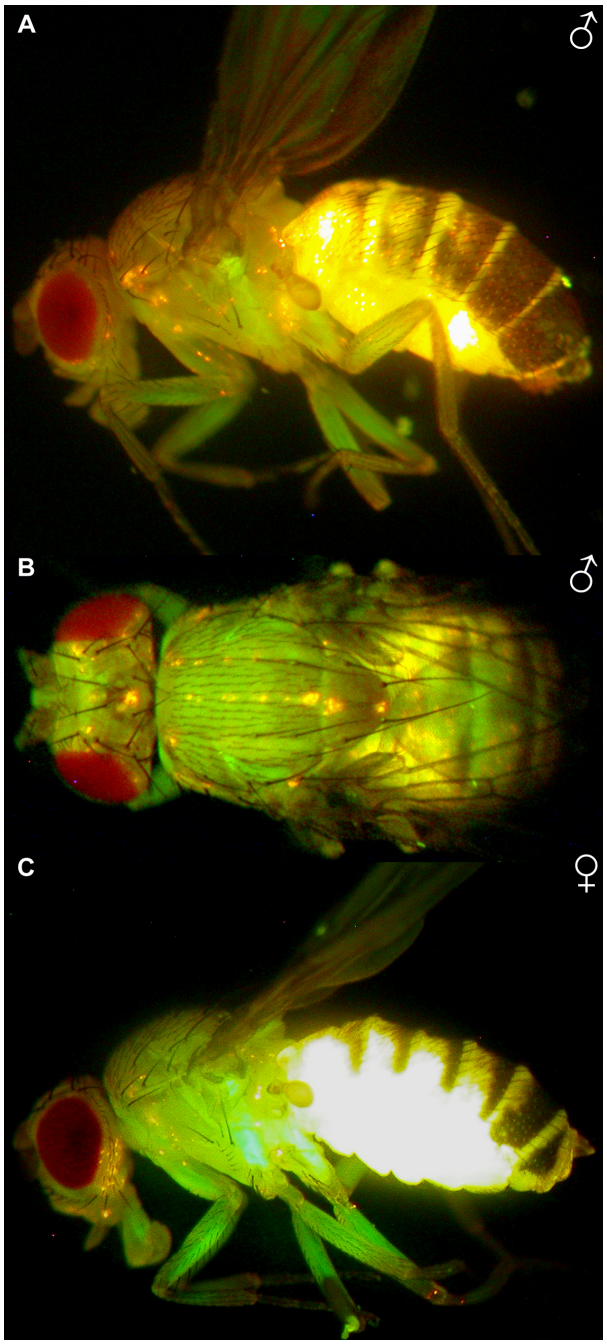

Figure 5-6 *dsx*^{GAL4} driven coincident expression of nuclear RFP and membrane bound GFP in whole mount 5 day old adult flies.
(A) Lateral and (B) dorsal view of adult male. (C) Lateral view of adult female. *dsx*^{GAL4} nRFP expression occurring in disassociated fat body, neuronal, non-neuronal and subcuticular cells. *dsx*^{GAL4} mGFP occurring in axonal projections throughout the head and body.

5.4.1 dsx^{GAL4} expression in cells of the adult fat body, oenocytes and associated with the external cuticle.

Expression of *dsx*^{GAL4} in such adult tissues as the fat body and oenocytes maybe inferred from previous genetic studies in which *dsx* function was demonstrated in the regulation of these tissues (Belote et al., 1985; Christiansen et al., 2002; Dauwalder et al., 2002; Ferveur et al., 1995; Fujii and Amrein, 2002; Lazareva et al., 2007). As such it was unsurprising to observe, in adults of both sexes, high levels of *dsx*^{GAL4} expression in the oenocytes and, throughout the body, in fat body cells (Figure 5.7A-C). This expression was observed to persist in animals expressing elav-Gal80 in conjunction with *dsx*^{GAL4} indicative of the non-neuronal nature of these cells (Figure 5.7D).

I also observed expression in cells associated with the external cuticles of both males and females (Figure 5.7B-E). This expression was comprehensively repressed in animals expressing *elav*-Gal80 in conjunction with *dsx*^{GAL4} (Figure 5.7F). The morphology of these cells, which appear disc-like, their positioning in a sub-cuticular plane at lines of flexure in the thorax, and more extensively in the abdomen, and finally the fact that expression in these cells is comprehensively repressed by *elav*-Gal80, indicative of the neuronal nature of these cells, would lead me to speculate that these cells are proprioceptive in nature and are analogous to the cells previously observed in the larval cuticle. However this again requires further investigation to definitively establish.

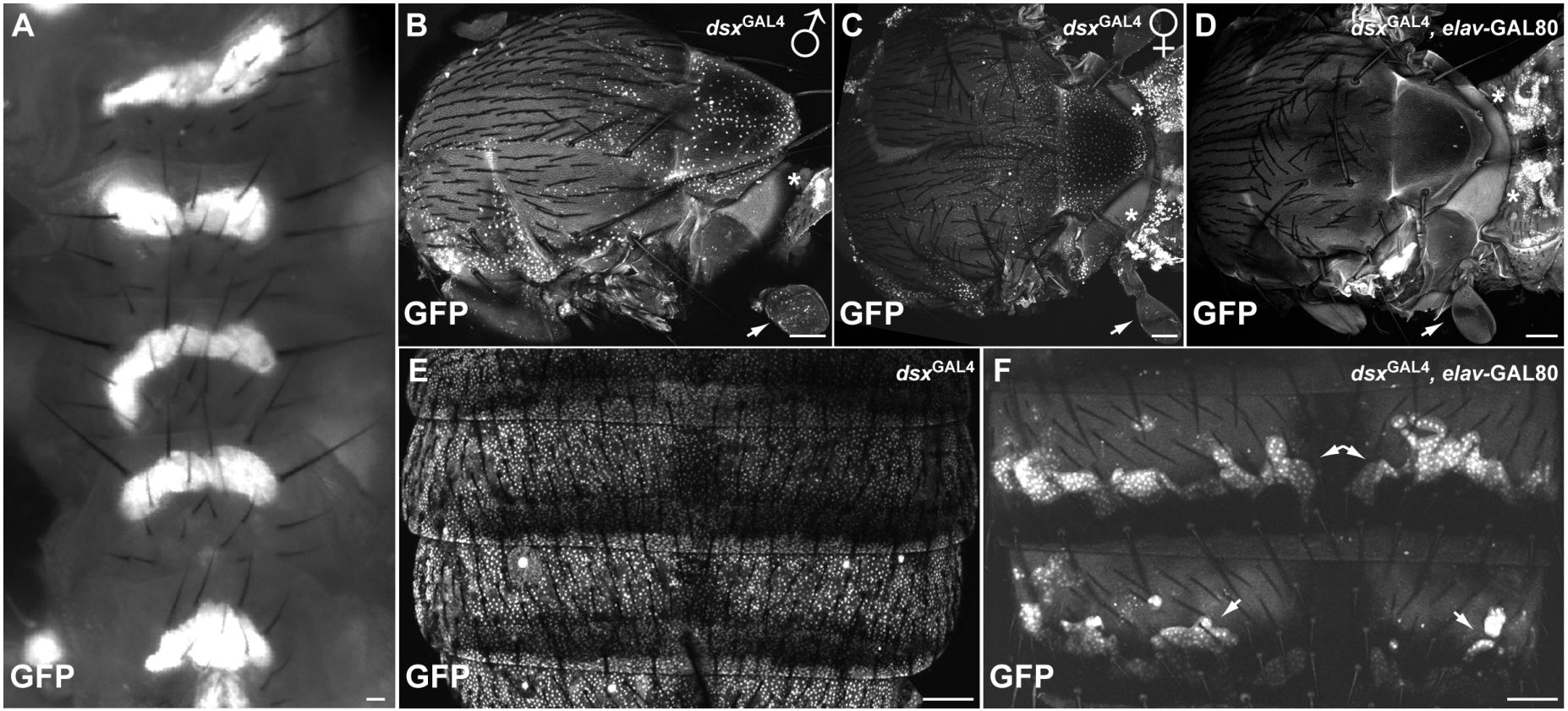

Figure 5-7 *dsx*^{GAL4} expression of nuclear GFP in subcuticular tissues of 5 day old adult flies.
(A) Whole mount image of adult oenocytes, midline ventral thorax. This pattern of expression is the same for both sexes and is not repressed in the presence of *elav*-GAL80 (data not shown). (B) Male and (C) female dorsal thoracic cuticle exhibiting subcuticular cell expression. Expression also visible in fat body cells in the abdomen (asterisks) and at low levels in the haltere (arrows). (D) Dorsal thoracic cuticle in which subcuticular cell expression in the thorax and haltere (arrow) are repressed in the presence of *elav*-GAL80. Expression persists in fat body cells in the abdomen (asterisks). This pattern of expression is the same for both sexes. (E) Dorsal abdominal cuticle with extensive subcuticular cell expression. Underlying tissues such as the fat body and muscle have been removed to allow the cells to be fully realised. This pattern of expression is the same for both sexes. (F) Dorsal abdominal cuticle in which subcuticular cell expression is repressed in the presence of *elav*-GAL80. Expression persists in structures such as the oenocytes and fat body cells (arrows). This pattern of expression is the same for both sexes. (A-C, E) as per Rideout et al., 2010. Scale bar = 100 µm.

5.4.2 dsx^{GAL4} expression in the alimentary tract.

I observed *dsx*^{GAL4} expression within the digestive tract and associated tissues, which appeared to be the same in both sexes. This expression was initially apparent at lower levels in early larval stages with both the intensity and topographical distribution of expression increasing into the adult (Figure 5.8). In the pupa and adult expression is apparent in the salivary glands, predominantly in the proximal ends (Figure 5.8B). There appears to be little expression in the oesophagus and only light speckling in crop (Figure 5.8B). Expression is next apparent in the proventriculus (cardia) with numbers of cells and intensity of expression appearing to increase along the midgut (Figure 5.8B, E-F). In the midgut, through their morphology and localisation, these cells maybe identified as neurosecretory cells or perhaps intestinal stem cells (ISCs) and/or enteroblasts (EBs) (Chatterjee and Ip, 2009; Micchelli and Perrimon, 2006; Ohlstein and Spradling, 2006, 2007; Robinett et al., 2010). Strong levels of expression are apparent in the primary and 'tiny' cells of the malpighian tubules, though expression again is spatially restricted, appearing to be absent in the stellate cells, in all cells of the initial segments and in the most proximal part of the ureter where it attaches to the alimentary tract (data not shown) (Rideout et al., 2010; Sözen et al., 1997). Little to no expression is apparent in the hindgut, with expression again increasing in the rectum (Figure 5.8A-D). *elav*-Gal80 expression in conjunction with *dsx*^{GAL4} comprehensively represses this observed expression throughout the gut except in the malpighian tubules where the levels of expression appear undiminished (data not shown). However the tubules' tiny cells which are thought to be neuroendocrinal, monitoring fluid collection in the ureter and secreting neurohormones basally into the haemolymph to regulate muscle contractility or ion transport, have been shown to be labelled by anti-HRP (Sözen et al., 1997) and it may be that repression of *dsx*^{GAL4} expression in these cells was missed.

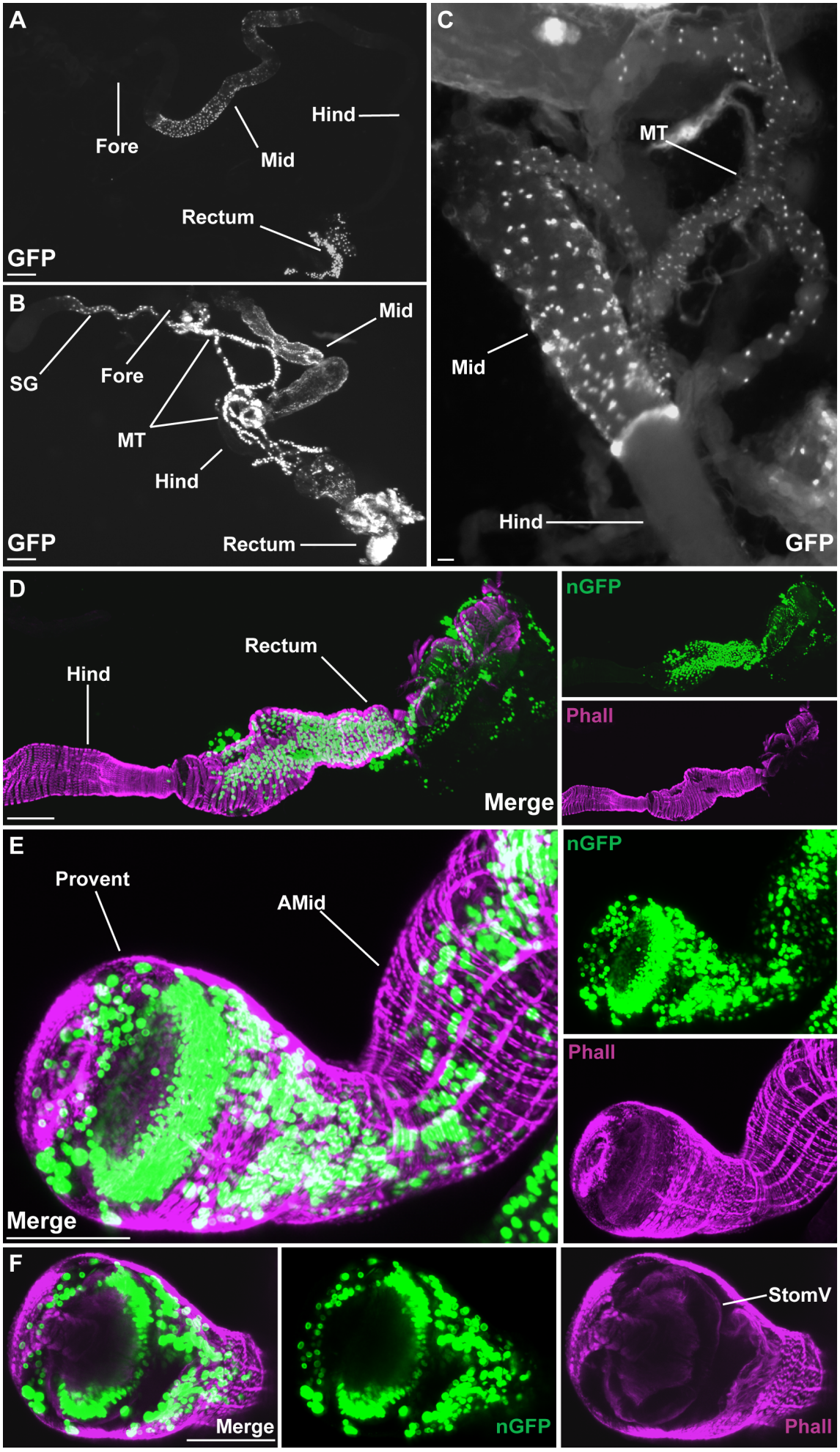
A
Fore
Mid
Hind
Rectum
GFP
B
SG
Fore
Mid
MT
Hind
Rectum
GFP
C
MT
Mid
Hind
GFP
D
Hind
Rectum
Merge
nGFP
Phall
E
Provent
AMid
Merge
nGFP
Phall
F
Merge
nGFP
StomV
Phall

Figure 5-8 *dsx*^{GAL4} driven expression of nuclear GFP in the digestive tract of the developing fly.
(A) Whole mount image of L3 larval digestive tract. Fore- (Fore), mid- (Mid) and hindgut (Hind) and rectum indicated. (B) Whole mount image of 2 day old pupal digestive tract. Salivary gland (SG), fore-, mid- and hindgut and, malpighian tubules (MT) and rectum indicated. (C) Detail of whole mount image of 5 day old adult alimentary canal. Mid- and hindgut and malpighian tubules indicated. (D) Detail of 5 day old adult alimentary canal highlighting transition from hindgut to rectum (indicated). (E) Detail of proventriculus (Provent) and anterior midgut (Amid) from a 5 day old adult alimentary canal. (F) Higher resolution image of the proventricuus from (E) highlighting *dsx*^{GAL4} nGFP expression in cells forming internal alimentary structures, such as the stomodeal valve (StomV) and associated with the internal lumen of the alimentary tract, but not with the external body wall. Nuclear GFP (nGFP), green. Anti-Phalloidin (Phall), magenta. The observed patterns of expression appear the same for both sexes. Cephalic, left; rectal, right. (C) as per Rideout et al., 2010. Scale bar = 100 µm.

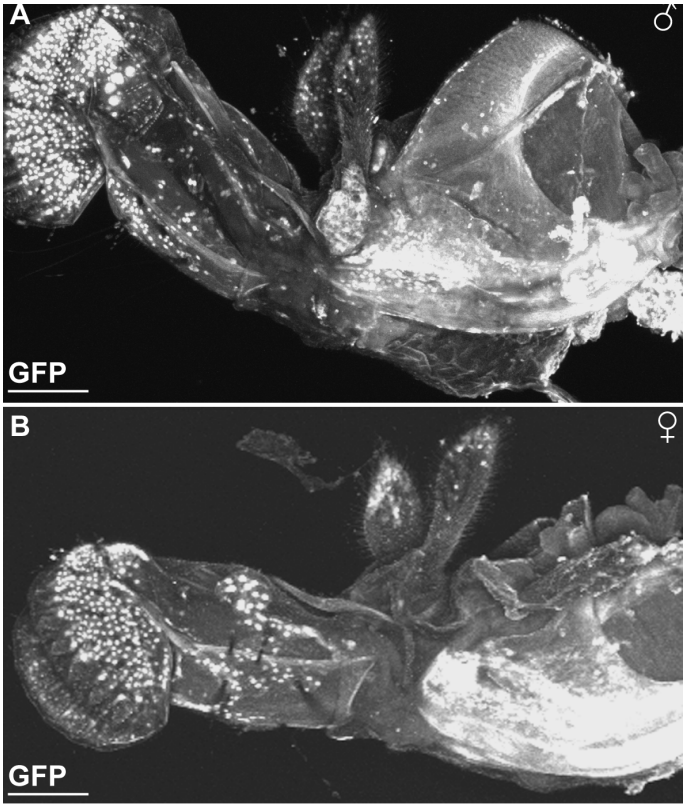

Figure 5-9 *dsx*^{GAL4} nuclear GFP expression in the proboscis and mouth parts of 5 day old male and female adults.
(A) Male and (B) proboscises and mouthparts demonstrating extensive, non-neuronal, expression. (A) as per Rideout et al., 2010. Scale bar = 100 µm.

dsx^{GAL4} also exhibited extensive nGFP expression within the proboscis and mouthparts of both males and females (Figure 5.9). This was especially associated with the labellum/labellar palpus, though individual cells are also scattered throughout including cells in the labrum, maxillary palps and the cibariaum (Rideout et al., 2010; Robinett et al., 2010). *elav*-Gal80 when expressed in conjunction with *dsx*^{GAL4} failed to repress this observed pattern of expression (data not shown) and no co-localisation was observed between *dsx*^{GAL4} nGFP

expression and antibodies specific to *elav* in the proboscis (E. Rideout, pers. comm.) indicative that these cells are non-neuronal in nature. Currently the lineage and function of these *dsx*^{GAL4} cells within the proboscis and mouthparts remains unknown.

5.4.3 dsx^{GAL4} in the genitalia of males and females.

As has been demonstrated in the previous chapter (see section 4.1.4) expression is apparent in innervations ramifying onto the male genitalia. However over and above this I was able to observe high levels of *dsx*^{GAL4} expression occurring in a restricted manner in differing tissues of both the male and female internal and external genitalia (Figures 5.10, 5.11 and 5.12) (Rideout et al., 2010; Robinett et al., 2010).

In the male this comprised a fine network of cells and neurites ramifying on the testes, seminiferous tubules, vas deferens, accessory glands and ejaculatory duct (Figures 5.10A and 5.11) (Rideout et al., 2010). I also observed expression in cells associated with the epithelium of the internal lumen of the seminiferous tubules, vas deferens, and ejaculatory duct (Figure 5.11A, C). Strikingly no expression was observed in the internal lumen of the accessory glands and no expression appeared in cells of the musculature surrounding the accessory glands or the seminiferous tubules, vas deferens, and ejaculatory duct (Figure 5.11C). Expression was apparent at high levels in the secondary cells in the apex of the accessory glands, in the muscles of the apodeme, in the secretory cells of the ejaculatory bulb and on the external genital plates (Figure 5.10C and 5.11A, C). The secondary cells are 40-50 binucleate cells containing large vacuoles, which are known to produce and secrete a variety of Acps (Bertram et al., 1992). Intriguingly *elav*-Gal80 expression in conjunction with *dsx*^{GAL4} comprehensively repressed this observed expression in all tissues, including the secondary cells of the accessory glands, except for that observed in the secretory cells of the ejaculatory bulb and at least some of the expression in the external genital plates indicative of the neuronal nature of the cells exhibiting *dsx*^{GAL4} expression in these tissues (Figure 5.10B).

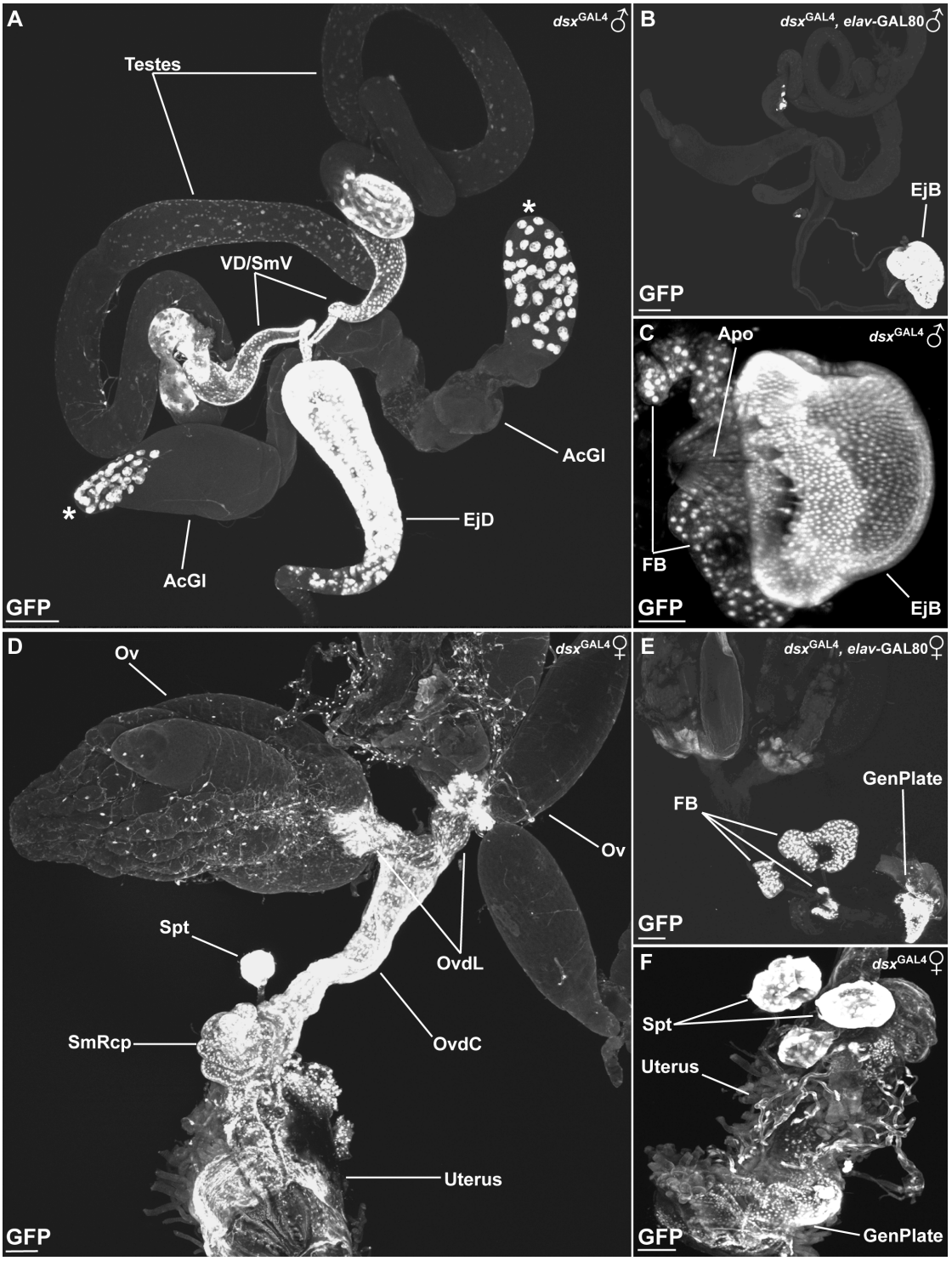

Figure 5-10 *dsx*^{GAL4} driven expression of nuclear GFP in the genitalia of 5 day old adult flies, with specific repression in tissues in the presence of *elav*-GAL80.
(A) *UAS-Stingerll*; *dsx*^{GAL4} male internal genitalia; testes, vas deferens (VD), seminal vesicles (SmV), ejaculatory duct (EjD), secondary cells (asterisks) of the accessory glands (AcGl) indicated. (B) *UAS-Stingerll*; *dsx*^{GAL4}, *elav*-GAL80 male internal genitalia. Expression in ejaculatory bulb (EjB) indicated, all other expression repressed. (C) (B) *UAS-Stingerll*; *dsx*^{GAL4}, *elav*-GAL80 male, detail of the ejaculatory bulb. Expression exhibited in fat body cells, musculature of the apodeme (Apo) and secretory cells of the EjB. (D) *UAS-Stingerll*; *dsx*^{GAL4} female internal genitalia; ovaries (Ov), lateral and common oviducts (OvdL and OvdC), seminal receptacle (SmRcp), spermathecae (Spt), and uterus indicated. (E) *UAS-Stingerll*; *dsx*^{GAL4}, *elav*-GAL80 female internal genitalia. Expression in external genital plates (GenPlate) and fat body cells (FB) indicated, all other expression repressed. (F) *UAS-Stingerll*; *dsx*^{GAL4} female detail of the external genital plates and uterus with expression apparent in both spermathecae. (A) and (D) as per Rideout et al., 2010. Scale bar = 100 µm.

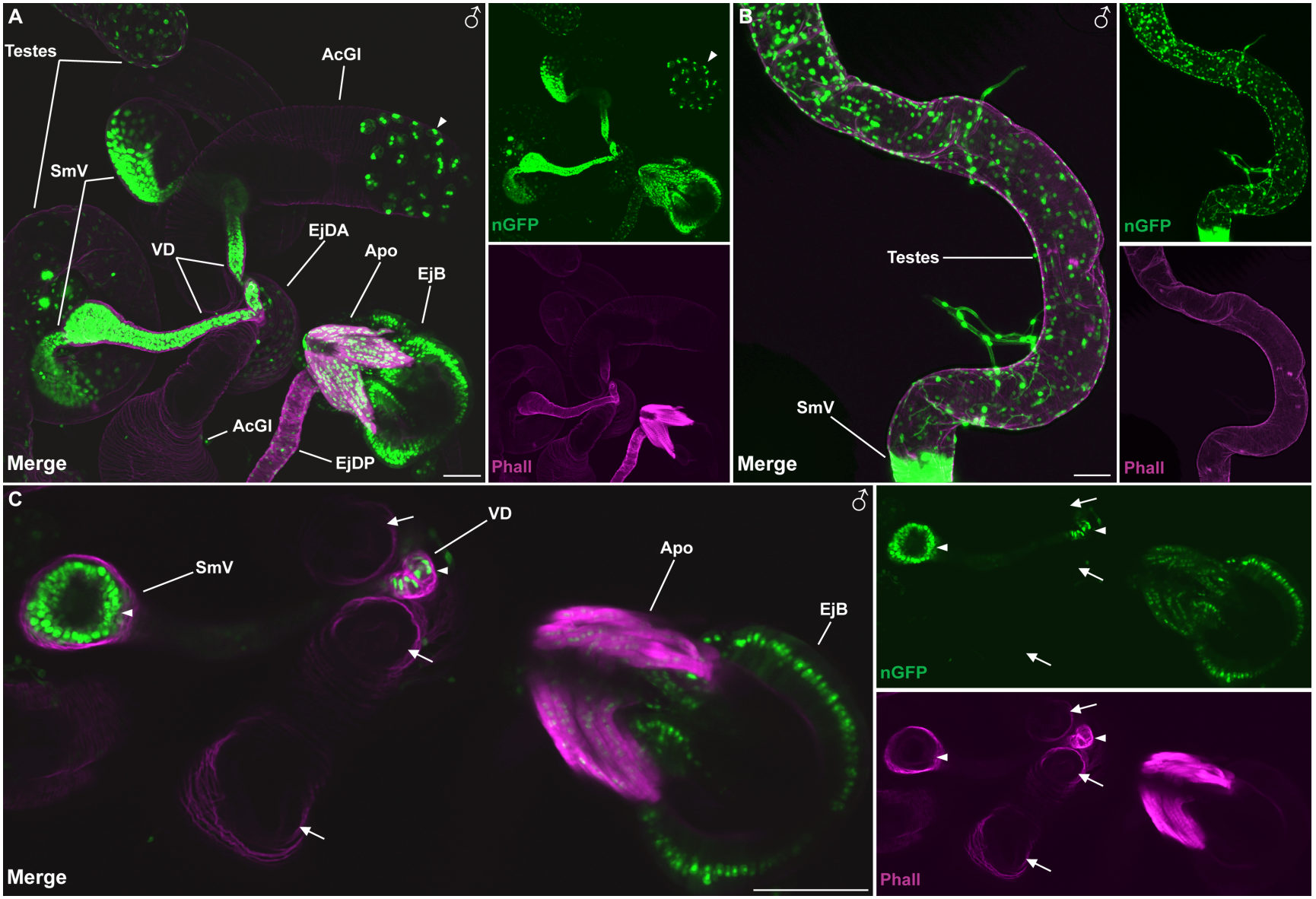
A
♂
Testes
AcGl
SmV
VD
EjDA
Apo
EjB
AcGl
EjDP
Merge
nGFP
Phall
B
♂
Testes
SmV
Merge
nGFP
Phall
C
♂
SmV
VD
Apo
EjB
Merge
nGFP
Phall

Figure 5-11 *dsx*^{GAL4} driven expression of nuclear GFP in the internal genitalia of 5 day old adult male flies counterstained with the F-actin specific antibody Phalloidin.
(A) Internal genitalia; testes, seminal vesicles (SmV), vas deferens (VD), accessory glands (AcGl), anterior (EjDA) and posterior (EjDP) ejaculatory ducts, apodeme (Apo) and ejaculatory bulb (EjB) indicated. *dsx*^{GAL4} expression in secondary cells of the AcGl indicated (arrowhead). (B) Detail demonstrating the filamentous network of cells and projections ramifying on the exterior of the testis. (C) Subset of the maximal confocal stack (A) highlighting *dsx*^{GAL4} expression in epithelial cells of the internal lumen of the seminiferous vesicle and vas deferen (arrowheads) but not the AcGl (arrows). Expression of *dsx*^{GAL4} in the internal lumen of the ejaculatory duct present but out of plane of view. Expression of *dsx*^{GAL4}in the musculature associated with the apodeme and the secretory cells of the ejaculatory bulb also indicated. Nuclear GFP (nGFP), green. Anti-Phalloidin (Phall), magenta. Scale bar = 50 µm.

In the female I observed a pattern of expression again comprising a fine network of cells and neurites encapsulating both ovaries and the lateral oviducts analogous to that seen ramifying on the male internal genitalia (Figure 5.10D and 5.12A-B) (Rideout et al., 2010). I also observed expression in the lateral and common oviducts (OvdL and OvdC respectively), the seminal receptacles (SmRcp), the spermathecae (Spt), the paravoria (Para), the uterus and the external genital plates (Figures 5.10D, F, 5.12 and 5.13) (Rideout et al., 2010). In the OvdL and OvdC, the SmRcp and the uterus this expression occurred in cells associated with the epithelium of the internal lumen (Figures 5.12C-D and 5.13). In contrast with the male however, in the OvdL and OvdC at least, expression was also apparent in cells associated with the surrounding muscular wall (Figure 5.12E). The uterus exhibited two discrete regions of *dsx*^{GAL4} expression (Figure 5.13). The first in the distal region of the uterus, presented as a series of cells associated with invaginations in the dorsal uterine luminal wall below the area of the SmRcp (Figure 5.13A-C). These cells appear to encircle the luminal openings for the SmRcp in an area consistent with that of the oviduct flap (OvF) (Figure 5.13 D-E) (Adams and Wolfner, 2007). The second area of cells is associated with the proximal uterine opening (Figure 5.13C). Again *elav*-Gal80 expression in conjunction with *dsx*^{GAL4} comprehensively repressed this observed expression in all tissues except that seen in external genital plates indicative of the neuronal nature of the cells exhibiting *dsx*^{GAL4} expression in these tissues (Figure 5.10E).

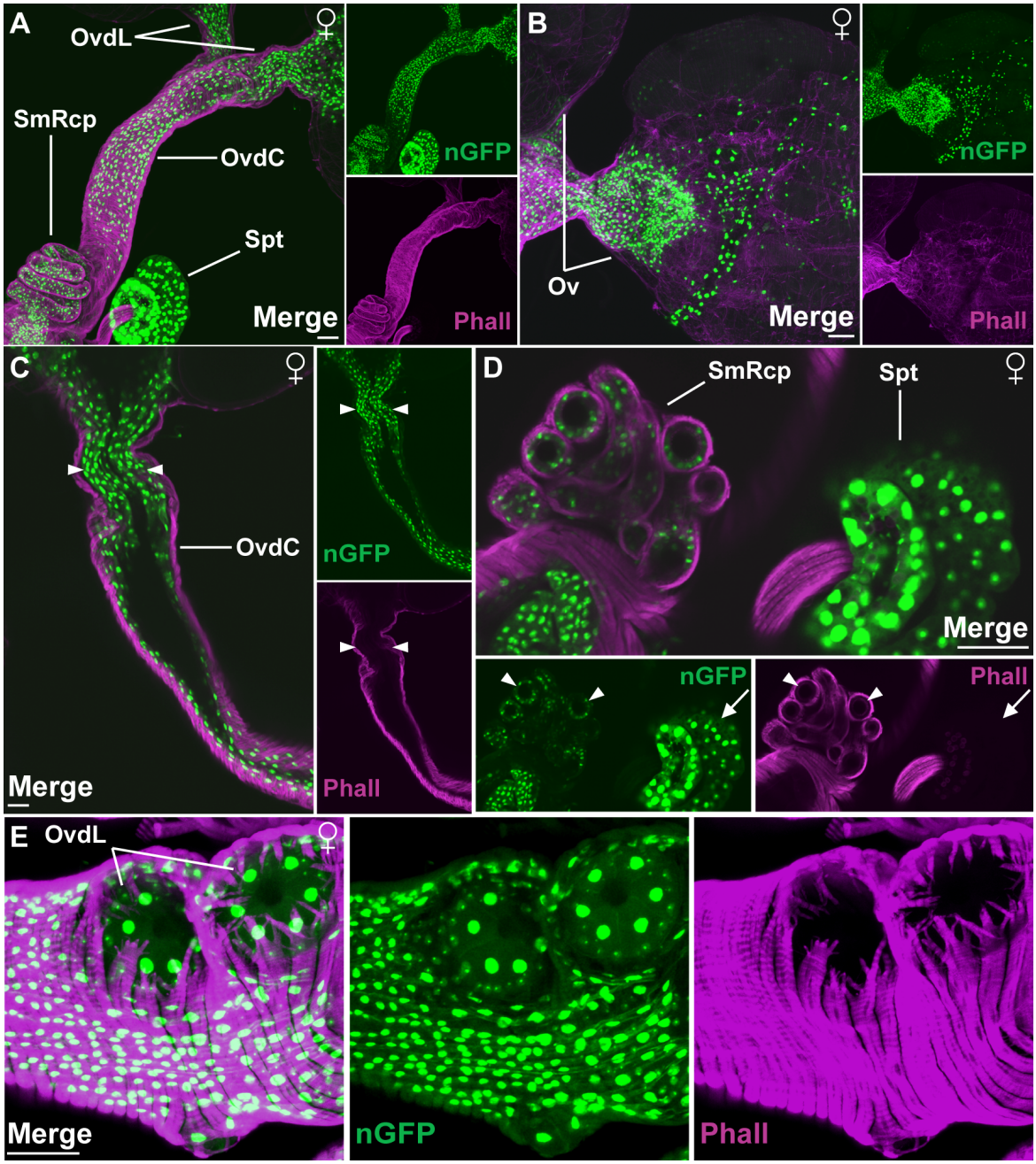

Figure 5-12 *dsx*^{GAL4} driven expression of nuclear GFP in the internal genitalia of 5 day old adult female flies counterstained with the F-actin specific antibody Phalloidin.
(A) Detail of female internal genitalia; lateral and common oviducts (OvdL and OvdC), seminal receptacle (SmRcp), and spermathecae (Spt) indicated. (B) Detail of female internal genitalia; ovaries (Ov) indicated. Demonstrating the filamentous network of cells and projections surrounding and ramifying on the exterior of the Ovaries. (C) Subset of maximal confocal stack highlighting *dsx*^{GAL4} expression in epithelial cells of the internal lumen of the oviducts (arrowheads). (D) Subset of the maximal confocal stack (A) highlighting *dsx*^{GAL4} expression in epithelial cells of the internal lumen of the seminal receptacles (arrowheads) and the absence of F-Actin in the main body of the spermatheca (arrows). (E) Subset of the maximal confocal stack (A) highlighting *dsx*^{GAL4} expression in epithelial cells of the internal lumens of the lateral oviducts (indicated) but also in cells within the surrounding muscular body wall. Nuclear GFP (nGFP), green. Anti-Phalloidin (Phall), magenta. Scale bar = 50 µm.

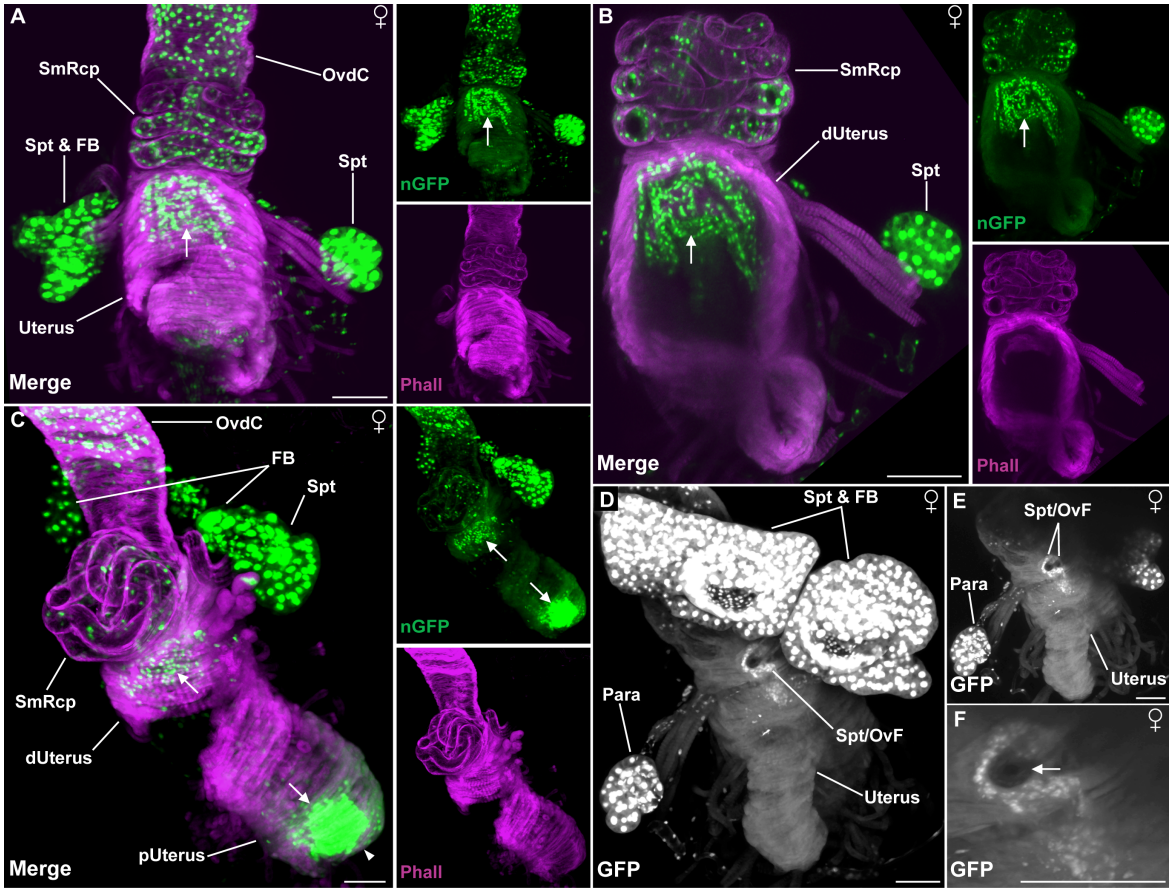

Figure 5-13 *dsx*^{GAL4} nuclear GFP expression in the uterus of 5 day old adult females. (A) Detail of female internal genitalia demonstrating *dsx*^{GAL4} nGFP expression in the common oviduct (OvdC), seminal receptacles (SmRcp), spermathecae (Spt), fat body (FB) and in the distal portion of the uterus (arrow). Proximal portion of the uterus not in plane of view. Ventral view; caudal, bottom. (B) Subset of the maximal confocal stack (A) highlighting *dsx*^{GAL4} expression in epithelial cells of the internal lumen of the distal portion of the uterus (dUterus), presenting in a series of invaginations of the luminal wall (arrow) but not expressed in the muscular body wall itself. Ventral view; caudal, bottom. (C) Detail of female internal genitalia demonstrating *dsx*^{GAL4} nGFP expression in the common oviduct (OvdC), seminal receptacles (SmRcp), spermathecae (Spt), fat body (FB) and restricted to areas in distal and proximal regions of the uterus (dUterus and pUterus; arrows). Uterine opening indicated (arrowhead). Lateral view; caudal, bottom. Nuclear GFP (nGFP), green. Anti-Phalloidin (Phall), magenta. (D) Detail of uterus demonstrating *dsx*^{GAL4} nGFP expression in the Spt, FB, paravoria (Para) invaginated luminal wall in area consistent with Spt luminal opening and oviduct flap (OvF). (E) Subset of confocal (D) stack highlighting the double opening in the uterine wall consistent with Spt lumenal opening (Spt/OvF). (F) Higher resolution image of Spt/OvF highlighting apparent dilatory flap in lumen (arrow). Dorsal view; caudal, bottom. Scale bar = 50 µm.

5.5 Discussion

Previous genetic studies have demonstrated the necessity for *dsx* function in the production of the stereotypical male or female soma (Billeter et al., 2006a; Camara et al., 2008; Christiansen et al., 2002; Rideout et al., 2010; Robinett et al., 2010; Simpson, 2002). Indeed some of these studies have identified specific tissues regulated by *dsx* that develop dimorphicaly or perform dimorphic functions in the adult to contribute to the overall male or female physical ‘state’ (reviewed in

Camara et al., 2008; Christiansen et al., 2002) and it is clear that the correct sexual identity (i.e. expressing DsxM or DsxF) in specific adult tissues is critical to the generation of normal sex-specific behaviours (Dauwalder et al., 2002; Fujii and Amrein, 2002; Fujii et al., 2008; Lazareva et al., 2007; Waterbury et al., 1999). However up till now there has been no encompassing understanding of where, and when, *dsx* may be expressed within the fly's soma. The investigations performed within this chapter have sought to provide a far more comprehensive survey of the spatial-temporal pattern of expression for *dsx* within the fly. Central to the findings of this survey is the fact that, as inferred by previous studies, *dsx* is not expressed in an unrestricted manner throughout the soma. The idea that certain cells and tissues do not require a sexual identity to function, even within a developing dimorphic animal such as the fly, makes logical developmental sense. The underlying genetic determinants and mechanisms which specify the overall development of the final (adult) animal are often required to be expressed in varying and/or iterative contexts. These genes and processes may be needed for regulation of other non-sex-specific paths and substrates and, as such, the expression of genes of the SDH would be, at the very least, superfluous. Indeed the ubiquitous expression of sexual identifiers such as *dsx* could be counter-productive to the fly's development, causing ectopic expression of dimorphic tissues or affecting the viability of the developing fly as a whole (Jursnich and Burtis, 1993). That is not to say that these non-sex-specific tissues are not themselves affected by the overall dimorphic development of the fly. The wings need not be physically dimorphic, yet maybe controlled in a sex-specific manner to generate a sex-specific output. However when dsx^{GAL4} is expressed within a specific tissue in the developing fly, this speaks volumes to the requirement for specification of a sexual identity in the development of both the individual tissue and for the achievement of the complete dimorphic adult animal as a whole.

As such, in keeping with the findings of previous studies, I observed dsx^{GAL4} expression within the male embryonic gonad (Hempel and Oliver, 2007). However I also observed novel expression within the developing oenocytes in the embryo and then in the larval fat body. This onset of expression in the embryo in both the male gonad and the oenocytes, appears indicative of the early requirement for sexual determinants in these tissues. While the persistence of this expression, as well as the later expression within the larval fat body in both males and females (which is continued into pupariation) appears to indicate a continuous

need for the maintenance of these sexual identifiers through to metamorphosis into the adult fly. This requirement for a sexual identity within the gonad may seem obvious but there is also developmental logic behind both the larval oenocytes and fat bodies also expressing sexual identifiers. The larval oenocytes, which are independent tissues from that of the adult oenocytes, are pyramidal shaped secretory cells of ectodermal origin positioned in a lateral and sub-epidermal location in ~7 abdominal segments (Bodenstein, 1950; Gutierrez et al., 2007; Hartenstein et al., 1992). These may vary between 4 – 9 cells per cluster though on average there are 6 cells per abdominal hemisegment (Bodenstein, 1950; Gutierrez et al., 2007; Hartenstein et al., 1992). These larval oenocytes appear to play a critical role in regulating growth, development and feeding behaviour especially with respect to lipid-processing in starvation conditions (Gutierrez et al., 2007). Again the dimorphic expression observed between the males and females in these tissues speaks to a previously unknown requirement for sex-specific regulation of non-sex-specific tissues within the embryo and larva, its expression in the larval oenocytes indicative of some form of modulation of the physiology of the developing animal.

The expression observed in the fat bodies of both males and females, as with the expression in the oenocytes, provides another novel example of dimorphic expression in larval tissue, again indicative that the mechanisms of sex determination, occurring in specific and restricted patterns, maybe a continuous process throughout development finally culminating in the production of the complete male and female soma. It should be noted that, like that of the larval and adult oenocytes, the larval fat body differs from that of the adult, with larval fat body cells differentiating from embryonic mesodermal cells while adult fat body cells are derived from larval histoblasts (presumably from adepithelial cells) associated with the imaginal discs (Aguila et al., 2007; Holz et al., 1997; Hoshizaki et al., 1994). The larval fat cells have been shown to be involved with a number of essential physiological functions, notably to do with immune responses and as a hormonal and nutritional sensor that regulates energy storage (Aguila et al., 2007; Liu et al., 2009; Petersen et al., 1999). The larval fat cells have proved refractive to the process of autophagic cell death that removes most larval cells during metamorphosis, thereby ensuring that these cells persist through pharate and early adult stages as disassociated fat cells until they are eventually replaced by their adult counterparts 3 -4 days post-eclosion (Aguila et al., 2007). This

presumably serves to ensure the newly eclosed animal has sufficient nutritional stores during the initial non-feeding adult developmental stage. It has been proposed that positional cues may regulate general fat cell specification, thereby acting to determine functional specialization within fat cells, giving rise to biochemically distinct regions in both the larval and adult fat bodies (Hoshizaki et al., 1995). *dsx* may be involved in this mechanism as demonstrated by the observed differential level of expression between the anterior and main portion of the larval fat body (Figure 5.4). Finally in keeping with the idea of sexual identity and cell determination as an ongoing developmental process (*cf.* the demonstrated persistence of dsx^{GAL4} expression in the embryo through to the larval stages), it may be also worthwhile to consider the cell-fate developmental relationship that exists between larval fat body and somatatopic gonadal precursor and cells, where mis-regulation in the genetic processes involved causes ectopic proliferation in one tissue at the cost of the other (Hayes et al., 2001).

Following this, in keeping with the idea of restricted expression of sexual identifiers, expression was seen to occur in a specific pattern in some, but not all, the imaginal discs (Rideout et al., 2010; Robinett et al., 2010). Again it appears to make logical developmental sense that those discs in which dsx^{GAL4} expression was observed, such as in the discs of the forelegs, developed into adult structures that possessed clear dimorphisms and/or dimorphic functions. Further novel expression was also observed in peri-cuticular cells within the larvae, the function of these cells requiring further investigation to be delineated.

In the adult dsx^{GAL4} expression was observed in cells of the fat body in both males and females (Rideout et al., 2010; Robinett et al., 2010). The adult fat body is a complex multi-modal tissue that acts not just as an energy store, but as a dynamic and responsive endocrinal signaling center performing a variety of metabolic functions to do with energy metabolism and growth, steroid hormone signaling, innate immune responses and aging (Camara et al., 2008; Hoshizaki, 2005). The fat body has already demonstrated sex-specific physiological attributes in both males and females. In the female the fat body *yolk protein* genes (*yp*) are transcriptionally activated by Dsx^F and repressed by Dsx^M (Bownes, 1994). *dsx* has been shown to continuously target the *yp* genes in the adult, demonstrating the requirement for persistent maintenance of this component of the female's sex-specific physiology for the assurance of proper sex-specific behavioural outputs

(Bownes, 1994). It has been demonstrated that feminization of the male adult fat body results in significant reduction in courtship behaviors, most likely due to disruption of synthesis of circulating male-specific secreted neuromodulatory proteins (Dauwalder, 2008). In the male Takeout (To), a factor secreted from the adult fat body involved in both nutritional survival mechanisms in response to starvation and the circadian cycle, has also been implicated in adult courtship behaviour and is apparently positively activated by the Dsx^M in conjunction with Fru^M and repressed by expression of Dsx^F (Dauwalder, 2008; Dauwalder et al., 2002; Lazareva et al., 2007). Similar to this role in the regulation of To, evidence appears to show that *dsx* may also be involved in the regulation sex-specific transcripts in the fat body, potentially in production of further soluble neuroendocrinal factors secreted into the haemolymph (Carney, 2007; Dauwalder, 2008; Lazareva et al., 2007). The adult fat body has also been demonstrated to express several other putative sex-specific genes, such as *female-specific independent of transformer* (*fit*) in females and *turn on sex-specificity* (*tsx*) in males, which encode odorant/pheromone binding proteins (Fujii and Amrein, 2002). These studies suggest that these soluble, circulating factors could play a significant role in the neuromodulation of sexual behavioural outputs and the associated sex-specific physiological processes, in a manner redolent of the hormonal control of behaviour in vertebrates. Highlighting another potential path in which way *dsx* may regulate sexual behaviour by the specification of sexual identity in non-neuronal tissues, imbuing them with sexually dimorphic physiological properties. As a corollary to this demonstrated requirement for *dsx* expression within the fat body; the fat body is also a pivotal site for production of the fly's innate immune responses and genes involved in immune responses have been shown to be induced/upregulated in mated females (Lawniczak and Begun, 2007; Mack et al., 2006; McGraw et al., 2004; Meister et al., 1997; Peng et al., 2005). This presumably occurring as a defence response against pathogenic challenges to their gametes/embryos and reproductive tracts, such as microbial attack, introduced during mating.

The adult oenocytes are specialized peri-cuticular cell clusters located in the abdomen, which have been shown to be the site of biosynthesis of cuticular hydrocarbons in *Drosophila* that are deposited on the surface of the fly (Billeter et al., 2009; Chertemps et al., 2007; Chertemps et al., 2006; Ferveur, 2005a; Ferveur et al., 1997; Grillet et al., 2006; Jallon et al., 1988; Lacaille et al., 2007; Legendre

et al., 2008; Savarit et al., 1999; Siwicki et al., 2005). Some of these cuticular hydrocarbon act to prevent desiccation, whilst other function as pheromones communicating sex and species identifiers, generating a characteristic profile of aphrodisiac and anti-aphrodisiac pheromones and therefore modulate behavioural outputs of both the progenitor and the target fly (Billeter et al., 2009; Ferveur, 2005a; Ferveur et al., 1997; Grillet et al., 2006; Lacaille et al., 2007; Savarit et al., 1999; Siwicki et al., 2005). Previous studies have shown that sex-specific pheromonal production is under the direct control of *dsx* (Jallon et al., 1988; Waterbury et al., 1999). Dsx expression likely influences pheromone production by regulating genes involved in pheromone synthesis, and a recent study demonstrated that Dsx^F directly activates the desaturase gene, *desatF*, in female oenocytes, to produce female pheromones that induce male courtship behavior in Drosophila melanogaster (Shirangi et al., 2009). As such the observed expression of dsx^{GAL4} in the oenocytes of both males and females likely reflects the requirement for *dsx* to modulate pheromonal production, presumably through the regulation of genes involved in pheromone biosynthesis (Billeter et al., 2009; Chertemps et al., 2007; Chertemps et al., 2006; Ferveur, 2005a; Ferveur et al., 1997; Grillet et al., 2006; Jallon et al., 1988; Lacaille et al., 2007; Legendre et al., 2008; Savarit et al., 1999; Shirangi et al., 2009; Siwicki et al., 2005).

Again, though the larval fat body and oenocytes and their adult counter-parts (with the fat bodies at least performing similar roles) have differing lineages, the presence of dsx^{GAL4} expression in all these tissues, and the persistence of expression from embryo to larva and then pupa to adult, argues convincingly that the process of sexual determination by *dsx* is one that begins at the earliest of stages and is then required continuously for the regulation and maintenance of sexual identity even in the developed adult.

Within the intestinal track homeostasis is a naturally occurring, ongoing process featuring constant basal levels of epithelium regeneration via differentiation of EBs (Buchon et al., 2010; Chatterjee and Ip, 2009; Jiang et al., 2009). However the metabolic pathways involved may also be upregulated in response to trauma or xenobiotic challenge (Buchon et al., 2009; Chatterjee and Ip, 2009; Jiang et al., 2009). As such homeostasis in the intestine is achieved through the complex inter-regulation of immune responses and developmental mechanisms for stem cell activity, epithelium proliferation and renewal utilising the

UPD, JAK-STAT and JNK pathways (Buchon et al., 2009; Buchon et al., 2010; Chatterjee and Ip, 2009; Jiang et al., 2009). The expression of *dsx*^{GAL4} within intestinal track makes logical sense as the homeostatic processes involved have already been shown to be dimorphic as both the basal and immune responsive turnover rates for epithelium are far higher in adult females than in males (Biteau et al., 2010; Jiang et al., 2009) (B. Edgar, pers. comm.). The increased rate exhibited by females occurs as a consequence of the greater numbers of ISCs, and consequently EBs, that exist in the female intestinal epithelium when normalized for size differences between the intestinal tracks of the two sexes (Jiang et al., 2009) (B. Edgar, pers. comm.). The requirement for this differential level of stem cell activity presumably due to the greater amount of ingestion required by the adult female's physiology, especially post-mating (Carvalho et al., 2006), and, as previously stated, the fact that successful copulation in females induces expression of genes of the immune response, probably in order to assure protection to the female and embryos from pathogenic attack introduced during mating (Lawniczak and Begun, 2007; Mack et al., 2006; McGraw et al., 2004; Meister et al., 1997; Peng et al., 2005; Wolfner, 2009).

Finally the requirement for expression of sexual identity in the male and female internal genitalia would seem obvious, but again the expression of *dsx*^{GAL4} within these tissues is not ubiquitous and as such the restricted nature of the expression patterns observed may give some insight into function. In the male, apart from the neural ramifications that exist to regulate activity in the testes, accessory glands, ejaculatory duct and bulb (presumably involved in the modulation of peristaltic movement for the transport of components of the seminal package), expression of *dsx*^{GAL4} appears largely restricted to the epithelium of the lumens of the seminiforous vesicles, vas deferens and ejaculatory duct. This *dsx*^{GAL4} expression may reflect a required function to modulate the constriction/relaxation of these lumens allowing transport of the seminal fluids, or indeed these cells may be neuro-endocrinal, contributing to the secretions within the seminal package (Ram and Wolfner, 2007a; Wolfner, 1997). Notably no expression is evident within the lumen of the accessory glands, though expression is evident in the secondary cells, large vacuolar cells that contribute components to the Acps as a whole (Bertram et al., 1992). The ejaculatory bulb exhibits a high level of expression within secretory cells that line the body of the bulb (Ram and Wolfner, 2007), and in the only place where it is evident within the genitalia

musculature, in the muscles associated with the apodeme. In the female the process of ovulation, fertilisation and deposition of an egg is a complex sequence of events dependent upon complementary orchestration of components of both male and female physiology. Successful transfer of the seminal package by males into the female has been shown to cause conformational changes in the female reproductive tract whereby the tract and the sperm storage organs (the seminiferous vesicles spermathecae) oviduct flap associated with the uterine wall are relaxed, allowing sperm entry into the lumen and into storage, perhaps through the release of neuromodulators from vesicles along the uterine duct induced or mediated by the reception of Acps, before further female inputs modulate the release of these seminal fluids for presentation of the sperm and the egg for fertilisation (Adams and Wolfner, 2007; Wolfner, 2009). As such the described *dsx*^{GAL4} pattern of expression in the female internal genitalia specifically in the lumen and muscle walls associated with these organs would appear to be of real importance. This seems especially true when you consider that Szabad and Fajszi (1981) identified a focus in the VNC involved in the modulation of post-mating physiological responses in the female specifically to do with ovulation and the transference of the mature unfertilized egg into the uterus for fertilization. Latterly it has been shown that mating, and successful transmission of the seminal package, activates octopaminergic neurons within the female Abg projecting to the oviducts stimulating the octopamine receptor in the mushroom bodies (OAMB) to cause fluid secretion from the epithelium of the oviducts into the lumen (Lee et al., 2009). Lee et al., 2009 also speculate this input to the oviducts may be processed by another octopamine receptor, effecting a relaxation of the muscular wall of the oviducts, the concerted affects of this secretion and relaxation being the transportation of the egg to the uterus for fertilization.

Up to this point I have demonstrated that cells expressing *dsx*^{GAL4} are required in the development of the adult external sexual morphology; in the assembly of sex-specific circuitry in males and females; and outwith the nervous system, throughout development, in key tissues required to assure sex-specific physiological properties and therefore proper maintenance of sex-specific behaviours. Following these spatial-temporal surveys, my investigations will centre on attempting to define the role(s) these *dsx*^{GAL4} expressing cells play in the generation of sex-specific behavioural outputs. The long-term goal of these studies is thus to try and provide insight into how *dsx* contributes to the development, and

maintenance, of both the sexually dimorphic nervous system (the “mind”) and soma (the “body”), and how these systems are then orchestrated to generate the ‘complete’ male or female adult.

6 The relationship of *dsx* and *fru* in specifying a sexually dimorphic nervous system

6.1 *dsx*^{GAL4} and Fru^{M} co-expression in the male CNS

As has been previously stated both *dsx* and *fru* are expressed within the pupal and adult CNS in discrete neuronal clusters (Billeter and Goodwin, 2004; Billeter et al., 2006a; Billeter et al., 2006b; Demir and Dickson, 2005; Lee et al., 2000; Lee et al., 2002; Rideout et al., 2010). Latterly, co-expression with Fru^{M} within at least a subset of the population of *dsx*-expressing neurons in each cluster has been demonstrated for the male pupa (Billeter et al., 2006b; Rideout et al., 2007; Rideout et al., 2010). However a systematic characterisation of this co-expression has been limited by the sensitivity of available reagents (specifically *dsx* antibodies). The *dsx*^{GAL4} allele allows a more detailed and comprehensive survey of the potential co-operation between *dsx* and *fru* to be completed.

The level of co-expression observed between neurons expressing *dsx*^{GAL4}-responsive nGFP and Fru^{M} remains relatively static, with no significant changes barring one notable exception (in *dsx*-pC2), between 48 hr pupae and 5 day old adult males (Figures 6.1, 6.2 & 6.3; Table 6.1). This despite the actual observed expression being dynamic in both *dsx*^{GAL4} and Fru^{M} clusters (see Figures 6.2 & 6.3; Table 6.1).

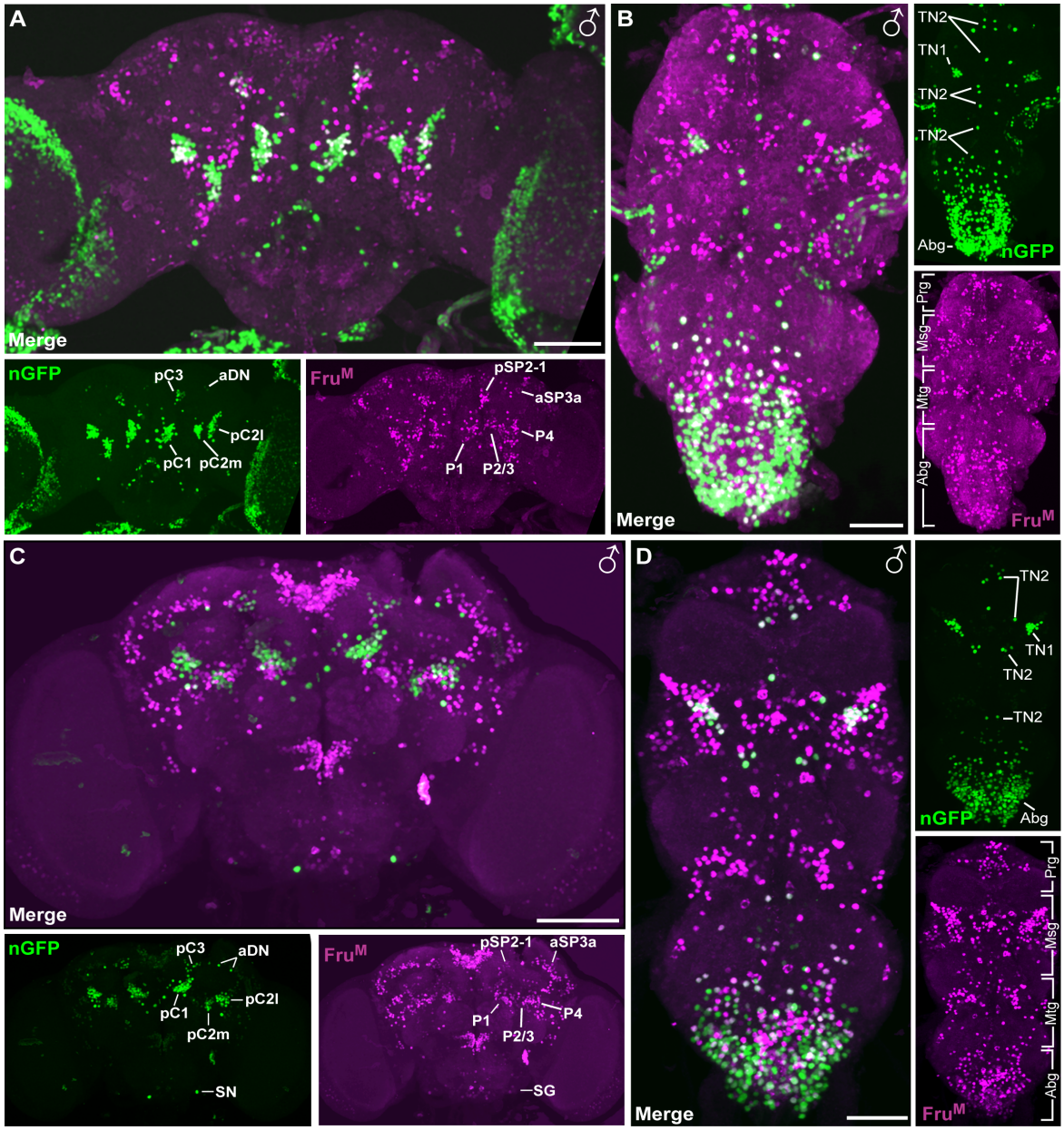

Figure 6-1 Co-expression of *dsx*^{GAL4} responsive nuclear GFP and Fru^{M} in 2 day old pupa and 5 day old adult male CNSs.
(A-B) 2 day old *dsx*^{GAL4} pupa expressing UAS-StingerII (nGFP, green), co-stained with anti-Fru^{M} (magenta) (A) brain and (B) VNC. *dsx* and *fru* neuronal clusters indicated. (C-D) 5 day old *dsx*^{GAL4} adult expressing UAS-StingerII (nGFP, green), co-stained with anti-Fru^{M} (magenta) (C) brain and (D) VNC. Prothoracic (Prg), mesothoracic (Msg), metathoracic (Mtg) and abdominal (Abg) ganglia. Ventral views; anterior top. *dsx* and *fru* neuronal clusters indicated. n ≥ 6. *fru* neuronal clusters as per Lee et al. 2000 and Kimura et al. 2008. *dsx* neuronal clusters as per Lee et al. 2002, Rideout et al. 2010 and Robinett et al. 2010. Scale Bars = 50 µm.

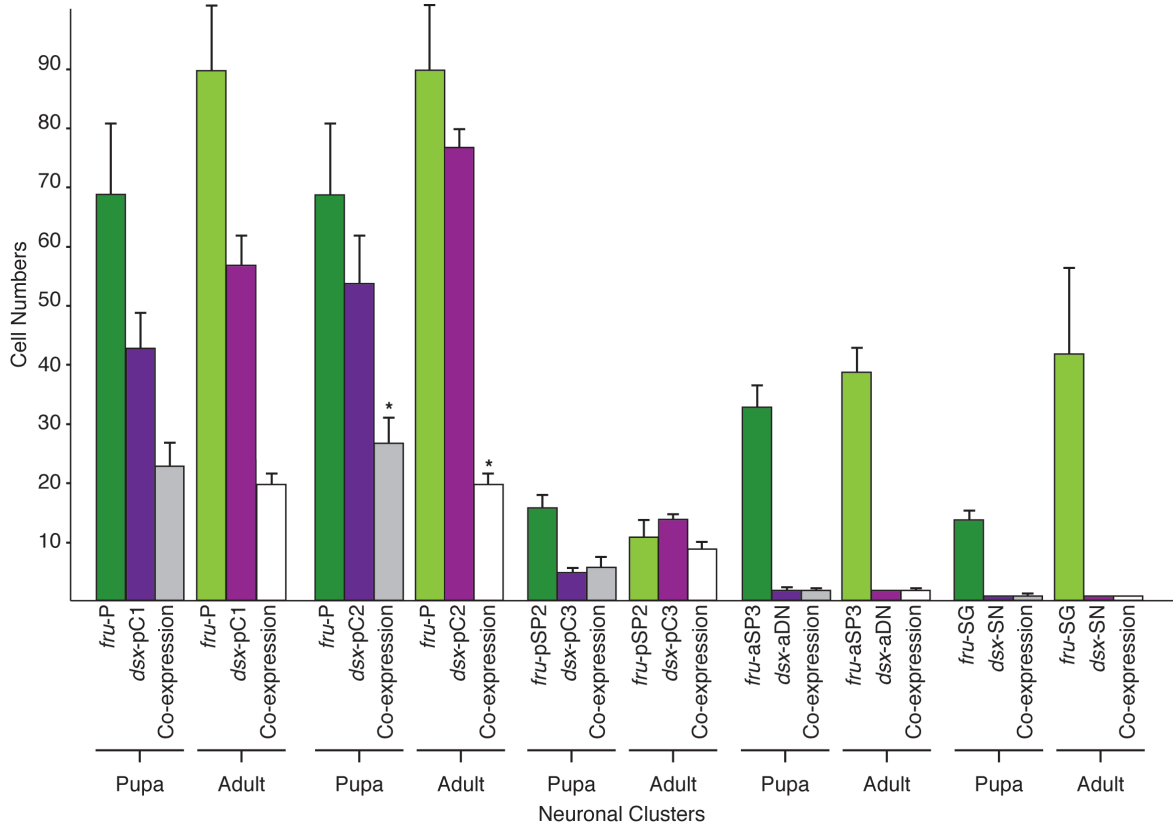

Figure 6-2 Graphical representations of the cell counts for *dsx*^{GAL4} responsive nuclear GFP, Fru^{M}, and the corresponding overlap, in 2 day old pupal and 5 day old adult male brains. **P*<0.05 (Student's t-test). n ≥ 6. *fru* neuronal clusters as per Lee et al., 2000 and Billeter and Goodwin, 2004. *dsx* neuronal clusters as per Lee et al. 2002 and Rideout et al 2010.

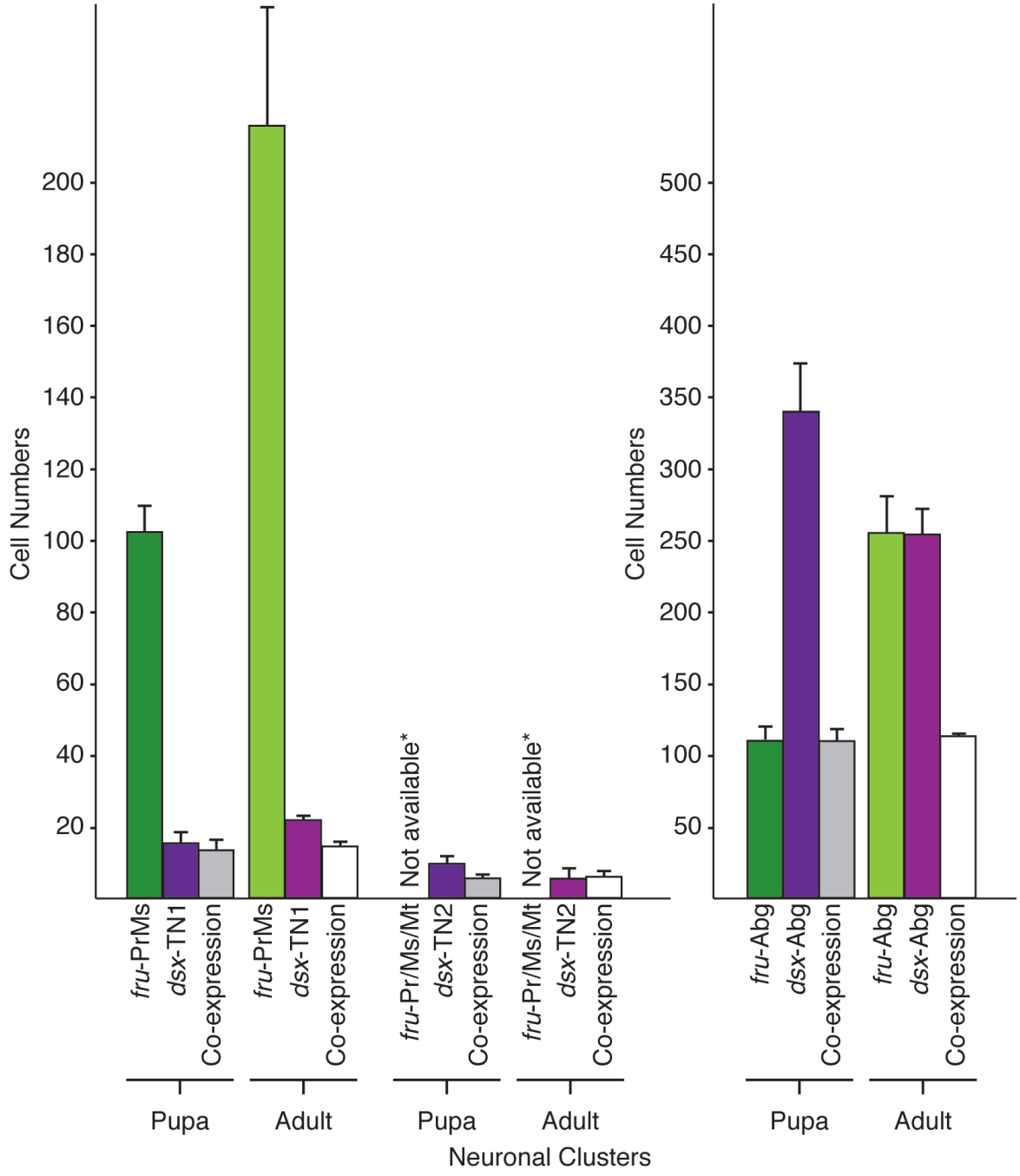

Figure 6-3 Graphical representations of the cell counts for *dsx*^{GAL4} responsive nuclear GFP, Fru^{M}, and the corresponding overlap, in 2 day old pupal and 5 day old adult male VNCs. n ≥ 6. *fru* neuronal clusters as per Lee et al., 2000 and Billeter and Goodwin, 2004. *dsx* neuronal clusters as per Lee et al. 2002 and Rideout et al 2010. *Neuronal counts unavailable, as neurons involved would be ascribed to more than one designated cluster.

TABLE 6.1 Co-expression of *dsx*^{GAL4} responsive nGFP and Fru^{M} in pupal and adult male CNSs

	48 hr Pupae				5 day old Adults				
	Dsx Neuronal clusters[1]	Cell Count[2]	Fru^{M} Neuronal Clusters[3]	Cell Count[4]	Colocalisation[5]	Dsx Neuronal clusters[1]	Cell Count[4]	Fru^{M} Neuronal Clusters[2]	Cell Count[4]	Colocalisation[5]
Brain										
1	*dsx*-pC1[6]	43 ± 6.0 (12)	*fru*-P[6]	69 ± 12.3 (5)	23 ± 4.2 (6)	*dsx*-pC1[6]	57 ± 5.0(10)	*fru*-P[6]	90 ± 11.2 (7)	20 ± 1.8 (6)
2	*dsx*-pC2[6]	54 ± 8.2 (12)	*fru*-P[6]	69 ± 12.3 (5)	27 ± 4.3 (6)*	*dsx*-pC2[6]	77 ± 3.1 (10)	*fru*-P[6]	90 ± 11.2 (7)	20 ± 1.8 (6)*
3	*dsx*-pC3[6]	5 ± 0.8 (10)	*fru*-pSP2[6]	16 ± 2.3 (6)	6 ± 1.7 (6)	*dsx*-pC3[6]	14 ± 1.0 (10)	*fru*-pSP2[6]	11 ± 3.0 (7)	9 ± 1.3 (7)
4	*dsx*-aDN[6]	2 ± 0.5 (10)	*fru*-aSP3[6]	33 ± 3.8 (3)	2 ± 0.5 (6)	*dsx*-aDN[6]	2 ± 0 (10)	*fru*-aSP3[6]	39 ± 4.1 (3)	2 ± 0.4 (6)
5	*dsx*-SN[6]	1 ± 0 (12)	*fru*-SG[6]	14 ± 1.7 (5)	1 ± 0.4 (7)	*dsx*-SN[6]	1 ± 0 (10)	*fru*-SG[6]	42± 14.4 (8)	1 ± 0 (6)
Ventral Nerve Cord										
6	*dsx*-TN1[6]	16 ± 2.6 (14)	*fru*-PrMs[6]	103 ± 3.5 (2)	14 ± 2.6 (12)	*dsx*-TN1[6]	22 ± 1.7 (10)	*fru*-PrMs[6]	216± 33.2 (5)	15 ± 1.4 (8)
7	*dsx*-TN2[6]	10 ± 1.3 (16)	*fru*-Pr/Ms/Mt[6]	n.a.[8]	6 ± 1.0 (6)	*dsx*-TN2[6]	7 ± 3.0 (10)	*fru*-Pr/Ms/Mt[6]	n.a.[8]	7 ± 1.5 (6)
8	*dsx*-MtAbg[7]	n.a.[8]	*fru*-MtAbg[7]	19 ± 5.7 (2)	n.a.[8]	*dsx*-MtAbg[7]	n.a.[8]	*fru*-MtAbg[7]	21 ± 5.5 (4)	n.a.[8]
9	*dsx*-Abg[7]	342 ± 34.2 (8)	*fru*-Abg[7]	111 ± 13.4 (3)	112 ± 9.2 (6)	*dsx*-Abg[7]	277 ± 22.1 (10)	*fru*-Abg[7]	256 ± 27.7 (6)	114 ± 1.8 (6)

Table 6-1 Co-expression of *dsx*^{GAL4} responsive nGFP and Fru^{M} in pupal and adult male CNSs.
[1]Nomenclature for Dsx neuronal clusters as per Lee et al. (2002) and Rideout et al. (2010). [2]Number of nuclei expressing *dsx*^{GAL4} responsive UAS-nGFP ± standard deviation as per Rideout et al. (2010). [3]Nomenclature for Fru^{M} neuronal clusters as per Lee et al. (2000). [4]Number of nuclei expressing Fru^{M} ± standard deviation as per Billeter and Goodwin (2004). [5]Number of nuclei co-expressing both *dsx*^{GAL4} responsive UAS-nGFP and Fru^{M} ± standard deviation. [6]Neuronal cluster away from CNS midline. Count represents one cluster per hemisegment of the CNS. [7]Neuronal cluster spans the CNS midline. Count given is for the complete VNC. [8]Neuronal counts unavailable, as neurons involved would be ascribed to more than one designated cluster. *P<0.005 (Student's t-test). n's listed in parentheses.

That is, while the numbers of cells expressing either *dsx*^{GAL4} or Fru^{M} may increase or decrease significantly for a given designated cluster from pupa to adult (Billeter and Goodwin, 2004; Lee et al., 2002; Rideout et al., 2010; Sanders and Arbeitman, 2008), the actual number exhibiting co-localization remains essentially the same. This is not to say that the individual cells demonstrating this co-expression are the same between the time-points. However it seems telling that this co-expression becomes apparent, and remains in place thereafter, at a crucial developmental time point in the male pupa (Arthur et al., 1998; Belote and Baker, 1987). The critical nature of this developmental time point is exemplified by the appearance of expression in the male-specific *dsx*-SN, *dsx*-TN1 and *dsx*-TN2 neurons at this juncture, coupled with the reduction in neuronal numbers in the *dsx*-Abg cluster (the latter neuronal numbers diminishing to less than that in the female). This developmental stage in the male pupa has previously been identified as crucial in the final specification of the male sexual behaviours (Arthur et al., 1998; Belote and Baker, 1987). One notable exception in the static nature of this co-expression involves *dsx*-pC2 where there appears to be a slight, but still significant, reduction in co-expression from pupa to adult despite a significant increase in both the *dsx*-pC2 and *fru*-P neuronal populations (Table 6.1).

It should be noted that differences in the tabulated counts presented here and previous co-expression data (Rideout et al., 2007) may be ascribed to the separation of cell counts between the previously identified cluster *dsx*-pC1 and the novel cluster *dsx*-pC3 as identified in Rideout et al. 2010 (and latterly in Robinett et al. 2010 as *dsx*-pCd). Previous tabulations incorporated cells (clearly visible in the relevant figures), now designated as neuronal cluster *dsx*-pC3, into the counts for the *dsx*-pC1 cluster (see Rideout et al., 2007).

6.2 Fru^M co-expression in the male-specific sub-clusters *dsx*-pC2m and *dsx*-pC2l

As previously discussed (section *4.1.3*) it would appear that the male *dsx*-pC2 cluster may be comprised of two distinct, yet topographically related, populations of neurons. This is based on the observations that, while only one distinct *dsx*-pC2 cluster is apparent in the female, the cluster is usually 'split' into two distinct medial (*dsx*-pC2m) and lateral (*dsx*-pC2l) subsets in the male. Further the distinct subsets contribute separate axonal projections to the overall *dsx* neural architecture (Figure 6.4B). Also as noted previously (see section *4.4.2*) performing axotomies on the foreleg above the sex comb in males results in a significant decrement in neurons in the *dsx*-pC2 cluster specifically in the –pC2l sub-cluster indicative of a bias of male-specific projections interacting with this cluster. While both subsets of the male *dsx*-pC2 cluster exhibit neurons that co-localize with Fru^M, the vast majority of co-expression appears localized to the lateral population of neurons (*dsx*-pC2l; Figure 6.4C). I would speculate that the significant alteration in level of co-expression between dsx^{GAL4} and Fru^M from pupa to adult (Figure 6.1, 6.2; Table 6.1) reflects first the generalized *dsx*-dependent proliferation of the male-specific neurons in the pupa and then the reduction in number of these neurons as they are re-organised and maintained in the adult as two related clusters, perhaps in a Fru^M-dependent manner and that the lateral *dsx*-pC2 neurons are essentially a novel male-specific *dsx* neuronal cluster. This could be occurring in a manner reminiscent of that described in Billeter et al. (2006b) with respect to the organization of the complete complement of ventral and dorsal male-specific serotonergic Abg neuronal clusters by Fru^M and Dsx, or may be the result of a continuation of neouroblast proliferation (*cf.* Taylor and Truman, 1992) or alternatively it may be that a program of cell death is occurring in the female to 'prune' the related female cluster (*cf.* Kimura et al., 2008). However it will require further clonal/lineage and mutant analyses to confirm both the distinct nature of the two clusters and also any cooperative developmental mechanism that might occur between Dsx^M and Fru^M in their specification.

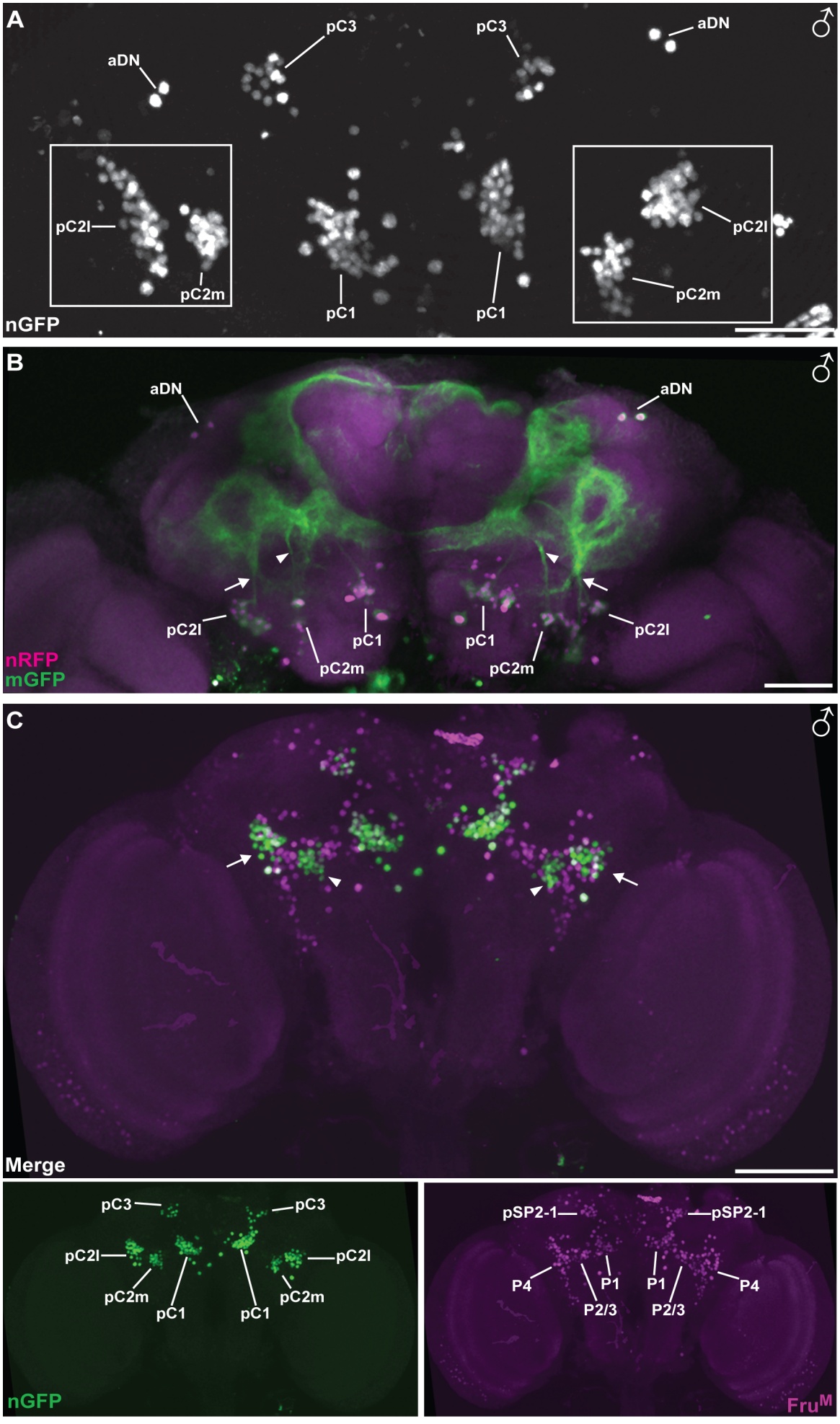
A
aDN
pC3
pC3
aDN
pC2l
pC2m
pC1
pC1
pC2l
pC2m
nGFP
B
aDN
aDN
pC2l
pC1
pC1
pC2l
pC2m
pC2m
nRFP
mGFP
C
Merge
pC3
pC3
pC2l
pC2l
pC2m
pC2m
pC1
pC1
nGFP
pSP2-1
pSP2-1
P4
P1
P1
P4
P2/3
P2/3
FruM

Figure 6-4 Demonstration of distinct medial and lateral subsets of the *dsx*-pC2 neuronal cluster in pupa and adult male brains.
(A) Detail of 2 day old *dsx*^{GAL4} pupal brain expressing UAS-StingerII (nGFP). *dsx* neuronal clusters indicated (Dorsal view, anterior top). (B) Detail of a horizontal plane of view 5 day old *dsx*^{GAL4} male adult brain expressing UAS-mCD8::GFP (mGFP, green) and UAS-StingerII (nGFP, magenta). Distinct individual fascicles associated with *dsx*^{GAL4}-pC2m (arrowheads) and *dsx*^{GAL4}-pC2l (arrows). *dsx* neuronal clusters indicated. (A-B) Shown previously in Figure 4.8 (Horizontal view, ventral top). (C) Detail of 5 day old *dsx*^{GAL4} male adult brain expressing UAS-StingerII (nGFP, green), co-stained with anti-Fru^{M} (magenta) to highlight the relationship of Fru^{M} co-expression with the distinct medial and lateral subsets of the *dsx*^{GAL4}-pC2 neuronal cluster. *dsx* and *fru* neuronal clusters indicated. Full maximal confocal stack of this image shown previously in Figure 6.1 (Dorsal view, anterior top). *fru* neuronal clusters as per Kimura et al., 2008. *dsx* neuronal clusters as per Lee et al. 2002, Rideout et al., 2010 and Robinett et al., 2010. Scale Bars = 50 µm.

6.3 Integration of *dsx* and *fru* neural circuitry

This described overlap between *fru*- and *dsx*-expressing neurons in the male CNS allows functional roles to be ascribed to certain *dsx* neurons due to their intersection with *fru* neurons with a defined role in male sexual behaviour. The relationship that these *dsx* neurons have to the male-specific *fru* circuitry may be extended by recent neuro-anatomical fine mapping of neuroblast clones and volumetric analyses describing *fru* neural circuitry (Cachero et al., 2010; Kimura et al., 2008; Ruta et al., 2010; Yu et al., 2010). This mapping has allowed more specific individual neurons and neuronal clusters associated with *fru* clonal groups to be identified, with a greater understanding of the relationship that these neurons have to each other and to the surrounding neural substrates and, by corollary, a greater understanding of how the *dsx*-specified neural circuit integrates into the overall male-specific neural architecture underlying the generation of courtship behaviours.

6.3.1 dsx-aDN

The bilateral pair of *dsx*-aDN neurons are the only *dsx*-expressing neurons positioned in the anterior compartment of the brain. The *dsx*-aDN neurons exhibit colocalization with the *fru*-aSP3 cluster, in a region of the brain that has been associated with the male courtship behaviours, initiation, following, tapping and wing extension via gynandromorph studies (Ferveur and Greenspan, 1998; Hall, 1977, 1979). This region has latterly been delineated as part of the *fru*-aSP3a cluster (Kimura et al., 2008), which in turn has been identified as comprising neurons arising from the *fru*-anterior Superior Protocerebrum (aSP) –f clonal group (Cachero et al., 2010).

fru-aSP-f (and thus the *dsx*-aDN neurons) is described as comprising third-order neurons associated with the olfactory neural circuitry and exhibits a sex-specific pattern of expression with respect to its neuronal complement (23.2 ± 2.59 in males compared with 18.6± 5.03 in females, $P<0.05$), axonal projections and the associated pattern of arborisation (Cachero et al., 2010). This cluster exhibits a sexually dimorphic projection pattern, where both males and females arborisation patterns can form discrete synaptic connections not possible in the other sex, the male aSP-f cluster forming extensive arbors within the male expanded regions absent in females while the opposite is true for females (Cachero et al., 2010). In keeping with these neurons being involved in higher-order processing of olfactory information, approximately 20% of the dendritic arborisation seen in the lateral horns (LHs) may be attributed to neurons of the aSP-f cluster, and again these arbors patterns were overtly dimorphic (Cachero et al., 2010). Intriguingly when these differences were overlapped they identified discrete changes of the neural architecture that potentially could result in the rerouting of sensory information/stimuli resulting in differential processing of this information by the different sexes (Cachero et al., 2010; Datta et al., 2008; Ruta et al., 2010).

6.3.2 dsx-pC1

dsx-pC1 colocalized with the medial area of the *fru*-P cluster, an area originally identified by gynandromorph studies to be a focus for licking and copulatory behaviours (Ferveur and Greenspan, 1998; Hall, 1977, 1979). Within this cluster *dsx*-pC1 may be identified as intersecting with a subset of *fru*-P1 neurons (Kimura et al., 2008). This is not only due to the positioning of the co-expressed neurons but also due to the fact that the *dsx*-pC1 cluster has associated with it a uniquely shaped, and therefore easily identifiable, fascicle. This fascicle, which is also characteristic of the *fru*-P1 cluster, projects straight up dorsally before hooking over to project antero-ventrally (see Figure 4.7) (Kimura et al., 2008). The 20 neurons of the P1 cluster have been shown to be both *fru* and *dsx* dependent requiring Fru^M for the proper organization of terminals of the associated axonal projections, while this cluster has been shown to undergo apoptosis in the presence of Dsx^F ensuring it's complete absence in females (Kimura et al., 2008). This male-specific cluster has been identified as being of extreme importance to the initiation of male courtship (Kimura et al., 2008) and has now been identified as male-specific interneurons with trans-midline neurites in which the courtship

initiation is generated in response to sensory stimuli from contact with non-volatile pheromonal cues (see Figure 4.7) (Kohatsu et al., 2011). Courtship specific stimuli from the female, received from multiple sensory inputs by the P1 cluster could initiate a bilateral coordinated neural program for male-specific courtship behavioural outputs, with signals transmitted to motor output centres in the VNC (Kohatsu et al., 2011).

fru-P1 (and therefore at least a subset of the *dsx*-pC1 cluster) has since been identified in volumetric/neuroblast clonal analyses as comprising neurons of the *fru*-posterior Medial Protocerebral (pMP) -e clone (Cachero et al., 2010). These neurons have been described, via their positioning and arborisation pattern, as a cluster of third-order neurons associated with the olfactory circuit (Cachero et al., 2010a), a circuit known to be of importance for sensory stimulation leading to courtship initiation (Billeter et al., 2009; Datta et al., 2008; Ferveur, 2005b; Jallon, 1984; Ruta et al., 2010). *fru*-pMP-e appears to be the most dimorphic of all *fru*+ elements within the central brain with a sex-specific pattern of expression with respect to its neuronal complement (38.4 ± 16.32 in males compared with 9.0 ± 1.41 in females, $P<0.05$), axonal projections and the associated pattern of arborisation (Cachero et al., 2010).

This *dsx*-pC1/*fru*-P1/*fru*-pMP-e neuronal ‘complex’ extends a primary neurite antero-dorsally with extensive ramifications in the lateral and medial protocerebrum, contributing to what is now described as the superior region of the ‘ring’, and to parts of the ‘lateral junction’ and ‘lateral crescent’ (Cachero et al., 2010; Rideout et al., 2010; Yu et al., 2010). Projections also extend to the corresponding contra-lateral region along the trans-midline superior-protocerebral bridge (forming part of the anterior dorsal commissure) also described as the ‘arch’ (Cachero et al., 2010; Kimura et al., 2008; Rideout et al., 2010; Yu et al., 2010). The pre-synaptic marker synaptotagmin is localized bilaterally on the medial side of the infero-lateral and ventro-lateral protocerebrum, as well as along the trans-commissural neurites, indicating that these regions are likely output sites for these neurons (see Figure 4.6C3-4) (Cachero et al., 2010; Rideout et al., 2010). Ipsi-lateral projections in the ventero-lateral and ventero-medial protocerebrum likely represent inputs into this neuronal complex (Cachero et al., 2010; Rideout et al., 2010). *fru*-pMP-e exhibits male-specific arborisations in the LH absent in females (Cachero et al., 2010). As it has been demonstrated that *fru*-P1 cluster is absent in

females due to PCD (Kimura et al., 2008) it seems likely that these neurons and, as a consequence neurons of the *dsx*-pC1 cluster, contribute to this male-specific arborisation. This extensive arborisation has been shown to overlap with the second most dimorphic clonal group, *fru*-anterior Superior Protocerebrum (aSP) -a, suggesting that these two sexually dimorphic neuronal clusters act in concert as multimodal integrators of higher-order sensory processing especially with respect to male-specific behavioural inputs and outputs (Cachero et al., 2010). This suggestion would be in keeping with the idea that the differing sensorium possessed by the fly allows courtship to be initiated (and subsequently maintained) by a variety of sensory stimuli in a coordinated manner, i.e. sensory input to the olfactory circuit stimulating higher order processing of the *dsx*-pC1/*fru*-P1/*fru*-pMP-e neuronal 'complex' receiving a re-iterative sensory signal from aSP-a neurons (or visa versa) leading to follow on male behavioural outputs of the courtship sequence (Krstic et al., 2009).

6.3.3 dsx-pC2

dsx-pC2 colocalized with the lateral region of the *fru*-P cluster (Figure 6.4C). Gynandromorph studies identified the *fru*-P cluster as a focus for licking and copulatory behaviours (Broughton et al., 2004; Ferveur and Greenspan, 1998; Hall, 1977, 1979). This region of the *fru*-P cluster has laterally been identified as *fru*-P2 to –P4 (Figure 6.4C) (Kimura et al., 2005). It would again seem to be of note that both neuronal clusters *fru*-P2 and *fru*-P4 exhibit overt sexual dimorphism with males possessing significantly mores neurons than females (22.2 ± 1.3 in males compared with 11.2± 2.8 in females, $P<0.005$ for *fru*-P2; 24.4 ± 0.09 in males compared with 15.0 ± 0.7 in females, $P<0.005$ for *fru*-P4). As previously stated *dsx*-PC2 in males seems to comprise two distinct clusters (*dsx*–pC2m and -pC2l). *dsx*-pC2m cluster is positionally related to the *fru*-P2 and (perhaps) –P3 clusters, while the *dsx*-pC2l cluster is more obviously related to the *fru*-P4 cluster.

fru-P2 (and therefore a subset of the *dsx*-pC2m cluster) has since been identified in volumetric/neuroblast clonal analyses as comprising neurons from the *fru*-posterior Inferior Protocerebrum (pIP) -a, *fru*-IP-h and *fru*-pMP-f clones (Cachero et al., 2010).

fru-pIP-a appears to comprise ‘second order neurons’ of the auditory neural circuit. The neurons associated with this clonal group are widely distributed throughout the male-enlarged region (MER) and have associated with them a pattern of projections that ‘descend’ in a bundle into the VNC with terminal arborisations in all three thoracic ganglia. These neurons are not thought to interact with motor neurons directly (Yu et al., 2010) implying that they make synaptic connections with localized inter-neurons (notably the male-specific *dsx*-TN2 neurons present in midline position in all three thoracic ganglia). *fru*-IP-a again exhibits a sex-specific pattern of expression with respect to neuronal numbers comprising the cluster (14.3 ± 3.06 in males compared with 96,4 ± 1.52 in females, $P<0.05$), axonal projections and the associated pattern of arborisation (Cachero et al., 2010). LH neurons are seen to arborise with *fru*-pIP-a descending neurons. *fru*-pIP-a extends projections throughout the medial and lateral infero-protocerebrum and contributes to the medial part of the ring, partly inferiorly but mainly extending superiorly to also comprise part of the lateral junction. *fru*-P2b which may also be identified as *fru*-pIP-a has latterly been identified as descending interneurons which are also involved in courtship initiation perhaps in response to sensory stimuli generated by contact with non-volatile pheromonal cues as with the *fru*-P1 neurons (Kohatsu et al., 2011).

fru-pIP-h and *fru*-pMP-f both appears to comprise ‘higher interneurons’ again associated with the auditory neural circuitry. *fru*-pIP-h neurons have a highly restricted pattern of expression localized to the more superior part of the protocerebral expression pattern which comprises the superior part of the ring. *fru*-pMP-f neurons have a far more extensive pattern of expression, contributing to all of the ring and part of the lateral junction. Both *fru*-pIP-h and *fru*-pMP-f clusters also exhibit male-specific projection patterns and arborisations.

fru-P4 (and again therefore a subset of the *dsx*-pC2l cluster) has since been identified in volumetric/neuroblast clonal analyses as comprising neurons from the *fru*-pIP-e clone. *fru*-pIP-e neurons appear to comprise higher interneurons associated with the visual neural circuitry. Again *fru*-pIP-e clones have a far more extensive pattern of expression, contributing to all of the ring and the lateral junction and with commissural projections to the corresponding contra-lateral region at the level of the protocerebral bridge, as well as both ispso- and contra-

lateral projections to the SOG. *fru*-pIP-e again also exhibits projection patterns and arborisations that are male-specific.

6.3.4 dsx-pC3

dsx-pC3 colocalized with part of the fru-pSP2 cluster, which has been identified as *fru*-posterior Superior Protocerebrum (pSP) 2-1 (or -pSP2-1a) (Figure 6.4C) (Kimura et al., 2008). This region of the brain has been associated with initiation, following, tapping and wing extension via gynandromorph studies (Ferveur and Greenspan, 1998; Hall, 1977, 1979).

fru-pSP2-1 (and again therefore a subset of the *dsx*-pC3 cluster) has since been identified in volumetric/neuroblast clonal analyses as comprising neurons arising from the *fru*-pMP-b clone (Cachero et al., 2010). *fru*-pMP-b is described as comprising third-order neurons associated with the visual neural circuitry (Cachero et al., 2010a). *fru*-pMP-b clones exhibit dimorphic projections patterns, with projections appearing overtly more extensive in males and projecting further ipsilaterally into the SOG (see Figure 4.7) (Cachero et al., 2010), *fru*-pMP-b is also described as a ‘descending clone’ with dimorphic projections into the VNC and with more extensive projections again occurring in males (Cachero et al., 2010). Again the presence of these descending dimorphic expressions might speak to the dsx-pC3/ fru-pSP2/ *fru*-pSP2-1 ‘neuronal complex’s’ involvement in such motor outputs as following, tapping and/or wing extension in response to visual stimuli during courtship.

6.3.5 dsx-SN

The bilateral *dsx*-SN neurons, which, unlike the other describe neuronal groups within the adult brain, are completely male-specific, colocalized with *fru* neurons within the *fru*-SG cluster. This region, extending ventro-dorsally, receives and processes non-volatile (contact gustatory) pheromonal information thought to facilitate sex and species discrimination (Bray and Amrein, 2003; Jallon, 1984; Miyamoto and Amrein, 2008; Spieth, 1974), and latterly has been shown to be involved in mate choice in males (Certel et al., 2007; Chan and Kravitz, 2007) as well as courtship posture associated with unilateral wing extension towards a target female (Koganezawa et al., 2010). Though as the *dsx*-SN neurons are restricted to the posterior Suboesophageal (pSOG) neuronal compartment, they

do not appear to be directly involved in these latter behavioural processes. Indeed the positional variation displayed by these two neurons in conjunction with the more extensive number and dispersed nature of the *fru*-expressing neurons within this region renders it difficult to conclusively identify which *fru*-clonal group they colocalize with. Intriguingly dsx^{GAL4} driven expression of the pre-synaptic marker synaptotagmin demonstrated that projections to the ventral SOG exhibit dimorphic arborisation patterns, with overtly expanded expression in males compared with females throughout the ventral and dorsal SOG compartments (Figure 4.5C vs. 4.5F) (Rideout et al., 2010). More specifically, a concentration of synapses may be observed in an area positionally associated with the *fru*-mCAL cluster (Lee et al., 2000; Rideout et al., 2010), a region that has been implicated in control of sequential courtship steps and in male-specific aggressive behaviours (Chan and Kravitz, 2007; Manoli and Baker, 2004).

6.3.6 dsx expression in the VNC

The region between the pro- and mesothoracic ganglai has been identified by gynandromorph studies to contain a focus for tapping in males (Ferveur and Greenspan, 1998), a necessary adjunct to the reception of non-volatile pheromonal cues (Bray and Amrein, 2003; Jallon, 1984; Miyamoto and Amrein, 2008; Spieth, 1974). Latterly this area has also been implicated in male-specific aggressive behaviours (Chan and Kravitz, 2007). Within this region exists 3-4 bilateral individual male-specific *dsx*-TN2 neurons, which co-express Fru^{M} (Figure 6.1D) and which appear to synapse with the surrounding neural circuitry contributing to the ‘mesothoracic triangle’ (Yu et al., 2010). A large part of the neuronal architecture of this triangle is comprised of projections originating from neuronal cell bodies within the tarsi of the foreleg, a region known to contain gustatory sensilla (Nayak and Singh, 1983; Possidente and Murphey, 1989; Singh and Nayak, 1985; Wang et al., 2004). These projections, entering the prothoracic neuromere before projecting into the mesothoracic ganglia, appear to synapse locally to *dsx*-TN2 neurons as well as sending projections both ispsi- and contralaterally up to the SOG as part of the higher-order processing network of the gustatory circuit**.**

Again in the mesothoracic area are three, medially placed, bilateral individual male-specific *dsx*-TN2 neurons, as well as the more laterally positioned bilateral

male-specific clusters of *ca.*22 *dsx*-TN1 neurons. Each TN1 neuronal cluster appears to communicate with these locally associated TN2 cells and, via contralateral commisural projections, to the opposite corresponding region, as well as with regions in the brain responsible for higher-order processing (either directly or indirectly). In fact all of these male-specific neurons, which co-express *fru*, appear to contribute to the mesothoracic triangle, with contra- and ispsi-lateral projections adding a high degree of complexity to the neural architecture in comparison with that displayed in the female. With this overtly increased, localized, neural complexity in mind it is perhaps unsurprising to find that gynadromorph studies identified the ventral mesothoracic ganglia as a focus for wing vibration (von Schilcher and Hall, 1979). More recently studies have shown that restrictive feminization of this region results in perturbation of male-courtship song, that there is a requirement for *dsx*-specification of a sexually dimorphic population of *fru*-expressing neurons within the Msg and that there exists in this region a localized song-pattern generator (Clyne and Miesenböck, 2008; Rideout et al., 2007; Rubinstein et al., 2010). All of which compellingly pinpoints this area as the site for the generation of the male-specific song. Again, tellingly, clonal analyses of *fru*-specified circuitry have identified 'descending' neuronal clones such as *fru*-pMP2, which receive inputs from the medial part of the protocerebral ring, and send outputs to the SOG and the ganglia of the VNC, particularly to the mesothoracic triangle (Yu et al., 2010). Here these projections appear to synapse with localized inter-neurons (vPR6 and dMS2), which themselves then project to the direct flight muscles the motor effectors for male-specific song output (Ewing, 1977; Ewing, 1979a; Nilsen et al., 2004; Rideout et al., 2007) and aggressive wing displays (Nilsen, Chan et al. 2004). A circuit with the reversed polarity to *fru*-pMP2, derived from *fru*-vPR1 neurons, was also identified sending ascending projections from the mesothoracic triangle up to the pMP2 neurons (Yu et al., 2010). Importantly both the pMP2 and vPR1 neural circuits are male specific with no corresponding neurons in the female (Yu et al., 2010). The presence of these higher-order neural relays may go along way to explain the finding that, while they posses the localized circuitry capable of generating a form of courtship song, females never normally sing (Clyne and Miesenböck, 2008; Yu et al., 2010). These described male-specific circuits directly reflect the topographical position and neuroanatomical pattern of projections associated with the male-specific *dsx*-TN1 clusters and -TN2 cells described by this study, and it would not be

unreasonable to assume that these *dsx* neurons contribute, at least in part, to these circuits.

Finally the Abg has been shown via gynadramorph studies to contain a foci for copulatory behavious (Ferveur and Greenspan, 1998). The larger population of *dsx* neurons observed (relative to the brain and the rest of the VNC) and the high degree of co-expression observed with Fru^M speaks to the importance of this region with respect to modulation of male-specific behavioural ouputs. *dsx* has previously been shown to govern the sex-specific pattern of proliferation of a group of abdominal neuroblasts (Taylor and Truman, 1992) and to cooperate with the Fru^M in the specification and organization of 20 male-specifc serotonergic neurons organized into 2 bilateral clusters (dorsal and ventral) of 10 cells each (Billeter et al., 2006b), which then project to the internal genitalia. Again the importance of this region towards these behaviours is exemplified not only by the presence of ascending and descending projections associated with the protocerebrum, but also those projections which ramify on the internal genitalia and external genital plates. Clonal analyses of *fru*-neurons has identified both descending projections, which presumably direct motor behaviours, as well as ascending projections (such as vAB3), which project to the SOG and the protocerebrum, providing necessary sensory inputs for the modulation of motor outputs associated with both courtship and copulatory behaviours (Yu et al., 2010).

However further fine characterisation of these circuits, both topographically and, more importantly, functionally needs to be performed to delineate their individual contributions to the *dsx*-*fru* specified dimorphic neural architecture and the male-specific behaviours that this architecture underlies.

6.4 *dsx* and *fru* act co-operatively to specify sexual dimorphism in the CNS

Fru^M expression has been shown to protect specific neurons in the brain from sex-specific PCD (Kimura et al., 2005), whereas Dsx^M expression prolongs neuroblast divisions in the Abg (Taylor and Truman, 1992). Again, significant overlap between *fru*- and *dsx*-expressing neurons has been demonstrated in the CNS, suggesting these two genes play cooperative or complementary roles in specifying the development of a sexually dimorphic CNS (Billeter et al., 2006; Rideout et al., 2007; Kimura et al., 2008). As previously described an examination of co-

expression of male-specific *fru* and *dsx*^{GAL4} expression within pupal and adult CNS demonstrated extensive overlap (Figure 6.1; Table 6.1). Therefore to examine the contributions of *fru* and *dsx* to the specification of these dimorphic populations of neurons, I assayed the number of *dsx*^{GAL4}-expressing neurons in *fru* and *dsx* mutant backgrounds using preparations generated both by Dr. Elizabeth Rideout and by myself (Figure 6.5; Table 6.2).

Table 6.2. *dsx*^{Gal4} driven nuclear GFP expression in CNSs of Fru^{M}-null Males, and Females Expressing Fru^{M}, Dsx^{M}, or the Anti-apoptotic Transgene UAS-*p35*

	5 Day Adult Male		5 Day Adult Female			
	CS	*fru*^{F}/*dsx*^{GAL4}, Df(3R)*fru*$^{4-40}$	CS	*fru*^{M}/*dsx*^{GAL4}, Df(3R)*fru*$^{4-40}$	*dsx*^{GAL4}/*dsx*^{Dom}	UAS-*p35*; *dsx*^{GAL4}
	(10)	(10)	(10)	(10)	(10)	(10)
Fru^{M}	+	-	-	+	-	-
Dsx^{M}	+	+	-	-	+	-
Dsx^{F}	-	-	+	+	+	+
Neuronal clusters						
Brain						
1 -PC1[a]	56.9 ± 5.0	48.2 ± 8.6**	8.7 ± 2.0	9.6 ± 1.1	45.8 ± 6.4**	11.1 ± 2.8
2 -PC2[a]	78.6 ± 3.1	67.4 ± 8.8*	11.2 ± 1.9	10.7 ± 1.5	56.3 ± 4.7**	16.1 ± 1.8*
3 -PC3[a]	13.6 ± 1.0	10.7 ± 1.2**	6.4 ± 1.4	6.3 ± 1.9	7.0 ± 1.3	11.7 ± 2.1**
4 -SN[a]	1.0 ± 0.0	1.0 ± 0.0	0.0 ± 0.0	0.0 ± 0.0	1.0 ± 0.0**	1.0 ± 0.0 **
5 -aDN[a]	2.0 ± 0.0	2.0 ± 0 .0	2.0 ± 0.0	2.0 ± 0.0	2.0 ± 0.0	2.2 ± 0.4
Ventral Nerve Cord						
6 -TN1[a]	22.4 ± 1.7	23.0 ± 2.2	0.0 ± 0.0	0.0 ± 0.0	15.5 ± 2.2**	3.0 ± 0.6**
7 -TN2[a]	6.9 ± 3.0	6.6 ± 0.7	0.0 ± 0.0	0.0 ± 0.0	6.0 ± 2.5**	7.0 ± 2.0**
8 -Abg[b]	276.9 ± 22.1	280.3 ± 12.9	311.6 ± 15.9	377.7 ± 23.9**	307.8 ± 19.0	326.6 ± 13.1

Table 6-2 *dsx*^{Gal4} driven nuclear GFP expression in CNSs of adult Fru^{M}-null males, and females expressing Fru^{M}, Dsx^{M}, or the anti-apoptotic transgene UAS-*p35*.
The presence or absence of Fru^{M}, Dsx^{M} and Dsx^{F} expression is noted below genotypes. Counts represent mean number of nuclei expressing *dsx*^{GAL4} responsive UAS-nGFP ± standard deviation as per Rideout et al. (2010). n's listed in parentheses. [a]Neuronal cluster away from CNS midline. Count represents one cluster per hemisegment of the CNS. [b]Neuronal cluster spans the CNS midline. Count given is for the complete VNC. **P*<0.005, ** *P*<0.001.

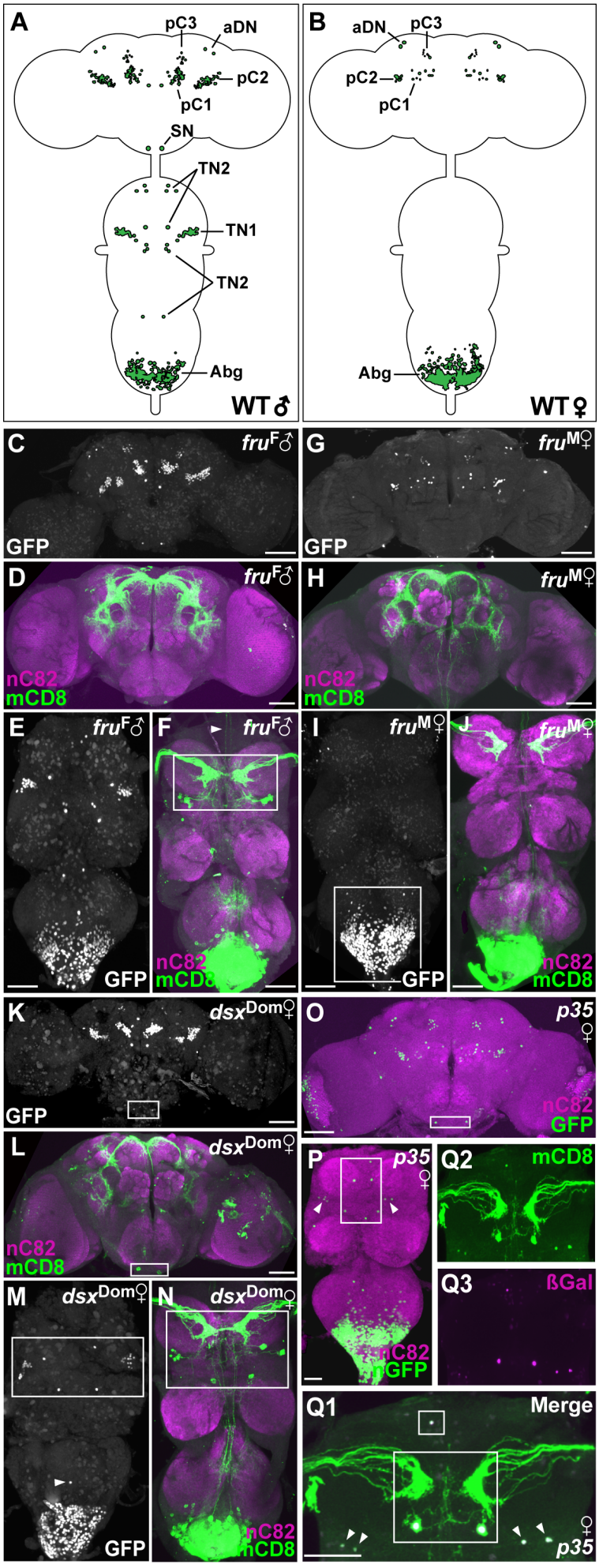
A
pC3
aDN
pC2
pC1
SN
TN2
TN1
TN2
Abg
WT♂
B
aDN
pC3
pC2
pC1
Abg
WT♀
C
fruF♂
GFP
G
fruM♀
GFP
D
fruF♂
nC82
mCD8
H
fruM♀
nC82
mCD8
E
fruF♂
GFP
F
fruF♂
nC82
mCD8
I
fruM♀
GFP
J
fruM♀
nC82
mCD8
K
dsxDom♀
GFP
O
p35
♀
nC82
GFP
L
dsxDom♀
nC82
mCD8
P
p35
♀
nC82
GFP
Q2
mCD8
Q3
ßGal
M
dsxDom♀
GFP
N
dsxDom♀
nC82
mCD8
Q1
Merge
♀
p35

Figure 6-5 *dsx*^{GAL4} Expression in CNSs of Fru^{M}-null Males, and Females Expressing Fru^{M}, Dsx^{M}, or the Anti-apoptotic Transgene UAS-*p35*.
(A-B) Trace contour schematic of *dsx*^{GAL4} nGFP expression in wild-type adult male (A) and female (B) CNSs. Individual neuronal clusters designated. (C) nGFP and (D) Membrane-bound GFP in Fru^{M}-null adult male brain. (E) nGFP and (F) Membrane-bound GFP in Fru^{M}-null adult male VNC, reduction in prothoracic contralateral (boxed area) and cervical connective projections (arrow). (G) nGFP and (H) Membrane-bound GFP in adult female brain expressing Fru^{M}. (I) nGFP and (J) Membrane-bound GFP in adult female VNC expressing Fru^{M}. Increased neuronal expression in Abg (boxed area). (K) nGFP and (L) Membrane-bound GFP in adult female brain expressing both Dsx^{F} and Dsx^{M}. Supernumerary SN cells (boxed area). (M) nGFP adult female VNC expressing both Dsx^{F} and Dsx^{M}. Supernumerary male-specific TN1 and TN2 cells (boxed area, arrow). (N) Membrane-bound GFP in adult female brain expressing both Dsx^{F} and Dsx^{M}. Prothoracic contralateral projections (boxed area). (O) UAS-*p35*; *dsx*^{GAL4} adult female brain, supernumerary SN cells (boxed area). (P) UAS-*p35*; *dsx*^{GAL4} adult female VNC, supernumerary TN1 (arrowheads) and TN2 (boxed area) neurons. (Q1-3) UAS-*nLacZ*,-*mCD8::GFP*,-*p35*;*dsx*^{GAL4} adult female prothoracic ganglion (Prg) (Q1) Merged image, co-expression of membrane-bound GFP, green (Q2) and nuclear ßGal, magenta (Q3). Supernumerary TN1 (arrowheads) and TN2 cells (boxed area) and ectopic contralateral projections. Ventral views; anterior up. (C, E, G, I, K, M) anti-GFP, green. (D, F, H, J, L, N, O, P) anti-mCD8, green and neuropil counter-stained with anti-nC82, magenta. Genotypes as per Experimental Procedures. Scale bar = 50 µm Figure modified from Rideout et al. 2010.

In Fru^{M}-null males (expressing Dsx^{M} but lacking Fru^{M}) the number of *dsx*^{GAL4} neurons in *dsx*-pC1, -pC2 and -pC3 were significantly reduced compared with wild-type males (Figure 6.5C-D, P; Table 6.2). This reduction in neuronal numbers causes a consequent diminishment in fascicles in the cervical connection and perhaps also in the contra-lateral commissural connections in the prothoracic ganglion (Figure 6.5F). However there was no observed reduction in *dsx*-TN1, -TN2, or -SN cell numbers (Figure 5.6F-G; Table 6.2). Indeed the observed reduction in the contra-lateral commissural connections may also arise through a diminishment in the Fru^{M}-specified gustatory sensilla in the tarsi of the foreleg, which send projections into the prothoracic neuromere and contribute both to the ispsi- and male-specific contra-lateral ascending fascicles (Mellert et al., 2010; Possidente and Murphey, 1989). Previously there has been a demonstrated reduction in *dsx* cells in the Abg in the absence of Fru^{M} expression (Billeter et al., 2006). In this study the overall cell counts in these animals did not appear significantly different from that seen in wild-type males (P>0.05, n=10; Table 6.2). However as this Fru^{M}-dependent specification of *dsx* cells involves a sub-population of 20 serotonergic neurons organized into 2 bilateral clusters (dorsal and ventral) of 10 cells each (Billeter et al., 2006b), this effect may be so subtle as to be lost in the overall larger Abg cell count of *ca.* 280 neurons. One way of definitively resolving this issue would be to counterstain *dsx*^{GAL4} males deficient for Fru^{M} with anti-5HT and compare the number and organisation of the male-specific serotonergic neuronal clusters in these Abgs with that of wild-type males.

I then looked at the effects on *dsx*^{GAL4} neurons in females expressing Fru^{M}, and found the number of neurons within the brain was not significantly different from wild-type females (Figures 6.5G-H; Table 5.2). However unexpectedly the number of *dsx*^{GAL4} neurons in the *dsx*-Abg cluster was significantly increased to those levels observed in wild-type 2 day old female pupae (Figures 6.5I-J; Table 6.2; *cf.* Table 4.1). This significant increase in the normal adult female neuronal population may be a consequence of *dsx*-expressing neurons present in the female pupa being somehow protected from normal cellular processes such as PCD by the presence of Fru^{M}, and thus remaining extant in the adult (*cf.* Kimura et al., 2005). Alternatively these neurons may reflect the aberrant proliferation of neurons not normally present in the female, essentially male-specific *dsx* neurons, generated by the ectopic expression of Fru^{M}.

In heterozygous *X/X*; *dsx*^{Swe}/*dsx*^{GAL4} flies, where both forms of Dsx are present (endogenous Dsx^{F} from the *dsx*^{GAL4} allele and exogenous Dsx^{M} from the *dsx*^{Swe} allele), the numbers of *dsx*^{GAL4} neurons were significantly increased in *dsx*-pC1, -pC2 and -SN neurons in the brain and all clusters counted in the VNC with a consequent increase in axonal projections and appearance of contralateral commissural connections (Figures 6.5K-N; Table 6.2). However tellingly these cell numbers were still significantly reduced in pC1 and pC2 clusters compared to numbers exhibited in wild-type males (Figure 6.5K; Table 6.2). It has been demonstrated that expression of Dsx^{F} precipitates PCD in ~20 cells of the *fru*-P1 neuronal cluster (Kimura et al., 2008). This cluster represents a sub-population of neurons of the *dsx*-pC1 cluster and, as such, a reduction in overall cell numbers is to be expected. It is reasonable to speculate that this same process of cell death occurs in the pC2 and pC3 clusters. The Abg shows no significant reduction in neuronal numbers in comparison with the level of expression in wild-type female (P>0.05, n=10; Table 6.2). However it is of interest to note that the comparative cell counts in the Abg clusters between *dsx*^{Swe}/*dsx*^{GAL4} females (expressing both Dsx^{F} and Dsx^{M}) and that of males expressing Dsx^{M} but lacking Fru^{M} are not significantly different (P>0.05, n=10; Table 6.2). Indicative that either the absence of Fru^{M} in the males has had some effect towards increasing the neuronal population in the male Abg cluster, or that the competing presence of Dsx^{M} and Dsx^{F} has resulted in a slight reduction of neurons in the female Abg cluster, or perhaps that both these effects are occurring.

As sex-specific PCD has been shown to be responsible for creating dimorphisms in the brain (Kimura et al., 2005; Kimura et al., 2008) I investigated how and when this developmental mechanism might operate in the determination of the *dsx* neural clusters. As shown in Figures 4.3, 4.4H and Table 4.1, *dsx*-SN and -TN2 cells are present in 48 hr female pupae, however in the adult female these cells are absent, implying that these have undergone a process of sex-specific PCD (see Figures 4.3, 4.4J and Table 4.1). As such I assayed dsx^{GAL4} neuronal cell numbers in adult females expressing the cell death inhibitor *p35* (Hay et al., 1994; Zhou et al., 1997) and found that *dsx*-SN and -TN2 cells are indeed protected from PCD, as their numbers were not significantly different from wild-type males (Figures 6.5O-P; Table 6.2). In addition 3 neurons of the *dsx*-TN1 cluster (± 0.4, n=14; Figures 6.5P-Q; Table 6.2) that are never normally apparent in females were also observed. This supernumerary expression of *dsx*-TN1 and -TN2 cells has the added effect of inducing contra-lateral commissural projections not normally present in adult females (Figure 6.5Q). While the *dsx*-Abg cluster shows an increase in neuronal numbers this level is not significantly different from wild-type female expression levels ($P>0.05$, n=10; Table 6.2). In the brain the numbers of cells is significantly increased in the *dsx*-pC2 and -pC3 clusters, though only in -pC3 is this to the level of wild-type males (Figure 6.5O; Table 6.2). The *dsx*-pC1 cluster, like the -Abg, while exhibiting an increased number of neurons is not significantly different from wild-type female expression ($P>0.05$, n=10; Table 6.2). dsx^{GAL4} neuronal cell numbers in adult males expressing the cell death inhibitor *p35* showed no significant change in all clusters and cells in the brain and VNC ($P>0.05$, n=10; data not shown). These preliminary findings suggest that there exists a cell-death program that removes specific dsx^{GAL4}-expressing neurons specifically in the female brain.

It should be noted that no induction of prothoracic contra-lateral projections from gustatory neurons in the foreleg in females expressing Fru^{M} was apparent, while these projections were reduced but still present in males expressing Dsx^{M} but not Fru^{M} (Figure 6.5I and F, respectively). Again in heterozygous *X/X*; dsx^{Swe}/dsx^{GAL4} flies, where both forms of Dsx are present (endogenous Dsx^{F} from the dsx^{GAL4} allele and exogenous Dsx^{M} from the dsx^{Swe} allele) but Fru^{M} is absent, prothoracic contra-lateral projections from gustatory neurons in the foreleg were overtly present (Figure 6.5N). This somewhat contradicts previous findings that determined that Fru^{M} expression (specifically the Fru^{MC} isoform) was necessary to

regulate the midline crossing of projections from gustatory neurons in the foreleg (Mellert et al., 2010). One argument might be that the presence of Dsx^{M} is inducing restoration of some of the contra-lateral projections, as this appears to have also been observed in females possessing the masculine Dsx isoform by Mellert et al. 2010, while the presence of Dsx^{F} may be having the opposite negative regulatory effect on these projections. The projections visualized as Fru^{M}-positive may also, in part, be different to those represented by dsx^{GAL4} expression. However none of these arguments are completely compelling and further investigation is warranted to delineate the necessity of each isoforms for both *fru* and *dsx* in the determination of these prothoracic projections.

Taken altogether, these results demonstrate that Dsx^{M} and Dsx^{F} are the primary regulators of dimorphisms in dsx^{GAL4} neurons, though Fru^{M} function is required to obtain a full complement of male-specific dsx^{GAL4} neurons within the protocerebrum and VNC, and that sex-specific PCD is one mechanism used to assemble this dimorphic neural circuit. Further it can be seen that even small changes in neuronal populations can substantially alter the subsequent neural organization and connectivity of the associated neural projections, and that these changes could provide an anatomical basis for the production of sex-specific behavioural outputs, through the creation, and maintenance, of dimorphic neural circuitry.

6.5 Discussion

As stated Dsx^{M} and Fru^{M} have been shown to co-express in a restricted number of regions in the male CNS (Billeter et al., 2006b; Kimura et al., 2008; Rideout et al., 2007; Rideout et al., 2010). However the dsx^{GAL4} allele has allowed a far more complete and sensitive spatio-temporal survey of this pattern of co-expression to be performed. This survey demonstrated that, while individual *dsx* and *fru* clusters exhibit dynamic levels of expression between early pupal and adult stages, the level of co-expression between Dsx^{M} and Fru^{M} relevant to each particular cluster remains largely the same. The idea that *fru* is involved in the regulation of male neuronal differentiation during metamorphosis is demonstrated by analyses of ectopic Fru^{M} expression in females, expression of specific *fru* isoforms in *fru* mutant backgrounds and is supported by the observation that Fru^{M} expression appears to peak during pupal development (Billeter et al., 2006b; Demir and

Dickson, 2005; Lee et al., 2000; Manoli et al., 2005; Stockinger et al., 2005). That *dsx* has been shown to be expressed earlier than male-specific *fru* transcripts, implies that it may act to specify a neural substrate, a 'canvas' upon which *fru* might act (Billeter et al., 2006a; Lee et al., 2002; Rideout et al., 2007). Again this idea is supported by the demonstrated co-operation between *dsx* and *fru* in the specification and organization to the male-specific serotonergic clusters in the Abg and of a male-specific cluster of Fru^M neurons in the Msg (Billeter et al., 2006b; Rideout et al., 2007). So the apparent persistence in co-expression of Dsx^M and Fru^M in these restricted neuronal clusters is of significance as it implies that expression in these neurons is important both in the specification of the male nervous system as it undergoes metamorphosis during the pupal stage, from that which regulates and maintains larval behavioural outputs to that of the mature adult, and the maintenance of this male-specific neural circuitry thereafter. Indeed 24 hours into pupariation has been shown to be critical in the final determination of the adult males neural circuitry, especially with respect to sex-specific behaviours (Arthur et al., 1998; Belote and Baker, 1987).

This cooperation between *dsx* and *fru* was again demonstrated by their mutual contributions towards the sculpting of the male-, and female-, specific neural architecture. Dsx^M and Dsx^F demonstrably the primary regulators in the specification of the *dsx* dimorphic neuronal populations, which in turn engender a dimorphic pattern of projections and associated connectivity within the CNS of each sex. However Fru^M was still required to obtain and maintain the full complement of male-specific neurons within the protocerebrum and, perhaps, the Abg.

However this survey of *dsx* and *fru* co-expression in the adult male goes beyond merely topographic description of the *dsx*/*fru* neuronal expression and the consequent neural architecture that is created. The overlap between *fru*- and *dsx*-expressing neurons in the male CNS allows the assignation of functions (or at least functional involvement) to certain *dsx* neurons due to their intersection with *fru* neurons with known, or suspected, roles in male sexual behaviour. In the interim this mapping has allowed me to identify the association of specific individual dsx^{GAL4} neurons and neuronal clusters with *fru* clonal groups, which along with along with evidentiary analyses gained form gynadramorph studies and the use of other transgenic tools, provides a greater understanding of the

relationship that these neurons have to each other and to the surrounding neural substrates and, by corollary, a greater understanding of how the *dsx*-specified neural circuit therefore integrates into the overall male-specific neural architecture. In the protocerebrum gynadromorph studies have identified the areas containing the dsx^{GAL4}neurons as being involved in such processes as initiation, following tapping, wing extension and copulatory behaviours. Latterly clonal analyses has allowed me to associate the neural clusters with involvement in higher order processing of multi-modal sensory stimuli inputs, specifically the auditory, visual and olfactory circuitry. This circuitry essential, acting both individually and in concert, for the initiation of courtship via the reception and processing of differing sensory inputs (which may themselves be sex-specific) and for the assurance of the continuation of courtship through coordination of the sequential behavioural steps, culminating in successful copulation.

Within the VNC the assignation of potential roles via intersection of *dsx*- and *fru*-expressing cells was aided by the restricted nature of dsx^{GAL4} neuronal expression, even when considering the added complexity of the neuronal architecture engendered by the presence of male-specific *dsx*-neurons. Again dsx^{GAL4} neurons appear to be expressed in areas that gynandromorph studies have identified as possessing foci associated with tapping, wing extension, courtship song and with copulatory behaviours. However assignation of potential functional roles was complicated by the far more diffuse topographical positioning of *fru* neurons, exemplified by the original neuronal cluster designations (i.e. PrMS, MsMt, MtAbg and Abg; Lee et al., 2000) and the less definitive nature of the clonal analyses performed in the VNC by recent studies. Added complexity arises from the multiplicity of potential inputs, such as from the foreleg tarsi where gustatory neurons send projections to synapse on localized interneurons within these regions as well as sending projections to higher centers in the brain (Mellert et al., 2010; Rideout et al., 2010) and outputs, both sex-specific (e.g., genitalia) and non-sex-specific (e.g., direct flight muscles controlling the wings). Though again it should be remembered that even these latter non-sex-specific motor tissues can also be controlled to render sex-specific behavioural outputs, such as with the generation of male-specific courtship song. Again further complexity is added by the dimorphic pattern of expression of these projections, as in the axons originating from the tarsi of the foreleg, which in male project both contra- and ipsi-laterally, whereas in females the pattern is restricted to ipsi-lateral projections

(Mellert et al., 2010; Possidente and Murphey, 1989; Rideout et al., 2010; Wang et al., 2004). Overall however the neurons of the Prg and Msg may be reasonably associated with transmission and processing of stimulatory inputs for the gustatory circuit and the subsequent regulation of higher order signals resulting in generation of unilateral wing extension and song production (Koganezawa et al., 2010; von Philipsborn et al., 2011). The latter behaviours, arising from multi-modal cues generated via a target female's rapidly changing position, are by necessity extremely sensitive and highly reactive (Dornan and Goodwin, 2008; Koganezawa et al., 2010; Tauber and Eberl, 2001a). The description of the neural circuits potentially involved in the generation of behaviours calls to mind classical models of positive/negative loop feedback circuits. These behaviours do not just require the generation of a motor output from the wing ipsi-lateral to the target but also the assurance that no motor output will be generated on the corresponding contra-lateral side; this almost certainly arises from stimulatory and inhibitory inputs which act on, and through, discrete bilateral neural pathways, but also involves communication between the two corresponding paths resulting in the coordination of positive and negative stimuli to orchestrate which is the active and which the passive wing (Dornan and Goodwin, 2008; Koganezawa et al., 2010). Again supporting evidence for this model of reciprocal excitatory/inhibitory signalling to modulate the courtship behaviour has been demonstrated in the silk moth Bombyx mori, involving exposure of the left and right antennae to transient pheromonal cues (Kanzaki et al., 1994).

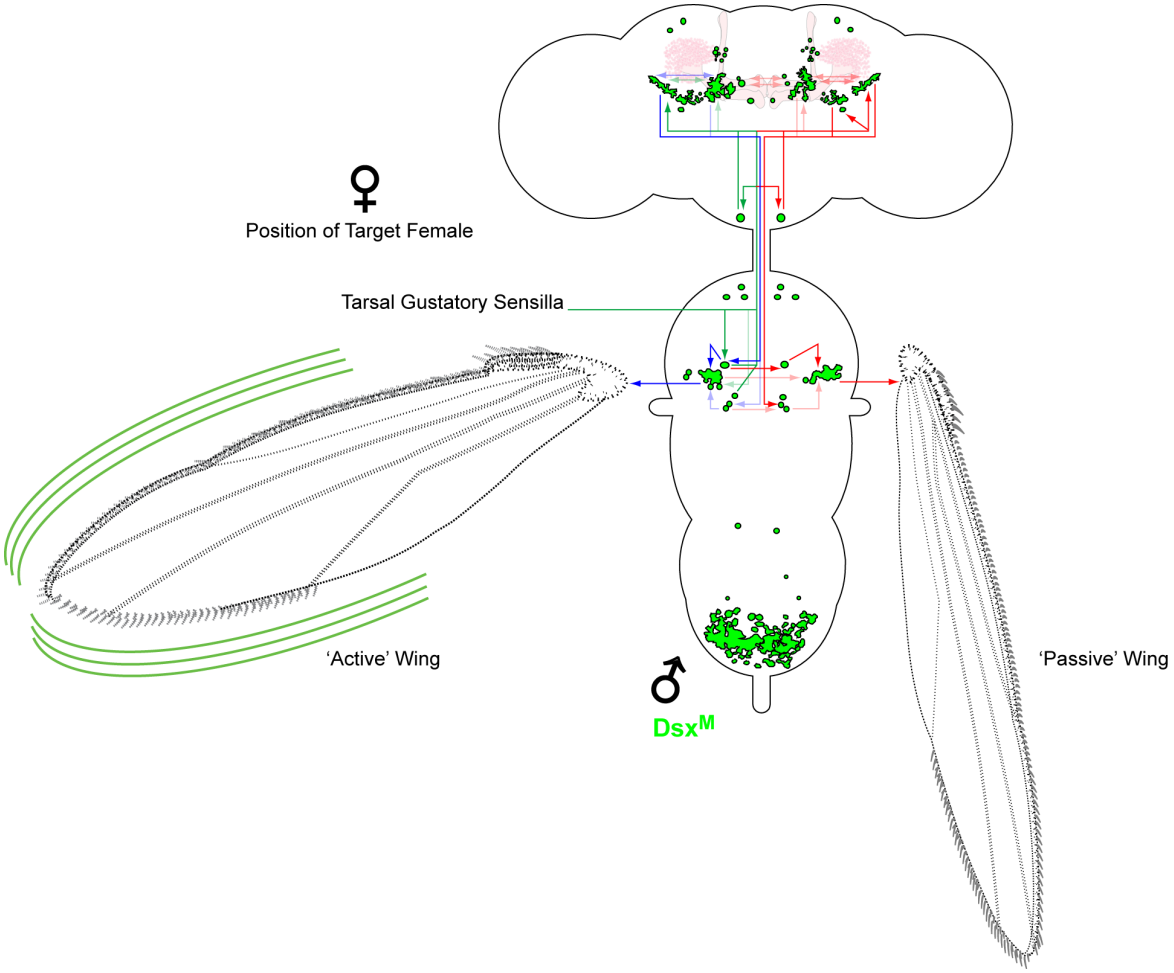

Figure 6-6 Schematic of the potential *dsx*^{GAL4} circuitry involved in generating unilateral wing extension in the adult male in response to non-pheromonal tarsal gustatory inputs received through sensilla in the foreleg.
Target female on the left. Sensory inputs from the tarsal sensilla to localised interneurons and ascending positive stimuli signals to higher order neural clusters indicated by green lines. Descending excitatory response signals to interneurons and then to motor effector tissues on 'active' wing side indicated by blue lines. Ascending and descending inhibitory signals repressing motor output on 'passive' wing side indicated by red lines. Polarity of projections indicated by arrowheads. Transparent lines represent potential connections, which are not considered as likely to transmit excitatory/inhibitory signals. Dsx^{M} neural clusters in green.

Finally the level of *dsx*^{GAL4} expression within the Abg with the associated projections, both descending to the internal and external genitalia and ascending to the protocerebrum (with presumably the reverse polarity circuitry also in place), speaks to the involvement of these neurons in copulatory behaviours.

The evidential information derived from the intersection of *fru* neurons and neuronal clusters of defined function with *dsx*^{GAL4}-expressing neurons allows a reasonable level of insight into what behaviours these neurons might impinge. Specifically, males in which the activity of these neurons are impaired would be predicted to present with aberrant behavioural phenotypes related to latency (the time it takes to initiate courtship) and the proper co-ordination and expression of any subsequent steps; again with emphasis on tapping; wing extension and song

generation; and finally, copulatory behaviours. As greater amounts of clonal analyses and fine circuit mapping become available, this, coupled with other tools such intersectional reagents, will allow more restricted analyses of individual regions and neuronal clusters, providing more definitive understanding of the *'co-operative'* nature of *dsx* and *fru* expression in determining the underlying male-specific neural substrates and the associated individual neurons and neural clusters that serve to generate distinct behavioural outputs.

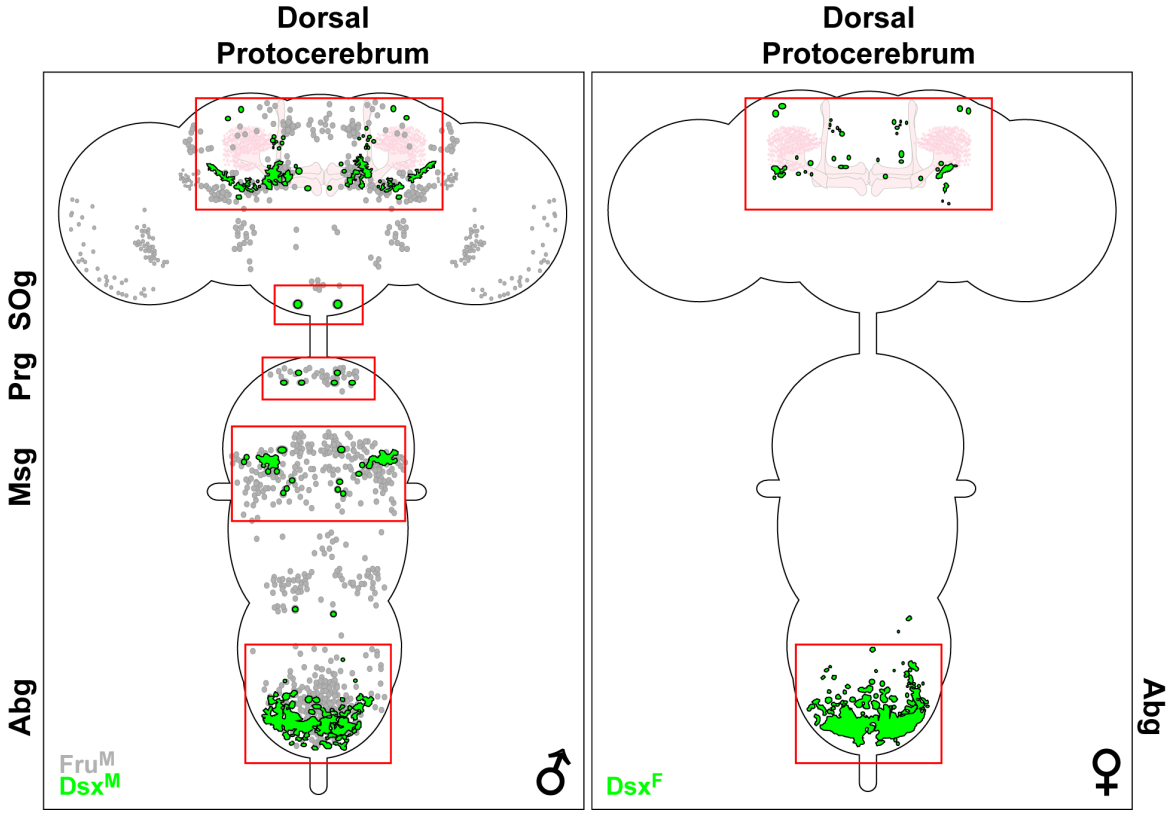

Figure 6-7 Schematic representation of the expression of Fru^M with Dsx^M in males and Dsx^F alone in females in the adult CNS.
Fru^M neuronal clusters in grey. Dsx^M and Dsx^F clusters in green. Red boxes highlight specific areas in the male and female CNSs in which behavioural foci have been localized.

One final and important point needs be re-emphasised. *fru* expression in adults is restricted to the male (Figure 6.7). While the expression of fru^{GAL4} demonstrates that much of what might be described as the 'male-specific *fru* neural circuitry' is present within the female as well, expression of Fru^M in these neurons is necessary for the specification of male-specific courtship behavioural outputs (Demir and Dickson, 2005). Though this (as has been previously stated) is not sufficient, requiring *dsx* expression to sculpt the associated male neural circuitry and the presence of Dsx^M to assure a complete male-behavioural repertoire (Kimura et al., 2008; Rideout et al., 2007; Rideout et al., 2010). *dsx* however is endogenously expressed in both the adult female as well as the male.

In the female CNS *dsx*-expressing neuronal clusters have been localized to areas in the protocerebrum and Abg implicated by gynandromorph studies to contain foci involved in receptivity and copulatory behaviours (Figure 6.7). Thus it would seem not unreasonable to predict that, in the female, functional analyses would demonstrate that female-specific behavioural outputs would be sub-served by the Dsx^{F} specified dimorphic neural architecture in a manner analogous to that of the Dsx^{M}/Fru^{M} specified circuitry regulating male-specific behavioural outputs. The following chapter will apply behavioural analyses to determine if the dsx^{GAL4} neurons and neuronal clusters (both male and female) are required for the specification of sex-specific behaviours, and if these are the behavioural outputs predicted by the findings of previous studies and the inferences drawn by the investigations within this study.

7 Characterisation of *dsx*^{GAL4}'s ability to direct distinct behavioural outputs in both males and females

dsx mutant males are known to display aberrant courtship behaviours (McRobert and Tompkins, 1985; Villella and Hall, 1996; Waterbury et al., 1999; Rideout et al., 2007); however, the anatomical or neurobiological basis for the anomolous behaviour is unknown. Changes in normal development during sexual differentiation of both neuronal and non-neuronal tissues likely play roles in generating these aberrant phenotypes. I have shown that *dsx* is required in the assembly of sexually dimorphic neural architecture in males and females and that it is likely that these *dsx*-specified dimorphic neural substrates are involved in the reception and higher-order processing of stimuli, and in turn direct male and female behavioural outputs. However I have also shown that dsx^{GAL4} is expressed in both sexes in somatic tissues that are likely to be necessary for the successful completion of sexually dimorphic behaviours. So there remains the question, do *dsx*-expressing neurons play direct roles in the generation of sex-specific courtship behaviours?

In order to determine this I, in conjunction with Drs. Megan Neville and Elizabeth Rideout, performed a series of behavioural assays on both male and female dsx^{GAL4} flies. However as the results for individual behavioural experiments are really only meaningful when considered in concert and, as many assays were conducted as a joint effort, the experiments presented within this chapter must, as a necessity, reflect the work performed not only by myself, but by my colleagues Megan Neville and Elizabeth Rideout and will in large part be presented as per our paper, Rideout et al., 2010.

Expressing the tetanus neurotoxin light chain (TNT) in dsx^{GAL4} cells disrupted synaptic activity in *dsx*-expressing neurons by acting specifically on neuronal synaptobrevin (n-Syb) (Sweeney et al., 1995). However given the previously demonstrated expression of dsx^{GAL4} in a variety of tissues outside the nervous system it was also necessary to determine whether any aberrant behaviours exhibited by *UAS-*TNT_G; dsx^{GAL4} animals occurred as a direct consequence of disrupting neuronal function, or if some physiological impairment was also a factor. To verify the neural specificity of any observed behavioural defects, we also used *elav-GAL80* (a kind gift from S. Sweeney) to inhibit GAL4-driven expression of TNT specifically in neurons. *elav-GAL80* targets expression of the GAL4 inhibitor GAL80 specifically to postmitotic neurons using the *elav*

promoter thereby allowing us to determine if any observed behavioural deficit arose through a specific neural aetiology for (Lee and Luo, 1999). This intersectional tool has been validated by examining *dsx*^{GAL4}-nuclear GFP expression in neuronal and non-neuronal tissues in the presence of *elav-GAL80* demonstrating that marker expression is indeed comprehensively suppressed throughout the nervous system (see Figure 4.13) (Rideout et al., 2010).

7.1 Courtship deficits in *dsx*^{GAL4} flies expressing tetanus toxin are not a result of defects in sensorimotor function

In order to demonstrate conclusively that any courtship defects observed in *dsx*^{GAL4} males and females expressing TNT were neural in aetiology and arose as a direct consequence of impairing *dsx*^{GAL4} neuronal function, it was first necessary to establish that they did not arise as a result of more general defects in morphology or sensorimotor function. As such we examined the genitalia and reproductive systems, including neuronal innervation, in *UAS-TNT*$_G$; *dsx*^{GAL4} males and females and established that they did not exhibit any gross anatomical abnormalities (data not shown). We also demonstrated that these animals performed at least as well as wild-type and control flies in locomotion (Kulkarni and Hall, 1987), flight (Benzer, 1973; Elkins et al., 1986), olfaction (Mackay et al., 1996) and taste assays (Gordesky-Gold et al., 2008) (Figure 7.1) (Rideout et al., 2010). Each of these assays is of importance in ensuring that no physical, or physiological, impairment underlies any observed deficit in courtship behaviours. They demonstrate simply that the test flies have the physical capability to engage in courtship behaviours; that is they can orientate and follow, decide to fight or escape; they can assay both volatile and non-volatile cues; and, as the direct flight muscles are also used for the generation of courtship song (Rideout et al., 2007), in the case of the male they can sing. Finally we ascertained that no overt differences are apparent in the cuticular hydrocarbon profiles for either males or females expressing *dsx*^{GAL4} alone or driving expression of the GAL4 responsive transgene *UAS-TNTg* (Sweeney et al., 1995) and therefore no disruption to the pheromonal signature of individuals had occurred (J.-C. Billeter, pers. comm).

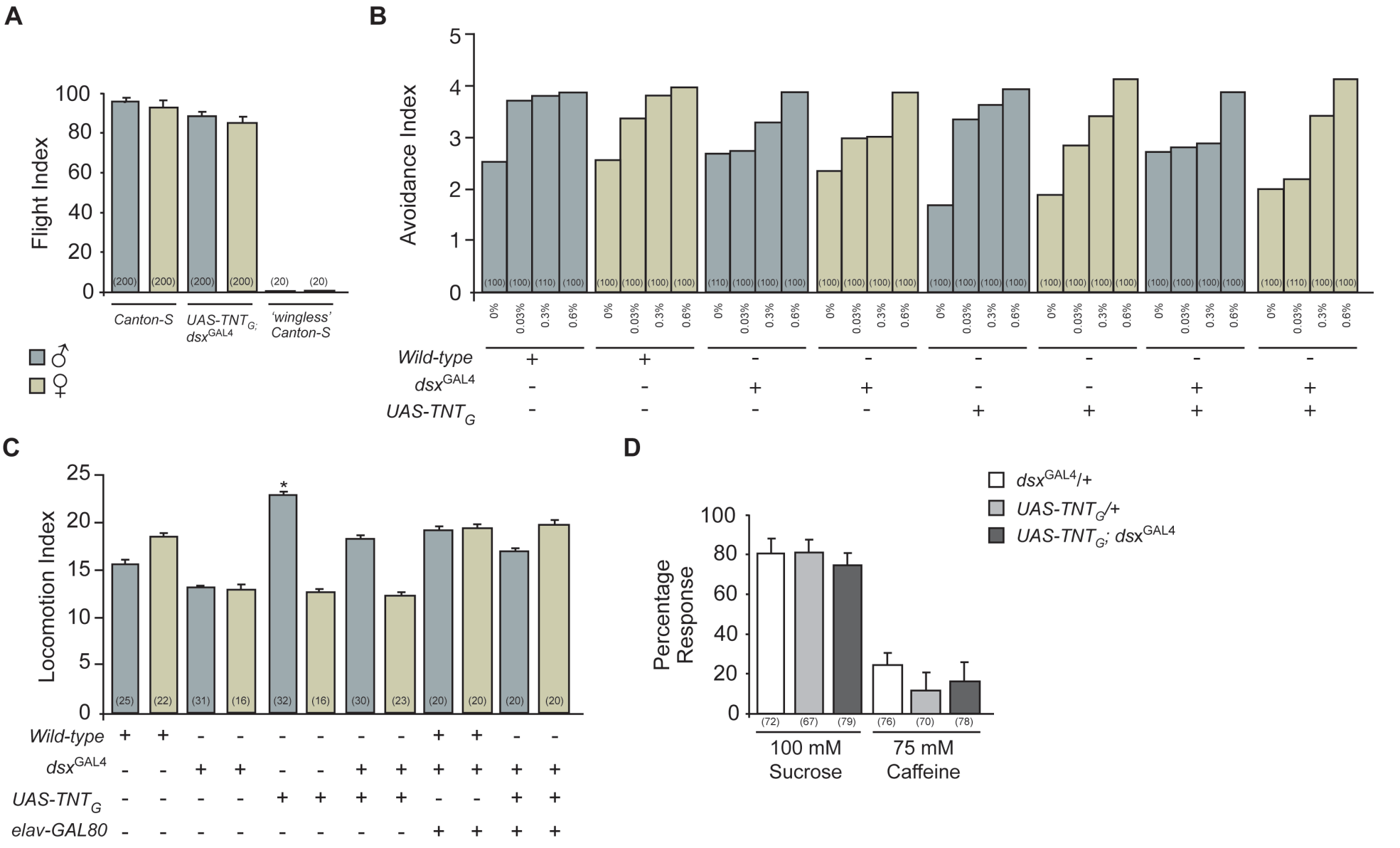
A
Flight Index
100
80
60
40
20
0
(200)
(200)
(200)
(200)
(20)
(20)
Canton-S
UAS-TNT$_G$; dsx^{GAL4}
'wingless' Canton-S
♂
♀
B
Avoidance Index
5
4
3
2
1
0
0%
0.03%
0.3%
0.6%
Wild-type
dsx^{GAL4}
UAS-TNT$_G$
C
Locomotion Index
25
20
15
10
5
0
*
(25)
(22)
(31)
(16)
(32)
(16)
(30)
(23)
(20)
(20)
(20)
(20)
Wild-type
dsx^{GAL4}
UAS-TNT$_G$
elav-GAL80
D
Percentage Response
100
80
60
40
20
0
(72)
(67)
(79)
(76)
(70)
(78)
100 mM Sucrose
75 mM Caffeine
dsx^{GAL4}/+
UAS-TNT$_G$/+
UAS-TNT$_G$; dsx^{GAL4}

Figure 7-1 General sensorimotor behavioural assays performed on *UAS-TNT*$_G$; *dsx*^{GAL4}, control and wild-type male and female adult flies.
(A) Flight tests measuring the percentage of flies able to fly as per Benzer, 1973. Tests were performed on groups of 20 flies, 10 replicates per genotype. Wild-type 'dewinged' flies used as a flightless control. (B) Odour avoidance olfactory assay performed as per Anholt et al., 1996. All genotypes behaved as well as control flies between the baseline (0%) and higher assay (0.6%), *P*<0.0001. Number of replicate scores for a given genotype in parentheses. (C) Locomotor activity measured as the number of line crossings per minute during a 10 minute recording interval as per Kulkarni and Hall, 1987. Asterisk indicates significant difference *P*>0.005. (D) Probosis extension reflex (PER) taste assay performed on males and females with both 100 mM Sucrose and 100 mM Sucrose + 75 mM Caffeine as per Gordesky-Gold et al., 2008. A '+' indicates the presence of a wild-type or transgenic chromosome. Mean ± SEM. n's in parentheses. Figure as per Rideout et al., 2010.

7.2 *dsx*^{GAL4} neurons are required for male sexual behaviours

As stated, having demonstrated *dsx*'s requirement in the assembly of sex-specific neural substrates, we asked whether the *dsx*-expressing neurons are directly involved in the generation of male courtship behaviours? To this end we specifically disrupted synaptic activity in *dsx*^{GAL4} neurons by expressing TNT (Sweeney et al., 1995) and found *UAS-TNT*$_G$; *dsx*^{GAL4} males to be completely infertile (n=60; Figure 7.2A) (Rideout et al., 2010). A more detailed investigation of these males determined this disruption in fertility was a consequence of defects in courtship and mating. The time to initiate courtship by *UAS-TNT*$_G$; *dsx*^{GAL4} males was significantly increased (Figure 7.2B) and, once initiated, courtship was severely diminished (Figure 7.2C) with a courtship index (CI) in *UAS-TNT*$_G$; *dsx*^{GAL4} males of 8.1 ± 2.1, compared to 85.1 ± 5.5, 91.8 ± 2.4 and 89.7 ± 3.3 for *UAS-TNT*$_G$ or *dsx*^{GAL4} alone or wild-type control males respectively. Unlike ~95% of controls, no *UAS-TNT*$_G$; *dsx*^{GAL4} males copulated in 4 hrs of observation (Figure 7.2D) (Rideout et al., 2010). Again it should be emphasised that these defects are not due to general sensorimotor defects, as *UAS-TNT*$_G$; *dsx*^{GAL4} males exhibited no gross abnormalities in genitalia or reproductive system, including their neuronal innervations, and performed as well as controls in locomotion, olfaction and taste assays (Figure 7.1B-D) (Rideout et al., 2010).

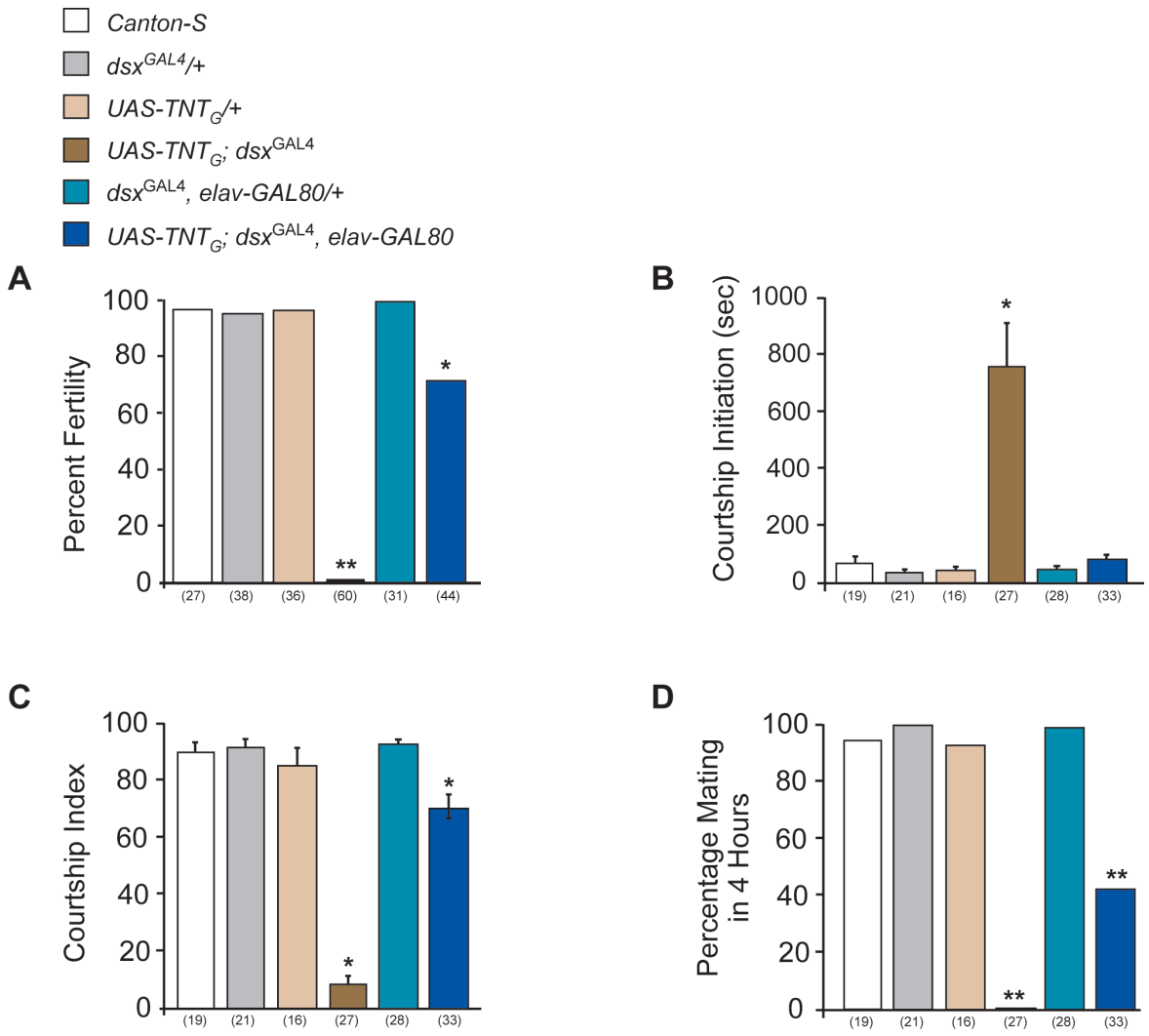

Figure 7-2 *dsx*^{GAL4} neurons control male sexual behaviour.
(A) Male fertility (P*<0.05, ***P*<0.0001, Fisher exact test). (B) Courtship initiation (mean ± SEM, **P*<0.05, Tukey-Kramer HSD statistical test). (C) Courtship index (mean ± SEM, **P*<0.05, Tukey-Kramer HSD test). (D) Percentage males mating in 4 hr (mean ± SEM, ***P*<0.0001, Fisher exact test). Genotypes indicate males. Target females were wild-type. n values are shown in parentheses. Figure modified from Rideout et al., 2010.**

The observed courtship behaviours in *UAS-TNT*$_G$; *dsx*^{GAL4} males consisted entirely of brief intermittent bouts of orientation and following. Conspicuously these males showed no wing extension, with a consequent complete absence of both sine- and pulse-song components of courtship song (Figure 7.3B) (Rideout et al., 2010). Again this defect is specific to courtship as these males are normal for flight, indicative that the direct flight muscles used for generating courtship song are still functional (Figure 7.1A) (Rideout et al., 2007; Rideout et al., 2010).

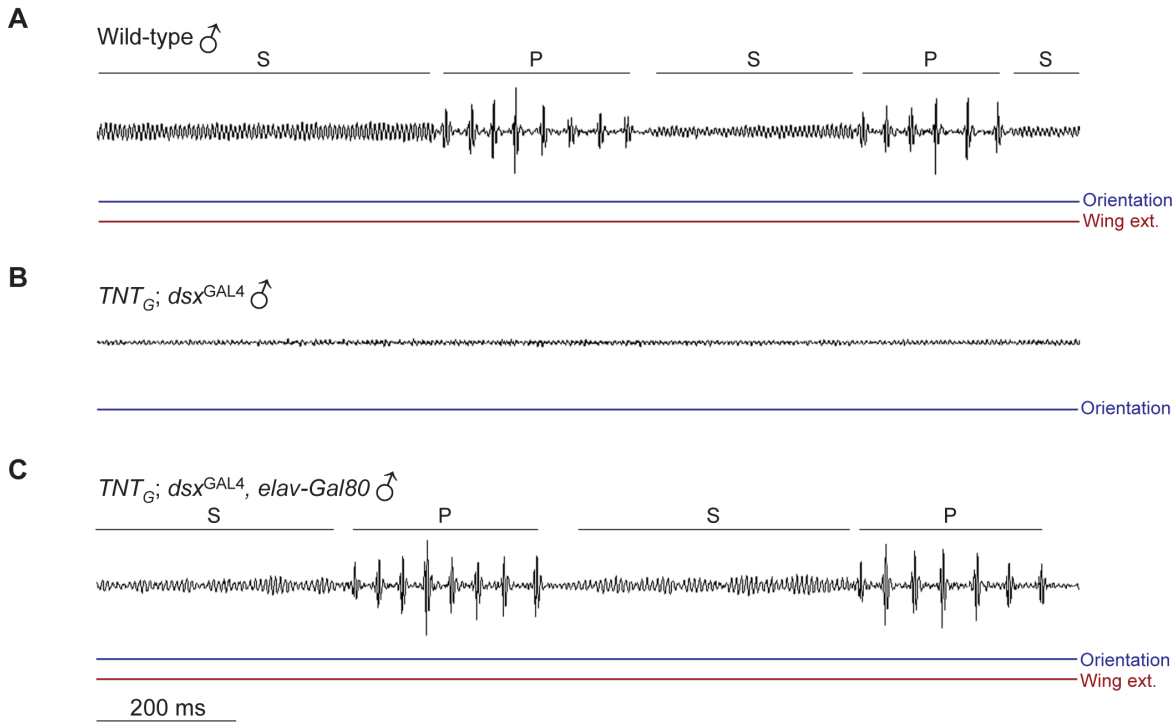

Figure 7-3 *dsx*^{GAL4} neurons control male courtship song output.
(A-C) Song recording traces for 5 - 7 D old (A) wild-type, (B) *UAS-TNT*$_G$; *dsx*^{GAL4} and (C) *UAS-TNT*$_G$; *elav*-GAL80, *dsx*^{GAL4} males. Pulse (P) and sine (S) song components are indicated above traces and courtship is shown below. Each trace represents a fraction of a 10-min recording. Scale bar represents 200 ms. Genotypes indicate males. Target females were wild-type. For 15 wild-type males, there were 18.6 ± 2.2 sine bouts per min, 19.9 ± 1.4 pulse trains per min, 8.1 ± 0.3 mean pulses per train and a 31.7 ± 3.0 ms interpulse interval. For 10 *UAS-TNT*$_G$; *dsx*^{GAL4} males, there was no recordable data. For 10 *UAS-TNT*$_G$; *elav*-GAL80, *dsx*^{GAL4} males, there were 18.4 ± 1.5 sine bouts per min, 26.6 ± 3.8 pulse trains per min, 10.0 ± 0.4 mean pulses per train and a 34.0 ± 0.4 ms interpulse interval. Figure modified from Rideout et al., 2010.

Given the demonstrated expression of *dsx*^{GAL4} in a variety of tissues outside the nervous system we verified that the observed aberrant courtship behaviour in *UAS-TNT*$_G$; *dsx*^{GAL4} males was a direct result of disrupted neuronal function using *elav-GAL80* to specifically inhibit GAL4-driven expression of TNT in neurons. Males expressing *UAS-TNT*$_G$; *elav*-GAL80, *dsx*^{GAL4} showed greatly improved levels of fertility (Figure 7.2A), courtship initiation (Figure 7.2B), and a significant recovery in CI's (with consequent restoration of courtship modalities such as licking, tapping and wing extension) when compared to *UAS-TNT*$_G$; *dsx*^{GAL4} males (Figure 7.2C) (Rideout et al., 2010). The percentage of males copulating within 4 hrs was also significantly improved in *elav-GAL80* males (Figure 7.2D), as was the ability to generate the sine and pulse components of courtship song (Figure 7.3C) (Rideout et al., 2010). These results confirming the neuronal aetiology of the observed *UAS-TNT*$_G$; *dsx*^{GAL4} male's aberrant courtship behaviour. It should be noted that not all behaviours have been restored to control levels; this most likely

reflects the dynamics of GAL80's ability to fully repress GAL4 function. However, the possibility that TNT expression is affecting some non-neuronal *dsx*^{GAL4} cells cannot be completely ruled out.

Thus inhibition of *dsx*^{GAL4} neuronal function in males leads to disruption of the early steps of courtship (orientation, following) and the complete absence of the later steps (wing extension, courtship song and attempted copulation), resulting in complete behavioural sterility in these animals, suggesting that *dsx* neurons are directly and specifically contributing to male courtship behaviours. Collectively, these results demonstrate that *dsx*^{GAL4} neurons play a critical role in generating male courtship behaviours. That this disruption of function of the ~640 *dsx*^{GAL4} neurons within the CNS comprising the *dsx* male neural architecture (of which only a subset, 7%, are shared with the ~2000 neurons of the more extensive Fru^{M} neural substrate) so effectively leads to suppression of male courtship behaviours allows us to define a far more minimal neural substrate necessary to specify these male-specific behavioural outputs.

7.3 *dsx*^{GAL4} neurons are critical for female sexual behaviours

Compared with males the neurobiological basis of female sexual behaviour is poorly defined, though it has been suggested that *dsx*'s influence on the sex of the nervous system might be critical to female behaviour (Waterbury et al., 1999). As we have now demonstrated that *dsx*^{GAL4} neurons are expressed in female-specific, as well as male-specific, neural architecture in the CNS, we investigated the effects on female behaviour of disrupting *dsx*^{GAL4} neuronal function through expression of TNT (Figure 7.4) (Rideout et al., 2010). We also used *elav-GAL80* to restrict expression of TNT exclusively to non-neuronal tissues to confirm the neuronal contribution of *dsx*^{GAL4} cells to direct female sexual behaviour.

UAS-TNT$_{G}$; *dsx*^{GAL4} females were completely infertile (Figure 7.4A) (Rideout et al., 2010). Significantly, unlike successfully mated wild-type females in which oviposition and egg deposition is markedly increased or even mature virgin females who will deposit a number of eggs over a period of several days, these females laid no eggs at all over five consecutive days post-mating (Figure 7.4B) (Rideout et al., 2010). The abdomens of these *UAS-TNT*$_{G}$; *dsx*^{GAL4} females

became noticeably distended over time with permanently extruded ovipositors (Figure 7.5A), and all test subjects dissected were found to have mature eggs atrophying in their oviducts (n>35; Figure 7.5B) (Rideout et al., 2010).

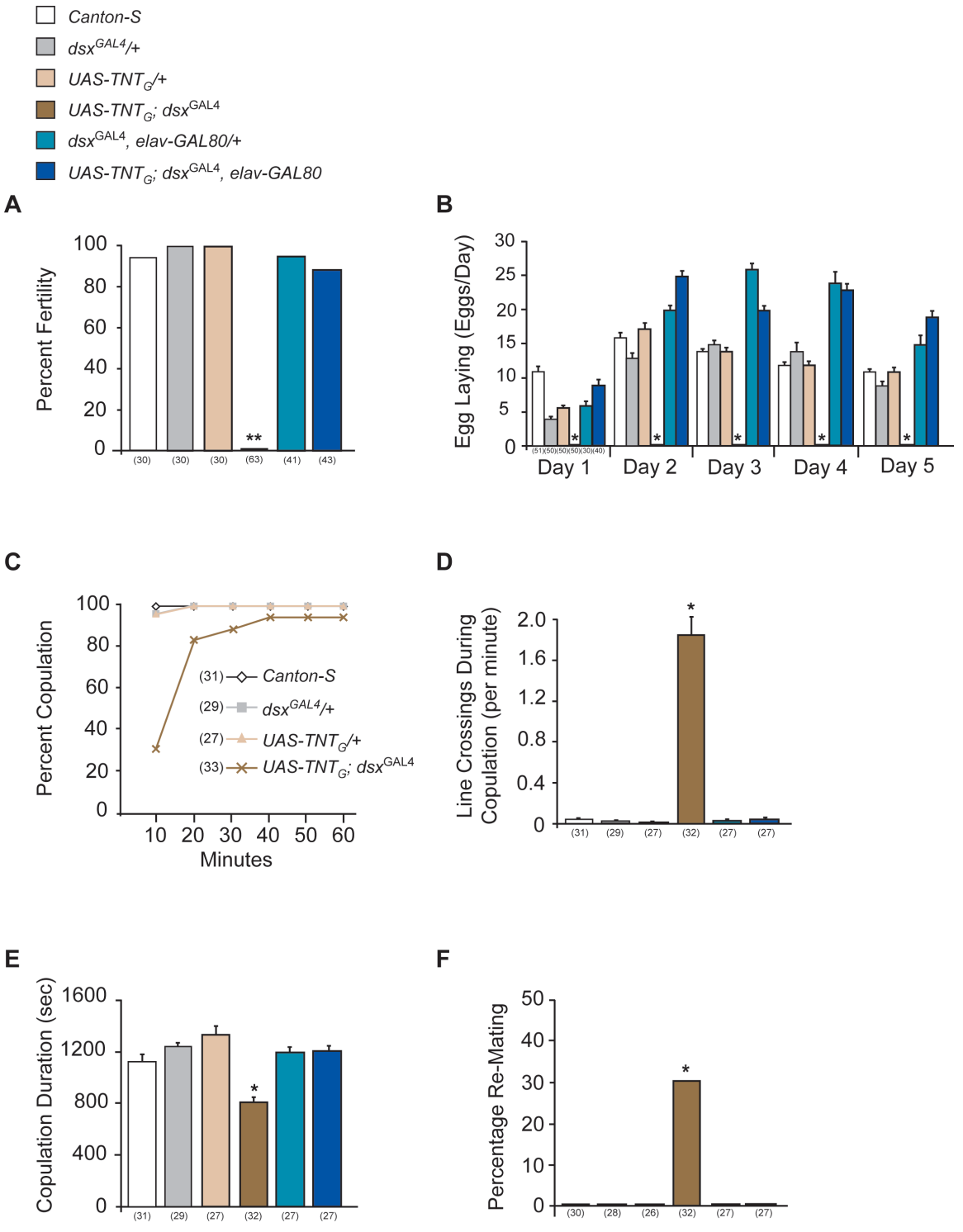

Figure 7-4 *dsx*^{GAL4} neurons control female sexual behaviour.
(A) Female fertility (*P*<0.0001, Fisher exact test). (B) Egg-laying (mean ± SEM, **P*<0.0001, Dunnett's test). (C) Percent copulation over time (10 min intervals over a 1 hr period). (D) Line crossings during copulation (mean ± SEM, **P*<0.05, Tukey-Kramer HSD test). (E) Copulation duration (mean ± SEM, **P*<0.05, Tukey-Kramer HSD test). (F) Percentage females re-mating with the same male in 4 hr period (**P*<0.05, Tukey-Kramer HSD test). Genotypes indicate females. Target males were wild-type. n values are shown in parentheses. Figure modified from Rideout et al., 2010.**

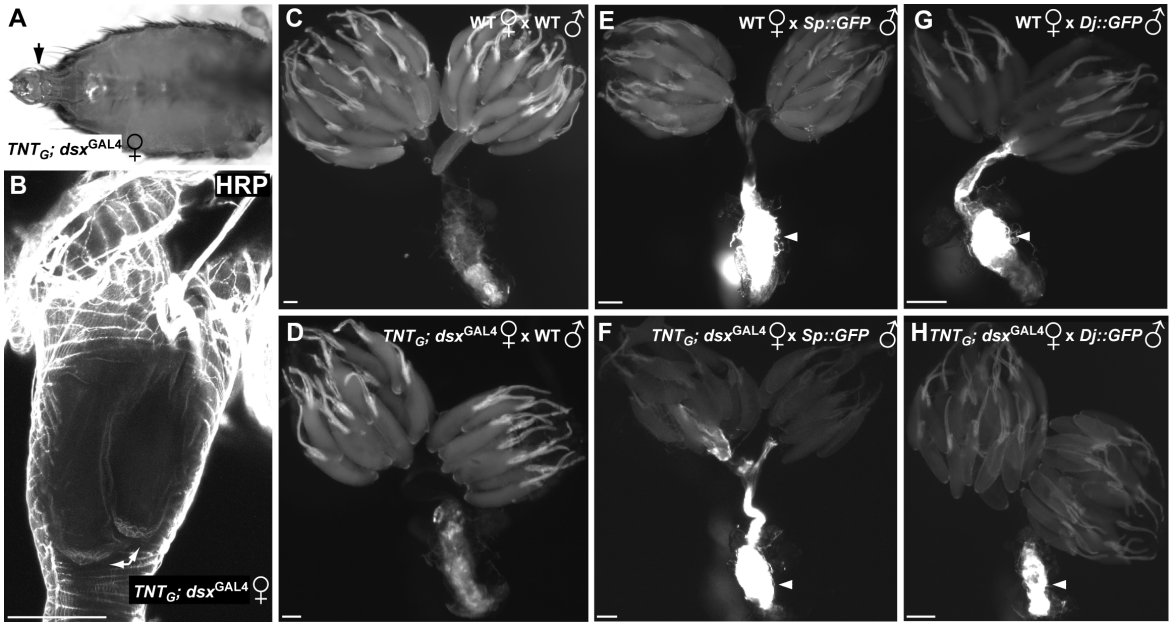

Figure 7-5 Assay of reproductive function and sperm and seminal fluid transfer in *UAS-TNTG*; *dsx*^{GAL4} females.
(A) Whole-mount image 5 day old *UAS-TNTG*; *dsx*^{GAL4} female abdomen exhibiting extruded ovipositor (arrow). (B) 5 day old *UAS-TNTG*; *dsx*^{GAL4} female, detail of common oviduct containing two atrophying mature eggs (arrows) (n>35). (C-H) Whole-mount images of ovaries dissected within 15 min after target female mated with either wild-type (WT), or *Sp*::GFP (GFP fused to Sex-peptide), or *Dj*::GFP (GFP fused to sperm) genotype males. (C) Ovaries of WT female mated to control WT male exhibiting background epifluorescence levels. (D) Ovaries of *UAS-TNTG*; *dsx*^{GAL4} female mated to control WT male exhibiting background epifluorescence levels. (E) Ovaries of WT female mated to *Sp*::GFP male. (F) Ovaries of UAS-*TNTG*; *dsx*^{GAL4} female mated to *Sp*::GFP male. (G) Ovaries of WT female mated to Dj::GFP male. (H) Ovaries of *UAS-TNTG*; *dsx*^{GAL4} female mated to Dj::GFP male. Arrowheads indicate GFP-positive female reproductive tracts, fluorescence demonstrating seminal fluid transfer. Scale bar = 100 µm. Figure as per Rideout et al., 2010.

During a 1hr period, virgin *UAS-TNT*$_G$; *dsx*^{GAL4} females were observed to be less receptive within the first 10 minutes; however, by 40 minutes the percentage of *dsx*^{GAL4} females expressing TNT that had copulated was near control levels (>93% vs. 100%; Figure 7.4C) (Rideout et al., 2010). Though this appears more a testament to the persistence of the courting wild-type male than any increased receptivity of the *UAS-TNT*$_G$; *dsx*^{GAL4} target females (see Supplementary Video 3, Rideout et al., 2010). In depth observation of the copulatory behaviour of *UAS-TNT*$_G$; *dsx*^{GAL4} females showed a complete lack of any receptive response; these females apparently actively rebuffing wild-type males throughout copulation, through sustained wing flicks, kicking, and a failure to remain stationary (see Supplementary Video 3, Rideout et al., 2010). Although males often managed to grasp hold of a female they never managed to spread the female's wings during copulation (see Supplementary Video 3, Rideout et al., 2010). The result of this aberrant copulation with *UAS-TNT*$_G$; *dsx*^{GAL4} females is a dramatic increase in locomotion of copulating pairs (Figure 7.4D; see Supplementary Video 3, Rideout

et al., 2010), and a significant decrease in copulation duration, presumably a consequence of the vigorous rejection displayed by these females (Figure 7.4E). Intriguingly, during a 4hr observation period, approximately 30% of *UAS-TNT*$_G$; *dsx*^{GAL4} females re-mated with the same male, some as many as four times (Figure 7.4F); control females never re-mated (Rideout et al., 2010).

The observed infertility was not failure to transfer sperm during the shorter copulation time, as *UAS-TNT*$_G$; *dsx*^{GAL4} females exhibited GFP-positive reproductive tracts when mated to males carrying the sperm-enriched mitochondrial marker Don Juan-GFP (Santel et al., 1997) (Figures 7.5F) (Rideout et al., 2010). Similarly seminal fluid transfer, required for post-mating rejection responses, was confirmed using a transgene encoding the accessory gland protein Sex-Peptide (Sp) fused to GFP (Figures 7.5H) (Rideout et al., 2010; Villella et al., 2006). Importantly no “live births” were observed, suggesting that this infertility is due to an inability to ovulate eggs into the uterus, preventing sperm, stored in the seminal receptacle and spermathecae, to penetrate through the egg’s micropyle and fertilize the embryo (Miller, 1950). Again it should be emphasised that these defects are not due to general sensorimotor defects, as *UAS-TNT*$_G$; *dsx*^{GAL4} females exhibited no gross abnormalities in genitalia or reproductive system, including their neuronal innervations (data not shown), and performed as well as controls in locomotion, flight, olfaction and taste assays (Figure 7.1) (Rideout et al., 2010).

To understand the observed unusual re-mating phenotype, we compared post-mating responses in mated *UAS-TNT*$_G$; *dsx*^{GAL4} females against mated control females, retesting for receptivity 24hrs post-copulation with a second naïve male. During a 1hr observation period 69% of mated *UAS-TNT*$_G$; *dsx*^{GAL4} females remated (n=13), in contrast to 0% of mated control females (n=14) (Rideout et al., 2010). In addition, mated *UAS-TNT*$_G$; *dsx*^{GAL4} females continued to elicit vigorous courtship (CI= 82.4% ± 4.4) compared to mated control females (CI=28.4% ± 6) (Rideout et al., 2010). The increased remating frequency observed with *UAS-TNT*$_G$; *dsx*^{GAL4} females may be accounted for by a failure to suppress wild-type male courtship behaviours.

To confirm that the observed infertility and courtship defects were due to disruption of *dsx*^{GAL4} neurons, we again used *elav-GAL80* to inhibit GAL4-driven

expression of TNT in the nervous system. Fertility and egg laying in *UAS-TNT*$_G$; *elav*-GAL80, *dsx*^{GAL4} females was restored to levels not significantly different from controls (Figure 7.4A-B) (Rideout et al., 2010). Similarly, locomotion during copulation, copulation duration, and re-mating after copulation, were also restored to wild-type levels (Figure 7.4D-F) (Rideout et al., 2010). This suggests that the abnormal behaviours exhibited by *UAS-TNT*$_G$; *dsx*^{GAL4} females are primarily a result of disrupting *dsx*^{GAL4} neurons.

That the specific disruption of function in these ~370 *dsx*^{GAL4} neurons, forming the *dsx*-specified female neural architecture, so effectively impinges on such distinct female-specific behaviours indicates the necessity of this neural substrate for the specification of female behavioural outputs necessary to the successful completion of the wild-type courtship repetoire.

7.4 Impaired induction of post-mating changes in *dsx*^{GAL4} females expressing TNT and the '*fru*$^+$/*ppk*$^+$' post-copulatory neural circuitry

During the process of successful copulation a wild-type female will receive from the male a seminal package containing sperm, to fertilize the eggs, and a mixture of various accessory gland proteins (Acps) including sex-peptide (SP), which induces post-copulatory responses (Kubli, 2003; Liu and Kubli, 2003). These post-copulatory changes in the mated female include reducing female receptivity, and therefore the propensity to remate for ~1 week, and increasing ovulation and oviposition (Liu and Kubli, 2003; Ram and Wolfner, 2007b). The immediate short-term effects and long-term potentiation of these effects have been demonstrated to arise as a consequence of successful uptake of SP in the female (Liu and Kubli, 2003).

In the female, SP activates a specific G protein-coupled receptor (SPR), (Yapici, et al., 2008). It has been shown that SP regulates post-mating responses by modulating a restricted number of *fru* positive (*fru*$^+$) neurons in the female reproductive tract (Häsemeyer et al., 2009; Yang et al., 2009). These neurons, designated as *fru*$^+$ as they are labeled by GAL4 responsive reporters when *fru-GAL4* is expressed in the female, have also been shown to be co-labeled with a sub-population of *pickpocket-GAL4* (*ppk-GAL4)* expressing neurons and as such

are also designated as *ppk*$^{+}$ type IV dendritic arborisation neurons (Grueber et al., 2003; Grueber et al., 2007; Häsemeyer et al., 2009; Yang et al., 2009). *ppk* neurons are implicated as acting as proprioceptive peripheral sensory neurons (Grueber et al., 2003; Grueber et al., 2007; Häsemeyer et al., 2009; Yang et al., 2009). These *ppk*$^{+}$ neurons innervating the female genitalia are described as having two neurons ramifying on each lateral oviduct with approximately a further thirty neurons organized in three bilateral clusters on each side of the uterus (Yang et al., 2009). Eight of these neurons were also found to be *fru*$^{+}$, one each on the lateral oviducts and a cluster of three on the sides of the uterus (Häsemeyer et al., 2009; Yang et al., 2009). These *fru*$^{+/}$*ppk*$^{+}$ neurons were also shown to express SPR (Häsemeyer et al., 2009; Yang et al., 2009). No co-expression between *fru-GAL4* and *ppk-GAL4* positive cells is observed anywhere else within the nervous system (Häsemeyer et al., 2009; Yang et al., 2009).

7.4.1 Absence of co-expression of *dsx*^{GAL4} with *fru*$^{+}$/*ppk*$^{+}$ neurons ramifying on the female internal genitalia

As *dsx*^{GAL4} demonstrates strong levels of expression in the female internal genitalia and as disrupting synaptic activity of *dsx*-expressing neurons in females strongly suppressed post-mating behaviours, effectively phenocopying SPR null females who, lacking the Sex Peptide Receptor (SPR), remain receptive, exhibiting virgin-like behaviours even after an initial mating or SP injection.

(Rideout et al., 2010) I therefore attempted to ascertain if the *fru*$^{+}$/*ppk*$^{+}$ neurons involved in the modulation of post-mating responses in response to SP signaling were also *dsx* neurons. As such I co-expressed the *ppk-eGFP* transgene (Grueber et al., 2003) alongside *UAS-nRFP* in *dsx*^{GAL4} females. Unfortunately expression of the red fluorescent reporter by the *dsx*^{GAL4} driver was so strong as to cause ectopic fluorescent emission in the 488 nm wavelength with consequent associated excitation of eGFP. This manifested as artifactual co-expression between *ppk-eGFP* and *UAS-nRFP*; *dsx*^{GAL4} in both the VNC and internal genitalia of the female preps (see Figure 7.6). The artifactual nature of this co-expression evidenced by the much more restricted expression observed in the VNC when *ppk-eGFP* is expressed alone (Figure 7.6C). However, importantly, what was also evident was that there was absolutely no co-expression observed (artifactual or

real) between *dsx*^{GAL4} and the described *fru*$^{+}$/*ppk*$^{+}$ neurons that ramify on the oviducts and uterus (Figure 7.6D).

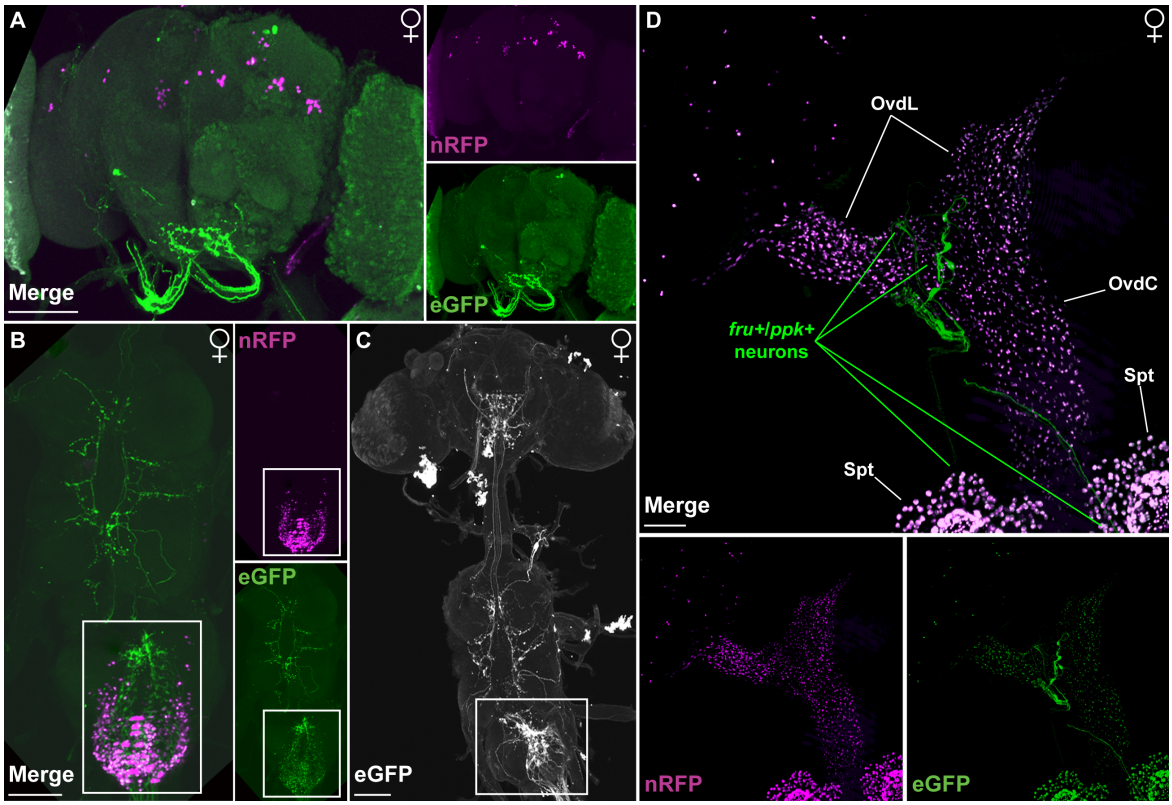

Figure 7-6 *dsx*^{GAL4} nRFP and *ppk-eGFP* expression in the CNS and internal genitalia of 5 day old adult females.
(A-B) UAS-RedStinger/ *ppk-eGFP*; dsxGAL4 female (A) brain showing no apparent co-localisation and (B) VNC. Apparent co-localisation in the Abg (boxed) is artifactual, the result of excitation of the 488 nm wavelength by nRFP signal (for comparison see expression pattern Abg of C). eGFP (green), nRFP (magenta). Ventral view; anterior up. (C) CNS female expressing only *ppk-eGFP*. Expression pattern in Abg (boxed) restricted to sensory projection inputs. Dorsal view, anterior up. (D) UAS-RedStinger/ *ppk-eGFP*; dsxGAL4 female genitalia. Large fru^{+}/ppk^{+} neurons ramifying on the lateral and common oviducts (OvdL and OvdC) and spermathecae (Spt) demonstrating no co-localisation with *dsx*^{GAL4} neurons indicated. Cell bodies associated with projections originating from the Spt and uterus out of field of view. Apparent co-localisation in the OvdL, OvdC and Spt is artifactual, the result of excitation of the 488 nm wavelength by nRFP signal. Scale bars = 50 µm.

Given the inherent problems with the co-labeling experiment described above, further validation of the absence of this co-expression of *dsx*^{GAL4} and *fru*$^{+}$/*ppk*$^{+}$ neurons was needed. I took advantage of the lexA/lexAop binary system (Lai and Lee, 2006b; Pfeiffer et al., 2010), to demonstrate the presence or absence of co-expression between *dsx*^{GAL4} and *fru*^{P1} in flies carrying the GAL4 responsive reporter *UAS-StingerII* with *fru*^{P1lex} driving expression of *lexAop* dsTomato (a kind gift from D. Mellert). In the CNS expression levels for both *dsx*^{GAL4} and *fru*^{P1LexA} realisation of the expression patterns of *UAS-StingerII, lexAop dsTomato*;

dsx^{GAL4}/*fru*^{P1LexA} in females appeared variable (Figure 7.7). What was of real interest was the paucity of any apparent co-expression between *dsx*^{GAL4} and *fru*^{P1LexA} driven expression patterns. Indeed it would appear that, while *dsx*^{GAL4} expression in the female CNS is contiguous with that associated with *fru*^{P1LexA} expression, there is no co-expression within the brain and, at most, ~3 neurons exhibit co-expression in the Abg (Figure 7.7). This lack of co-expression is in keeping with the findings of Sander and Arbeitman (2008) that saw no co-localisation between *fru*^{P1} and *dsx* in the –pC1, -pC2 and -TN1 neuronal clusters. In the male the general anatomy of *dsx*-expressing neurons is strongly reminiscent of *fru*-expressing neurons. However we know that only ~138 neurons of *dsx*^{GAL4}-expressing neurons are also *fru* positive, that is only ~7% of the total number of ~2000 *fru* neurons in the CNS overlap with *dsx* (see 6.1). In females there appears to be no overlap whatsoever. Since Fruitless has no action in the female nervous system, any circuits that are actively specified in the female (as opposed to a default ground plan) are likely to depend on *dsx*. This is important as it emphasizes that the *dsx*^{GAL4}-specified neural architecture is *fru*-independent and female-specific. While *fru-GAL4* expression in females demonstrates that the majority of neurons, which express Fru^{M} in the male exist in the female (Kvitsiani and Dickson, 2006; Stockinger et al., 2005), these need not necessarily contribute to the generation of sex-specific behavioural outputs as they do in the male. However once again what was clear in these *dsx*^{GAL4}/*fru*^{P1LexA} females was that absolutely no co-expression was observed between *dsx* and *fru*$^{+}$/*ppk*$^{+}$ neurons (Figure 7.7).

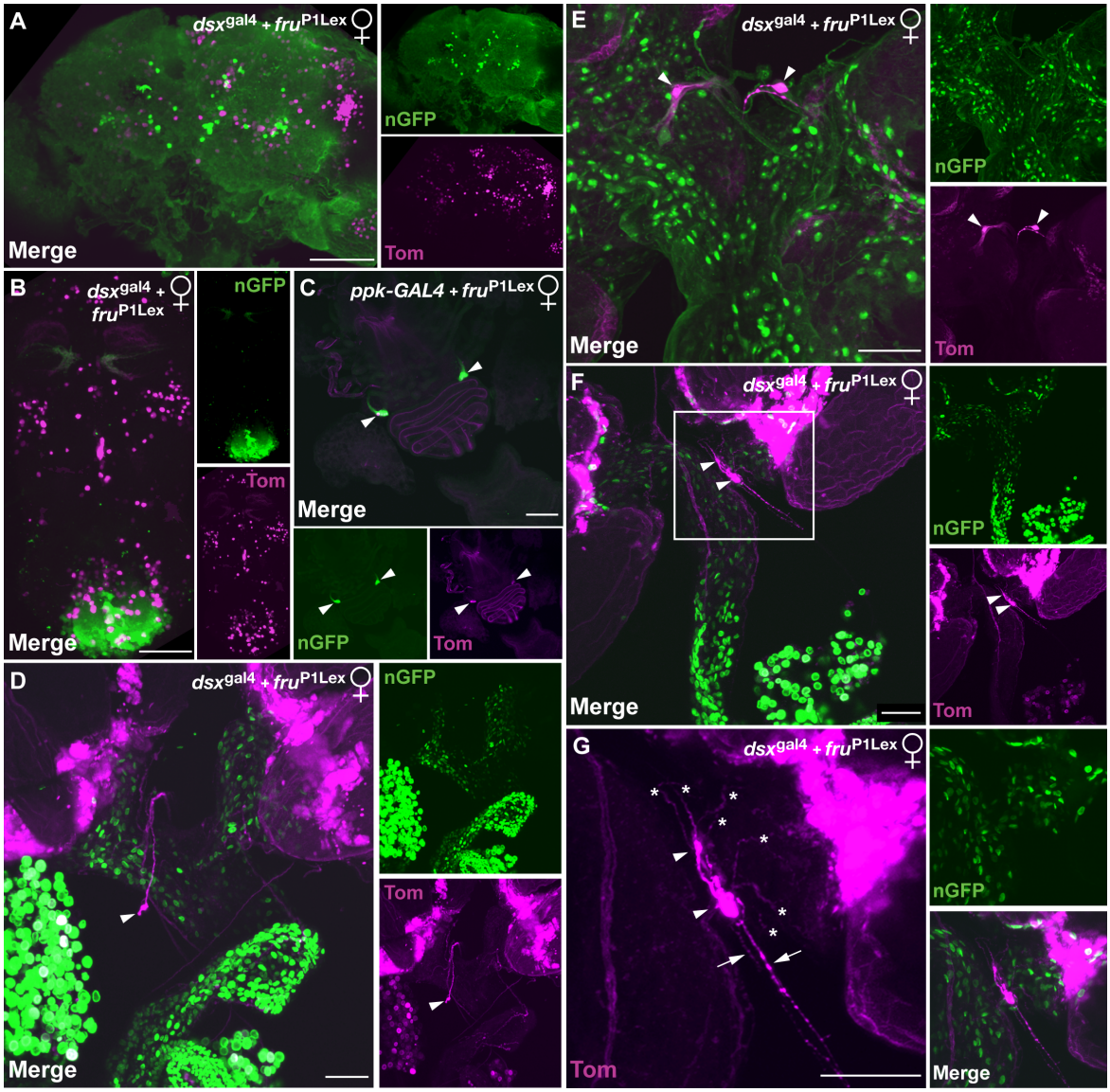

Figure 7-7 *dsx*^{GAL4} nGFP and *fru*^{P1Lex} *dsTomato* expression in the CNS and internal genitalia of 5 day old adult females.
(A-B) *UAS-StingerII, lexAop dsTomato*; *fru*^{P1Lex}/ *dsx*^{GAL4} female (A) brain and (B) VNC showing no apparent co-localisation. Dorsal views, anterior up. (C-G) Details of the internal female genitalia (C) *UAS-StingerII, lexAop dsTomato/ ppk*-GAL4; *fru*^{P1Lex} female demonstrating co-localisation on a bilateral cluster of cells ramifying on the seminal receptacle. (D) *UAS-StingerII, lexAop dsTomato*; *fru*^{P1Lex} / *dsx*^{GAL4} female exhibiting *fru*$^{+}$ neurons and projections associated with the oviducts and uterus, demonstrating no co-localisation with *dsx*^{GAL4}. (E) *UAS-StingerII, lexAop dsTomato*; *fru*^{P1Lex} / *dsx*^{GAL4} female exhibiting bilateral pairs of *fru*$^{+}$ neurons and projections associated with the lateral oviducts, demonstrating no co-localisation with *dsx*^{GAL4}. (F) *UAS-StingerII, lexAop dsTomato*; *fru*^{P1Lex} / *dsx*^{GAL4} female exhibiting the pair of *fru*$^{+}$ neurons and projections associated with the lateral oviduct, demonstrating no co-localisation with *dsx*^{GAL4}. (G) Higher resolution detail from (F) demonstrating the ramification of the two *fru*$^{+}$ neuronal cell bodies on the lateral oviduct (asterisks) and their individual associated projections (arrows), again no co-localisation with *dsx*^{GAL4} is apparent. GAL4 responsive nGFP, green. Lex responsive dsTomato, magenta. Scale bars = 50 µm.

7.4.2 ppk-GAL80 expression fails to repress the post-copulatory physiological changes deficits in dsx^{GAL4} females expressing TNT

It has previously been demonstrated that the intersectional tool *ppk-GAL80* is an effective inhibitor of *ppk-GAL4*, specifically blocking *fru-GAL4* driven expression in the *fru*$^{+}$/*ppk*$^{+}$ neurons that ramify on the oviducts and uterus while leaving the remaining pattern of *fru-GAL4* expression within the CNS intact (Häsemeyer et al., 2009; Yang et al., 2009). Further it has been demonstrated that expression of *ppk-GAL80* 'largely' suppresses the anomalous behavioural phenotypes associated both with *fru-GAL4* driven expression of membrane bound SP in virgin females (increased egg-laying and reduced receptivity) or SPR RNAi expression in mated females (reduced egg-laying and increased receptivity); restoring the assayed females to more wild-type behavioural outputs (Yang et al., 2009).

I therefore examined *UAS-StingerII*; *dsx*^{GAL4} females also expressing *ppk-GAL80* (a kind gift of S. Rumpf) and found no repression of nGFP expression within the CNS and internal genitalia (Figures 7.8- 7.9 and Table 7.1) indicative that *dsx*^{GAL4} and *ppk* do not colocalise. I then expressed *ppk-GAL80* in *dsx*^{GAL4} flies expressing TNT and found no restoration of fertility in females (n=40; Figure 7.10). Again these females showed no suppression of the egg-laying deficit (Figure 7.10) and exhibited permanently extruded ovipositors after 5 days (data not shown), as previously demonstrated in *dsx*^{GAL4} TNT females. The persistence of these phenotypes again indicative that the neuronal paths impaired by expression of TNT under the aegis of *dsx*^{GAL4} is again separate from that of the described '*fru*$^{+}$*/ppk*$^{+}$' neural circuit in the female.

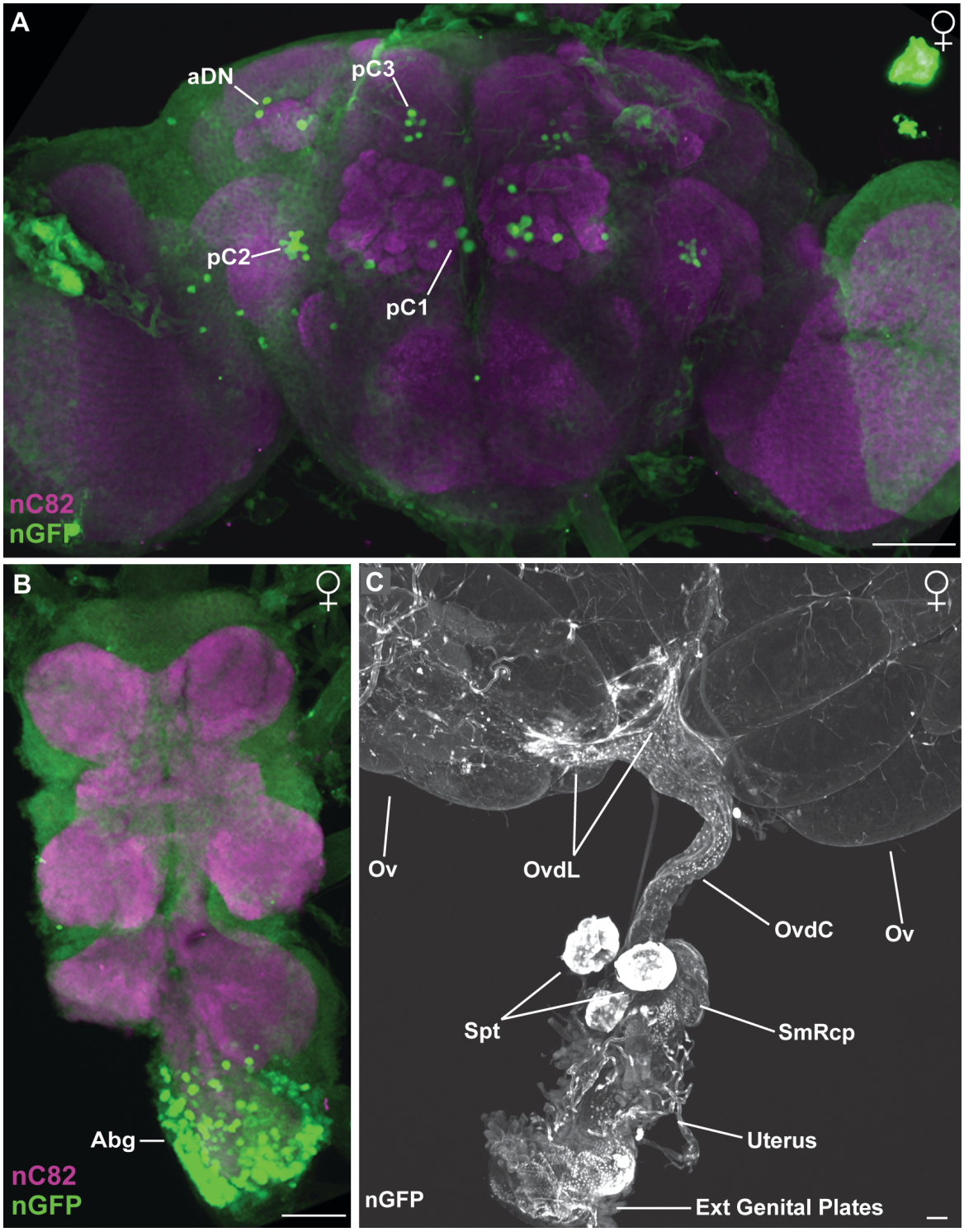

Figure 7-8 *ppk-GAL80* fails to suppress *dsx*^{GAL4} driven nGFP expression in the CNS and genitalia of 5 day old adult females.
(A-C) *UAS-StingerII/ppk-GAL80; dsx*^{GAL4} female. (A) brain and (B) VNC demonstrating persistence of *dsx*^{GAL4} driven nGFP expression (green). Neuropil counterstained with anti-nC82 (magenta). Ventral views, anterior up. (C) Genitalia demonstrating persistence of *dsx*^{GAL4} driven nGFP expression in the ovaries (Ov), lateral and common oviducts (OvdL and OvdC), seminal receptacle (SmRcp), spermathecae (Spt), uterus and external genital plates (Ext Genital Plates). Scale bar = 50 µm.

TABLE 7.1 *dsx*^{GAL4} responsive nGFP cell counts demonstrating the lack of repression in the CNSs of adult females also expressing *ppk*-GAL80

	Dsx Neuronal clusters[1]	5 day old Adult Females *UAS-StingerII*; *dsx*^{GAL4} Cell Counts[2]	*UAS-StingerII*/*ppk*GAL80; *dsx*^{GAL4} Cell Counts
Brain			
1	*dsx*-pC1[3]	8.7 ± 2.0 (10)	8.5 ± 1.8 (10)
2	*dsx*-pC2[3]	11.2 ± 1.9 (10)	11.1 ± 2.7 (14)
3	*dsx*-pC3[3]	6.4 ± 1.4 (10)	7.0 ± 1.5 (12)
4	*dsx*-aDN[3]	2.0 ± 0.0 (12)	2.0 ± 0.0 (10)
Ventral Nerve Cord			
9	*dsx*-Abg[4]	311.6 ± 15.9 (10)	296.0 ± 28.6 (12)

Table 7-1 *dsx*^{GAL4} responsive nGFP cell counts demonstrating the lack of repression in the CNSs of adult females also expressing *ppk*-GAL80.
[1]Nomenclature for Dsx neuronal clusters as per Lee et al. (2002) and Rideout et al. (2010).
[2]Number of nuclei expressing *dsx*^{GAL4} responsive nGFP ± SD as per Rideout et al. (2010).
[3]Neuronal cluster away from CNS midline. Count represents one cluster per hemisegment of the CNS. [4]Neuronal cluster spans the CNS midline. Count given is for the complete VNC.n's listed in parentheses. No significant difference between any counts *P*>0.05 (Student's t-test).

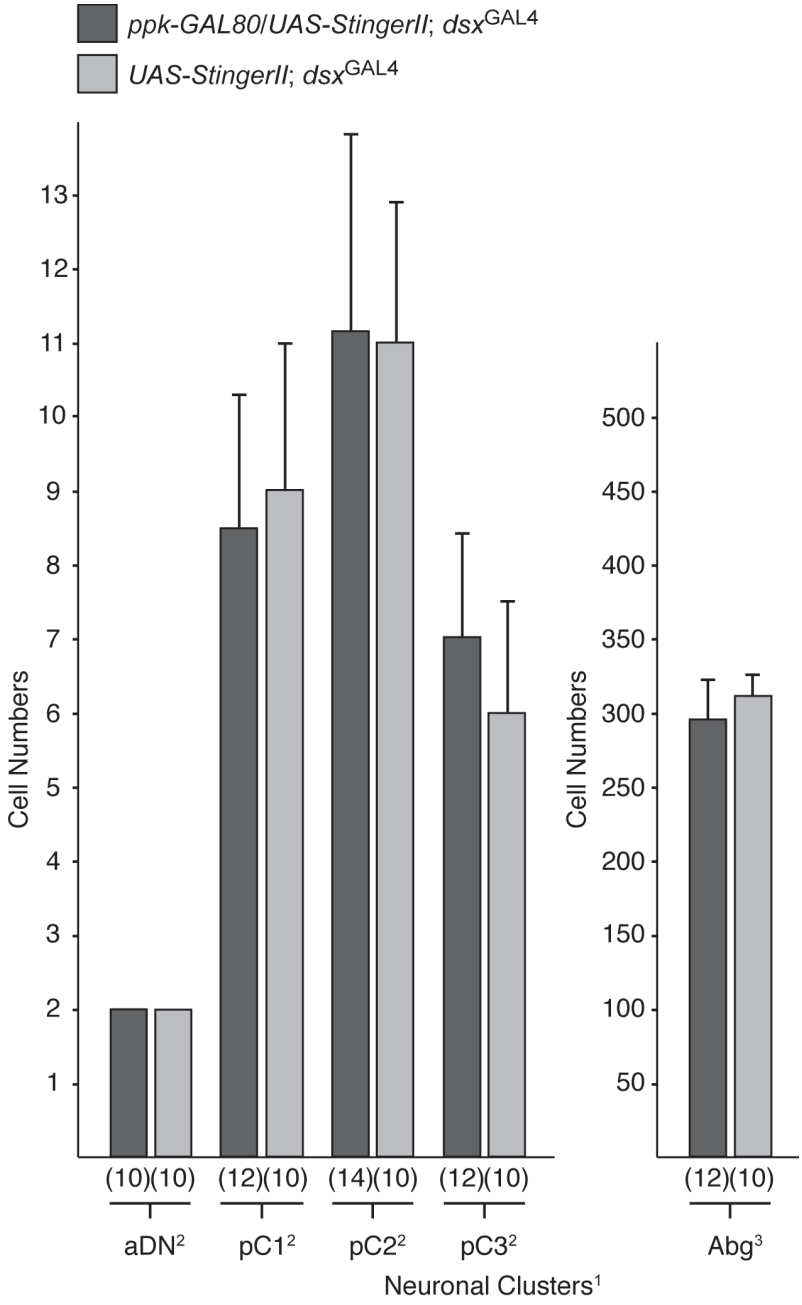

Figure 7-9 Comparison between GAL4 responsive nGFP cell counts driven in the CNSs of adult females expressing either *dsx*^{GAL4} with *ppk-GAL80*, or *dsx*^{GAL4} alone.
[1]Nomenclature for Dsx neuronal clusters as per Lee et al. (2002) and Rideout et al. (2010). [2]Neuronal cluster away from CNS midline. Count represents one cluster per hemisegment of the CNS. [3]Neuronal cluster spans the CNS midline. Count given is for the complete VNC. n's listed in parentheses. No significant difference between any counts *P*>0.05 (Student's t-test).

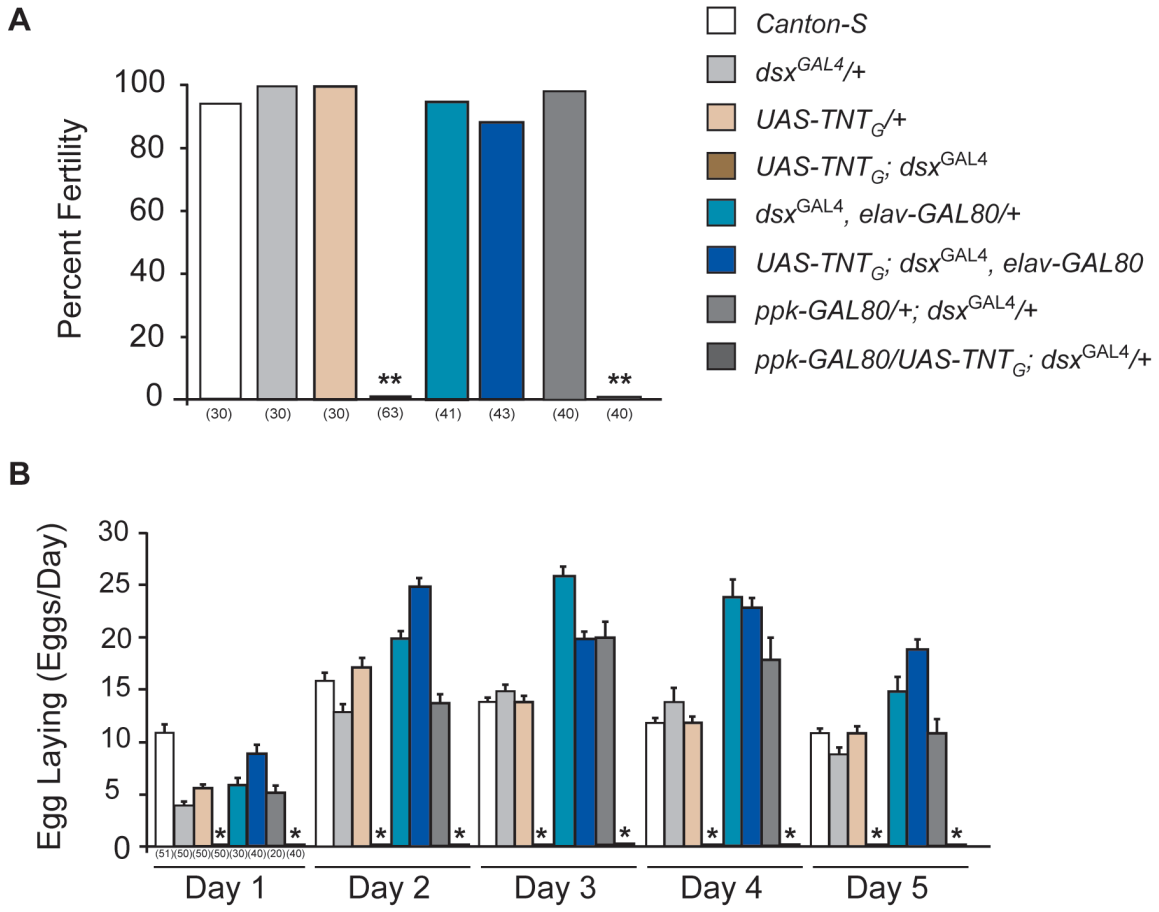

Figure 7-10 *ppk*-GAL80 expression is not sufficient to restore post-copulatory behaviours in mated *UAS-TNT$_G$;* dsx^{GAL4} females.
(A) Female fertility (P<0.0001, Fisher exact test). (B) Egg-laying (mean ± SEM, *P<0.0001, Dunnett's test). Genotypes indicate females. Target males were wild-type. n values are shown in parentheses. Assays for *ppk*-GAL80/+; dsx^{GAL4} and *ppk*-GAL80/*UAS-TNT$_G$;* dsx^{GAL4} flies performed on different date than other experimental and control animals. Experimental and controls as per Figure 7.4.**

As such it appears that *ppk-GAL80* expression is not sufficient to restore the suppression of post-mating behaviours in *dsx*^{GAL4} females expressing TNT and that this, coupled with the absence of any co-expression between *dsx*^{GAL4} and the *fru*$^+$/*ppk*$^+$ neurons in the female, implies that these post-copulatory deficits arise from the impairment of a novel neural pathway, which is distinct from that described by the '*fru*$^+$/*ppk*$^+$" SPR circuit.

7.5 Discussion

I have, in the previous chapters, demonstrated the profound differences that exist in the neural architecture of adult males and females arising from differences in cell numbers in homologous clusters and the presence, or absence, of sex-specific neurons and neuronal clusters; with consequent dimorphisms in the associated projections, the paths they follow and connections they make. It is these

differences, created during the assembly of the circuits in development that would appear to be functionally relevant to the generation of distinct adult sexual behaviours in both males and females.

Furthermore, through the overlapping relationship between *dsx* and *fru*, I have attempted to predict what individual modalities of courtship behaviour might be affected when the function of *dsx*^{GAL4} neurons is specifically impaired in the male. In the brain *dsx*^{GAL4} neurons are localised to areas that gynadromorph studies have identified as containing foci involved in initiation, following, tapping, wing extension and copulatory behaviours (Hall, 1977, 1979; Hotta and Benzer, 1976; von Schilcher and Hall, 1979). Latterly clonal analyses of *fru* neurons (Cachero et al., 2010; Kimura et al., 2005; Yu et al., 2010) allowed me to associate the intersecting *dsx*^{GAL4} neurons/neuronal clusters with involvement in higher-order processing of multi-modal sensory stimuli inputs; specifically the auditory, visual and olfactory circuitry (Cachero et al., 2010; Kimura et al., 2008; Kohatsu et al., 2011; Yu et al., 2010). Within the VNC the *dsx*^{GAL4} neurons appear to be expressed in areas identified by gynandromorph studies as containing foci associated with tapping, wing extension, courtship song and with copulatory behaviours (Hall, 1977, 1979; Hotta and Benzer, 1976; von Schilcher and Hall, 1979). These studies coupled with more recent analyses allowed me to infer that the *dsx*^{GAL4} neurons of the Prg and Msg may be associated with the transmission and processing of stimulatory inputs for the gustatory circuit, and the subsequent modulation of transmitted higher-order signals involved in the generation of unilateral wing extension and song production (Cachero et al., 2010; Kimura et al., 2008; Kohatsu et al., 2011; Rideout et al., 2007; Rideout et al., 2010; Yu et al., 2010). Finally the neurons of the Abg and their associated projections, both descending to the genitalia and ascending to the protocerebrum, may be associated with regulation and generation of copulatory behaviours (Billeter et al., 2006b; Cachero et al., 2010; Kimura et al., 2008; Kohatsu et al., 2011; Rideout et al., 2010; Yu et al., 2010). All these neural substrates potentially describe circuitry essential for the initiation of courtship and for the assurance of the continuation of the individual courtship modalities (*e.g.*, tapping, courtship song etc.) in a coordinated manner, culminating in successful copulation. This evidentiary somatotopic mapping allows the informed prediction to be made that males in which *dsx*^{GAL4} neuronal activity is impaired would present with aberrant behavioural phenotypes related to latency (the time it takes to initiate courtship)

and the proper coordination and expression of any subsequent courtship steps. That is presenting with significant decrements in the later courtship steps, such as tapping, wing extension and song generation, and copulatory behaviours. It is therefore telling that specific disruption of *dsx*^{GAL4} neuronal function in males resulted in a behaviourally sterile animals that, in keeping with the predicted phenotypic disruptions, exhibited significantly extended time to initiate any courtship behaviour. This behaviour, again in keeping with the predicted pattern of behavioural impairment, is limited to little more than occasional bouts of orientation on the target female with none of the latter stages of courtship ever displayed. No tapping and no wing extension, and thus consequently a complete absence of courtship song, and no copulation are ever attempted. This somatotopic mapping of these *dsx*^{GAL4} neurons, and the relationship they have with known parts of the *fru* male-specific neural substrates, coupled with the demonstrated abrogation of almost all male-specific courtship behaviours by specific impairment of *dsx*^{GAL4} neural function provides compelling evidence that these neurons comprise the neural circuitry necessary for the specification of male-specific courtship behavioural outputs.

Sexual behavioural studies in *Drosophila melanogaster* have almost exclusively focused on the robust and quantifiable sequential program of behaviours performed by the male (Billeter et al., 2006a), the female seeming in comparison largely passive. However while females appear largely submissive they are known to exhibit some subtle behaviours, though those identified so far appear to consist mostly of rejection behaviours such as wing flicking (in young virgins) or kicking (in mature virgins) (Connolly and Cook, 1973; Ejima et al., 2001; Spieth and Ringo, 1983). Again little is quantitatively known about the effects these female rejection responses have on the behaviour of courting males, and what stimuli might trigger these behaviours. However it would seem an imperative that if the female is to make an assured judgement of a prospective mate, not only of species type but also perhaps of individual fitness, she must be able to assay the courting male through a variety of stimulatory cues, such as audition and pheromonal signaling, prior to allowing copulation to occur. That the mature (and therefore potentially receptive) virgin female changes her apparent rejection behaviour from wing-flicks to kicking with her hind-legs (which exhibit a significantly increased number of *dsx*^{GAL4} cells compared to males; see Figure 4.14) is of interest as this may in fact be another method by which the female may

assay the fitness of a courting male, in a manner analogous to the males tapping the female with his fore-legs. It is worth noting that in some species of Drosophilids the females exhibit an acceptance posture, which allows, or may even initiate, male attempted copulation (Spieth, 1974). These behaviours can consist of the female spreading her wings up and out, holding them extended until the male mounts and spreading their vaginal plates (Spieth and Ringo, 1983). Despite this known repertoire of acceptance postures, the number of studies utilising female-specific behaviours (rather than the act of copulation itself) to assay female receptivity in courtship has, to date, been extremely limited (Ikeda et al., 1981; Ritchie et al., 1998; Tomaru et al., 1885). It is known that, in response to a courting male, receptive *melanogaster* females will slow down and cease rejection behaviours, allowing the male to lick her genitals but it is unclear if these females exhibit other acceptance behaviours (Spieth and Ringo, 1983). However while it has been shown that a persistent male can overcome female rejection to successfully copulate, our results do suggest that female cooperation does occur to facilitate copulation (Rideout et al., 2010). During attempted copulation and copulation the male curls his abdomen under and forward, rearing upwards, thrusting his head under the female's wings, and grasping her body with his fore- and mid-legs. If successful intromission occurs, the pair will then remain largely stationary (Spieth and Ringo, 1983). In females, gynandromorph studies have suggested a requirement for a receptivity focus in the dorsal brain (Hotta and Benzer, 1976; Szabad and Fajszi, 1982; Tompkins and Hall, 1983), the region in which *dsx* neurons are positioned. It would seem likely that these neurons are contributing to female mating decisions in an analogous manner to the involvement of *dsx* neurons in male mating decisions (Broughton et al., 2004; Kimura et al., 2008) as disruption of the synaptic activity of these neurons in females again specifically impairs courtship behaviours. dsx^{GAL4} females expressing TNT presenting as apparently oblivious to the male's advances during courtship (Rideout et al., 2010). This seeming incapability of the female to sample male-specific courtship stimuli is evidenced by the complete lack of receptivity, or provision of any acceptance response by these females. This then results in extended courtship indices by the male directed at these females until, finally, the female's rejection behaviours are overcome (Rideout et al., 2010). However even then the positioning of the male is often less than optimum, with the female continuing to appear oblivious to the mounted male's attentions as evidenced by

the anomalous locomotion levels displayed by these copulating pairs (see Supplementary Video 3, Rideout et al., 2010).

That successful transmission of a seminal package in these copulating pairs has occurred is reasonably demonstrated through the use of the GFP encoding sperm and SP transgenes (Rideout et al., 2010). However these mated females display none of the SP induced post-mating physiological changes that normally would occur after successful mating; that is they continue to elicit male courtship, will re-mate and display no increased egg-production and consequent oviposition (Rideout et al., 2010). It has been shown that SP (Yapici et al., 2008) can activate a specific G protein-coupled receptor (SPR) to regulate post-mating responses by modulating fru^{+}/ppk^{+}-sensory neurons in the female reproductive tract (Häsemeyer et al., 2009; Yang et al., 2009). While dsx^{GAL4} is extensively expressed throughout the internal genitalia in the female, I have demonstrated that there appears to be no co-expression between these fru^{+}/ppk^{+} and dsx^{GAL4} neurons. It would seem therefore that the suppression of post-mating changes exhibited in dsx^{GAL4} females expressing TNT is operating on a pathway independent of that described by the fru^{+}/ppk^{+} neurons. As dsx^{GAL4} neurons in the Abg innervate the female internal genitalia, these neurons might effect some direct control on these tissues modulating such processes as egg fertilization and oviposition.

Szabad and Fajszi, 1982 describe more than one foci involved in eliciting post-mating changes. The first foci, mapping to the brain, directs increased oviposition and egg deposition and decreased receptivity in the successfully post-mated female. While the second foci, mapped to the VNC, is involved in transmission of mature eggs along the oviducts and positioning of eggs for successful fertilisation prior to ovipositor deposition. It seems significant that in females in which the fru^{+}/ppk^{+} post-copulatory path is impaired some egg deposition still occurs; that these deposited eggs hatch and develop normally is used as evidence that the process of copulation is unaffected in these females (Yang et al., 2009). Whereas in dsx^{GAL4} females expressing TNT absolutely no egg deposition is observed with mature eggs atrophying in the lateral oviducts and, as no ‘live births’ are observed, no successful fertilisation of eggs by transmitted sperm can have occurred (Rideout et al., 2010). In keeping with this it has been demonstrated that *Octopamine receptor in the mushroom body* (OAMB),

a Drosophila G-protein-coupled receptor for octopamine, expressed both in the nervous and the reproductive system, is required for ovulation upon induction after successful copulation (Lee et al., 2009; Lee et al., 2003). In the nervous system OAMB is enriched in the brain in the MBs and central complex while in the VNC it is also expressed in octopamanergic neurons in the Abg, which project to the oviduct epithelium (Lee et al., 2009; Lee et al., 2003). In the female genitalia OAMB has been shown to be restrictively expressed in the epithelial layer in the oviducts, where it is thought to stimulate fluid secretions, and perhaps also in the oviduct muscles where it induces relaxation of the oviduct muscular wall (Lee et al., 2009). These concerted activities appearing to be critical in the process of egg transfer through the oviduct to the uterus. I have previously demonstrated that *dsx*^{GAL4} expression within the internal genitalia appears to occur both within the epithelium and the muscular wall and that the suppression of this by *elav-GAL80* might therefore indicate that this expression is in some way neuronal (see section 5.4.3). One model for the interaction of the two independent behaviours of egg transfer and egg deposition is that SPs transmitted by the seminal package inhibit the activity of the *fru*$^{+}$/*ppk*$^{+}$ SPR neurons which project to the brain and interact with OAMB receptors (Lee et al., 2009). These then activate the OAMB neurons in the Abg which project to the oviducts and act to induce egg transfer to the uterus for fertilization and subsequent deposition, with the very act of transfer through the oviducts and uterus also generating a mechanistic stimulatory signal which activates the mature egg and facilitates further post-copulatory changes in the mated female (Lee et al., 2009). Therefore it may be that the described *fru*$^{+}$/*ppk*$^{+}$ neurons modulate both the initiation of these post-mating changes and more ‘downstream’ physiological processes required for successful deposition of these fertilized eggs from the uterus via the ovipositor. While *dsx*^{GAL4} neurons are involved both in higher-order processing of the received SPR signal, but also represent a ‘downstream’ target of SPR activity, directing post-mating physiological processes specific to transfer and successful fertilization of eggs in the female uterus. These processes, independent but related, describing the complete mated (and therefore unreceptive) female repertoire of post-copulatory behavioural outputs, with this model effectively explaining how the impairment of the *dsx*^{GAL4} neural function blocks any further progression in the process of post-copulatory physiological change in these females despite the *fru*$^{+}$/*ppk*$^{+}$ neurons being activated by successful transmission of a the complete seminal package. Alternatively as silencing *ppk* neurons by expressing *shibire*^{ts} induces high egg-

laying rates, and reduces receptivity in virgins, Yang et al. (2009) proposed that SP acts by reducing neuronal activity of fru/ppk neurons to produce post-mating behaviors. While mated *dsx*^{GAL4} expressing TNT do not lay eggs, activating *dsx*^{GAL4} neurons via TRPA1 (Parisky et al., 2008; Pulver et al., 2009; Shang et al., 2008) leads to increased oviposition in virgin females which might indicate that these neurons are activated by SP to trigger post-mating responses (C. Rezaval, pers. comm),.

Finally it is important to note that the presence of *fru*^{GAL4} expressing neurons in females, and the consequent ability of these females to exhibit male-specific behaviours, has been used as evidence of a shared neural circuitry between the sexes (Kvitsiani and Dickson, 2006). However the apparent absence of any co-expression between *dsx*^{GAL4} and *fru*^{P1} in the female indicates that the *dsx*-specified neural architecture is indeed sex-specific and that the dimorphic neural substrates, while positionally contiguous with each other in relation to the underlying neuro-anatomy, do appear to represent independent neural paths. Therefore the resultant deficits in male- and female-specific sexual behaviours (and not general sensory function or motor control), which occur when *dsx*^{GAL4} neuronal function is specifically disrupted within the CNS, compellingly argues that these *dsx*^{GAL4} neurons instruct sex-specific neural networks. Unequivocal proof however that the *dsx* neurons are involved in both male and female copulatory decision-making again will require individual courtship modalities to be functionally mapped to specific subset(s) of *dsx* neurons.

8 Summary discussion

8.1 Investigative conclusions

The insertion of a GAL4 element into the *dsx* locus by homologous recombination has created an important transgenic tool, allowing a systematic spatial-temporal survey to be performed of the endogenous expression of *dsx*'s sex-specific isoforms throughout development in males and females. This topographical understanding of the gene's expression has been expanded, by functional analyses and somatotopic mapping, to provide insight into the processes underlying the development of a dimorphic nervous system and associated somatic tissues, and how these then are coordinated in the generation of sex-specific behavioural outputs.

These investigations first required validation of the dsx^{GAL4} transgenic. As previously stated the dsx^{GAL4} allele presented as a duplication at the *dsx* locus of the endogenous gene and the donor construct containing the GAL4 element. I performed Northern analyses to demonstrate that the dsx^{GAL4} allele produced both the expected endogenous wild type *dsx* and GAL4-containing transcripts in both sexes. Further, I showed that dsx^{GAL4} males and females exhibited no overt morphological abnormalities either in their internal genitalia or external sexual characteristics and were viable and fertile. As such I concluded that integration of this novel construct had not impinged on normal gene expression. I also demonstrated that dsx^{GAL4} accurately reiterated the endogenous gene expression in the CNS in both sexes in pupae and adults. Beyond this I demonstrated that manipulating *dsx* function specifically in dsx^{GAL4} cells is sufficient to reprise the known functional roles of the endogenous *dsx* isoforms in the direction of a male- or female-specific program of development of somatic sexual characteristics.

Following the tenet that to understand function you must first understand structure, I performed a comprehensive survey of dsx^{GAL4} expression throughout development in the nervous system of both sexes. This provided a time line progression of the dynamic manner in which these dsx^{GAL4} neurons and neuronal clusters develop, are maintained or are lost, before finally arriving at the final adult expression patterns. I observed significant neuro-anatomical dimorphisms between males and females arising from differences in neuronal numbers in non-sex-specific clusters and in the presence of sex-specific neurons and neuronal

clusters; with changes in neural complexity, axonal density, and connectivity a consequence of the differences in the architecture of the associated neuronal projections and synapses (Rideout et al., 2010).It is important to note that in the adult those areas with sexually dimorphic *dsx*^{GAL4} expression have previously been demonstrated to be important with respect to sex-specific behaviours in both males and females (Billeter et al., 2006a; Ferveur and Greenspan, 1998; Hall, 1977, 1979; Villella and Hall, 2008; von Schilcher and Hall, 1978). In keeping with the idea that metamorphosis occurs not only to achieve the adult sexually dimorphic physical state but also ensure that a sexually dimorphic neural circuitry is specified as well, it is significant that the 48 hr pupal stage, a developmental time point previously identified as critical in the establishment of the neural substrates governing sex-specific reproductive behaviours (Arthur et al., 1998; Belote and Baker, 1987), appears to be a pivotal moment in the determination of the final adult *dsx*-specified dimorphic male and female CNS (Rideout et al., 2010).

I also observed a restricted and dimorphic pattern of expression of *dsx*^{GAL4} in the PNS, particularly in cells within the foreleg (Rideout et al., 2010). In keeping with previous studies some of these *dsx*^{GAL4}-expressing cells were male-specific gustatory neuronal receptors that projected, in a male-specific manner, into the CNS (Mellert et al., 2010; Possidente and Murphey, 1989; Rideout et al., 2010). Axotomy at the level above the sex comb resulted in complete degeneration of the associated projections (Rideout et al., 2010). In keeping with the observations of Koganezawa et al. (2010) these amputated males displayed aberrant courtship postures towards a target female. These animals also exhibited significant reduction in neuronal numbers in two *dsx* clusters in the brain, perhaps through loss of anterograde signals from synaptic inputs of projecting neurons. The observed anomalous behaviour may therefore arise from loss, or altered neural processing, of sensory inputs.

The observed dimorphisms in the connectivity of the *dsx*^{GAL4} neural substrates (both in the CNS and PNS) begins to provide an insight into how stimuli might undergo differential sensori-motor processing, resulting in altered behavioural outputs. It is not unreasonable to infer that the creation of these differences during the developmental assembly of the neural circuitry are

consequently functionally relevant in the generation of distinct adult sexual behaviours in both males and females.

As *dsx* is central to somatic sex determination and the establishment of sexual characteristics in both males and females I also performed a spatial-temporal survey of dsx^{GAL4} expression outwith the nervous system in both the sexes. Rather than a ubiquitous pattern of expression, I observed dsx^{GAL4} expression to be restricted (Rideout et al., 2010). With only those tissues that were sexually physiologically relevant, such as in the developing gonads, oenocytes, fat body cells and specific imaginal discs of the embryo and larva, or in the oenocytes, fat body cells, gut and genitalia of the pupae and adult requiring specification of a sexual identifier (Rideout et al., 2010; Robinett et al., 2010). The novel expression in the larval fat body and oenocytes, as well as that seen in the male gonad, is indicative of an early requirement for the establishment of sexual identity. The persistence of expression in these and later sexually physiologically relevant tissues indicates the requirement for the regulation and maintenance of gender appropriate sexually identity for the assurance of the 'complete' sexual state (*cf. dsx* regulation of *yp* genes; Bownes, 1994).

It has been demonstrated that *dsx* and *fru* are required to cooperate for the establishment of the complete wild-type nervous system and have been shown to co-express in within the CNS (Billeter et al., 2006b; Kimura et al., 2008; Rideout et al., 2007; Rideout et al., 2010). As such I comprehensively surveyed the spatial pattern of dsx^{GAL4} and *fru* co-expression in the male pupal and adult CNSs. Despite the dynamic nature of both dsx^{GAL4} and *fru* expression individually between the pupal and adult developmental stages, the actual level of co-expression remains relatively static. While it has not been determined in this study that individual cells demonstrating this co-expression are the same between the time-points, it seems telling that this co-expression becomes apparent in 48 hr male pupae, a critical developmental time point for the establishment of the neural substrates governing male courtship behaviours (Arthur et al., 1998; Belote and Baker, 1987), and is maintained thereafter.

The demonstrated co-operative nature of *fru* and *dsx* in the establishment of the male CNS (Billeter et al., 2006b; Kimura et al., 2008; Rideout et al., 2007; Rideout et al., 2010) also meant that I assayed dsx^{GAL4} neural architecture in *fru*

and *dsx* mutant backgrounds in adult males and females. I found that male and female isoforms of *dsx* appear to be the primary regulators of dimorphisms in *dsx*^{GAL4} neurons, though Fru^{M} function is required to obtain a full complement of male-specific *dsx*^{GAL4} neurons within the protocerebrum and VNC, and that sex-specific PCD is one mechanism used to assemble this dimorphic neural circuit (Rideout et al., 2010). Further it can be seen that even small changes in neuronal populations can substantially alter the subsequent neural organization and connectivity of the associated neural projections, again demonstrating one process whereby neuro-anatomical changes could provide the basis for production of sex-specific behavioural outputs, through the creation, and maintenance, of dimorphic neural paths and connectivities.

During performance of the spatio-temporal survey in *dsx*^{GAL4} of expression in the CNS I noted that that the male *dsx*-pC2 cluster was comprised of two distinct, yet topographically related, populations of neurons with distinct axonal projections (Robinett et al., 2010). Performing axotomies on male forelegs resulted in significant decrement in neurons specifically in the –pC2l sub-cluster, perhaps indicative of a bias of male-specific projections interacting with this cluster. Again while I observed that both the *dsx*-pC2l and m subsets in the male exhibit neurons that co-localize with Fru^{M}, the vast majority of co-expression appears localized to the lateral population of neurons. It is tempting to speculate that the lateral *dsx*-pC2 cluster in fact represents a novel male-specific cluster however it would require clonal/lineage analysis to confirm this.

The overlap between *fru*- and *dsx*-expressing neurons in the male CNS allowed me to infer function for *dsx*^{GAL4} neurons due to their intersection with *fru* neurons with known, or suspected, roles in male sexual behaviour (Cachero et al., 2010; Datta et al., 2008; Kimura et al., 2008; Kimura et al., 2005; Rideout et al., 2010; Ruta et al., 2010; von Philipsborn et al., 2011; Yu et al., 2010). Allowing me to associate individual *dsx*^{GAL4} neuronal clusters with involvement, in the brain, of higher order processing of multi-modal sensory stimuli inputs (specifically auditory, visual and olfactory circuitry) as well as, in the VNC, of sensiro-motor processing of stimuli for wing extension, song production and copulatory behaviours. Circuitry that is essential, individually and in concert, to ensure the success of courtship through assurance of the coordinated courtship behavioural steps. This more restricted analyses of individual regions and neuronal clusters by clonal analyses,

coupled with other tools, such intersectional reagents, continues to provide greater understanding of the nature of the *dsx* and *fru* 'co-operative' circuitry and of the functional roles individual neurons and neural clusters have in the generation of distinct behavioural outputs.

Finally I, in conjunction with Drs. Megan Neville and Elizabeth Rideout, performed a series of behavioural assays on both male and female dsx^{GAL4} flies (Rideout et al., 2010). We demonstrated that inhibition of dsx^{GAL4} neuronal function in males leads to disruption of the early steps of courtship (orientation, following) and the complete absence of the later steps (wing extension, courtship song and attempted copulation), resulting in complete behavioural sterility in these animals (Rideout et al., 2010). Demonstrating that these ~640 male dsx^{GAL4} neurons are directly and specifically contributing towards the generation of male courtship behaviours and that disruption of the function of the *dsx* male neural architecture so effectively leads to suppression of male courtship behaviours that it therefore defines a far more minimal neural substrate necessary to specify these male-specific behavioural outputs than that previously described by the far more extensive *fruitless* circuit.

Similarly to the male, disrupting synaptic activity of dsx^{GAL4}-expressing neurons in females impaired distinct female courtship behaviours (Rideout et al., 2010). These females appeared incapable of sampling the male's courtship display and were thus incapable of providing any acceptance response and when copulation did occur, lack of female cooperation was evidenced by continuous movement and rejection behaviours (Rideout et al., 2010). Although sperm and seminal fluids were successfully transferred to these females, they laid no eggs, re-mated and remained incapable of actively rejecting or suppressing further courtship; indicative that disrupting dsx^{GAL4} neuronal function in females also suppressed normal post-mating behaviours (Rideout et al., 2010). The necessity of the *dsx*-specified female neural architecture for specification of female behavioural outputs required for successful completion of the wild-type courtship repertoire may be demonstrated by that fact that specific disruption of function in these ~370 dsx^{GAL4} neurons so effectively impinges on the female-specific behaviours observed. It seems likely that these neurons contribute to female mating decisions, as homologous neurons in males are involved in male decisions.

8.2 Future work

The work presented in this thesis hopefully represents another step along the path to understanding the genetic principles that determine the development of the nervous system and the processes behind the reception of sensory stimuli, their processing and the generation of a behavioural response. At least these findings provide an insight as to how we might continue to delineate the developmental logic surrounding the formation of the *doublesex*- and *fruitless*-specified neural circuitry in *Drosophila* and how these circuits are coordinated with the gender-appropriate physiology and sensori-motor tissues to generate sex-specific behavioural outputs.

Key to gaining further understanding about the development and function of the dimorphic neural circuitry is continuing the process of somatotopic mapping of these circuits. Targeting individual *dsx* neurons and/or neuronal clusters with fine mapping to determine projection paths, connectivity and the relation each part of the circuit has with the surrounding neuroanatomy. Both the associated parts of the *dsx*-specified neural architecture itself and beyond this with other neural circuits, as and when they are identified. Central to this however is the ability to assign function to individual parts of the overall circuit. One approach using the extant dsx^{GAL4} transgene is to take advantage of available enhancer-trap FLP lines to intersect parts of the dsx^{GAL4} expression patterns (Bohm et al., 2010). Two similar, but variant, schemes may be employed for functional clonal mapping of the dsx^{GAL4}-specified neural architecture. The first involves crossing an ET^{FLP} line with dsx^{GAL4} and a *UAS>stop>mCD8::GFP* reporter and *UAS>stop>TNT* effector to express membrane bound GFP and TNT in all intersecting neurons in which FLP has excised the transcriptional stop cassette (>*stop*>). The second involves crossing an ET^{FLP} line with a strain containing the dsx^{GAL4} driver, *tub>GAL80>*, a *UAS-mCD8::GFP* reporter and a *UAS-TNT* effector. In this scheme GAL80 repression is removed in the intersected *dsx* neurons via FLP-mediated recombination allowing expression of the reporter and TNT effector transgenes. These strategies present a retroactive approach for the elucidation of function in clonal groups, as flies employed in the two schemes must first undergo behavioural screens to assay for behavioural deficit(s) prior to dissection to elucidate which neurons/tissues are exhibiting reporter expression. Thereby identifying and assigning functional roles to the cells whose impairment has

resulted in the associated behavioural anomalies. Again the advantage of the *dsx*^{GAL4} allele is that it is expressed in both males and females allowing the above strategies to be employed in elucidating those neural substrates involved in the generation of sex-specific behavioural outputs in both sexes.

Beyond this however will be the requirement to develop more sophisticated 'next generation' tools for intersectional investigations; allowing reproducible 'genetic access' to defined sub-populations of the *dsx* neurons for circuit analyses. One such tool is the 'Split-Gal4' system, in which separation of DNA-binding and transcription-activating functions within GAL4 (the Gal4-DB and -AD domains respectively) (Brent and Ptashne, 1985; Fields and Song, 1989; Keegan et al., 1986) allowed the development of a ternary GAL4 approach in which the activity of the GAL4-DB and -AD domains may be driven by separate gene-specific enhancers. In this system GAL4-responsive UAS transgenic expression is restricted to those cells in which the split-GAL4 has been reconstituted via a leucine zipper attached to each domain; that is GAL4 expression occurs only in those cells in which endogenous expression of both proteins normally occurs (spatially and temporally) and therefore only those cells expressing both domains of the split-GAL4 system (Luan et al., 2006; Pfeiffer et al., 2010a). As *dsx*^{GAL4} expression occurs in both the nervous system and in non-neuronal adult tissues, such as the fat body and oenocytes (Rideout et al., 2010) the development of a *dsx*$^{Split\ GAL4}$ transgene would allow separation of neural and non-neural tissues providing the ability to anatomically and functionally dissect distinct types of *dsx* cells. This novel dsx GAL4 hemi-driver may then be employed in conjunction with extant Split GAL4 enhancer-trap lines (ET^{VP16AD}) to isolate and identify components of the overall *dsx* circuit in males and females. Novel hemi-drivers may be also be designed that will allow directed dissection of *dsx*-expressing tissues; such as the use of neurotransmitter specific hemi-drivers to identify neuronal subtypes, (*e.g.*, octopaminergic *tbh*^{VP16AD} and glutamatergic *vGlut*^{VP16AD} transgenes). This idea of reconstituting split functional domains has also been applied to the LexA/LexAop system in which the DNA-binding and *trans*-activating moieties are independently targeted using distinct promoters to achieve highly restricted, intersectional expression patterns (Ting et al., 2011). This 'Split-LexA' system can again be employed in compliment with the GAL4/UAS system to allow the opportunity to refine the expression patterns observed in existing GAL4 lines (Ting et al., 2011). Further developments utilising these systems are ongoing, for

example the refinement in *Drosophila* of the system for GFP reconstitution across synaptic partners (GRASP) (Feinberg et al., 2008) in which complementary use of the LexA and GAL4 systems allows a greater degree of specificity in expression of the reconstituted trans-membrane GFP both *in vivo* and in fixed tissues, with further restriction of expression being possible through application of MARCM strategems (Gordon and Scott, 2009). Another approach would be to target the insertion of *Drosophila* codon-optimized FLP recombinase into the *dsx* locus by homologous recombination, creating a dsx^{FLP} allele that drives FLP-mediated recombination specifically in *dsx* neurons. The efficacy and reach of this system may be expanded by the use of selected GAL4 drivers in conjunction with the dsx^{FLP} expressing active *UAS*>*stop*>reporters/effectors in the intersecting cells where FLP has excised the transcriptional stop cassette (>stop>). Newer more sophisticated techniques are continuing to be developed in response to perceived limitations of extant systems and as technological advances become available. One recently developed strategy to overcome the inherent difficulties of homologous recombination utilises conditionally amplifiable BAC vectors combined with *in vivo* recombination-mediated genetic engineering techniques for the manipulation of large DNA fragments in these vectors ('recombineering') (Copeland et al., 2001; Heintz, 2001; Muyrers et al., 2001; Sawitzke et al., 2007). These BAC constructs are then integrated into the *Drosophila* genome via PAC/BAC transgenesis techniques employing the system of PhiC31 integrase ensuring repeated targeting of the integrants to the same genomic 'docking/landing' sites (Bischof et al., 2007; Groth et al., 2004; Venken and Bellen, 2007; Venken et al., 2009; Venken et al., 2006; Venken et al., 2008). This latter process allowing control of local genomic environmental influences on transgenic expression and effectively eliminating problems associated with positional/insertional effects, something that is highly desirable when comparing variant mutagenised constructs derived from the same transgene for structure/function analyses.

In combination with the continued somatotopic mapping of the *dsx* neural architecture and the development of new technologies must come the continuation of analyses of the *dsx*-modulated sex-specific behavioural outputs. Functional analyses of female behaviours using dsx^{GAL4} indicated that *dsx*-positive neurons are involved in both pre- and post-copulatory female reproductive behaviors. Disrupting *dsx* neuronal function in females suppressed post-mating responses

(PMRs) suggesting an overlap between *dsx*$^{+}$ and the previously described sex peptide (SP) -responsive *fru*$^{+}$/ *ppk*$^{+}$-expressing neurons in the reproductive system (Häsemeyer et al., 2009; Yang et al., 2009; Yapici et al., 2008). However no colocalisation is apparent between *dsx* and these neurons in the genital tract and expression of *ppk*-GAL80 does not ameliorate the observed behavioural deficits. Indicating that additional neurons expressing *dsx* (independent of the *fru*$^{+}$/ *ppk*$^{+}$ pathway) must play a role in the underlying physiological and behavioural changes triggered by SP upon mating. Discerning how this *dsx* regulated (*fru*$^{+}$/ *ppk*$^{+}$ independent) pathway operates in the female demands further investigation. Such as *dsx*^{GAL4} driven expression of membrane-bound SP (mSP) in virgin females, to see if this will induce PMRs, or expression of SPR RNAi, to see if this will knock down PMRs in mated females (Häsemeyer et al., 2009; Yang et al., 2009; Yapici et al., 2008). Again co-expressing *elav*-GAL80 will allow confirmation of the neural aetiology of any observed consequences of manipulating SP expression driven by *dsx*^{GAL4} (Rideout et al., 2010). While co-expressing *ppk*-GAL80 will identify if these observed effects are indeed *fru*$^{+}$/ *ppk*$^{+}$ independent (Häsemeyer et al., 2009; Yang et al., 2009; Yapici et al., 2008).

Identifying which specific *dsx* neurons control different components of the sex-specific behavioural repertoires is an essential step towards dissecting the circuitry required for the performance of *Drosophila* sexual behaviours in both males and females. Providing insight into the neuronal events underlying behavioural choices and the genetic developmental logic that governs the assembly of these dimorphic neural circuits.

9 List of References

Acharyya, M., and Chatterjee, R.N. (2002). Genetic analysis of an intersex allele (ix5) that regulates sexual phenotype of both female and male Drosophila melanogaster. Genet Res *80*, 7-14.

Adam, G., Perrimon, N., and Noselli, S. (2003). The retinoic-like juvenile hormone controls the looping of left-right asymmetric organs in Drosophila. Development *130*, 2397-2406.

Adams, E.M., and Wolfner, M.F. (2007). Seminal proteins but not sperm induce morphological changes in the Drosophila melanogaster female reproductive tract during sperm storage. J Insect Physiol *53*, 319-331.

Ahmad, S.M., and Baker, B.S. (2002). Sex-specific deployment of FGF signaling in Drosophila recruits mesodermal cells into the male genital imaginal disc. Cell *109*, 651-661.

Ahuja, A., and Singh, R.S. (2008). Variation and evolution of male sex combs in Drosophila: nature of selection response and theories of genetic variation for sexual traits. Genetics *179*, 503-509.

Aigaki, T., Fleischmann, I., Chen, P.S., and Kubli, E. (1991). Ectopic expression of sex peptide alters reproductive behavior of female D. melanogaster. Neuron *7*, 557-563.

Amrein, H., and Thorne, N. (2005). Gustatory perception and behavior in Drosophila melanogaster. Curr Biol *15*, R673-684.

Anand, A., Villella, A., Ryner, L.C., Carlo, T., Goodwin, S.F., Song, H.J., Gailey, D.A., Morales, A., Hall, J.C., Baker, B.S.*, et al.* (2001). Molecular genetic dissection of the sex-specific and vital functions of the Drosophila melanogaster sex determination gene fruitless. Genetics *158*, 1569-1595.

Arbeitman, M.N., Kopp, A., Siegal, M.L., and Van Doren, M. (2010). Everything You Always Wanted to Know about Sex ... in Flies. Sexual development : genetics, molecular biology, evolution, endocrinology, embryology, and pathology of sex determination and differentiation.

Aguila, J.R., Suszko, J., Gibbs, A.G., and Hoshizaki, D.K. (2007). The role of larval fat cells in adult Drosophila melanogaster. J Exp Biol *210*, 956-963.
Arbeitman, M.N., Kopp, A., Siegal, M.L., and Van Doren, M. (2010). Everything You Always Wanted to Know about Sex ... in Flies. Sexual development : genetics, molecular biology, evolution, endocrinology, embryology, and pathology of sex determination and differentiation.

Arthur, B.I., Jallon, J.M., Caflisch, B., Choffat, Y., and Nöthiger, R. (1998). Sexual behaviour in Drosophila is irreversibly programmed during a critical period. Curr Biol *8*, 1187-1190.

Baker, B.S., and Ridge, K.A. (1980). Sex and the single cell. I. On the action of major loci affecting sex determination in Drosophila melanogaster. Genetics *94*, 383-423.

Baker, B.S., Taylor, B.J., and Hall, J.C. (2001). Are complex behaviors specified by dedicated regulatory genes? Reasoning from Drosophila. Cell *105*, 13-24.

Barmina, O., and Kopp, A. (2007). Sex-specific expression of a HOX gene associated with rapid morphological evolution. Dev Biol *311*, 277-286.

Barmina, O., Gonzalo, M., McIntyre, L.M., and Kopp, A. (2005). Sex- and segment-specific modulation of gene expression profiles in Drosophila. Dev Biol *288*, 528-544.

Barolo, S., Carver, L.A., and Posakony, J.W. (2000). GFP and beta-galactosidase transformation vectors for promoter/enhancer analysis in Drosophila. Biotechniques *29*, 726, 728, 730, 732.

Bellen, H.J., Tong, C., and Tsuda, H. (2010). 100 years of Drosophila research and its impact on vertebrate neuroscience: a history lesson for the future. Nat Rev Neurosci *11*, 514-522.

Bennet-Clark, H.C., and Ewing, A.W. (1967). Stimuli provided by Courtship of Male Drosophila melanogaster. Nature *215*, 669-671.

Bernstein, A.S., Neumann, E.K., and Hall, J.C. (1992). Temporal analysis of tone pulses within the courtship songs of 2 sibling Drosophila species, their interspecific hybrid, and behavioral mutants of Drosophila melanogaster (Diptera: Drosophilidae). J Insect Behav *5*, 15-36.

Bertram, M.J., Akerkar, G.A., Ard, R.L., Gonzalez, C., and Wolfner, M.F. (1992). Cell type-specific gene expression in the Drosophila melanogaster male accessory gland. Mech Dev *38*, 33-40.

Bi, X., and Rong, Y.S. (2003). Genome manipulation by homologous recombination in Drosophila. Brief Funct Genomic Proteomic *2*, 142-146.

Billeter, J.-C., and Goodwin, S.F. (2004). Characterization of Drosophila fruitless-gal4 transgenes reveals expression in male-specific fruitless neurons and innervation of male reproductive structures. J Comp Neurol *475*, 270-287.

Billeter, J.-C., Rideout, E.J., Dornan, A.J., and Goodwin, S.F. (2006a). Control of male sexual behavior in Drosophila by the sex determination pathway. Curr Biol *16*, R766-776.

Billeter, J.-C., Villella, A., Allendorfer, J.B., Dornan, A.J., Richardson, M., Gailey, D.A., and Goodwin, S.F. (2006b). Isoform-specific control of male neuronal differentiation and behavior in Drosophila by the fruitless gene. Curr Biol *16*, 1063-1076.

Bischof, J., Maeda, R.K., Hediger, M., Karch, F., and Basler, K. (2007). An optimized transgenesis system for Drosophila using germ-line-specific phiC31 integrases. Proceedings of the National Academy of Sciences of the United States of America *104*, 3312-3317.

Bohm, R.A., Welch, W.P., Goodnight, L.K., Cox, L.W., Henry, L.G., Gunter, T.C., Bao, H., and Zhang, B. (2010). A genetic mosaic approach for neural circuit mapping in Drosophila. Proc Natl Acad Sci USA *107*, 16378-16383.

Bownes, M. (1994). The regulation of the yolk protein genes, a family of sex differentiation genes in Drosophila melanogaster. Bioessays *16*, 745-752.

Brand, A. (1995). GFP in Drosophila. Trends Genet *11*, 324-325.

Brand, A.H., and Perrimon, N. (1993). Targeted gene expression as a means of altering cell fates and generating dominant phenotypes. Development *118*, 401-415.

Brent, R., and Ptashne, M. (1985). A eukaryotic transcriptional activator bearing the DNA specificity of a prokaryotic repressor. Cell *43*, 729-736.

Burtis, K.C., Coschigano, K.T., Baker, B.S., and Wensink, P.C. (1991). The doublesex proteins of Drosophila melanogaster bind directly to a sex-specific yolk protein gene enhancer. EMBO J *10*, 2577-2582.

Burtis, K.C., and Baker, B.S. (1989). Drosophila doublesex gene controls somatic sexual differentiation by producing alternatively spliced mRNAs encoding related sex-specific polypeptides. Cell *56*, 997-1010.

Butler, B., Pirrotta, V., Irminger-Finger, I., and Nothiger, R. (1986). The sex-determining gene tra of Drosophila: molecular cloning and transformation studies. EMBO J *5*, 3607-3613.

Cachero, S., Ostrovsky, A.D., Yu, J.Y., Dickson, B.J., and Jefferis, G.S. (2010). Sexual dimorphism in the fly brain. Curr Biol *20*, 1589-1601.

Camara, N., Whitworth, C., and Van Doren, M. (2008). The creation of sexual dimorphism in the Drosophila soma. Curr Top Dev Biol *83*, 65-107.

Carvalho, G.B., Kapahi, P., Anderson, D.J., and Benzer, S. (2006). Allocrine modulation of feeding behavior by the Sex Peptide of Drosophila. Curr Biol *16*, 692-696.

Cermak, T., Doyle, E.L., Christian, M., Wang, L., Zhang, Y., Schmidt, C., Baller, J.A., Somia, N.V., Bogdanove, A.J., and Voytas, D.F. (2011). Efficient design and assembly of custom TALEN and other TAL effector-based constructs for DNA targeting. Nucleic acids research *39*, e82.

Chan, Y.-B., and Kravitz, E.A. (2007). Specific subgroups of FruM neurons control sexually dimorphic patterns of aggression in Drosophila melanogaster. Proc Natl Acad Sci USA *104*, 19577-19582.

Chase, B.A., and Baker, B.S. (1995). A genetic analysis of intersex, a gene regulating sexual differentiation in Drosophila melanogaster females. Genetics *139*, 1649-1661.

Christian, M., Cermak, T., Doyle, E.L., Schmidt, C., Zhang, F., Hummel, A., Bogdanove, A.J., and Voytas, D.F. (2010). Targeting DNA double-strand breaks with TAL effector nucleases. Genetics *186*, 757-761.

Chintapalli, V.R., Wang, J., and Dow, J.A. (2007). Using FlyAtlas to identify better Drosophila melanogaster models of human disease. Nat Genet *39*, 715-720.

Christiansen, A.E., Keisman, E.L., Ahmad, S.M., and Baker, B.S. (2002). Sex comes in from the cold: the integration of sex and pattern. Trends Genet *18*, 510-516.

Cline, T.W., and Meyer, B.J. (1996). Vive la différence: males vs females in flies vs worms. Annu Rev Genet *30*, 637-702.

Clyne, J.D., and Miesenböck, G. (2008). Sex-specific control and tuning of the pattern generator for courtship song in Drosophila. Cell *133*, 354-363.

Clynen, E., Ciudad, L., Bellés, X., and Piulachs, M.-D. (2011). Conservation of fruitless' role as master regulator of male courtship behaviour from cockroaches to flies. Dev Genes Evol *221*, 43-48.

Connolly, K., and Cook, R.M. (1973). Rejection responses by female Drosophila melanogaster: Their ontogeny, causality and effects upon the behavior of the courting male. Behavior *44*, 142-167.

Cook, R.M. (1977). Behavioral role of the sexcombs in Drosophila melanogaster and Drosophila simulans. Behav Genet *7*, 349-357.

Cook, R.M. (1979). The courtship tracking of Drosophila melanogaster. Biol Cybern *34*, 91-106.

Copeland, N.G., Jenkins, N.A., and Court, D.L. (2001). Recombineering: a powerful new tool for mouse functional genomics. Nat Rev Genet *2*, 769-779.

Couderc, J.L., Godt, D., Zollman, S., Chen, J., Li, M., Tiong, S., Cramton, S.E., Sahut-Barnola, I., and Laski, F.A. (2002). The bric a brac locus consists of two paralogous genes encoding BTB/POZ domain proteins and acts as a homeotic and morphogenetic regulator of imaginal development in Drosophila. Development *129*, 2419-2433.

Court, D.L., Sawitzke, J.A., and Thomason, L.C. (2002). Genetic engineering using homologous recombination. Annu Rev Genet *36*, 361-388.

Coutelis, J.B., Petzoldt, A.G., Spéder, P., Suzanne, M., and Noselli, S. (2008). Left-right asymmetry in Drosophila. Semin Cell Dev Biol *19*, 252-262.

Coyne, J.A. (1985). Genetic studies of three sibling species of Drosophila with relationship to theories of speciation. Genet Res *46*, 169-192.

Datta, S.R., Vasconcelos, M.L., Ruta, V., Luo, S., Wong, A., Demir, E., Flores, J., Balonze, K., Dickson, B.J., and Axel, R. (2008). The Drosophila pheromone cVA activates a sexually dimorphic neural circuit. Nature *452*, 473-477.

Dauwalder, B. (2008). Systems behavior: of male courtship, the nervous system and beyond in Drosophila. Curr Genomics *9*, 517-524.

Davis, T., Kurihara, J., Yoshino, E., and Yamamoto, D. (2000). Genomic organisation of the neural sex determination gene fruitless (fru) in the Hawaiian species Drosophila silvestris and the conservation of the fru BTB protein-protein-binding domain throughout evolution. Hereditas *132*, 67-78.

DeFalco, T.J., Verney, G., Jenkins, A.B., McCaffery, J.M., Russell, S., and Van Doren, M. (2003). Sex- specific apoptosis regulates sexual dimorphism in the Drosophila embryonic gonad. Dev Cell 5, 205–216.

de Vries, G.J., and Södersten, P. (2009). Sex differences in the brain: the relation between structure and function. Horm Behav *55*, 589-596.

Demir, E., and Dickson, B.J. (2005). fruitless splicing specifies male courtship behavior in Drosophila. Cell *121*, 785-794.

Dickson, B.J. (2008). Wired for sex: the neurobiology of Drosophila mating decisions. Science *322*, 904-909.

Dietzl, G., Chen, D., Schnorrer, F., Su, K.-C., Barinova, Y., Fellner, M., Gasser, B., Kinsey, K., Oppel, S., Scheiblauer, S*., et al.* (2007). A genome-wide transgenic RNAi library for conditional gene inactivation in Drosophila. Nature *448*, 151-156.

Dornan, A.J., Gailey, D.A., and Goodwin, S.F. (2005). GAL4 enhancer trap targeting of the Drosophila sex determination gene fruitless. Genesis *42*, 236-246.

Dornan, A.J., and Goodwin, S.F. (2008). Fly courtship song: triggering the light fantastic. Cell *133*, 210-212.

Duffy, J.B. (2002). GAL4 system in Drosophila: a fly geneticist's Swiss army knife. Genesis *34*, 1-15.

Ejima, A., Nakayama, S., and Aigaki, T. (2001). Phenotypic association of spontaneous ovulation and sexual receptivity in virgin females of Drosophila melanogaster mutants. Behav Genet *31*, 437-444.

Engels, W.R. (1996). P Elements in Drosophila In Transposable Elements, H. Saedler, and A. Gierl, eds. (Berlin, Springer-Verlag), pp. 103-123.

Erdman, S.E., and Burtis, K.C. (1993). The Drosophila doublesex proteins share a novel zinc finger related DNA binding domain. EMBO J *12*, 527-535.

Erdman, S.E., Chen, H.J., and Burtis, K.C. (1996). Functional and genetic characterization of the oligomerization and DNA binding properties of the Drosophila doublesex proteins. Genetics *144*, 1639-1652.

Ewing, A.W., and Bennet-Clark, H.C. (1968). The courtship songs of Drosophila. Behaviour *31*, 288-301.

Fahrbach, S.E. (2006). Structure of the mushroom bodies of the insect brain. Annu Rev Entomol *51*, 209-232.

Feinberg, E.H., Vanhoven, M.K., Bendesky, A., Wang, G., Fetter, R.D., Shen, K., and Bargmann, C.I. (2008). GFP Reconstitution Across Synaptic Partners (GRASP) defines cell contacts and synapses in living nervous systems. Neuron *57*, 353-363.

Ferveur, J.F., and Greenspan, R.J. (1998). Courtship behavior of brain mosaics in Drosophila. J Neurogenet *12*, 205-226.

Fields, S., and Song, O. (1989). A novel genetic system to detect protein-protein interactions. Nature *340*, 245-246.

Finley, K.D., Edeen, P.T., Foss, M., Gross, E., Ghbeish, N., Palmer, R.H., Taylor, B.J., and McKeown, M. (1998). Dissatisfaction encodes a tailless-like nuclear receptor expressed in a subset of CNS neurons controlling Drosophila sexual behavior. Neuron *21*, 1363-1374.

Finley, K.D., Taylor, B.J., Milstein, M., and McKeown, M. (1997). dissatisfaction, a gene involved in sex-specific behavior and neural development of Drosophila melanogaster. Proc Natl Acad Sci U S A *94*, 913-918.

Fitzpatrick, M.J., Ben-Shahar, Y., Smid, H.M., Vet, L.E.M., Robinson, G.E., and Sokolowski, M.B. (2004). Candidate genes for behavioural ecology. Trends Ecol Evol *20*, 96-104.

Fujii, S., and Amrein, H. (2002). Genes expressed in the Drosophila head reveal a role for fat cells in sex-specific physiology. EMBO J *21*, 5353-5363.

Gailey, D.A., Billeter, J.-C., Liu, J.H., Bauzon, F., Allendorfer, J.B., and Goodwin, S.F. (2006). Functional conservation of the fruitless male sex-determination gene across 250 Myr of insect evolution. Mol Biol Evol *23*, 633-643.

Gailey, D.A., and Hall, J.C. (1989). Behavior and cytogenetics of fruitless in Drosophila melanogaster: different courtship defects caused by separate, closely linked lesions. Genetics *121*, 773-785.

Gailey, D.A., Ho, S.K., Ohshima, S., Liu, J.H., Eyassu, M., Washington, M.A., Yamamoto, D., and Davis, T. (2000). A phylogeny of the Drosophilidae using the sex-behaviour gene fruitless. Hereditas *133*, 81-83.

Gailey, D.A., Taylor, B.J., and Hall, J.C. (1991). Elements of the fruitless locus regulate development of the muscle of Lawrence, a male-specific structure in the abdomen of Drosophila melanogaster adults. Development *113*, 879-890.

Garrett-Engele, C.M., Siegal, M.L., Manoli, D.S., Williams, B.C., Li, H., and Baker, B.S. (2002). intersex, a gene required for female sexual development in Drosophila, is expressed in both sexes and functions together with doublesex to regulate terminal differentiation. Development *129*, 4661-4675.

Gill, K.S. (1963). A mutation causing abnormal mating behavior. Drosophila Inform Serv 38, 33.

Godt, D., Couderc, J.L., Cramton, S.E., and Laski, F.A. (1993). Pattern formation in the limbs of Drosophila: bric a brac is expressed in both a gradient and a wave-like pattern and is required for specification and proper segmentation of the tarsus. Development *119*, 799-812.

Gohl, D.M., Silies, M.A., Gao, X.J., Bhalerao, S., Luongo, F.J., Lin, C.-C., Potter, C.J., and Clandinin, T.R. (2011). A versatile in vivo system for directed dissection of gene expression patterns. Nat Methods *8*, 231-237.

Goldman, T.D., and Arbeitman, M.N. (2007). Genomic and functional studies of Drosophila sex hierarchy regulated gene expression in adult head and nervous system tissues. PLoS Genet *3*, e216.

Golic, K.G., and Lindquist, S. (1989). The FLP recombinase of yeast catalyzes site-specific recombination in the Drosophila genome. Cell *59*, 499-509.

Gong, S., Yang, X.W., Li, C., and Heintz, N. (2002). Highly efficient modification of bacterial artificial chromosomes (BACs) using novel shuttle vectors containing the R6Kgamma origin of replication. Genome Res *12*, 1992-1998.

Goodwin, S.F., Taylor, B.J., Villella, A., Foss, M., Ryner, L.C., Baker, B.S., and Hall, J.C. (2000). Aberrant splicing and altered spatial expression patterns in fruitless mutants of Drosophila melanogaster. Genetics *154*, 725-745.

Gordesky-Gold, B., Rivers, N., Ahmed, O.M., and Breslin, P.A.S. (2008). Drosophila melanogaster prefers compounds perceived sweet by humans. Chem Senses *33*, 301-309.

Gordon, M.D., and Scott, K. (2009). Motor control in a Drosophila taste circuit. Neuron *61*, 373-384.

Greenspan, R.J., and Ferveur, J.F. (2000). Courtship in Drosophila. Annu Rev Genet *34*, 205-232.

Groth, A.C., Fish, M., Nusse, R., and Calos, M.P. (2004). Construction of transgenic Drosophila by using the site-specific integrase from phage phiC31. Genetics *166*, 1775-1782.

Grueber, W.B., Ye, B., Moore, A.W., Jan, L.Y., and Jan, Y.N. (2003). Dendrites of distinct classes of Drosophila sensory neurons show different capacities for homotypic repulsion. Curr Biol *13*, 618-626.

Gutierrez, E., Wiggins, D., Fielding, B., and Gould, A.P. (2007). Specialized hepatocyte-like cells regulate Drosophila lipid metabolism. Nature *445*, 275-280.

Haerty, W., Jagadeeshan, S., Kulathinal, R.J., Wong, A., Ravi Ram, K., Sirot, L.K., Levesque, L., Artieri, C.G., Wolfner, M.F., Civetta, A.*, et al.* (2007). Evolution in the fast lane: rapidly evolving sex-related genes in Drosophila. Genetics *177*, 1321-1335.

Hall, J.C. (1977). Portions of the central nervous system controlling reproductive behavior in Drosophila melanogaster. Behav Genet *7*, 291-312.

Hall, J.C. (1978). Courtship among males due to a male-sterile mutation in *Drosophila melanogaster*. Behav Genet 8, 125-141.

Hall, J.C. (1979). Control of male reproductive behavior by the central nervous system of Drosophila: dissection of a courtship pathway by genetic mosaics. Genetics *92*, 437-457.

Hall, J.C., and Greenspan, R.J. (1979). Genetic analysis of Drosophila neurobiology. Annu Rev Genet *13*, 127-195.

Hartenstein, V. (1993). Atlas of Drosophila Development. In The Development of Drosophila, M. Bate, and A. Martinez-Arias, eds. (Cold Spring Harbor, Cold Spring Harbor Laboratory Press).

Häsemeyer, M., Yapici, N., Heberlein, U., and Dickson, B.J. (2009). Sensory neurons in the Drosophila genital tract regulate female reproductive behavior. Neuron *61*, 511-518.

Hastings, P.J., McGill, C., Shafer, B., and Strathern, J.N. (1993). Ends-in vs. ends-out recombination in yeast. Genetics *135*, 973-980.

Hasty, P., Rivera-Pérez, J., and Bradley, A. (1991a). The length of homology required for gene targeting in embryonic stem cells. Mol Cell Biol *11*, 5586-5591.

Hasty, P., Rivera-Pérez, J., Chang, C., and Bradley, A. (1991b). Target frequency and integration pattern for insertion and replacement vectors in embryonic stem cells. Mol Cell Biol *11*, 4509-4517.

Hausen, K., and Strausfeld, N.J. (1980). Sexually dimorphic interneuron arrangements in the fly visual system. Proc R Soc Lond B *208*, 57-71.

Hayes, S.A., Miller, J.M., and Hoshizaki, D.K. (2001). serpent, a GATA-like transcription factor gene, induces fat-cell development in Drosophila melanogaster. Development *128*, 1193-1200.

Heintz, N. (2001). BAC to the future: the use of bac transgenic mice for neuroscience research. Nat Rev Neurosci *2*, 861-870.

Heisenberg, M. (2003). Mushroom body memoir: from maps to models. Nat Rev Neurosci *4*, 266-275.

Heisenberg, M., Heusipp, M., and Wanke, C. (1995). Structural plasticity in the Drosophila brain. J Neurosci *15*, 1951-1960.

Hempel, L.U., and Oliver, B. (2007). Sex-specific DoublesexM expression in subsets of Drosophila somatic gonad cells. BMC Dev Biol *7*, 113.

Hildreth, P.E. (1965). Doublesex, Recessive Gene That Transforms Both Males and Females of Drosophila into Intersexes. Genetics *51*, 659-678.

Hockemeyer, D., Wang, H., Kiani, S., Lai, C.S., Gao, Q., Cassady, J.P., Cost, G.J., Zhang, L., Santiago, Y., Miller, J.C.*, et al.* (2011). Genetic engineering of human pluripotent cells using TALE nucleases. Nature biotechnology.

Hoshijima, K., Inoue, K., Higuchi, I., Sakamoto, H., and Shimura, Y. (1991). Control of doublesex alternative splicing by transformer and transformer-2 in Drosophila. Science *252*, 833-836.

Hoshizaki, D.K., Lunz, R., Ghosh, M., and Johnson, W. (1995). Identification of fat-cell enhancer activity in Drosophila melanogaster using P-element enhancer traps. Genome *38*, 497-506.

Ikeda, H., I., H., and Takabatake, I. (1981). Intraspecific variations in the thresholds of female responsiveness for auditory stimuli emitted by the male in Drosophila mercatorum. Zool Mag *90*, 325-332.

Ilius, M., Wolf, R., and Heisenberg, M. (1994). The central complex of Drosophila melanogaster is involved in flight control: studies on mutants and mosaics of the gene ellipsoid body open. J Neurogenet *9*, 189-206.

Ito, H., Fujitani, K., Usui, K., Shimizu-Nishikawa, K., Tanaka, S., and Yamamoto, D. (1996). Sexual orientation in Drosophila is altered by the satori mutation in the sex-determination gene fruitless that encodes a zinc finger protein with a BTB domain. Proceedings of the National Academy of Sciences of the United States of America *93*, 9687-9692.

Jones, W.D. (2009). The expanding reach of the GAL4/UAS system into the behavioral neurobiology of Drosophila. BMB Rep *42*, 705-712.

Jursnich, V.A., and Burtis, K.C. (1993). A positive role in differentiation for the male doublesex protein of Drosophila. Dev Biol *155*, 235-249.

Kanzaki, R., Ikeda, A., and Shibuya, T. (1994). Morphological and physiological properties of pheromone-triggered flip-flopping descending interneurons of the male silkworm moth, Bombyx mori. J Comp Physiol *175*, 1–14.

Kawanishi, M., and Watanabe, T.K. (1980). Genetic variations of courtship song of Drosophila melanogaster and D. Simulans. Jap J Genet *55*, 235-240.

Keegan, L., Gill, G., and Ptashne, M. (1986). Separation of DNA binding from the transcription-activating function of a eukaryotic regulatory protein. Science *231*, 699-704.

Keisman, E.L., Christiansen, A.E., and Baker, B.S. (2001). The sex determination gene doublesex regulates the A/P organizer to direct sex-specific patterns of growth in the Drosophila genital imaginal disc. Dev Cell *1*, 215-225.

Kimura, K.-I. (2011). Role of cell death in the formation of sexual dimorphism in the Drosophila central nervous system. Dev Growth Differ *53*, 236-244.

Kimura, K.-I., Hachiya, T., Koganezawa, M., Tazawa, T., and Yamamoto, D. (2008). Fruitless and doublesex coordinate to generate male-specific neurons that can initiate courtship. Neuron *59*, 759-769.

Kimura, K.-I., Ote, M., Tazawa, T., and Yamamoto, D. (2005). Fruitless specifies sexually dimorphic neural circuitry in the Drosophila brain. Nature *438*, 229-233.

Kitamoto, T. (2001). Conditional modification of behavior in Drosophila by targeted expression of a temperature-sensitive shibire allele in defined neurons. J Neurobiol *47*, 81-92.

Koganezawa, M., Haba, D., Matsuo, T., and Yamamoto, D. (2010). The shaping of male courtship posture by lateralized gustatory inputs to male-specific interneurons. Curr Biol *20*, 1-8.

Kohatsu, S., Koganezawa, M., and Yamamoto, D. (2011). Female Contact Activates Male-Specific Interneurons that Trigger Stereotypic Courtship Behavior in Drosophila. Neuron *69*, 498-508.

of sexual dimorphism in the olfactory brain of Hawaiian Drosophila. Proc Biol Sci *270*, 1005-1013.

Kopp, A., and Duncan, I. (2002). Anteroposterior patterning in adult abdominal segments of Drosophila. Dev Biol *242*, 15-30.

Kopp, A., Duncan, I., Godt, D., and Carroll, S.B. (2000). Genetic control and evolution of sexually dimorphic characters in Drosophila. Nature *408*, 553-559.

Krstic, D., Boll, W., and Noll, M. (2009). Sensory integration regulating male courtship behavior in Drosophila. PLoS One *4*, e4457.

Kubli, E. (2003). Sex-peptides: seminal peptides of the Drosophila male. Cell Mol Life Sci *60*, 1689-1704.

Kubli, E. (2008). Sexual behaviour: a receptor for sex control in Drosophila females. Curr Biol *18*, R210-212.

Kubli, E. (2010). Sexual behavior: dietary food switch induced by sex. Curr Biol *20*, R474-476.

Kulkarni, S.J., and Hall, J.C. (1987). Behavioral and cytogenetic analysis of the cacophony courtship song mutant and interacting genetic variants in Drosophila melanogaster. Genetics *115*, 461-475.

Kvitsiani, D., and Dickson, B.J. (2006). Shared neural circuitry for female and male sexual behaviours in Drosophila. Curr Biol *16*, R355-356.

Kyriacou, C.P., and Hall, J.C. (1980). Circadian rhythm mutations in Drosophila melanogaster affect short-term fluctuations in the male's courtship song. Proc Natl Acad Sci USA *77*, 6729-6733.

Kyriacou, C.P., and Hall, J.C. (1982). The function of courtship song rhythms in Drosophila. Anim Behav *30*, 794-801.

Kyriacou, C.P., and Hall, J.C. (1986). Interspecific genetic control of courtship song production and reception in Drosophila. Science *232*, 494-497.

Lai, S.-L., and Lee, T. (2006). Genetic mosaic with dual binary transcriptional systems in Drosophila. Nat Neurosci *9*, 703-709.

Lee, G., Foss, M., Goodwin, S.F., Carlo, T., Taylor, B.J., and Hall, J.C. (2000). Spatial, temporal, and sexually dimorphic expression patterns of the fruitless gene in the Drosophila central nervous system. J Neurobiol *43*, 404-426.

Lee, G., and Hall, J.C. (2001). Abnormalities of male-specific FRU protein and serotonin expression in the CNS of fruitless mutants in Drosophila. J Neurosci *21*, 513-526.

Lee, G., Hall, J.C., and Park, J.H. (2002). Doublesex gene expression in the central nervous system of Drosophila melanogaster. J Neurogenet *16*, 229-248.

Lee, G., Villella, A., Taylor, B.J., and Hall, J.C. (2001). New reproductive anomalies in fruitless-mutant Drosophila males: extreme lengthening of mating durations and infertility correlated with defective serotonergic innervation of reproductive organs. J Neurobiol *47*, 121-149.

Lee, H.-G., Rohila, S., and Han, K.-A. (2009). The octopamine receptor OAMB mediates ovulation via Ca2+/calmodulin-dependent protein kinase II in the Drosophila oviduct epithelium. PLoS ONE *4*, e4716.

Lee, T., and Luo, L. (1999). Mosaic analysis with a repressible cell marker for studies of gene function in neuronal morphogenesis. Neuron *22*, 451-461.

Li, H., and Baker, B.S. (1998a). Her, a gene required for sexual differentiation in Drosophila, encodes a zinc finger protein with characteristics of ZFY-like proteins and is expressed independently of the sex determination hierarchy. Development *125*, 225-235.

Li, H., and Baker, B.S. (1998b). hermaphrodite and doublesex function both dependently and independently to control various aspects of sexual differentiation in Drosophila. Development *125*, 2641-2651.

Lima, S.Q., and Miesenböck, G. (2005). Remote control of behavior through genetically targeted photostimulation of neurons. Cell *121*, 141-152.

Liu, W., and Hou, S.X. (2008). Genetic tools used for cell lineage tracing and gene manipulation in Drosophila germline stem cells. Methods Mol Biol *450*, 61-70.

Luan, H., Peabody, N.C., Vinson, C.R., and White, B.H. (2006). Refined spatial manipulation of neuronal function by combinatorial restriction of transgene expression. Neuron *52*, 425-436.

Luo, L. (2007). Single-Neuron Labeling Using the Genetic MARCM Method. CSH Protoc *2007*, pdb.prot4789.

Ma, J., and Ptashne, M. (1987). The carboxy-terminal 30 amino acids of GAL4 are recognized by GAL80. Cell *50*, 137-142.

MacDonald, J.M., Beach, M.G., Porpiglia, E., Sheehan, A.E., Watts, R.J., and Freeman, M.R. (2006). The Drosophila cell corpse engulfment receptor Draper mediates glial clearance of severed axons. Neuron *50*, 869-881.

MacDougall, C., Harbison, D., and Bownes, M. (1995). The developmental consequences of alternate splicing in sex determination and differentiation in Drosophila. Dev Biol *172*, 353-376.

Mackay, T.F., Hackett, J.B., Lyman, R.F., Wayne, M.L., and Anholt, R.R. (1996). Quantitative genetic variation of odor-guided behavior in a natural population of Drosophila melanogaster. Genetics *144*, 727-735.

Manning, A. (1959). The sexual isolation between Drosophila melanogaster and Drosophila simulans. Anim Behav *7*, 60-65.

Manoli, D.S., and Baker, B.S. (2004). Median bundle neurons coordinate behaviours during Drosophila male courtship. Nature *430*, 564-569.

Manoli, D.S., Foss, M., Villella, A., Taylor, B.J., Hall, J.C., and Baker, B.S. (2005). Male-specific fruitless specifies the neural substrates of Drosophila courtship behaviour. Nature *436*, 395-400.

Manoli, D.S., Meissner, G.W., and Baker, B.S. (2006). Blueprints for behavior: genetic specification of neural circuitry for innate behaviors. Trends Neurosci *29*, 444-451.

Markow, T.A. (1987). Behavioral and sensory basis of courtship success in Drosophila melanogaster. Proc Natl Acad Sci USA *84*, 6200-6204.

Markow, T.A., Bustoz, D., and Pitnick, S. (1996). Sexual selection and a secondary sexual character in two Drosophila species. Animal Behaviour *Volume 52*, 759-766. .

Martin, J.R., Ernst, R., and Heisenberg, M. (1998). Mushroom bodies suppress locomotor activity in Drosophila melanogaster. Learn Mem *5*, 179-191.

Martin, J.R., Raabe, T., and Heisenberg, M. (1999). Central complex substructures are required for the maintenance of locomotor activity in Drosophila melanogaster. J Comp Physiol A *185*, 277-288.

McGuire, S.E., Roman, G., and Davis, R.L. (2004). Gene expression systems in Drosophila: a synthesis of time and space. Trends Genet *20*, 384-391.

McNabb, S.L., Baker, J.D., Agapite, J., Steller, H., Riddiford, L.M., and Truman, J.W. (1997). Disruption of a behavioral sequence by targeted death of peptidergic neurons in Drosophila. Neuron *19*, 813-823.

McRobert, S.P., and Tompkins, L. (1985). The effect of transformer, doublesex and intersex mutations on the sexual behavior of Drosophila melanogaster. Genetics *111*, 89-96.

McRobert, S.P., Tompkins, L., Barr, N.B., Bradner, J., Lucas, D., Rattigan, D.M., and Tannous, A.F. (2003). Mutations in raised Drosophila melanogaster affect experience-dependent aspects of sexual behavior in both sexes. Behav Genet *33*, 347-356.

Meinertzhagen, I.A., and Hanson, T.E. (1993). The development of the optic lob. In The development of Drosophila melanogaster, M. Bate, and A. Martinez-Arias, eds. (New York, Cold Spring Harbor Laboratory Press), pp. 1363-1491.

Mellert, D.J., Knapp, J.-M., Manoli, D.S., Meissner, G.W., and Baker, B.S. (2010). Midline crossing by gustatory receptor neuron axons is regulated by fruitless, doublesex and the Roundabout receptors. Development *137*, 323-332.

Miller, A. (1950). The internal anatomy and histology of the imago of Drosophila melanogaster. In Biology of Drosophila, M. Demerec, ed. (New York, John Wiley & Sons), pp. 420-534.

Miller, J.C., Tan, S., Qiao, G., Barlow, K.A., Wang, J., Xia, D.F., Meng, X., Paschon, D.E., Leung, E., Hinkley, S.J.*, et al.* (2011). A TALE nuclease architecture for efficient genome editing. Nature biotechnology *29*, 143-148.

Muyrers, J.P., Zhang, Y., and Stewart, A.F. (2001). Techniques: Recombinogenic engineering--new options for cloning and manipulating DNA. Trends Biochem Sci *26*, 325-331.

Ng, C.S., and Kopp, A. (2008). Sex combs are important for male mating success in Drosophila melanogaster. Behav Genet *38*, 195-201.

Parisky, K.M., Agosto, J., Pulver, S.R., Shang, Y., Kuklin, E., Hodge, J.J.L., Kang, K., Kang, K., Liu, X., Garrity, P.A.*, et al.* (2008). PDF cells are a GABA-responsive wake-promoting component of the Drosophila sleep circuit. Neuron *60*, 672-682.

Nitabach, M.N., Wu, Y., Sheeba, V., Lemon, W.C., Strumbos, J., Zelensky, P.K., White, B.H., and Holmes, T.C. (2006). Electrical hyperexcitation of lateral ventral pacemaker neurons desynchronizes downstream circadian oscillators in the fly circadian circuit and induces multiple behavioral periods. J Neurosci *26*, 479-489.

Nojima, T., Kimura, K.-I., Koganezawa, M., and Yamamoto, D. (2010). Neuronal synaptic outputs determine the sexual fate of postsynaptic targets. Curr Biol *20*, 836-840.

O'Dell, K.M., and Goodwin, S.F. (2010). Courtship. Drosophila Neurobiology Manual CSH Press, 1-8.

Pan, Y., Zhou, Y., Guo, C., Gong, H., Gong, Z., and Liu, L. (2009). Differential roles of the fan-shaped body and the ellipsoid body in Drosophila visual pattern memory. Learn Mem *16*, 289-295.

Pathak, S.C., and Ghosh, S. (1990). Neurosecretory cells in Diptera. Folia Morphol (Praha) *38*, 174-185.

Pfeiffer, B.D., Ngo, T.T., Hibbard, K.L., Murphy, C., Jenett, A., Truman, J.W., and Rubin, G.M. (2010). Refinement of tools for targeted gene expression in Drosophila. Genetics *186*, 735-755.

Pilauri, V., Bewley, M., Diep, C., and Hopper, J. (2005). Gal80 dimerization and the yeast GAL gene switch. Genetics *169*, 1903-1914.

Possidente, D.R., and Murphey, R.K. (1989). Genetic control of sexually dimorphic axon morphology in Drosophila sensory neurons. Dev Biol *132*, 448-457.

Potter, C.J., and Luo, L. (2011). Using the Q system in Drosophila melanogaster. Nat Protoc *6*, 1105-1120.

Potter, C.J., Tasic, B., Russler, E.V., Liang, L., and Luo, L. (2010). The Q system: a repressible binary system for transgene expression, lineage tracing, and mosaic analysis. Cell *141*, 536-548.

Pultz, M.A., and Baker, B.S. (1995). The dual role of hermaphrodite in the Drosophila sex determination regulatory hierarchy. Development *121*, 99-111.

Pultz, M.A., Carson, G.S., and Baker, B.S. (1994). A genetic analysis of hermaphrodite, a pleiotropic sex determination gene in Drosophila melanogaster. Genetics *136*, 195-207.

Pulver, S.R., Pashkovski, S.L., Hornstein, N.J., Garrity, P.A., and Griffith, L.C. (2009). Temporal dynamics of neuronal activation by Channelrhodopsin-2 and TRPA1 determine behavioral output in Drosophila larvae. J Neurophysiol *101*, 3075-3088.

Rajashekhar, K.P., and Singh, R.N. (1994). Neuroarchitecture of the tritocerebrum of Drosophila melanogaster. J Comp Neurol *349*, 633-645.

Ram, K.R., and Wolfner, M.F. (2007). Seminal influences: Drosophila Acps and the molecular interplay between males and females during reproduction Integrative and Comparative Biology
47, 427-445.

Raymond, C.S., Murphy, M.W., O'Sullivan, M.G., Bardwell, V.J., and Zarkower, D. (2000). Dmrt1, a gene related to worm and fly sexual regulators, is required for mammalian testis differentiation. Genes Dev *14*, 2587-2595.

Raymond, C.S., Shamu, C.E., Shen, M.M., Seifert, K.J., Hirsch, B., Hodgkin, J., and Zarkower, D. (1998). Evidence for evolutionary conservation of sex-determining genes. Nature *391*, 691-695.

Rein, K., Zöckler, M., Mader, M.T., Grübel, C., and Heisenberg, M. (2002). The Drosophila standard brain. Curr Biol *12*, 227-231.

Rideout, E.J., Billeter, J.-C., and Goodwin, S.F. (2007). The sex-determination genes fruitless and doublesex specify a neural substrate required for courtship song. Curr Biol *17*, 1473-1478.

Rideout, E.J., Dornan, A.J., Neville, M.C., Eadie, S., and Goodwin, S.F. (2010). Control of sexual differentiation and behavior by the doublesex gene in Drosophila melanogaster. Nat Neurosci *13*, 458-466.

Ritchie, M., Townhill, R., and Hoikkala, A. (1998). Female preference for fly song: playback experiments confirm the targets of sexual selection. Anim Behav *56*, 713-717.

Ritchie, M.G., Halsey, E.J., and Gleason, J.M. (1999). Drosophila song as a species-specific mating signal and the behavioural importance of Kyriacou & Hall cycles in D. melanogaster song. Anim Behav *58*, 649-657.

Robinett, C.C., Vaughan, A.G., Knapp, J.-M., and Baker, B.S. (2010). Sex and the single cell. II. There is a time and place for sex. PLoS Biol *8*, e1000365.

Rong, Y.S., and Golic, K.G. (2000). Gene targeting by homologous recombination in Drosophila. Science *288*, 2013-2018.

Rong, Y.S., and Golic, K.G. (2001). A targeted gene knockout in Drosophila. Genetics *157*, 1307-1312.

Rong, Y.S., Titen, S.W., Xie, H.B., Golic, M.M., Bastiani, M., Bandyopadhyay, P., Olivera, B.M., Brodsky, M., Rubin, G.M., and Golic, K.G. (2002). Targeted mutagenesis by homologous recombination in D. melanogaster. Genes Dev *16*, 1568-1581.

Rubin, G.M., and Spradling, A.C. (1983). Vectors for P element-mediated gene transfer in Drosophila. Nucleic Acids Res *11*, 6341-6351.

Ruta, V., Datta, S.R., Vasconcelos, M.L., Freeland, J., Looger, L.L., and Axel, R. (2010). A dimorphic pheromone circuit in Drosophila from sensory input to descending output. Nature *468*, 686-690.

Ryner, L.C., and Baker, B.S. (1991). Regulation of doublesex pre-mRNA processing occurs by 3'-splice site activation. Genes Dev *5*, 2071-2085.

Ryner, L.C., Goodwin, S.F., Castrillon, D.H., Anand, A., Villella, A., Baker, B.S., Hall, J.C., Taylor, B.J., and Wasserman, S.A. (1996). Control of male sexual

behavior and sexual orientation in Drosophila by the fruitless gene. Cell *87*, 1079-1089.

Sadowski, I., Ma, J., Triezenberg, S., and Ptashne, M. (1988). GAL4-VP16 is an unusually potent transcriptional activator. Nature *335*, 563-564.

Salvemini, M., Polito, C., and Saccone, G. (2010). fruitless alternative splicing and sex behaviour in insects: an ancient and unforgettable love story? J Genet *89*, 287-299.

Sanchez, L., Gorfinkiel, N., and Guerrero, I. (2001). Sex determination genes control the development of the Drosophila genital disc, modulating the response to Hedgehog, Wingless and Decapentaplegic signals. Development *128*, 1033-1043.

Sanchez, L., and Guerrero, I. (2001). The development of the Drosophila genital disc. Bioessays *23*, 698-707.

Sandeman, R., Clarke, D., Sandeman, D., and Manly, M. (1998). Growth-related and antennular amputation-induced changes in the olfactory centers of crayfish brain. J Neurosci *18*, 6195-6206.

Sawitzke, J.A., Thomason, L.C., Costantino, N., Bubunenko, M., Datta, S., and Court, D.L. (2007). Recombineering: in vivo genetic engineering in E. coli, S. enterica, and beyond. Meth Enzymol *421*, 171-199.

Shang, Y., Griffith, L.C., and Rosbash, M. (2008). Light-arousal and circadian photoreception circuits intersect at the large PDF cells of the Drosophila brain. Proceedings of the National Academy of Sciences of the United States of America *105*, 19587-19594.

Shirangi, T.R., Dufour, H.D., Williams, T.M., and Carroll, S.B. (2009). Rapid evolution of sex pheromone-producing enzyme expression in Drosophila. PLoS Biol *7*, e1000168.

Shorey, H.H. (1962). Nature of the Sound Produced by Drosophila melanogaster during Courtship. Science *137*, 677-678.

Siegel, R.W., and Hall, J.C. (1979). Conditioned responses in courtship behavior of normal and mutant Drosophila. Proc Natl Acad Sci U S A *76*, 3430-3434.

Simpson, J.H. (2009). Mapping and manipulating neural circuits in the fly brain. Adv Genet *65*, 79-143.

Siwicki, K.K., and Kravitz, E.A. (2009). Fruitless, doublesex and the genetics of social behavior in Drosophila melanogaster. Curr Opin Neurobiol *19*, 200-206.

Spieth, H.T. (1974). Courtship behavior in Drosophila. Annu Rev Entomol *19*, 385-405.

Song, H.-J., Billeter, J.-C., Reynaud, E., Carlo, T., Spana, E.P., Perrimon, N., Goodwin, S.F., Baker, B.S., and Taylor, B.J. (2002). The fruitless gene is required for the proper formation of axonal tracts in the embryonic central nervous system of Drosophila. Genetics *162*, 1703-1724.

Song, H.-J., and Taylor, B.J. (2003). fruitless gene is required to maintain neuronal identity in evenskipped-expressing neurons in the embryonic CNS of Drosophila. J Neurobiol *55*, 115-133.

Spéder, P., Adám, G., and Noselli, S. (2006). Type ID unconventional myosin controls left-right asymmetry in Drosophila. Nature *440*, 803-807.

Spieth, H.T. (1952). Mating behavior within the genus Drosophila (Diptera). Bull Am Museum Nat Hist *99*, 395-474.

Spieth, H.T. (1974). Courtship behavior in Drosophila. Annu Rev Entomol *19*, 385-405.

Spieth, H.T., and Ringo, J.M. (1983). Mating behavior and sexual isolation in Drosophila. In The Genetics and Biology of Drosophila, M. Ashburner, H. Carson, and T. J., eds. (New York, Academic Press), pp. 223–284.

Steinmann-Zwicky, M., Amrein, H., and Nöthiger, R. (1990). Genetic control of sex determination in Drosophila. Adv Genet *27*, 189-237.

Stocker, R.F. (1994). The organization of the chemosensory system in Drosophila melanogaster: a review. Cell Tissue Res *275*, 3-26.

Stockinger, P., Kvitsiani, D., Rotkopf, S., Tirián, L., and Dickson, B.J. (2005). Neural circuitry that governs Drosophila male courtship behavior. Cell *121*, 795-807.

Strausfeld, N.J. (1976). Atlas of an insect brain (New York, Springer).

Strausfeld, N.J. (1980). Male and female visual neurones in dipterous insects. Nature *283*, 381-383.

Strausfeld, N.J. (1991). Structural organization of male-specific visual neurons in calliphorid optic lobes. J Comp Physiol A *169*, 379-393.

Strausfeld, N.J., and Meinertzhagen, I.A. (1998). The insect neuron: types, morphologies, fine structure, and relationship to the architectonics of the insect nervous system. In Microscopic anatomy of invertebrates, F.W. Harrison, and M. Locke, eds. (New York, Wiley), pp. 487-538.

Struhl, G. (1982). Genes controlling segmental specification in the Drosophila thorax. Proc Natl Acad Sci U S A *79*, 7380-7384.

Struhl, G., and Basler, K. (1993). Organizing activity of wingless protein in Drosophila. Cell *72*, 527-540.

Suster, M.L., Seugnet, L., Bate, M., and Sokolowski, M.B. (2004). Refining GAL4-driven transgene expression in Drosophila with a GAL80 enhancer-trap. Genesis *39*, 240-245.

Sweeney, S.T., Broadie, K., Keane, J., Niemann, H., and O'Kane, C.J. (1995). Targeted expression of tetanus toxin light chain in Drosophila specifically eliminates synaptic transmission and causes behavioral defects. Neuron *14*, 341-351.

Szüts, D., and Bienz, M. (2000). LexA chimeras reveal the function of Drosophila Fos as a context-dependent transcriptional activator. Proceedings of the National Academy of Sciences of the United States of America *97*, 5351-5356.

Taylor, B.J., and Truman, J.W. (1992). Commitment of abdominal neuroblasts in Drosophila to a male or female fate is dependent on genes of the sex-determining hierarchy. Development *114*, 625-642.

Taylor, B.J., Villella, A., Ryner, L.C., Baker, B.S., and Hall, J.C. (1994). Behavioral and neurobiological implications of sex-determining factors in Drosophila. Dev Genet *15*, 275-296.

Technau, G.M. (1984). Fiber number in the mushroom bodies of adult Drosophila melanogaster depends on age, sex and experience. J Neurogenet *1*, 113-126.

Thorne, N., Bray, S., and Amrein, H. (2005). Function and expression of the Drosophila gr genes in the perception of sweet, bitter and pheromone compounds. Chem Senses *30 Suppl 1*, i270-272.

Tinbergen, N. (1951). The Study of Instinct, XII edn (London, Oxford University Press).

Ting, C.-Y., Gu, S., Guttikonda, S., Lin, T.-Y., White, B.H., and Lee, C.-H. (2011). Focusing transgene expression in Drosophila by coupling Gal4 with a novel split-LexA expression system. Genetics *188*, 229-233.

Tokunaga, C. (1962). Cell lineage and differentiation on the male foreleg of Drosophila melanogaster. Dev Biol *4*, 489-516.

Tomaru, M., Matsubayashi, H., and Oguma, Y. (1885). Heterospecific interpulse intervals of courtshipsong elicit female rejection in Drosophila biaurarua. Anim Behav *50*, 905-915.

Tompkins, L., Siegel, R.W., Gailey, D.A., and Hall, J.C. (1983). Conditioned courtship in Drosophila and its mediation by association of chemical cues. Behav Genet *13*, 565-578.

Usui-Aoki, K., Ito, H., Ui-Tei, K., Takahashi, K., Lukacsovich, T., Awano, W., Nakata, H., Piao, Z.F., Nilsson, E.E., Tomida, J.*, et al.* (2000). Formation of the male-specific muscle in female Drosophila by ectopic fruitless expression. Nat Cell Biol *2*, 500-506.

Venard, R., Antony, C., and Jallon, J.-M. (1989). Drosophila chemoreceptors. In Neurobiology of Sensory Systems, R.N. Singh, and J.S. Strausfeld, eds. (New York, Plenum), pp. 377–385.

Venken, K.J.T., and Bellen, H.J. (2007). Transgenesis upgrades for Drosophila melanogaster. Development *134*, 3571-3584.

Venken, K.J.T., Carlson, J.W., Schulze, K.L., Pan, H., He, Y., Spokony, R., Wan, K.H., Koriabine, M., de Jong, P.J., White, K.P.*, et al.* (2009). Versatile P[acman] BAC libraries for transgenesis studies in Drosophila melanogaster. Nat Methods *6*, 431-434.

Venken, K.J.T., He, Y., Hoskins, R.A., and Bellen, H.J. (2006). P[acman]: a BAC transgenic platform for targeted insertion of large DNA fragments in D. melanogaster. Science *314*, 1747-1751.

Venken, K.J.T., Kasprowicz, J., Kuenen, S., Yan, J., Hassan, B.A., and Verstreken, P. (2008). Recombineering-mediated tagging of Drosophila genomic constructs for in vivo localization and acute protein inactivation. Nucleic Acids Res *36*, e114.

Villella, A., Gailey, D.A., Berwald, B., Ohshima, S., Barnes, P.T., and Hall, J.C. (1997). Extended reproductive roles of the fruitless gene in Drosophila melanogaster revealed by behavioral analysis of new fru mutants. Genetics *147*, 1107-1130.

Villella, A., and Hall, J.C. (1996). Courtship anomalies caused by doublesex mutations in Drosophila melanogaster. Genetics *143*, 331-344.

Villella, A., and Hall, J.C. (2008). Neurogenetics of courtship and mating in Drosophila. Adv Genet *62*, 67-184.

von Philipsborn, A.C., Liu, T., Yu, J.Y., Masser, C., Bidaye, S.S., and Dickson, B.J. (2011). Neuronal control of Drosophila courtship song. Neuron *69*, 509-522.

von Schilcher, F. (1976a). The function of pulse song and sine song in the courtship of Drosophila melanogaster. Anim Behav *24*, 622-625.

von Schilcher, F. (1976b). The role of auditory stimuli in the courtship of Drosophila melanogaster. Anim Behav *24*, 18-26.

von Schilcher, F., and Hall, J.C. (1979). Neural topography of courtship song in sex mosaics of Drosophila melanogaster. J Comp Physiol *129*, 85–95.

Vosshall, L.B. (2007). Into the mind of a fly. Nature *450*, 193-197.

Waterbury, J.A., Horabin, J.I., Bopp, D., and Schedl, P. (2000). Sex determination in the Drosophila germline is dictated by the sexual identity of the surrounding soma. Genetics *155*, 1741-1756.

Waterbury, J.A., Jackson, L.L., and Schedl, P. (1999). Analysis of the doublesex female protein in Drosophila melanogaster: role on sexual differentiation and behavior and dependence on intersex. Genetics *152*, 1653-1667.

Wheeler, D.A., Fields, W.L., and Hall, J.C. (1988). Spectral analysis of Drosophila courtship songs: D. melanogaster, D. simulans, and their interspecific hybrid. Behav Genet *18*, 675-703.

Wheeler, D.A., Kulkarni, S.J., Gailey, D.A., and Hall, J.C. (1989). Spectral analysis of courtship songs in behavioral mutants of Drosophila melanogaster. Behav Genet *19*, 503-528.

Wild, J., Hradecna, Z., and Szybalski, W. (2002). Conditionally amplifiable BACs: switching from single-copy to high-copy vectors and genomic clones. Genome Res *12*, 1434-1444.

Williams, T.M., Selegue, J.E., Werner, T., Gompel, N., Kopp, A., and Carroll, S.B. (2008). The regulation and evolution of a genetic switch controlling sexually dimorphic traits in Drosophila. Cell *134*, 610-623.

Xu, T., and Rubin, G.M. (1993). Analysis of genetic mosaics in developing and adult Drosophila tissues. Development *117*, 1223-1237.

Yang, C.-H., Rumpf, S., Xiang, Y., Gordon, M.D., Song, W., Jan, L.Y., and Jan, Y.-N. (2009). Control of the postmating behavioral switch in Drosophila females by internal sensory neurons. Neuron *61*, 519-526.

Yang, X.W., Model, P., and Heintz, N. (1997). Homologous recombination based modification in Escherichia coli and germline transmission in transgenic mice of a bacterial artificial chromosome. Nat Biotechnol *15*, 859-865.

Yapici, N., Kim, Y.-J., Ribeiro, C., and Dickson, B.J. (2008). A receptor that mediates the post-mating switch in Drosophila reproductive behaviour. Nature *451*, 33-37.

Yu, J.Y., Kanai, M.I., Demir, E., Jefferis, G.S., and Dickson, B.J. (2010). Cellular organization of the neural circuit that drives Drosophila courtship behavior. Curr Biol *20*, 1602-1614.

Yun, S.J., Hiraoka, Y., Nishizawa, M., Takio, K., Titani, K., Nogi, Y., and Fukasawa, T. (1991). Purification and characterization of the yeast negative regulatory protein GAL80. J Biol Chem *266*, 693-697.

Zarkower, D. (2001). Establishing sexual dimorphism: conservation amidst diversity? Nat Rev Genet *2*, 175-185.

Zarkower, D. (2002). Invertebrates may not be so different after all. Novartis Found Symp *244*, 115-126; discussion 126-135, 203-116, 253-117.

Zars, T. (2000). Behavioral functions of the insect mushroom bodies. Curr Opin Neurobiol *10*, 790-795.

Zhang, S.D., and Odenwald, W.F. (1995). Misexpression of the white (w) gene triggers male-male courtship in Drosophila. Proc Natl Acad Sci U S A *92*, 5525-5529.

Zhang, W., Ge, W., and Wang, Z. (2007). A toolbox for light control of Drosophila behaviors through Channelrhodopsin 2-mediated photoactivation of targeted neurons. Eur J Neurosci *26*, 2405-2416.

Zhou, L., Schnitzler, A., Agapite, J., Schwartz, L.M., Steller, H., and Nambu, J.R. (1997). Cooperative functions of the reaper and head involution defective genes in the programmed cell death of Drosophila central nervous system midline cells. Proceedings of the National Academy of Sciences of the United States of America *94*, 5131-5136.

10 Accompanying materials